Electrochemical Synthesis of Melanin-Like Polyindolequinone

A thesis presented to
The Queensland University of Technology

In fulfilment of the requirements for the degree of
Doctor of Philosophy

by
Surya Subianto
Bachelor of Applied Science (Hons)

Under the Supervision of:
Dr. Geoffrey Will
Dr. Paul Meredith

Inorganic Materials Research Program
School of Physical and Chemical Sciences
Queensland University of Technology

July 2006

This thesis is dedicated to my parents,
without whom I would not be where I am today

Acknowledgement

The author would like to thank the following people

- My principal supervisors, Dr. Geoffrey Will and Dr. Paul Meredith
- Dr. Barry Wood
- Prof. Andrew Whittaker
- Dr. Llew Rintoul
- Mr. Loc Duong
- Dr. Thor Bolstrom
- Members of the Inorganic Materials Research Program
- The Staff and Postgraduates of the School of Physical and Chemical Sciences, Queensland University of Technology
- Members of the Soft Solid State Materials Research Group, University of Queensland

Declaration

The work contained in this thesis has not been previously submitted for a degree or diploma at any higher educational institution. To the best of my knowledge and belief, the thesis contains no material previously published or written by another person except where due reference is made

Surya Subianto
July 2006

Abstract

Conducting polymer is a rapidly developing area of research due to its potential in combining the physical properties of polymers with electrical properties previously found only in inorganic systems. These conducting polymers owe their unique properties to a conjugated polymer backbone and become conducting upon oxidation or reduction.

Melanin, a biopolymer, possess a conjugated backbone required of a conducting polymer, and has shown properties of an amorphous semiconductor. However, there has not been much study done in this area despite its potential, and this is partially due to the lack of processing methods as melanin is generally synthesised as an intractable powder. Thus, a better synthetic method was required, and a possible solution is the use of electrochemical synthesis.

In our previous study we have shown that melanin can be synthesised electrochemically as a free-standing film, which was the first step towards the use of melanin as a bulk material. This project aims to continue from this preliminary work, investigating the various synthetic parameters and possible modifications as well as investigating possible applications for the electrochemically synthesised melanin film.

Table of Contents

Chapter 2. Synthesis and Characterisation – Effect of Synthetic Parameters

Chapter 4. Electrochemically Synthesised Melanin as Light Harvester in Dye-Sensitised Solar Cells

Chapter 5. Conclusion and Future Work

List of Figures

Chapter 1

Chapter 2

Chapter 3

Chapter 4

List of Tables

Chapter 2

Chapter 3

Chapter 4

Chapter 1

Introduction

1.1. Conducting Polymers

1.1.1. Introduction

Traditionally, polymers are regarded as excellent insulators and indeed they are the most widely used material in applications that demands good insulating properties. In most polymers, conductivity is regarded as an undesirable property and can mostly be assigned to impurities or loosely bound protons.

In the last few decades, however, the opposite trend has led to studies done towards the use of polymers as conducting materials. A lot of this research interest is generated by the discovery of Conducting Polymers (CP), which are unique in that unlike traditional polymeric materials, they are intrinsically conducting and do not rely on conductive fillers in order to achieve their conductivity. These conducting polymers can be regarded as a new class of polymer materials which possess novel optical and electrical properties previously found only in inorganic systems.

Conducting polymers are conjugated polymers possessing an extended π-system and highly delocalised electronic states. This extended π-electron conjugation is what gives rise to its electrical conductivity. However, unlike inorganic semiconductors which are atomic solids, conducting polymers are typically amorphous polymeric materials, and so phenomena such as charge transport in conducting polymer can be quite different to those encountered in conventional semiconductors.

The polymers themselves are not new, with many CPs such as polypyrrole and polyaniline being well known in their nonconducting form long before their conductivity was discovered. Indeed, it may be said that the discovery of conducting polymers is not the discovery of the polymer but rather of its unique properties.

The breakthrough came in 1976 when Shirakawa in collaboration with Heeger and MacDiarmid discovered that the conductivity of polyacetylene can be increased by several orders of magnitude by exposure to iodine vapours. This was very unique in that the intrinsic electrical, magnetic, and optical properties of these polymers can be changed

significantly by oxidation or reduction, and this discovery sparked the interest in conducting polymers as a new class of electronic material[1-4]. Nowadays, many different conducting polymers have been developed with a wide range of properties and potential applications (See Figure 1.1).

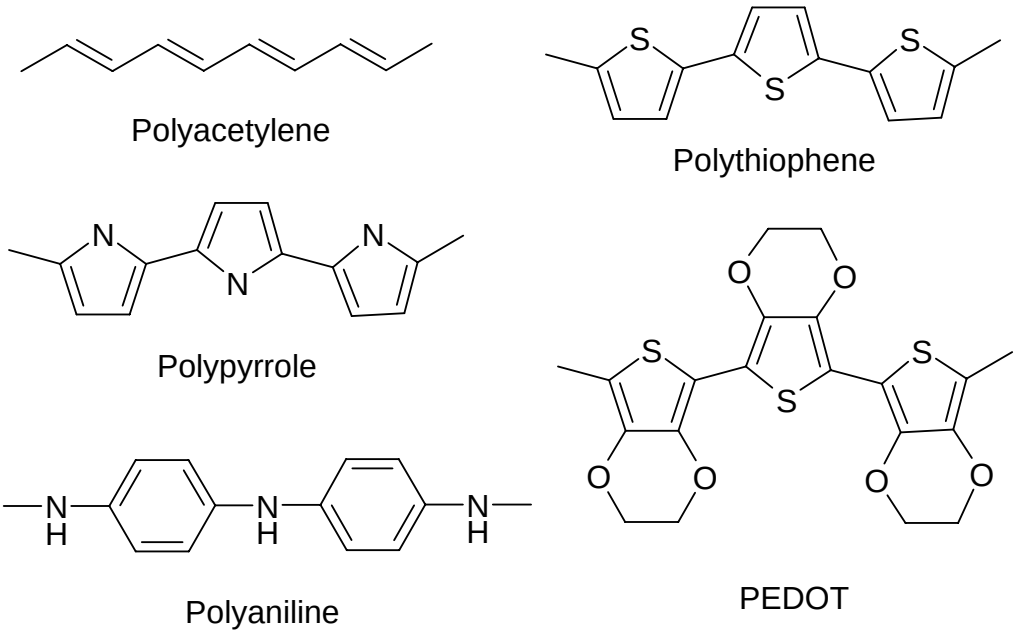

Figure 1.1. Some of the more well-studied conducting polymers

Initially, the most well studied of the CPs was polyacetylene, being the first conducting polymer to have been 'discovered'. However, despite its high conductivity it is also chemically unstable in air, making it unsuitable for use in most applications. Nowadays the polyheterocycles such as polypyrrole, polythiophene, and polyaniline make the bulk of conducting polymer research due to their good stability and ease of synthesis[5, 6]. Other variations of the heterocycles have also been developed, most notably poly(ethylene-dioxy thiophene) or PEDOT which is widely used as solid electrolyte in various applications.

1.1.2. Doping in Conducting Polymer

The concept of doping is the unique, central theme which distinguishes conducting polymers from all other type of polymers[7]. It must be noted, however, that doping in CP is different to doping in conventional inorganic semiconductor in that it is purely a redox

process. The dopant counterion is therefore incorporated to balance the charges created during doping and does not create the charge carriers itself.

There are two types of redox doping, anionic and cationic doping. Anionic doping is when the polymer is oxidised, creating positive charges and therefore a dopant anion is incorporated to balance the charge. Anionic doping is termed p-type doping, in analogy to solid-state physics terminology. Cationic doping or n-type doping is when the polymer is reduced and a dopant cation is incorporated into the polymer matrix. Most heterocycles such as polypyrrole and polythiophene are only susceptible to p-type doping, but some CPs such as polyacetylene or poly(para-phenylene) are susceptible to both p-type and n-type doping.

A non-redox doping also exists in some special cases where the number of electrons associated with the polymer backbone does not change. This type of doping can be observed in polyaniline, where the emeraldine base from of polyaniline can be treated with protonic acids to gain a nine to ten order of magnitude increase in conductivity.

Doping can occur chemically or electrochemically. Chemical doping is achieved by using a suitable oxidising/reducing agent in solution, while electrochemical doping is achieved by applying a suitable electrical potential to the polymer in a suitable electrolyte solution. Chemical doping has the benefit of being a simple and straightforward process, however it can be difficult to control when one tries to obtain an intermediate doping level. Electrochemical doping, on the other hand, is usually applicable only to solid films, but the doping level in it can be precisely controlled by controlling the potential applied to the polymer. Electrochemical doping is often part of the electrochemical synthetic process of CP since the oxidation potential of the CP is lower than that of the monomer, hence the CP is synthesised in its oxidised, conducting form.

Since dopant counterions are incorporated in the polymer in significant amounts, it plays an important part in determining the properties of the polymer. These dopants are generally incorporated into the CPs during the synthesis, however, they may also be

incorporated later through chemical or electrochemical means. The nature of the dopants varies depending on the desired properties of the polymer, and can range from small ions to polymers with ionic pendant groups. The doping level is expressed as the proportion of dopant ion/molecules incorporated per monomer unit, and varies for different CPs and dopants.

1.1.3. Conductivity in Conducting Polymers

Since CPs have an extensive π-electron delocalisation over the length of the polymer chain similar to graphite, one may anticipate that conjugated polymers would behave as a one dimensional metal with a half filled conduction band, as best illustrated with polyacetylene. This, however, is not the case in conjugated polymer.

It appears that for one-dimensional systems, the polymer can more efficiently lower its energy by introducing bond alternations of short and long bonds throughout its length. The direct consequence of bond alternation is that it limits the extent of electronic delocalization along the polymer backbone, with electron delocalisation limited to a small number of monomer units[8]. Therefore there is a periodic modulation of the charge density on the polymer chain with the region of space occupied by the shorter bonds carrying a greater share of electron density. In such systems, the length of the polymer chain does not affect the extent of electron delocalisation in the polymer, so properties directly related to electronic delocalisation such as electronic and optical properties will reach their limiting values at chain lengths much shorter (15-20 multiple bonds) than the overall length of the chain (which can readily exceed 10^4 in some cases). This bond alternation is not present in graphite because of the symmetry and rigidity of its structure.

Bond alternation is a direct consequence of the strong coupling that exist between the backbone skeletal vibrations (phonons) and the π-electrons[8]. A phonon can be described as lattice vibration or a standing wave in the lattice. Although bond alternation means an energy increase due to lattice vibrations, this is more than compensated for by the decrease in electronic energy.

The restriction that bond alternation places on the extent of delocalisation creates an energy gap at the Fermi level, creating a filled valence band and an empty conduction band. This means that all conjugated polymers are large band gap semiconductors, with band gaps generally in excess of 1.5 eV.

In order to make these materials into a conductor, charge carriers must be introduced into the polymer by means of oxidation or reduction, a process commonly known as doping. Based on the concept of traditional semiconducting materials such as silicon, one may expect doping to simply remove electron from the valence band thereby facilitating conduction by free unpaired electrons (and reduction would be the reverse), but it does not explain the fact that the concentration of free spins in conducting polymers is too low to account for the conductivity observed. Furthermore, the concentration of free spins only increases with dopant concentration up to a certain point, and as the doping level increases, it saturates and eventually decreases to undetectable amounts at higher doping levels.

This lack of free spin is related to the nature of the charge in CPs. Unlike traditional semiconductor, the charges in a CP are balanced by a counterion, thus forming an ionic complex with low mobility. This confines the charge to a small section of the polymer backbone, and prevent a full delocalisation of electrons.

There are two types of charge carriers in CPs: bipolarons and solitons. Bipolarons are formed in conducting polymers with non-degenerate ground state structure such as polypyrrole and polythiophene, while solitons are formed in those with degenerate ground state structure, the only known example being polyacetylene (See Figure 1.2). For polypyrrole, a CP with a non-degenerate ground state, the quinoid form is of higher energy compared to the benzenoid form.

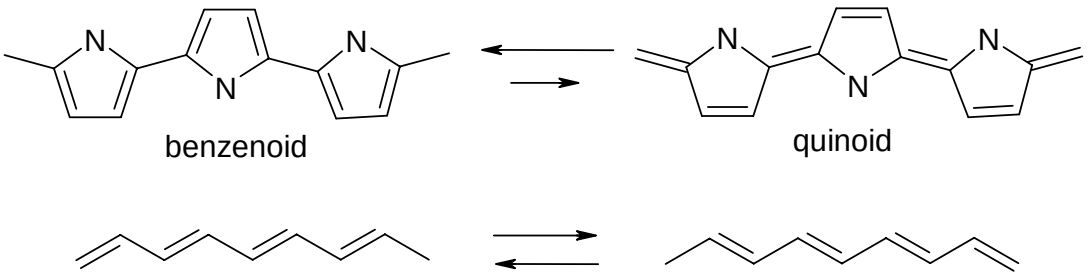

Figure 1.2. Ground state structures of polypyrrole (top) and polyacetylene (bottom)

In polypyrrole, when an electron is removed a cation and a free radical are created which are connected to each other via a local lattice distortion, in this case the quinoid structure of polypyrrole (See Figure 1.3). This radical-cation pair is called a polaron. A polaron has a spin, and its formation creates new localised electronic states in the band gap. Upon further oxidation, another electron can be removed from the polaron, creating a dication which is called a bipolaron. Oxidation can also produce new polarons, but formations of bipolarons are preferred over the formation of new polarons since it produces a larger decrease in ionisation energy. The bipolaron levels are spinless since they are either empty (p-type doping) or fully occupied (n-type doping). At higher doping levels, it is also possible for two polarons to combine to create a bipolaron. Overlaps of the localised bipolaron states forms a continuous bipolaron band, and theoretically, in heavily doped polymers the bipolaron bands will eventually merge with the conduction and valence band, giving metallic-like conductivity.

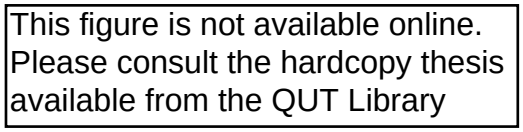

Figure 1.3. Oxidation of polypyrrole[9]

In the case of conducting polymers with degenerate ground state structure (i.e. the two resonance forms are of equal energy), the situation is slightly different. In polyacetylene, the oxidation process is quite similar to polypyrrole in that first a polaron is formed, then another electron is removed from the polaron to form a bipolaron. However, unlike in

polypyrrole, the two cations in the bipolaron are not bound together by high energy bonding configuration and therefore can freely move along the chain (See Figure 1.4). In essence, the charge defects are isolated and do not interact with each other. These defects form domain walls separating two phases of opposite orientation but identical energy (See Figure 1.5). Such defects are called solitons and they can be charged or neutral in nature. In trans-polyacetylene, neutral solitons are also formed naturally as a result of unpaired π-electrons resulting from an odd number of carbon atoms in the polymer chain.

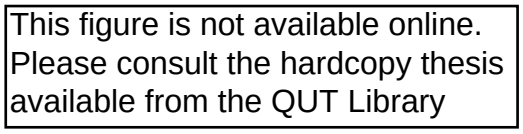

Figure 1.4. Oxidation of polyacetylene[9]

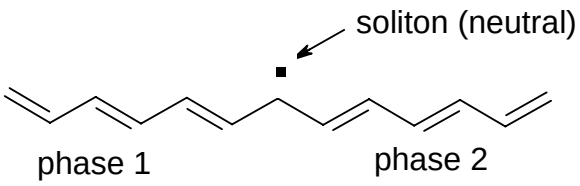

Figure 1.5. A soliton as a domain wall between two phases.

The bipolarons and solitons are mobile defects, and become the charge carrier for conducting polymers. The exact charge transfer mechanism in conducting polymers is still unknown due to its complex structure. However, it is generally accepted that the presence of counterions incorporated in the polymer means that these defects are localised, and the main mechanism involves hopping of charge carrier between the defect sites (see Figure 1.6).

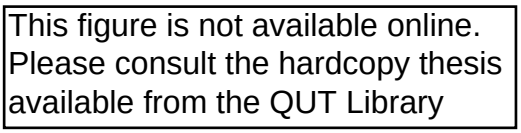

Figure 1.6. Hopping of charge carrier in conducting polymers [9]

The nature of the charge carrier in conducting polymer is also different to that of conventional semiconductor in that they are slow moving, and are present at much higher concentration. Unlike silicon, the polymer backbone can be oxidised until it is saturated with bipolarons resulting in a high number of charge carriers in the polymer. The large number of charge carrier is required for metallic conduction due to the amorphous nature of the polymer and hence the barrier it presents on charge carrier mobility. So if in silicon conduction is a result of fast movement of a small amount of charge carrier (holes or free electrons), conduction in conjugated polymers is a result of the slow movement of a large amount of charge carrier.

1.1.4. Potential Applications of Conducting Polymers

1.1.4.1. Processable conducting materials

Compared to traditional electronic materials such as metals or silicon, polymeric materials offer a much greater degree of control, customisation, and processability[1, 2]. Furthermore, unlike silicon, CPs are less affected by various impurities and thus can be made at a much lower cost, making them an ideal electronic material for cheap, disposable mass produced electronics in the future.

However, because of its conjugated backbone and the ionic nature of the doped polymer, CPs tend to be insoluble and infusible. This raised some doubts as to whether or not suitable processing methods can be developed for these polymers. Nowadays, however, significant progress has been made in the synthesis of processable CPs[10, 11], with several basic approaches. The most widely used methods are side chain functionalisation and dopant induced processing[12, 13].

Side chain functionalisation is perhaps the more traditional approach[14, 15], and has been successfully applied to polythiophenes where an alkyl side chain has been introduced to achieve a solution or melt-processible polymer[16, 17]. Similarly, functionalised side chains can also be used to alter the optical properties of the CP[18, 19].

An alternative is to functionalise the dopant counterion rather than introducing functional groups to the polymer chain itself[20]. By using bifunctional counterions, the dopant can greatly improve the solubility of the polymer. An example is the use of dodecylbenzenesulfonate in conducting polyaniline[1, 21], where the SO_3^- head group forms an ionic bond with the polymer chain, while the hydrocarbon 'tail' remains lyophilic and therefore greatly increases its solubility in organic solvents.

Even though it is unlikely that they can replace traditional metallic materials as conductors, these processable polymers would be of great use in applications such as electromagnetic shielding or lithography resists. Angelopolous et al[22-24] described the use

of polyaniline as discharge layers in electron-beam lithography and also in SEM. The water soluble polyaniline provides a non-destructive masking technique compared to the traditional metal deposition technique, with the applied mask removed simply with a water rinse.

1.1.4.2. Energy Storage and Conversion

In the modern world, energy has become one of the basic necessities of our society. Conducting polymers have attracted a lot of interest in this field due to their versatility and relatively low cost, not only as charge transfer and storage material, but also in solar energy conversion[2, 5, 7, 9, 25-28].

The concept of polymer batteries have great potential in various applications, and conducting polymer film can be used as an electrode material for rechargeable batteries due to their reversible doping[5, 7, 9]. Their main limitation for use in batteries is the fact that very few polymers can be electrochemically reduced (n-doped), thus their use is limited mostly as cathodes in battery system.

Even so, they are an attractive replacement of traditional dry cell cathode materials since they are rechargeable and have higher energy density compared to the MnO_2 based dry cell as well as a wider operating temperature range.

Another application in this field is the use of conducting polymers as electrodes in supercapacitors[29], which require a high capacitance and high discharge rates. Compared with the traditional carbon materials conducting polymers have an increased stability against breakdown from loss of conductivity at higher field strength. The use of conducting polymers also opens the possibility to deposit large area electrodes with low cost and relative ease, while still being able to tailor the material for desired properties.

In the last decade there has also been a rapidly increasing interest in the use of conducting polymer material in solar cells[30-33]. But despite recent progress in the field, there are inherent limitations to conducting polymer materials in photovoltaics. Since the

intermolecular Van der Waals forces in conducting polymers are weaker compared to bonds in inorganic crystals, all electronic states are localised on single molecules. This results in low mobility of the charge carrier and charge transport proceeds by hopping between the localised states rather than transport within a band. Furthermore, the often high degree of disorder found in polymer material aggravates this problem, and as a result it is difficult for CP-based solar cells to match inorganic system in terms of efficiency[9].

While it appears that the inorganic systems would always have the edge in efficiency, conducting polymers remain attractive prospects for photovoltaics due to: the potential of high throughput manufacturing, the possibilities of thin, flexible devices which can be integrated into various appliances or building materials, and also the ability to tailor their optical properties by altering their chemical structure.

The first all polymer p-n junction device was reported by Ozaki et al[34], made with pressure contact of p-type and n-type polyacetylene films. However, due to polyacetylene's instability towards air and moisture, recent efforts have been directed towards more stable polyheterocycles[31, 32, 35-37], particularly when it was discovered that polythiophene can be electrochemically doped with cations[38, 39] (cation doping has not been observed in polypyrrole). However, single layer solar cells of this type generally deliver low quantum efficiencies (less than 1%), focusing research efforts into heterojunction solar cells[40-45] which show better efficiencies.

In heterojunction devices, an electron acceptor and an electron donor are combined together, and some of the best efficiencies (quantum efficiencies of over 50% and power conversion efficiencies of 2-3%) were obtained with fullerene particles (as the electron transport material) dispersed in a conducting polymer matrix (which acts as the hole-transporting material)[9, 46]. This type of heterojunction is called the dispersed heterojunction, since the two materials are blended together rather than layered like a conventional solar cells, and they offer interesting design prospects since there are no restrictions on their geometry other than their overall thickness.

Figure 1.7. Device structure of a heterojunction solar cell utilising Poly (2-methoxy,5-(3',7'-dimethyl-octyloxy))-*p*-phenylene-vinylene (MDMO-PPV) and Phenyl C_{61}-butyric acid methyl ester (PCBM) as the optically active layer[46].

CPs have also been used either as charge transport material or as a sensitiser in Dye-Sensitised Solar cells (DSSC), which will be discussed in more detail in chapter 4.

1.1.4.3. Optical and Photonic Devices

Conducting polymers have great potential as electrochromic material[47-51] since some CPs can be rapidly reduced or oxidised electrochemically with high contrast in the optical properties of the polymer. These colour changes are due to modifications to the polymer's electronic structure upon doping and undoping, which can be controlled by sweeping the potential.

When compared to inorganic electrochromic materials such as liquid crystals, CPs do not represent an improvement as far as switching time is concerned. However, they do offer potential advantages of unlimited visual angle and open-circuit optical memory. Furthermore, being polymers, they have the advantage of conformational flexibility, and the greater variety of colour contrast that can be achieved by tailoring their synthesis[52, 53].

CPs can also be used in electroluminescent devices such as polymer based LEDs[54-56]. These polymer based devices offer significant advantages compared to conventional semiconductors in terms of mechanical properties and geometries. Another favourable aspect of conducting polymer materials is the ability to tailor their spectral range from visible to near infrared within a single family of polymer such as polythiophene.

Furthermore, polymer materials also offer the possibility of obtaining polarised light from oriented polymers, extending the possibilities of fabricating exotic polymer devices.

1.1.4.4. Sensors

Conducting polymers have attracted a lot of interest as a sensor material due their properties being affected by their environment[6, 27, 57-61]. The presence of certain gases, changes in humidity or other environmental variables can cause changes in the electrical properties[62, 63], and these changes can be monitored by various electrochemical means.

Greater selectivity and specificity can be achieved by functionalisation of the polymer. The organic nature of conducting polymer means that various functional molecules can be incorporated into the polymer either as a side chain or as dopants. Changes in these functional molecules would be reflected as changes in the electrical or optical properties of the polymer.

CPs are especially attractive in the field of enzyme-based biosensors[64-66]. This is because biosensors do not require as high an electrical conductivity as other polymer sensors. Also, many conducting polymers can be used in neutral aqueous solutions. There has been significant research in this area, and various enzyme and antibodies has been successfully immobilised in a CP matrix to impart selectivity[58, 64, 65, 67, 68]. This functionalisation capability also extends to living cells, in that intact red blood cells has been successfully immobilised in a polypyrrole matrix[69, 70], and PC-12 cells can be cultured on a polypyrrole composite where cell differentiation can be stimulated by electrically generated release of growth promoters[66, 67].

Another advantage of CPs compared to inorganic materials is in their synthesis. Most CPs can be synthesised electrochemically, which provides better control over polymerisation conditions. The electrochemical synthesis would be a significant complement to the trend towards miniaturisation, since it enables controlled deposition of the material in a small and geometrically complex area, as well as opening the possibility of layered structures.

1.1.4.5. Actuators

Another unique property in CPs is the volumetric changes that accompany the doping process[71, 72]. Due to the nature of the process, the dopant molecule is physically incorporated into the CP and thus a volumetric change occurs upon doping. Since the doping process is reversible, so is the volumetric change, and by controlling the doping state through application of electrical potential a reversible mechanical actuation can be achieved[73-77].

A basic CP actuator was demonstrated by Otero et al[78] who used a bilayer of CP and an adherent, flexible non conducting polymer to achieve mechanical movement (See Figure 1.8). Upon electrochemical oxidation or reduction, the CP layer contracts or expands, promoting an asymmetric strain on the system which results in bending of the bilayer. The magnitude and rate of dopant adsorption determines the distance and speed of the movement achieved by the actuator, and this can be controlled by controlling the applied potential.

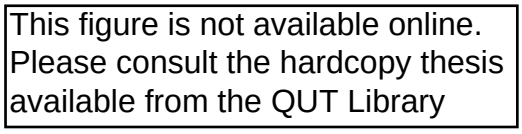

Figure 1.8. Schematic of a bilayer CP actuator[78]

Although studies in this area are still in an early stage, the performance of a conducting polymer actuator was very promising[79-83]. The theoretical performance limit of conducting polymers are much greater than the strongest muscle system in the animal kingdom, and compared to actual muscle fibre a conducting polymer actuator could produce a much greater maximum force with response times an order of magnitude faster[74, 84].

The major drawback of conducting polymer actuators is in the cycle lifetime, with a much shorter effective lifetime compared to muscular tissue. However CP displays have been shown to reach cycle lifetimes of 10^6 cycles[85], and direct comparison with natural muscle is biased by the fact that natural muscles undergo repairs as part of the biological process.

1.1.4.6. Functionalised membrane materials

Conducting polymers are attractive membrane since they offer flexibility in synthesis, and they are a suitable matrix material for many functional molecules which can be incorporated directly onto the polymer backbone or as dopant counterions[86]. Unlike traditional polymers, functionalisation in CP can also be controlled to some degree by the application of electrical potential.

Furthermore, CP can also achieve actuation at molecular levels, offering an interesting prospect for controlled selectivity in membranes[87]. It has been shown that the permeability of certain ions through a CP membrane could be changed by two orders of magnitude under polarisation at different potentials[88-90]. The redox doping can also change the hydrophilicity of the material, changing its water permeability[64]. Despite the excellent separation effect for some system and the possible selectivity switching technical realisation of conducting polymer membranes are rare due to lack of stability and difficulties in synthesising pinhole free materials which are especially important for separations of gases.

1.1.4.7. Drug delivery systems

The reversibility of the doping process in CP offers an interesting prospect for drug delivery systems[91-95]. The reversible doping in CP means that active substances or drugs can be taken up in the conducting polymer, and released into the body by an applied electrical signal. In the past, polypyrrole films have been used in a neurotransmitter as a drug release system into the brain[96].

1.2. Melanin

1.2.1. Introduction

Despite the extensive studies in the field of conducting polymer, there is one common biopolymer which technically fulfils the requirement of being a conducing polymer, but has not received any significant attention with regards to its use as an electronic material.

Melanins are the major pigment present in the surface structure of vertebrates, and are responsible for colouration in animals and some plants. The melanins can be classified as carbonaceous polymers, which is the generic name for dark coloured macromolecular compounds of biogenic and pyrogenic origin and includes humic and fulvic acids as well as oxygen-containing derivative of polycyclic aromatic hydrocarbons.

Melanins can be divided into two groups: pheomelanins and eumelanins. Eumelanins are the black, nitrogen containing pigment of animal origin, and are of higher molecular weight compared to pheomelanins. In humans, eumelanins are synthesised in specialized cells called melanocytes. The melanins are located in the cytoplasm of the melanocyte as distinctive units called melanosomes in which the pigment is synthesised and then deposited onto a protein matrix. Eumelanins are predominantly made of indole subunits, with the major monomer being 5,6-dihydroxyindole (DHI) (See Figure 1.9) with some 5,6-dihydroxyindole-2-carboxylic acid units present.

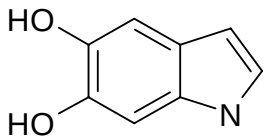

Figure 1.9. 5,6-Dihydroxyindole

Pheomelanins are the lower molecular weight, nitrogen and sulphur containing polymer which are generally yellow to red in colour. Unlike eumelanins, pheomelanins consist mainly of benzothiazine units, with some of those degraded into benzothiazoles.

1.2.2. Melanin Formation

In nature, eumelanins are made by the oxidation of the amino acid tyrosine with the enzyme tyrosinase, and the subsequent autooxidation of dopa (See Figure 1.10). Tyrosine is first oxidised to dopa by the enzyme tyrosinase, followed by the autooxidation process of dopa into melanin. When dopa is oxidised into its quinone form, it becomes susceptible to intramolecular Michael addition, resulting in spontaneous cyclisation into dopachrome. Tautomerisation of dopachrome yields leucodopachrome, and the final oxidation process results in the monomer, 5,6-dihydroxyindole (DHI).

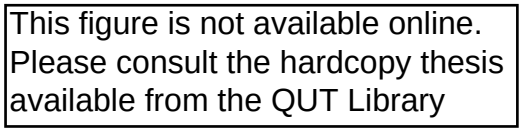

Figure 1.10. Raper-Mason Scheme of melanin formation[97]

In some cases the carboxylic acid group may not leave and therefore there are also some 5,6-dihydroxyindole-2-carboxylic acid (DHICA) formed. DHICA formation is much less

than DHI, however some researchers suggest that the balance between the two can be controlled by the presence of transition metal ions[98, 99].

In the laboratory melanin is generally synthesised chemically by the auto-oxidation of dopa in alkali solution using suitable oxidizing agents such as air or hydrogen peroxide. Dopa is often used in place of tyrosine because selective oxidation of tyrosine can be difficult to achieve without the enzyme. A typical melanin synthesis involves bubbling oxygen through an alkali aqueous solution dopa for several days, and after all the dopa has been oxidised the melanin is precipitated by the addition of acid and extracted as powder by filtration. Commercially available melanin powder, however, is synthesised by the autooxidation of tyrosine by hydrogen peroxide in the presence of tyrosinase. In the case of pheomelanins, the synthesis generally follows similar procedure to eumelanins, however cysteine-dopa is used as the precursor instead of dopa.

1.2.3. Structure of melanin

The chemical structure of melanin is not yet fully known, but several models have been proposed with the basic structure being covalently linked units of dihydroxyindole. The first structure was proposed by Mason[97], with DHI units bonded regularly through the 2,3 or the 4,7 position (See Figure 1.11).

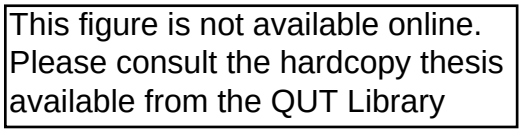

Figure 1.11. Model of melanin structure proposed by Mason[97]; left: linked through the 2,3 position; and right: linked through the 4,7 position

However, Nicolaus[100] and Swan[101] proposed a different model where the monomer units are randomly linked (See Figure 1.12). The main feature of the Nicolaus models is a strong heterogeneity, with the dihydroxyindole units being able to form bonds at the 2,3,4, and 7 positions making it unlikely that it will form a simple linear chain. Furthermore, although the polymer appears to be based on indolic units other pre-indolic products of the synthetic pathway may also be present as well as some pyrollic units, further adding to the heterogeneity of the system.

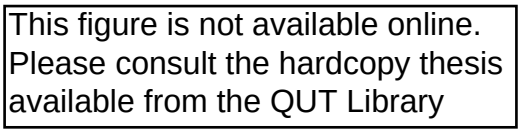

Figure 1.12. The Nicolaus model of melanin structure with randomly linked DHI units[100, 101]

Currently the Nicolaus model is the most widely accepted, however it was also thought that the oligomers can form a planar, macrocylic structure[102], giving rise to the 'stacked island' model proposed by Zajac et al[103]. In this model, planar oligomers may be stacked by Van der Waal's interaction giving layer spacing of about 3.4 A (See Figure 1.13), but the irregular interposition of other residues make the polymer essentially amorphous.

Figure 1.13. The 'stacked island' model of melanin structure[103]

Depending on the pH, the monomer unit, DHI, can exist in different oxidation states (See Figure 1.14). The oxidation states are pH dependent, with the hydroquinone dominating at lower pH and the quinone at higher pH. This means that, depending on its oxidation state, melanin can act as an electron donor or acceptor (See Figure1.15).

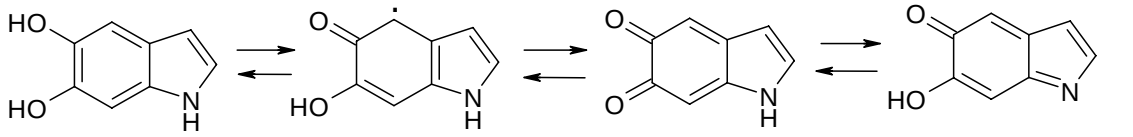

Hydroquinone (quinol) Semiquinone Quinone Quinone-Imine

Figure 1.14. The various oxidation states of DHI

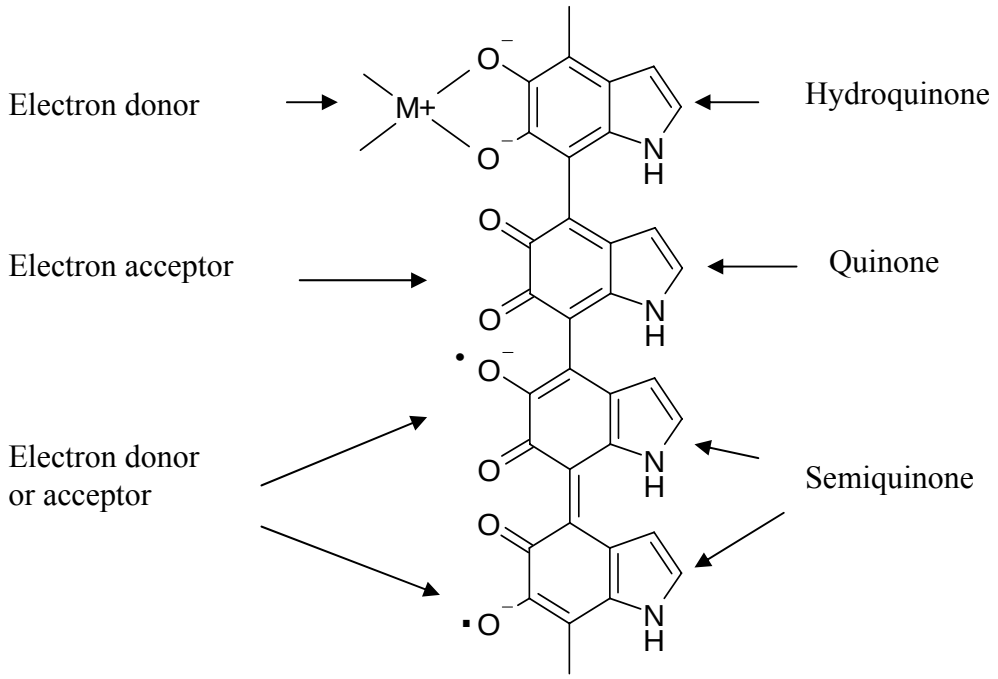

Figure 1.15. Melanin as electron donor or acceptor

Natural melanins are quite complex due to addition of various proteins and metal ions to the polymer, but in general synthetic melanin made from dopa are regarded as a good model for their natural counterpart[104]. Several studies have found that natural and synthetic melanins are quite similar in properties and structure. It must also be noted that the differences may be due to the presence of residual proteins or other organic matter as well as the isolation procedure for natural melanin.

One of the significant differences between synthetic and natural melanin is in their conductivity value, in which synthetic melanin has a far higher conductivity compared to melanin isolated from natural sources. This is understandable since conductivity, assuming similar conduction mechanism to other conducting polymers, would depend on how ordered the structure of the polymer is and harsh isolation procedure and the extra defects caused by proteins in the polymer matrix are likely to lower the conductivity of natural melanin.

1.2.4. Biological functions of melanin

Even after years of investigation, the role of melanin is still not yet fully understood. Melanins are found all over the body from the skin and blood plasma to the nervous system, but the role of melanin in all these different systems is not clear. However, some biological functions have been postulated[105-109], with the main one being photoprotection[110-112].

Melanins absorbs very strongly in the UV-visible region of the electromagnetic spectrum. Large melanosomes in biological systems are very potent shield against UV radiation, and is the reason why Caucasians are more prone to develop skin cancer compared to Negroid and Mongoloid where melanin granules are produced in large quantities and are concentrated on top of the nucleus of the keratinocytes in the basal layer of the epidermis[106].

This visible absorbance is due to the extensive conjugation on the polymer backbone, while the UV absorbance is attributed to the carbonyl groups present in the quinone form of the monomer unit. It is widely accepted that that melanin in human skin plays a crucial part in protecting the nuclei of epidermal cells from damage by solar radiation. The melanin in the eye may also serve a photoprotective role, but their overall biological activity in this regard is still not very well understood. It has been observed, however, that there is a significant change in retinal melanin upon overexposure to blue light.

Although most people know melanin only as a sunscreen, it also plays a part in the thermoregulation system where absorbed solar radiation is converted into heat. In mammals, the heat is then dissipated between hairs or capillary blood vessels. This is evident in that the dermal vascular network in dark-skinned people are up to four times more developed compared to caucasians[106].

Melanin has also been attributed to strengthening of structures through cross-linking of proteins. By doing this, melanin supply mechanical strength and may protect the protein

from degradation. Melanisation of seedpods confers increased rigidity, as does the browning of fruits in response to surface injuries[106].

Melanins also have powerful cation chelating properties through the carboxyl and the deprotonated hydroxyl groups[113-115]. They also possess reactivity towards nucleophilic groups such as thiols and amino groups which gives them potential antibiotic properties. Some have speculated that melanin may have acted as an antibiotic in insects and cephalopods, and it is may also function as a chemoprotective agent by acting as a free radical sink[116] or as a means of binding potentially toxic substances[117, 118].

The free radical nature of melanin[119-123] means that melanin can act as a free radical sink, protecting the body against free radical damage. This function of melanin may play a part in our nervous system. Melanin is what gives our brain its greyish colour, but its role in the nervous system is still unclear.

The free radical nature of melanin also gives rise to hypothesis regarding the toxicity of melanin. Some researchers have shown that cells containing small amounts of melanin are more susceptible to damage from irradiation. This observation has been linked to the iron content of melanin[124-126], in that when melanin is saturated with transition metal ions such as iron it may actually produce free radicals and therefore accelerate cell death rather than protecting it.

1.2.5. Melanin as a conducting polymer

Since melanin is made of covalently linked dihydroxyindole units, it fulfils the main requirement of a conducting polymer: a conjugated polymer backbone. In this case, one may expect that melanin would behave similarly to conducting polymers such as polyindole.

Indeed, melanin has been regarded as an amorphous semiconductor as early as 1974, when a paper was published in *Science* describing the amorphous semiconductor switching in melanin[127]. In that paper McGinness showed that melanin exhibited

threshold switching, a property that until then has only been observed in inorganic systems. The observed switching was also reversible and therefore is not a breakdown of the material, and the potential gradient required was also two or three orders of magnitude lower than reported for inorganic thin films and is comparable to gradients existing in some biological system.

In 1982 Strzelecka[128, 129] published two papers regarding the semiconductor properties of melanin and also a band model for synthetic dopa melanin. She studied the IV characteristic of melanin extracted from bovine eye, dark human hair, and banana peel as well as synthetic dopa melanin.

In that study, the conductivity of the natural melanin was found to be in the order of 10^{-11} S cm while the synthetic melanin showed a greater conductivity in the order of 10^{-8} S cm. This difference in the conductivity value of natural and synthetic melanin is most likely caused by greater heterogeneity in natural melanin due to the presence of various proteins in the material. Furthermore, extraction of natural melanin requires harsh extraction and isolation procedure which may have damage or alter the polymer structure, thereby affecting its conductivity.

Osak[130] followed up on this study with another investigation of the IV characteristics and electrical conductivity of synthetic eumelanin, and concluded the presence of traps in the melanin polymer.

Jastrzebska et al[131] studied the dark and photoconductivity of synthetic pheomelanins, and she reported a dark conductivity value in the order of 10^{-11} S cm, similar to what was previously reported for natural melanin. The lower conductivity of pheomelanins may be caused by extra disorder in the structure of the material due to the presence of benzothiazine, therefore lowering its conductivity value. Furthermore, unlike eumelanin, pheomelanin may not be conjugated, as for conjugation to occur the benzothiazine units need to be bonded through the already crowded benzene ring due to the lack of an indolic

moiety in pheomelanin. It must also be noted, however, that the pheomelanin also exhibited photoconductivity.

Another study regarding the photoelectronic properties of melanin was done by Rosei et al[132] who studied synthetic dopa-melanin suspension. They concluded that melanin can be described as a network of nanometre-sized conjugated clusters[133], where photogenerated electron-hole pairs undergo either germinate recombination or dissociation depending on the photon energy.

Jastrzebska et al[134] also published a later study regarding the conductivity of melanin for different hydration states and temperature, and found that the conductivity in melanin is highly dependent on humidity, with changes of 8 orders of magnitude from 10^{-13} up to 10^{-5} depending on the relative humidity.

They have also observed the presence of two parts of water in the 'dry' melanin sample, with the presence of water adsorbed on the surface and also in the molecular structure. It was postulated that the water molecules may be present between the layers composed of planar indole-quinone monomer units. The presence of tightly bound water molecules may be due to hydrogen bonding with the hydroxyl or quinine groups present on the monomer unit.

1.3. Rationale for this research project

As mentioned before, much of the work on melanin has been done on its biological function and little has been done regarding its use as a bulk material until recently[135]. However, despite this lack of research interest, melanin is an attractive material for conducting polymer applications for several reasons:

- Being a natural photoprotective agent, it is very stable chemically and photochemically
- It is a biopolymer, and thus offer potentially the ultimate in biocompatibility

- Melanin can be synthesised from relatively non-toxic chemicals and in aqueous solution using simple processes.

In order for melanin to be of use as a conducting polymer material, one of the main requirements is that a better synthetic method is found. The currently used method of chemical synthesis results in the formation of melanin powder, which is insoluble in most solvents except in highly alkaline aqueous solutions. The answer to this processability problem may lie in altering the synthetic process itself, rather than post-synthetic process of the intractable polymer.

Electrochemical polymerisation has often been the method of choice in the synthesis of conducting polymer due to the control and ease that it afforded. It can give polymer films with excellent quality and controlled properties. It is often preferred over chemical polymerisation because it offers several advantages, such as:

- Greater control over the polymerization process – the polymerization rate can be controlled quite precisely by controlling the applied potential and current flow
- The polymer is deposited as a film on the electrode, removing the need for post-processing
- Doping occurs during synthesis

Furthermore, although melanin has been widely investigated in the past, most studies regarding the electrical properties of melanin have been done on chemically synthesised samples. In this case, the chemically synthesised melanin powders would be dried and then pressed into pellets for measurements. Since it is quite likely that the conductivity would depend to some extent on the crystallinity of the polymer, these measurements may not represent the true properties of melanin because the amount of pressure applied to make the pellets may have damaged the polymer structure. Thus, compared to chemically synthesised powders electrochemically synthesised melanin films may better represent the bulk electrical and physical properties of this material, as well as having

better electrical properties since it is not subjected to the same harsh treatment post synthesis as its chemically synthesised counterpart.

In our previous study[136] we have shown that electrochemical synthesis can be used to synthesise not only thin films but also thicker, free standing films of melanin which was the first step in the investigation of the use of melanin as a bulk material. In that study we showed some initial results that suggests that the melanin free standing film synthesised was chemically different from dopa and was similar to a commercially available melanin sample. However, the investigation was preliminary, and was concerned mainly with the electrochemical synthesis of the material, with little characterisation of the material and no further study into possible applications.

This project aims to build on the basics established in our previous work, and investigate further into the properties of this material as well as investigating possible applications for electrochemically synthesised melanin.

Chapter 2

Synthesis and Characterisation: Effect of Synthetic Parameters

2.1. Introduction

2.1.1. Electrochemical Synthesis of Conducting Polymers

There are two main methods used in the synthesis of conducting polymers: chemical and electrochemical polymerisation. Although chemical methods have the advantage of potentially lower mass production cost, electrochemical synthesis offer the possibility of in-situ formation, removing all the cost and trouble of post-processing. Furthermore, in the case of polyheterocycles such as polypyrroles it also creates material with better conducting properties compared to chemical methods.

The principle of electrochemical synthesis involves the use of an electrical current through a solution containing the monomer and an electrolyte in order to generate radical cations that would react to form the polymer. Since the polymer is deposited as a continuous layer on the anode surface, electrochemical polymerisation is often utilised in the synthesis of conducting polymer in applications that require thin film electrodes such as sensors or energy storage/conversion.

Another main advantage to electrochemical synthesis is the direct control over the polymerisation reaction. The applied potential controlled the thermodynamics of the reaction, whereas the reaction kinetics depends on the rate of charge transfer and therefore is determined by the electrical current. Also, the film thickness is dependent on the amount of charge employed in the process, and therefore can be controlled by the polymerisation time.

Unlike chemical synthesis, electrochemical synthesis does not usually require the use of a catalyst, with the reaction driven by the applied potential. The main requirement of an electrochemical polymerisation solution other than the monomer is the electrolyte, which serves to impart sufficient conductivity to the solution. Furthermore, the polymer is generally deposited as a solid film on the electrode surface, which simplifies the synthetic process since no specific extraction or purification step is required.

In chemical synthesis the newly formed polymer generally has to be doped after synthesis, but in electrochemical synthesis the conducting polymer is synthesised in its doped, conducting form, with the electrolyte in solution incorporated as a dopant. This results from the oxidation potential of the polymer being lower than that of the monomer, and therefore the potential applied to form the polymer is also sufficient to oxidise it.

Electrochemical syntheses are addition polymerisations, where the initial step is the generation of a radical cation. The next step is widely believed to be a coupling of two radical cations to produce a dihydrodimer dication which becomes a dimer after aromatisation by the loss of two protons. This radical-radical coupling reaction would predominate over an attack by a radical cation on a monomer molecule since on the electrode surface the concentration of radical cations would be greater than that of the monomer molecule.

Since the dimer is more easily oxidised than the monomer due to the stability of its radical cation, the dimer is further oxidised and undergoes further coupling with a nearby radical cation. The reaction proceeds in this fashion until termination either when the radical cation of the growing chain becomes too unreactive, or when the reactive end of the chain becomes sterically hindered from further reaction.

In an electrochemical synthesis, there are several basic parameters that need to be considered[137-149]: applied potential, electrode material, electrolyte, and solvent.

Applied potential

The electropolymerisation reaction can be done potentiostatically or galvanostatically, or by application of potential/current sweeps or pulses. It is important that the applied potential is controlled as to provide sufficient potential for monomer oxidation while minimising side reaction or degradation due to over oxidation.

The applied potential also directly controls the current flow, and hence the rate of film formation. Thus it needs to be controlled to provide an efficient polymerisation rate, while minimising undesired side reaction and also gas formation as they often have detrimental effects on the morphology of the polymer.

Electrode material

Since the polymer is produced by an oxidative process, it is important that the material used for the electrode does not passivate or corrode at the required potential. For this reason the anode is usually made of inert materials such as platinum, gold, stainless steel, glassy carbon or conducting glass electrodes.

Electrolyte

The main requirements for a suitable electrolyte are its solubility in the solvent of choice and the reactivity of its anion and cation. The electrolyte needs to be sufficiently inert as to not undergo oxidation/reduction at the potential used for the electropolymerisation. As it is also incorporated in the final polymer as the dopant, the choice of counterion can affect the properties of the resultant polymer.

Solvent

Solvents have a very strong influence both on the mechanism of electropolymerisation and on the properties of the resultant polymer. The solvent need to be stable at the electropolymerisation potential, and it also needs a high dielectric constant to ensure the ionic conductivity of the electrolytic medium.

2.1.2. Electrochemical Synthesis of Melanin

Although electrochemical analysis has always been one of the main methods used in the investigation of dopa and other cathecols, it has not been widely thought of as a method of synthesis. The possibility of electrochemically synthesised melanin has been hinted at as early as 1974, when Brun et al[150] investigated the electrochemical characteristics of dopa and found that in alkaline pH the current decreases after repetitive cycles. However, they did not observe any deposit on the electrode, presumably due to the fact that they

only oxidised the solution for a short period of time. After that, the first direct reference towards the electrochemical polymerisation of melanin was in an abstract by Zielinski et al[151] in 1990. Zielinski claimed to have synthesised a thin film of melanin electrochemically, but was not followed by a full paper and no details were available regarding the actual study.

The first paper published on the oxidative electrochemical synthesis of melanin was by Horak et al[152] in 1993, who accidentally oxidised DAI to form melanin on an electrode surface by means of cyclic voltammetry. The effect of parameters such as scan rate, solution pH, concentration, and potential range were studied, and it was found that repeated scanning using fast scan rates seems to be ideal for thin film formation, demonstrating that once the oxidation occurs, the polymerisation process is quite rapid.

In this study, cyclic voltammetry was preferred over static scans because it seemed to result in better film formation. They postulated that this is because the film was deposited layer by layer, with each layer undergoing an oxidation and reduction cycle which was beneficial for the mechanical properties of the film.

However, in their study synthesis of free standing films was not achieved which they believe is due to the fact that thicker films prevent diffusion of the electrolyte. Indeed, another similar study with DHI also showed that the electrode is passivated with the cyclic voltammetric deposition of melanin[99].

The resultant polymer was found to be insoluble in aqueous or organic solvents including DMSO, which means that the polymer cannot be easily processed post-synthesis by traditional methods such as spin-casting. In contrast, it has been shown that chemically synthesised melanin can be spin-casted from certain solvents like DMSO[153].

Later, Gidanian et al[99] used the method reported by Horak et al[152] to investigate the effect of copper and zinc on the electrochemistry of melanin films. They found that the presence of copper or zinc ions alter the DHI/DHICA ratio in the final polymer, which

was attributed to complexation of the intermediates. The exact mechanism is still unknown, but it may be related to the action of the enzyme tyrosinase (catalyst for melanin synthesis in mammals) which is also a copper complex. Another thing to note is that similarly to Horak et al, Gidanian et al also claimed that the polymer films formed are mechanically stable and are insoluble in all the solvents tested.

Robinson et al[154] also electropolymerised melanin thin films, but they used l-dopa as the starting material rather than DAI. Like the other publications on electropolymerised melanin, electrochemical analysis methods such as cyclic voltammetry were used to investigate the electrooxidation process. In this paper, the different steps in the oxidation of dopa were studied in detail relative to their oxidation potential. However, this study was concerned mainly with the oxidation process, with no structural analysis or further characterization of the film.

In another study, Serpentini et al[155] investigated the redox properties of dopa melanin by incorporating chemically synthesised melanin into a carbon paste electrode. Although their study was done on chemically synthesised melanin, the use of carbon paste electrode meant that the melanin was present in thin layer condition and not in solution like conventional electrochemical analysis. Their study showed that only the monomer units on the surface are involved in electron exchange, thus ruling out a regular conjugated DHI arrangement and suggesting a compact structure with randomly linked monomer units.

Rubianes et al[156] used dopa-melanin as an electrode modifier to impart selectivity towards the electrode. In this study, dopa-melanin was incorporated into a carbon paste electrode by means of potentiostatic electrochemical oxidation of dopa in phosphate buffer. The resultant polymer film exhibits selectivity, strongly rejecting negatively charged species while allowing cationic species to pass through and be oxidised at the electrode. The method used in this study was based on that of Robinson et al[154], with potentiostatic oxidation of l-dopa in an air-saturated buffer solution.

Of the two melanin precursor (dopa and DHI), dopa is the one that is more widely used due to its commercial availability and cheaper cost. However, since it requires more oxidation steps to form melanin, the polymerization is not as efficient, as was indicated by Horak et al[152] in their paper. Theoretically, DHI would provide a more homogenous film and faster synthesis because the intermediate would not have sufficient time to diffuse away from the electrode, and the film would be more homogenous as it would not contain DHICA or any other intermediate of dopa oxidation.

These works were aimed at the synthesis of thin films, with suggested synthesis conditions of fast scan rate and low monomer concentration to be ideal. Although thin films are sufficient for applications such as coatings and electrode modifier, it would be difficult to study the morphology and electrical properties of those thin films in detail. Also, the surface effect is much greater in thin films and at the moment it is unknown whether the surface properties of the polymer differ to that of the bulk. This is a possibility because the polymer can exist in several oxidation states, so the surface which is exposed to air or light may be in a different oxidation state than the bulk.

2.1.3. Melanin from Organic Solvents

In the electrochemical synthesis of conducting polymers, organic solvents are much more widely used compared to aqueous solvents since they produce films with better electrical and mechanical properties.

In the case of melanin, most past studies have been done exclusively on aqueous systems due to the requirement of an alkaline pH for the reaction. Recently, however, it has been demonstrated by Deziderio et al[153] that melanin can be synthesised from organic solvent. In their work, a DMSO/DMF solvent system was used in the chemical synthesis of melanin, producing a suspension which could then be spin coated onto substrates. However, we found that our electrochemically synthesised melanin appeared to have lower solubility than its chemically synthesised counterpart, as was found by Horak[152]. Our attempt at the use of DMSO as a solvent was unsuccessful, and no film formation was observed.

2.1.4. Characterisation of Melanin

2.1.4.1. Cyclic Voltammetry

The electrochemical synthesis of conducting polymers has been well studied with various electroanalytical means. One of the most prominent is Cyclic Voltammetry (CV), due to its ability to rapidly provide information on the thermodynamics of redox processes and kinetics of heterogenous electron transfer reactions[157-161].

In the case of dopa oxidation, the initial step involves the oxidation of dopa into dopaquinone accompanied by the loss of two protons and two electrons. The study by Brun et al[150] claimed that this reaction occurs at 0.82 V vs SHE (in a 0.1M $HClO_4$ solution).

According to the Raper-Mason scheme, the dopaquinone is then subjected to an intra-molecular Michael addition where it cyclises into leucodopachrome, which then rearranges into dopachrome. The dopachrome is then further oxidised into DHI and then into indolequinone which polymerise into melanin. These subsequent steps occur spontaneously since the potential required for the subsequent oxidation steps are lower than that of dopa oxidation[161].

Based on previous study on DHI by Gidanian et al, the DHI oxidation into melanin occurs at around 0.15 V vs Ag/AgCl. However, in our study where dopa is used as the precursor the DHI oxidation is not likely to be observed since they are likely to be masked by the initial oxidation step.

2.1.4.2. Solid-State Nuclear Magnetic Resonance Spectroscopy

Melanin, being insoluble in most organic solvent, has not been widely analysed by solution-phase NMR. However, since solid-state NMR does not require the use of a solvent, it can be used to analyse melanin without using a highly alkaline solution.

Indeed, most published studies concerning NMR of melanin has been done using solid-state rather than solution phase NMR.

Duff et al[162] investigated the structure of synthetic and natural melanin by this technique, comparing chemically synthesised dopa-melanin with natural melanin extracted from squid ink (S*epia Officinalis*) and malignant melanoma cells. Investigation of the ^{13}C and ^{15}N spectra showed resonances consistent with known pyrrolic and indolic structure within the heterogenous biopolymer. However, the ^{13}C spectra also indicated that there are aliphatic residues remaining in the polymer, presumably from unoxidised dopa. They concluded that synthetic melanin is similar in structure to natural melanin, with the same structural features present in the solid-state NMR spectrum. They also observed significantly higher aliphatic carbons in the natural melanin, which was attributed to proteins present in the natural melanin. This result was supported by a latter study by Reinheimer et al[163] who used selectively labelled ^{13}C DHI melanin in their study.

A similar study was done by Katritzky et al[164] who investigated natural melanin by ^{1}H NMR. They also found aliphatic peaks to be present, however since they only studied natural melanin these aliphatic peaks could also be due to the presence of proteins. They also proposed a tentative structure of a 4-unit fragment of Sepia melanin based on the empirical formula and the ratio of aromatic protons to non-aromatic ones.

2.1.4.3. X-Ray Photoelectron Spectroscopy

X-ray Photoelectron Spectroscopy (XPS) (also known as Electron Spectroscopy for Chemical Analysis or ESCA) has been proven to be quite a powerful tool in the analysis of polymers because it is capable of obtaining information regarding the core and valence levels of any elements regardless of nuclear properties such as magnetic moments. It also has the benefit of being able to analyse involatile and insoluble solid state material, which is very beneficial in the analysis of polymers.

XPS utilises the photoelectric effect where the absorption of X-Ray by the surface layer of the sample leads to the ejection of an electron from one of the tightly bound core

levels. The emitted photoelectron is analysed, and since the excitation energy is known the binding energy of the photoemitted electron can be found by subtracting the kinetic energy of the photoelectrons from the energy of the exciting X-ray photons.

The use of XPS in the study of melanin was first demonstrated by Williams-Smith et al[165] in 1976 who investigated various natural and synthetic melanin. Their study showed that the nitrogen in melanin is most likely present in an indolic structure rather than a primary amine, supporting the notion that melanin is made of dihydroxyindole units. However, their work was preliminary and also focused on sulphur-containing natural melanins, with little information on synthetic melanins.

A more in depth study published by Clark et al[166] compared natural melanin (extracted from *Sepia Officianalis*) with synthetic melanin chemically synthesised from various precursor including dopa, DHI, DHICA, and N-Me-DHI. They discovered that in terms of elemental composition and functional group distribution, the dopa-melanin is quite close to the natural melanin, however, the other synthetic melanins showed some differences in these areas. This was most likely due to the fact that dopa melanin is a more heterogenous polymer compared to DHI or DHICA melanin, and therefore more closely resemble natural melanins which are biosynthesised from tyrosine.

The melanins were also found to have more carbonyl functions compared to what would be accounted for by the monomer units, which indicated that other oxidation process has occurred, or that there was some water present in the structure. The incorporation of water in the eumelanin microstructure may account for the presence of the higher oxygen count especially in the DHI melanin, which theoretically should consist only of DHI although some degradation products are also possible[167].

However, for water to be present it needs to be quite strongly bonded to the polymer due to the ultrahigh vacuum used in XPS. This would indicate that there may be two types of water present in the polymer, in that there may be tightly-bound water incorporated within the polymer structure itself. Furthermore, they also discover some evidence of

quinone, cyclohexadione, and carboxylic acid group which indicates that the monomer units of melanin exist in various oxidation states.

2.1.4.4. Scanning Electron Microscopy

Scanning electron Microscopy (SEM) has been widely used in investigating the morphology of various polymers. In the case of melanin, Nosfinger et al[168] studied natural and synthetic melanins, and found that they exhibit a granular appearance. The natural melanin consisted of aggregates of small, spherical particles while the synthetic melanins appeared as an amorphous solid with no discernable structure. The synthetic melanins showed a rough, granular surface, but without a well-defined substructure like the spherical ones observed in natural melanins.

Later, Liu et al[169] studied the effect of sample extraction and preparation of natural melanin, and found that the sample drying method has a significant impact on the morphology of the polymer. Initially, extracted squid ink powder of sepia melanin was observed as semi-spherical or nearly doughnut shaped particles which at higher magnifications was revealed to be made of spherical granules, which was consistent with previous observation by Nosfinger et al[168].

At first it was thought that the spherical structure may have been an artefact of the drying process as the different methods resulted in different morphology. Large micron-sized spheres were observed in the spray-dried sample, while the air dried sample showed a thin layer of deposited melanin and the freeze dried sample showed rod-like aggregates. In a sample dried with supercritical CO_2, the observed macrostructure was that of a porous aerogel with no real structured aggregates. However, in all these cases, the microstructure of the melanin sample remains the same, in that they all consist of small melanin granules about 150 nm in size, which correspond to the melanin granules synthesised in the melanosomes. Thus it would appear that while the bulk structure of the polymer is highly dependent on the drying process, the underlying granular structure of natural melanin remains unchanged.

2.2. Experimental

2.2.1. Electrochemical Synthesis

All chemicals were purchased from Sigma-Aldrich and were used as received. Electrochemical oxidation of dopa was performed in a two electrode setup, with the potential referenced to the counter electrode. The anode material used was Fluorine-doped Tin Oxide (FTO) conducting glass (100 Ω/cm), while the counter electrode used was copper or stainless steel. Copper sheet was used as a contact between the alligator clip and the FTO working electrode, while in the case of the counter electrode the wire was soldered directly onto the metal. Due to the nature of the power supply used, an external reference electrode was not used, and the applied potential was measured relative to the counter electrode.

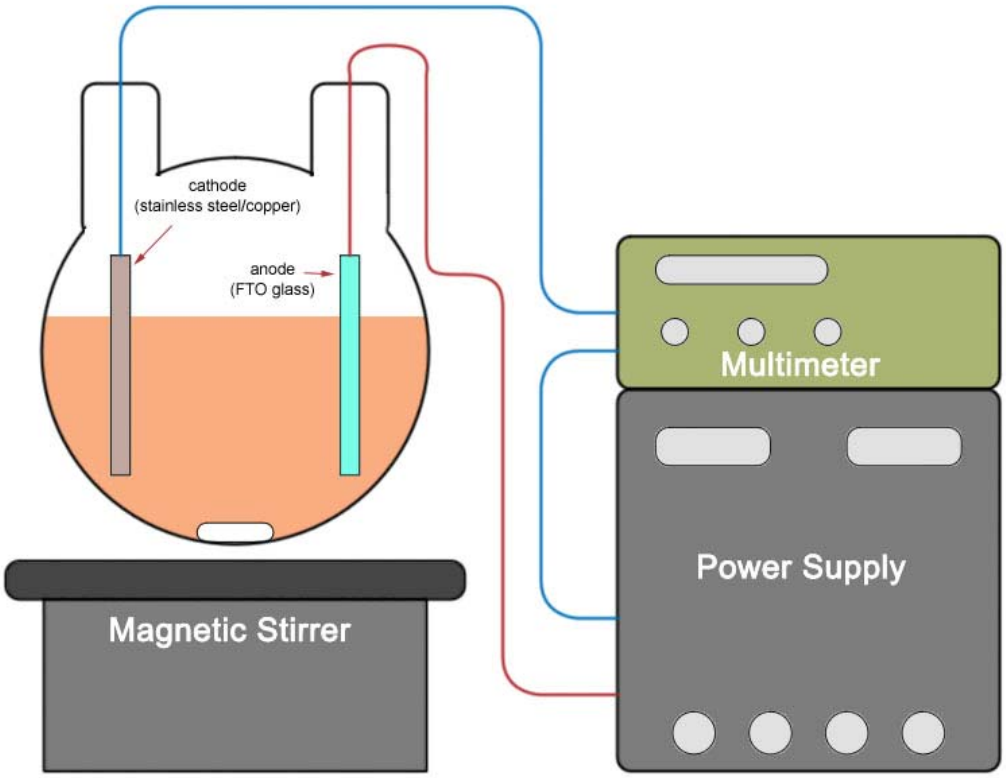

Figure 2.1. Electropolymerisation setup for the synthesis of melanin free-standing film

The setup was then connected to a Thandar power supply with a fluke 8050 A multimeter used to measure the current flow. In the case of borax buffer, the solution was first

preoxidised at 5-10 mA/cm^2 for 20 minutes with vigorous stirring before the stirrer was turned off and the current density brought back down to the polymerization current density of 0.5 mA/cm^2. The oxidation was carried out for 7-10 days, after which the film was taken out together with the FTO electrode and washed by several immersions in deionised water, and then extracted from the electrode surface with a scalpel.

The resultant film was then put onto a Teflon sheet and kept inside a desiccator for drying. The air in the desiccator was kept moist for the first 3 days in order to slow down the drying process. The final dried film was then kept in a desiccator in the dark.

2.2.2. Electrochemical Analysis

Cyclic Voltammetry experiments were carried out with a Princeton Applied Research 273A Potentiostat/Galvanostat running a PowerSuite software package using a three electrode setup. A platinum wire was used as the working electrode and a platinum flag was the counter electrode. The reference electrode used was silver/silver chloride (Ag/AgCl) electrode or Standard Calomel Electrode (SCE) as specified. The solutions were not degassed unless otherwise stated. Dopa solutions were made by dissolving dopa in minimal amount of 0.1 M buffer solution and making it up to the mark with deionised water.

Conductivity measurements were performed by sandwiching the polymer film in between two pieces of FTO conducting glass electrodes (100 Ω/cm). The sample was then put in a desiccator to obtain a constant environment, and the conductivity was measured by means of an IV curve. The potential was applied through a Princeton Applied Research 273A Potentiostat/Galvanostat in a two-electrode setup with the reference connected to the counter electrode. The IV curve was recorded repeatedly until no further change was observed before the measurement was taken.

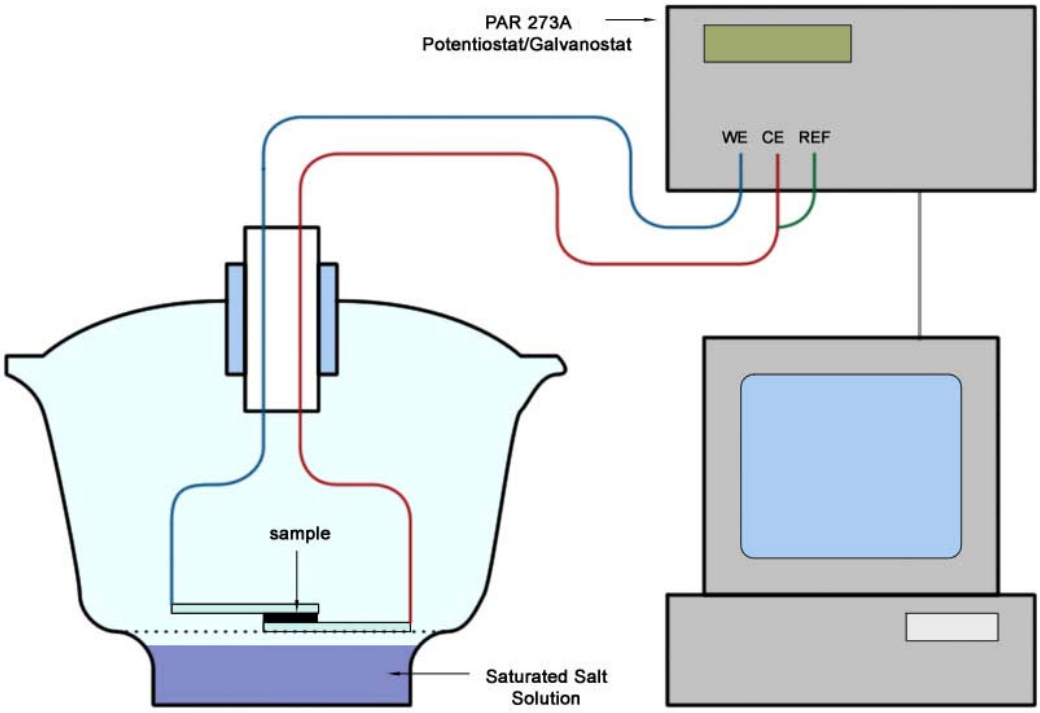

Figure 2.2. Experimental setup for conductivity measurements under constant humidity.

Humidity experiments were performed by means of saturated salt solutions. The sample was sandwiched in between two FTO glass electrodes and kept in a sealed container containing a saturated salt solution (See Figure 2.2), and a linear potential scan was performed after at least 3 hours, with another scan performed 5-10 minutes afterwards to ensure that the system had indeed reach equilibrium.

2.2.3. Characterisation of the Melanin Film

^{13}C solid state NMR was done using an MSL300 Spectrometer (Centre for Magnetic Resonance, University of Queensland). The parameters used were the ones outlined by Duff et al[162] for the solid state NMR analysis of synthetic melanin. The melanin samples were made by galvanostatic polymerisation of l-dopa in borax buffer at 0.5 mA/cm^2 for 8 days unless otherwise specified. The samples were rinsed with deionised water, dried in a desiccator, and ground into a fine powder for analysis.

High-Resolution XPS was performed on a Kratos Axis Ultra with a monochromated Al source. For the analysis, the sample was grounded into a powder and was put in the instrument's vacuum chamber for several hours to remove its water content. Analysis was also performed on melanin chemically synthesised from 5,6-Diacetoxyindole (DAI)[170] (provided by Dr. Sov Atkinson, University of Queensland).

SEM was performed on a JEOL 840A Electron Probe Microanalyser and a FEI Quanta 200 Environmental SEM. The samples were mounted by means of conducting carbon paste and were coated with gold prior to analysis. All samples were analysed under vacuum.

2.3. Effect of Synthetic Parameters

2.3.1. Effect of Electrode Material

2.3.1.1. Electrochemical Analysis

It was found that free standing films were formed only when conducting glass was used as the electrode. When a platinum electrode was used, there was only a thin, film on the electrode surface, and upon extended oxidation the melanin was deposited mainly as granules on the electrode's edge and in rough areas where the electrode has been scratched. There was no significant drop in the current density, and thus this is not caused by passivation of the electrode. Rather, this shows that there is little to no attraction between the melanin and the platinum electrode, and the melanin formed on the electrode surface did not stay on to form a film, but diffused away into the solution.

A thin, adherent film of melanin was formed when a cyclic potential method was used instead of the galvanostatic one, but as was found by Horak et al[152] this film did not appear to grow any thicker with further oxidation. Instead, it appears that the film passivates the electrode, as the current decreases with subsequent cycles. Furthermore, although it has good attachment to the platinum electrode, the melanin film can also be easily wiped off, indicating that it is not chemically attached to the metal.

When stainless steel electrodes were used, a thin film was formed on the electrode surface which does not grow thicker with further oxidation. Unlike the film synthesised on platinum electrodes, the melanin film formed on stainless steel was very adherent and could not be readily removed.

The galvanostatic oxidation profile of l-dopa on stainless steel (See Figure 2.3) showed that the electrode itself did not become fully passivated in that a current continues to flow through the system. In fact, the potential required to maintain the oxidation reaches a stable peak more quickly compared to when FTO conducting glass electrodes were used.

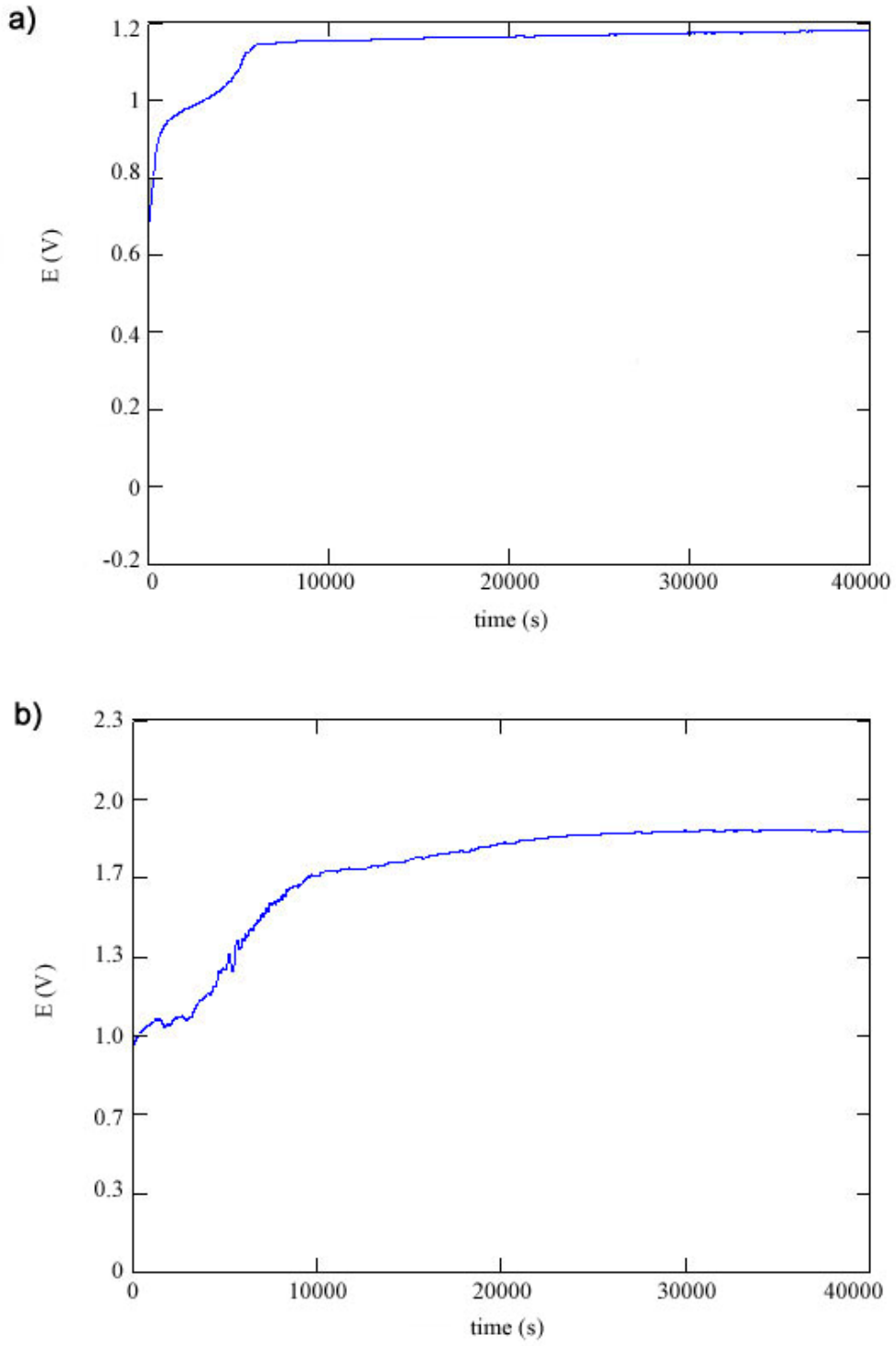

Figure 2.3. Galvanostatic oxidation profile of 0.02 M l-dopa in borax buffer on (a) stainless steel (b) FTO conducting glass electrode at 0.5 mA/cm^2.

Initially, there is an increase in the potential required to maintain the polymerisation current as the newly formed melanin film passivates the electrode. As the polymerisation proceeds, the system eventually reaches a diffusion-controlled equilibrium and the potential profile flattens out. This was the same for both electrodes, with a thick film formed only on the FTO glass and only a thin film observed on stainless steel. This indicates that the lack of thick film may not be due to electrode passivation, but rather in the case of stainless steel electrode melanin has complexed the metal surface forming a dense film that prevents further diffusion of monomer, but is permeable to the electrolyte ions and hence the current is still maintained. Due to the low conductivity of the material, the melanin film can only grow from the electrode surface rather than from the polymer itself, and thus if the monomer/oligomer cannot diffuse through to the electrode surface no further film growth can occur.

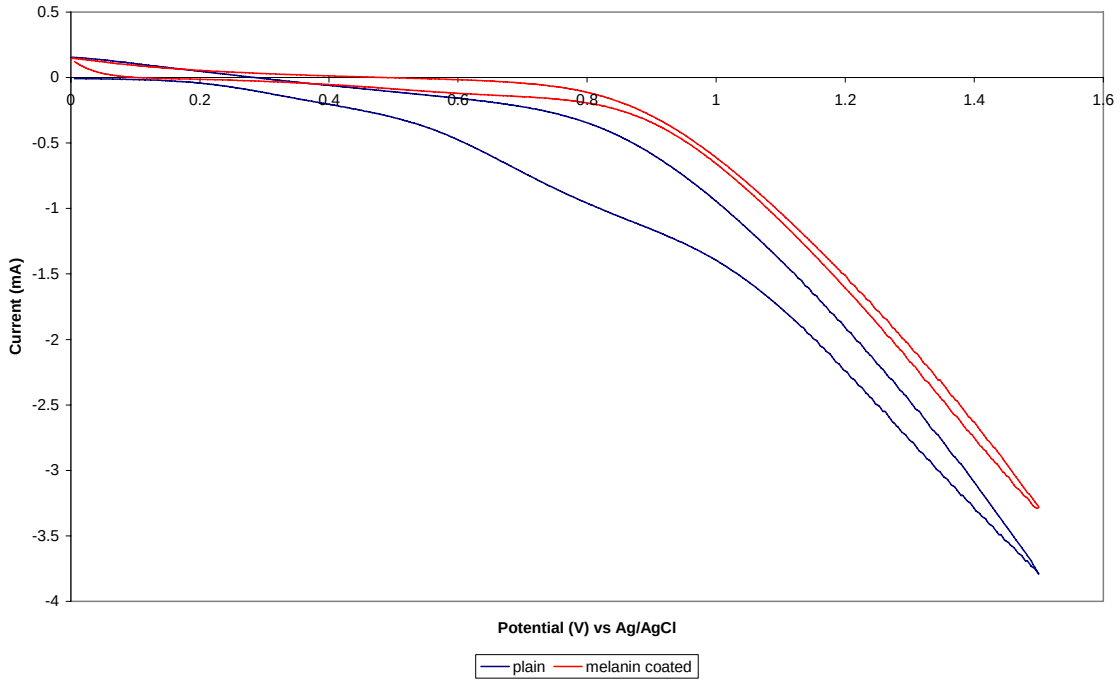

Figure 2.4. CV of 0.02M l-dopa in borax buffer on stainless steel electrodes at a scan rate of 50 mV/s before and after a film is formed on the stainless steel surface.

This is supported by the CV of l-dopa oxidation using stainless steel electrode (See Figure 2.4), comparing a clean electrode with one previously coated with melanin. As can be seen on the CV, when the melanin film is present on the electrode surface the broad

shoulder at 0.8 V indicative of dopa oxidation is no longer observed. This indicates that no further oxidation of dopa is occurring at the electrode surface, however since the melanin itself is a sufficiently good ionic conductor it does not fully passivate the electrode, and the smaller electrolyte ions are still able to pass through the melanin film and hence the decrease in current is only minimal.

It must be noted, though that the peak is not quite as sharp as when platinum electrodes are used since stainless steel is not fully inert, and thus the corrosion current of the stainless steel overlaps the current due to dopa oxidation.

2.3.1.2. SEM Analysis

SEM analysis (See Figure 2.5) showed flaky thin films which appeared to conform to the surface defects on the stainless steel. In the higher magnification image on the right the polymer appears as a thin coating on the electrode.

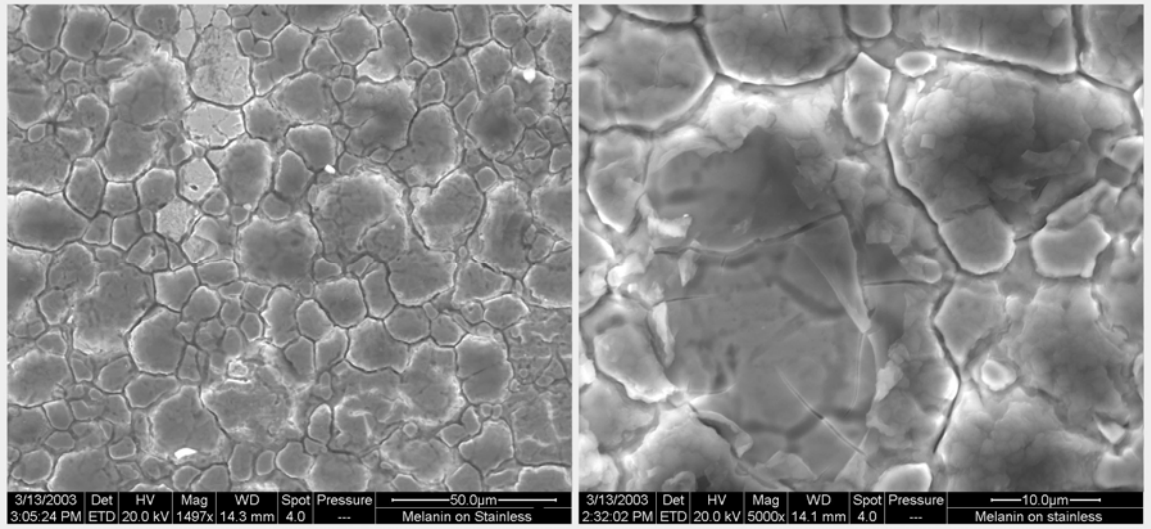

Figure 2.5. SEM images of electrochemically polymerised melanin on stainless steel electrode surface, electropolymerised at 0.3 mA/cm^2 for 6 days

This supports our theory that the polymerisation only occurs on the electrode surface, and not on the polymer surface itself[171]. In our previous study on polypyrrole, it was found that the pyrrole is capable of polymerising from the tip of the growing polymer when

diffusion into electrode surface becomes restricted[172]. However, it appears that melanin does not possess sufficient conductivity in order to transfer charges across to the film surface. Thus, when a sufficiently dense film is formed on the electrode surface the precursor to melanin was unable to diffuse to the electrode surface to be oxidised, and the film does not grow any thicker.

2.3.2. Polymerisation Current Density

The optimum polymerization current was determined to be 0.5 mA/cm^2. This was the maximum current density that can be obtained without oxygen formation on the electrodes. At higher current densities, oxygen bubbles formed on the electrodes can push the intermediates away from the electrode surface and therefore hinders the polymerization process. In the case where a film is already formed, oxygen formation results in mechanical damage to the film.

2.3.3. Polymerisation Method

Galvanostatic method was preferred over potentiostatic ones due to the fact that the growing polymer passivates the electrode by presenting a barrier to electrolyte diffusion, and hence an increasingly greater potential was required in order to maintain a sufficient reaction rate. By using galvanostatic methods the reaction rate is maintained and film formation can proceed, whereas with potentiostatic method the current density (and reaction rate) would decrease significantly with time and thus preventing efficient film formation.

The potential required to maintain the optimum current density initially increases as the melanin film is formed, up until a certain point where it flattened out and there was only a slight increase in potential over time (See Figure 2.6). This is attributed to initial film formation presenting a significant barrier to diffusion, while after reaching a certain thickness an equilibrium is achieved where diffusion through the polymer essentially remains constant, increasing only slightly with increasing film thickness.

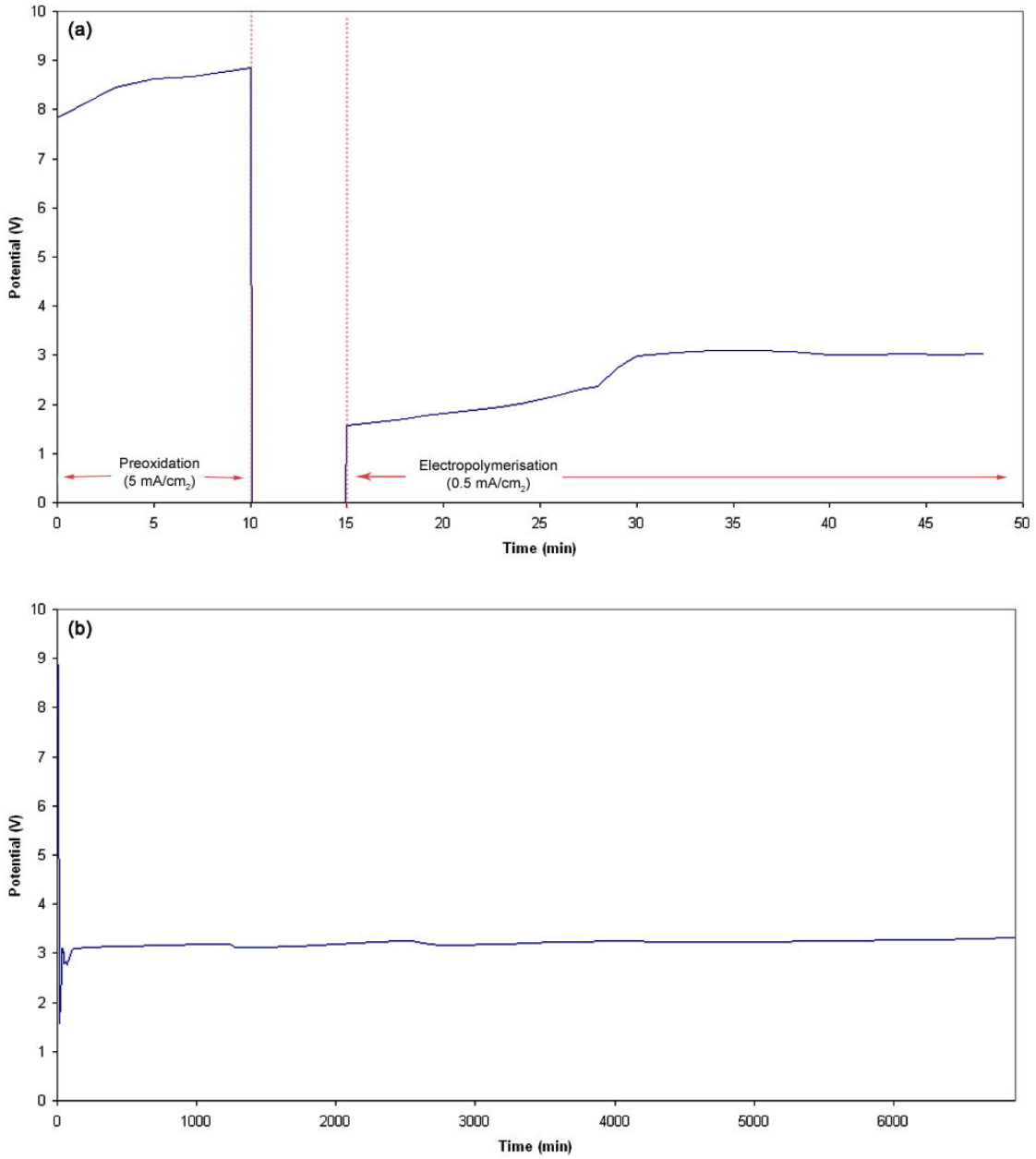

Figure 2.6. Potential profile of the galvanostatic polymerisation at 0.5 mA/cm^2 of melanin from 0.02 M l-dopa solution in borax buffer on FTO conducting glass electrode (a) in the first 50 minutes including 10 minutes of preoxidation at 5 mA/cm^2 (b) over several days

Interestingly, in the preoxidation there is also a similar increase in potential required to maintain the current. This is, however, unlikely to be caused by melanin since vigorous stirring would remove most of the oxidised species from the electrode surface and hence little to no film formation would occur. Instead, this indicates that under the conditions used in the preoxidation, some passivation of the electrode occurs as was shown by the CV of blank FTO in borax buffer (See figure 2.7) where there is an initial reduction in current after the first cycle before it stabilises. Although this increases the initial potential required for the polymerisation, it is unlikely that it will have any effect on the polymer since electrode passivation is expected occur to some degree during the electropolymerisation process itself.

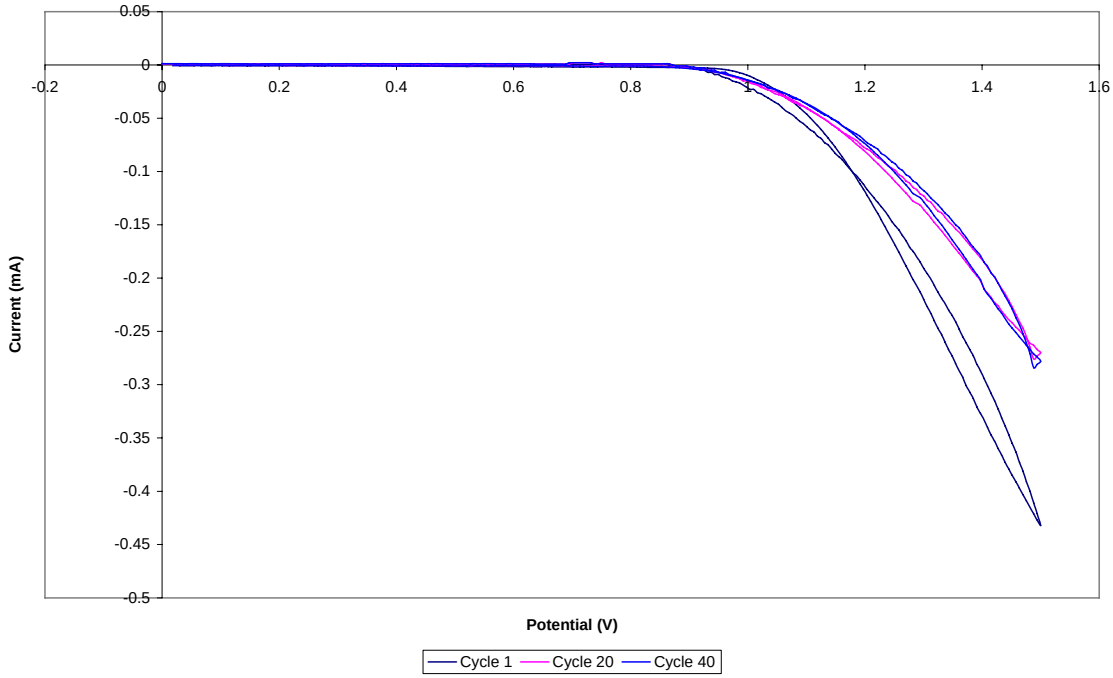

Figure 2.7. CV of FTO conducting glass in borax buffer, scan rate 50 mV/s

2.3.4. Solvent pH

It was found that film formation was favoured by the use of alkaline pH. At low pH the oxidation of dopa does not proceed as the reaction requires the deprotonation of the hydroxyl groups (see Figure 2.8), which is unfavourable in acidic environment. It is still possible to oxidise the dopa into dopaquinone even at lower pH, however the reaction is fully reversible[150] and thus would be inefficient as most intermediates would be reduced

back to dopa rather than oxidise further into melanin. Furthermore, dopa is less soluble in acidic solutions and therefore the concentration of dopa that can be used in acidic pH is much less than that in alkaline pH.

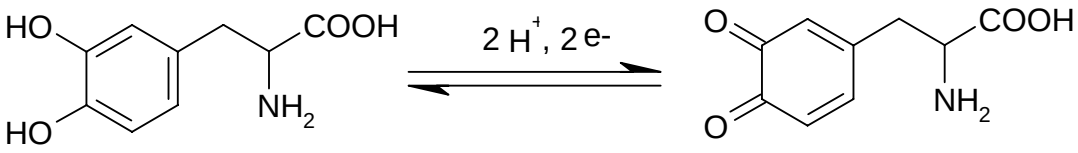

Figure 2.8. The oxidation of dopa into dopaquinone

At neutral pH, oxidation of dopa still occurs, however film formation was slow and inefficient and this was due to the oxidation of dopa into dopaquinone being partially reversible at neutral pH.

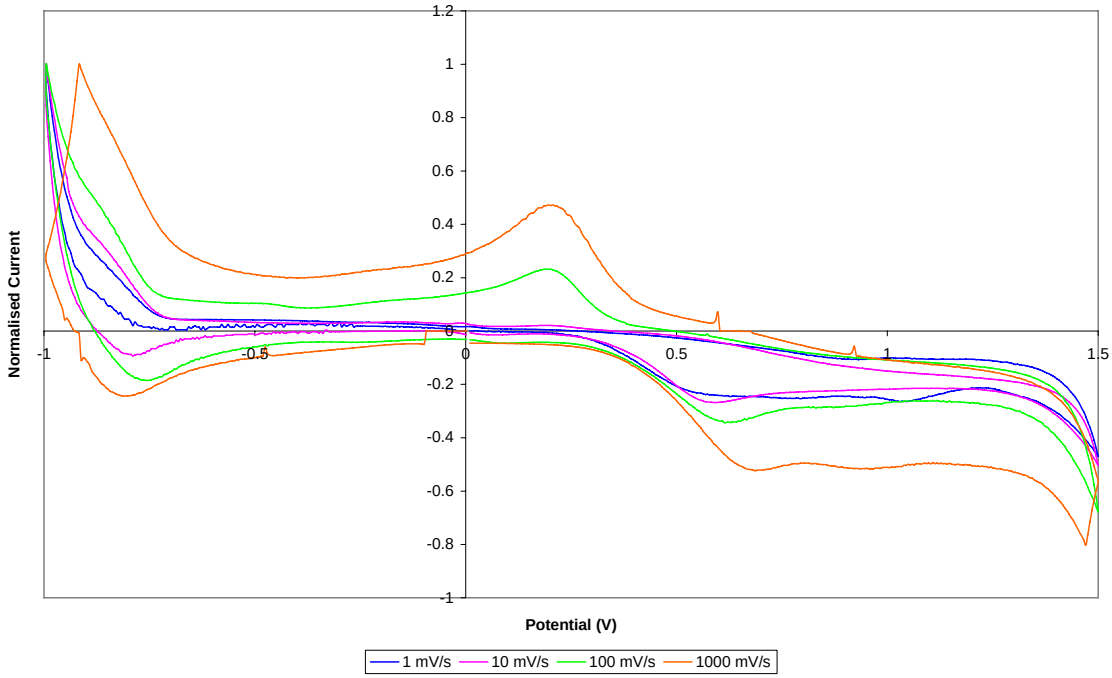

Figure 2.9. Cyclic voltammetry of the oxidation of 0.02 M l-dopa in neutral pH (phosphate buffer, pH 7.5) at scan rates of 1, 10, 100, and 1000 mV/s.

CV (See Figure 2.9) showed the oxidation peak accompanied by a reduction peak (which at faster scan rate was of the same intensity as the oxidation peak) on the reverse sweep, indicating that the reaction is quasi-reversible. There was also a large separation in peak

potential between the oxidation and reduction peak of greater than 118 mV for a fully reversible system (assuming a 2-electron transfer reaction).

Furthermore, the CV appears to be more irreversible at lower scan rate, which indicates an $E_{rev}C_{irrev}$ mechanism where a fast electron transfer is followed by an irreversible chemical reaction. This shows that the further oxidation of dopaquinone into melanin intermediates is still occurring at this pH, but the process is sufficiently slow that at faster scan rate the reaction appears reversible.

This reversibility means that melanin formation in neutral pH would not be as efficient as it is at higher pH. And indeed, it was found that at neutral pH, the reaction proceeds quite slowly, and hence only a small amount of melanin is formed even after a prolonged period of oxidation. It is possible that extending the oxidation time would eventually lead to the formation of free standing film, however, most of the dopa would have been subject to autooxidation and form smaller, soluble oligomers of melanin in solution rather than on the electrode surface. This would be detrimental to film formation since the oligomers would find it more difficult to diffuse through the newly formed polymer film onto the electrode surface where film formation can occur.

Another drawback of using neutral pH is that the solubility of dopa is greater at high pH, which means that the solutions at neutral pH would have a significantly lower initial concentration of dopa compared to the high pH solution. This means that less dopa molecule is available for oxidation at the electrode, further hampering film formation.

This was confirmed experimentally when phosphate buffer (pH 7.4) was used, film formation was very slow as expected. Preoxidation did not seem to be as effective as it was for higher pH solution, and after 6 days, there was only a very thin film of melanin formed on the electrode, despite visible colouration of the solution. The lack of film formation was attributed to the oxidation of dopa being reversible at this pH, hence film formation on the electrode would not be as efficient as in alkaline solution.

At neutral pH the solution also did not darken as rapidly as in higher pH solution, indicating that autooxidation in solution is also slower. Although slower autooxidation would be beneficial for film formation (as autoxidation competes with the electrochemical polymerisation process), it was not sufficient to compensate for the slower film formation. After extended period of 14 days there was no significant film formation observed but the solution was dark in colour, which indicates that autooxidation may dominate at neutral pH.

As mentioned before, the oxidation of dopa is favoured in higher pH. This is because the oxidation of dopa is accompanied by the deprotonation of the hydroxyl groups. Although the electron transfer itself is reversible, in order for the back reaction to occur it requires reprotonation of the quinone.

CV at higher pH (See Figure 2.10) showed that the reaction becomes irreversible regardless of scan rate, as the reduction peaks were only present at very negative potentials and were much smaller in intensity compared to the oxidation peak. This indicates that the reduction reaction is not favoured in high pH solutions, whereas in neutral pH it occurs more readily. It must also be noted that the peak for dopa oxidation has also been shifted due to the irreversibility of the reaction

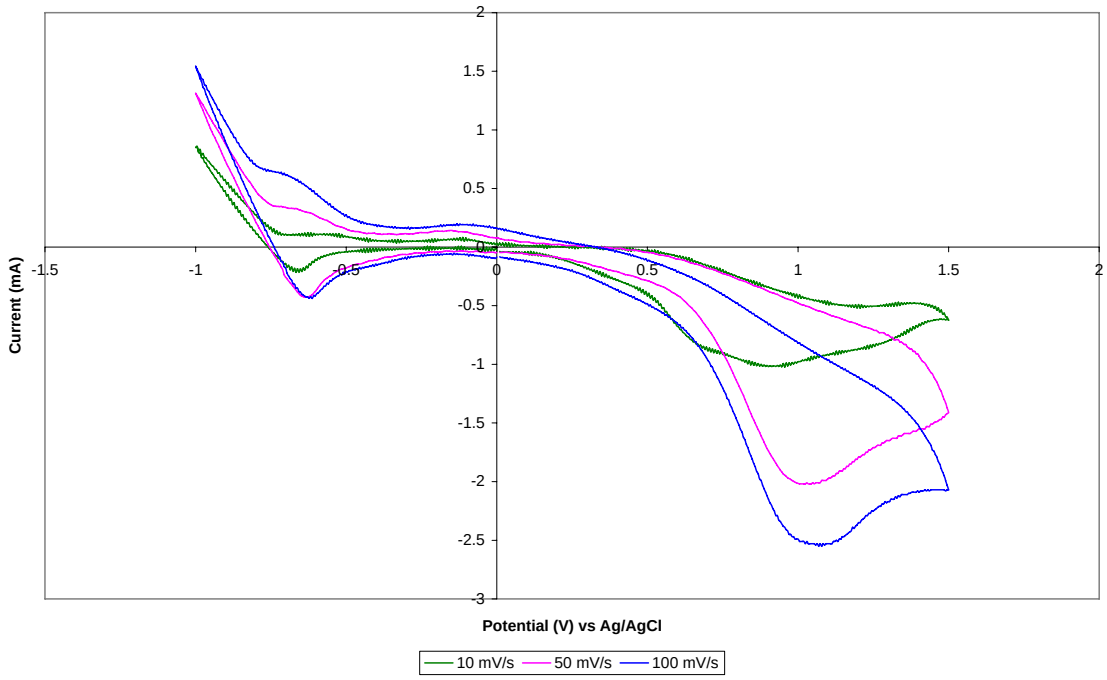

Figure 2.10. CV of 0.02 M l-dopa in borax buffer at scan rates of 10, 50, and 100 mV/s

At higher pH, the oxidation of dopachrome can also be observed as a second peak which appears in subsequent scans (See Figure 2.11). The first cycle of the CV showed only one oxidation peak at 0.9 V vs Ag/AgCl which was the oxidation of dopa into dopaquinone. However, subsequent scan showed a small peak at 0.35 V vs Ag/AgCl which was due to the oxidation of dopachrome into DHI, and this peak did not change significantly in intensity over subsequent scans since the dopachrome is a product of dopa oxidation and therefore the amount of dopachrome available on the electrode surface depended only on the oxidation of dopa during the previous cycle.

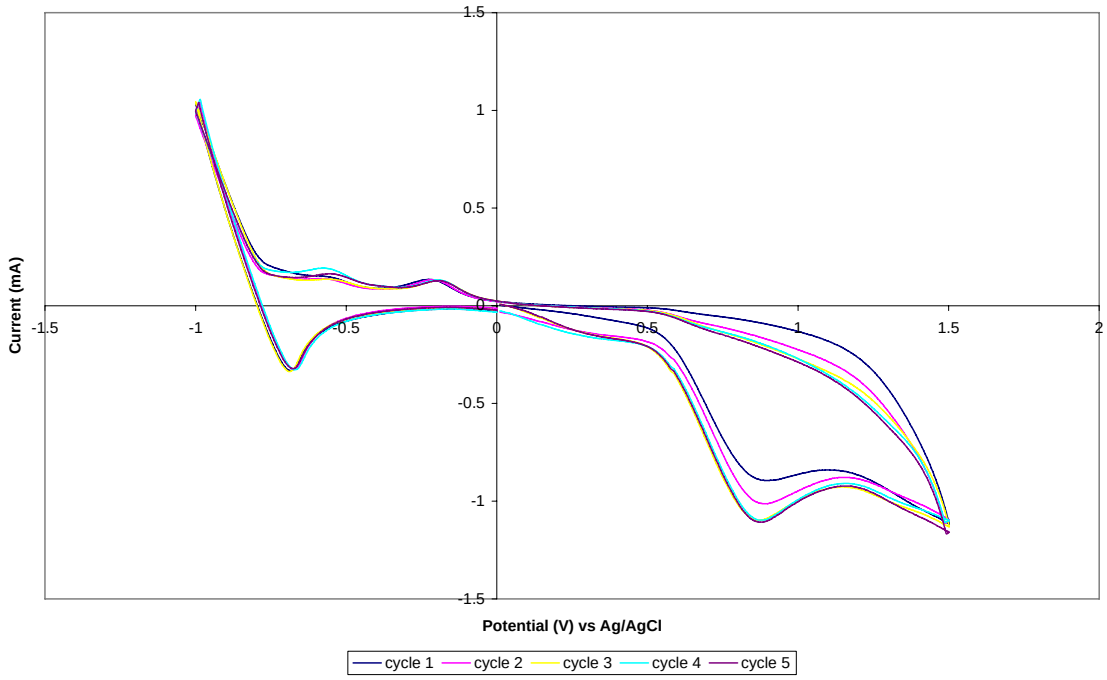

Figure 2.11. CV of 0.02 M l-dopa in borax buffer, scan rate 50 mV/s

The two reduction peak, at -0.2 and -0.5V vs Ag/AgCl appeared to be due to dopaquinone and dopachrome respectively. The peak at -0.5 V showed a slight increase in subsequent scans, while the peak due to reduction of dopaquinone at -0.2V remained practically constant.

2.3.5. Dopa Concentration

When a lower concentration of 5-10 mM was used films did form, however they were not of sufficient thickness to be able to be removed from the electrode, and prolonged oxidation did not result in a free standing film. This means that concentrations below 10 mM were too low for free standing films to form, in that there was insufficient precursor material to maintain the polymerisation rate required to form a free standing film.

It was thought that by increasing the dopa concentration, the reaction would proceed more efficiently due to the availability of reactive intermediates in the vicinity of the electrode surface. However, although it does appear that higher concentration helps improve filming, it was found that using a higher precursor concentration was less

efficient since a significant amount of the precursor are wasted. Extending the polymerisation time would presumably resulted in full oxidation of the material, however prolonged oxidation of 12-14 days would not significantly increases the thickness of the polymer film due to electrode orientation.

In the experimental setup, the film was oriented vertically in solution, and once it reaches a certain thickness it may fall off the electrode due to its own weight. Although this problem can be overcome by placing the electrode horizontally this did not seem to significantly increase film thickness with longer polymerisation time. Additionally, by placing the electrode horizontally the electrical contacts for the anode was put in contact with the solution and in some cases where the seal was not perfect the contact appeared to corrode thereby hindering the process.

This signifies that once the film reaches certain thickness diffusion would be slowed down significantly and the polymerisation rate would be greatly reduced, and hence the remaining precursor in the solution would mainly be consumed by autooxidation rather than the electropolymerisation process. It is possible that the film synthesised at longer time would be slightly thicker than those synthesised at shorter times, however this difference could not be easily measured since the hydrated film had the consistency of a thick paste on the side exposed to the solution.

Furthermore, ^{13}C solid-state NMR result showed that when high concentration of dopa was used a significant amount of dopa remains within the polymer. The solid state NMR spectrum of melanin synthesised from a 50 mM solution of l-dopa (See Figure 2.12) show peaks that are sharp and well resolved, however the aliphatic peak indicative of dopa is very prominent and there is only a small peak at 110 ppm which is indicative of melanin. This indicates that the solid state NMR spectrum is dominated by dopa, with the melanin appearing as the smaller peaks next to the dopa peaks.

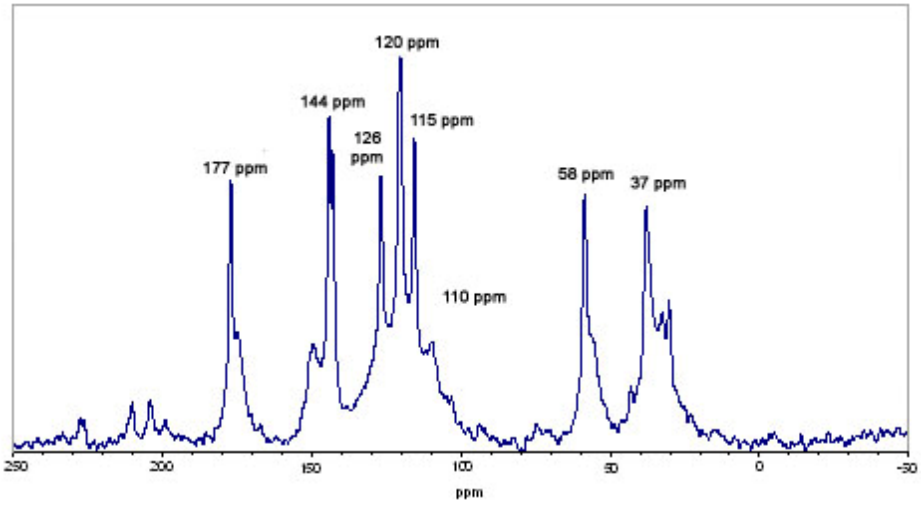

Figure 2.12. ^{13}C solid-state NMR of an electropolymerised melanin film made with dopa concentration of 50 mM in borax buffer.

Although in solid state NMR the peak area is proportional to the number of atoms, the spectra we obtained were only qualitative and quantitative analysis was not possible due to the poor resolution of the spectra. Peak fitting analysis of the NMR spectra showed deviations from the expected value, even in the aliphatic peaks that are exclusive to dopa in that they are not equal to each other. This is similar to what has been encountered in the literature by Duff et al[162], with very broad, overlapping peaks observed in their ^{13}C solid-state NMR spectra.

After taking these factors into consideration, a concentration of 20-30 mM was considered optimum, since it provided sufficient rate of electropolymerisation to form a free-standing film within 6-8 days. Lower concentration results in inefficient film formation, while higher concentration appears to result in an excess of starting material in the polymer.

2.3.6. Polymerisation time

The optimum polymerisation time appears to be dependent on dopa concentration, but for our optimised concentration it was found that 8 days was the optimum polymerisation

time, in that it produces sufficiently thick film with the reaction going into completion where no more of the precursor was available for polymerisation.

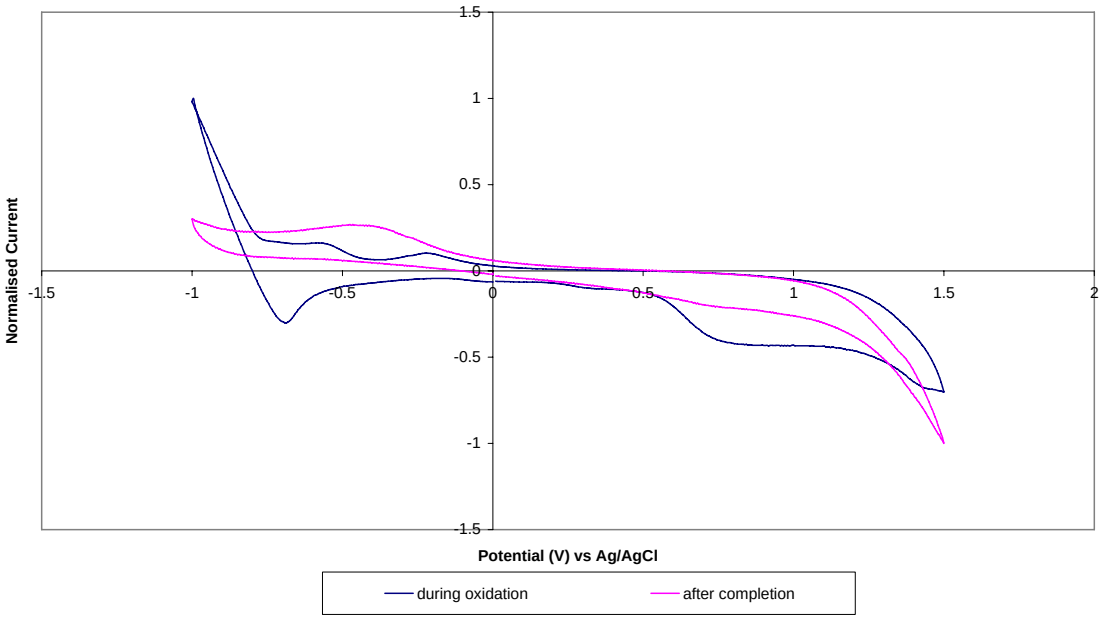

Figure 2.13. CV of the electropolymerisation solution (0.03 M l-dopa in borax buffer) during oxidation (2 days) and after completion (8 days), scan rate 50 mV/s.

During the oxidation period the CV of the solution exhibits an oxidation peak around 0.7 V which is indicative of the oxidation of dopa into dopaquinone (See Figure 2.13). A small peak around 0.3V indicative of dopachrome oxidation and two reduction peaks at -0.2 V and -0.6 V which were due to dopaquinone and dopachrome were also observed. After completion, the CV showed no dopa oxidation peak, and the reduction peak was now a single, broad peak at -0.4 V which is likely due to the reduction of the low-molecular weight melanin species in solution, as the same reduction peak can be observed in the CV of melanin films (See Figure 2.14).

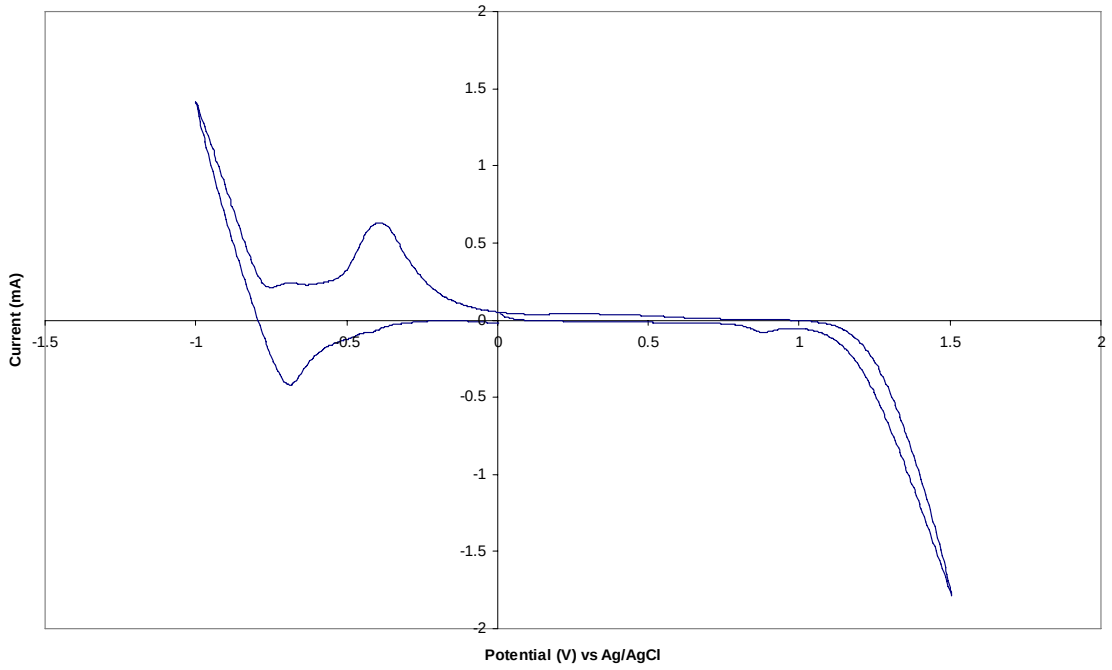

Figure 2.14. CV of a thin film of melanin on platinum electrode synthesised from 0.02M l-dopa in borax buffer by potentiostatic electropolymerisation for 12 hours at 1.5 V. CV taken in a 0.05 M borax solution with a scan rate of 50 mV/s.

This indicates that after 8 days, the dopa has been almost fully oxidised into melanin. The dark colour of the solution indicated that there were still soluble melanin species (possibly oligomers and lower molecular weight polymer species) in solution, but due to their size these oligomers may not be able to diffuse to the electrode surface for further oxidation into higher molecular weight species that can form the melanin film.

2.3.7. The Use of Organic Solvent

Due to the requirement of an alkaline pH, the range of usable solvent was rather limited. Since our previous attempt using basic organic solvent such as acetonitrile was unsuccessful, it was thought that it may be possible to use a mixed solvent system such as an ethanol/water system combined with alkaline buffer salts such as borax.

This again was unsuccessful, with no film formation observed. There was some precipitation of melanin on the working electrode, however, they were random and

granular in appearance and non adherent. Some precipitation near the surface of the solution was observed and may indicate that the melanin did not form as a film on the electrode surface, and the dominant process was more likely the precipitation of melanin from solution with the rougher edge of the electrode acting as nucleating sites.

2.4. Characterisation of the Melanin Film

2.4.1. Solid State NMR

The ^{13}C solid-state NMR spectrum of the electrochemically synthesised melanin (see Figure 2.15) showed a peak at 110 ppm, indicative of an indolic carbon and not present in dopa. This shows that the polymer contains indolic moieties, indicating that ring closure has occurred and significant amount of dopa has been oxidised to dihydroxyindole. It must be noted that the NMR spectra in Figure 2.12 showed peaks that are mainly due to dopa and not melanin, as reflected by the difference in chemical shift.

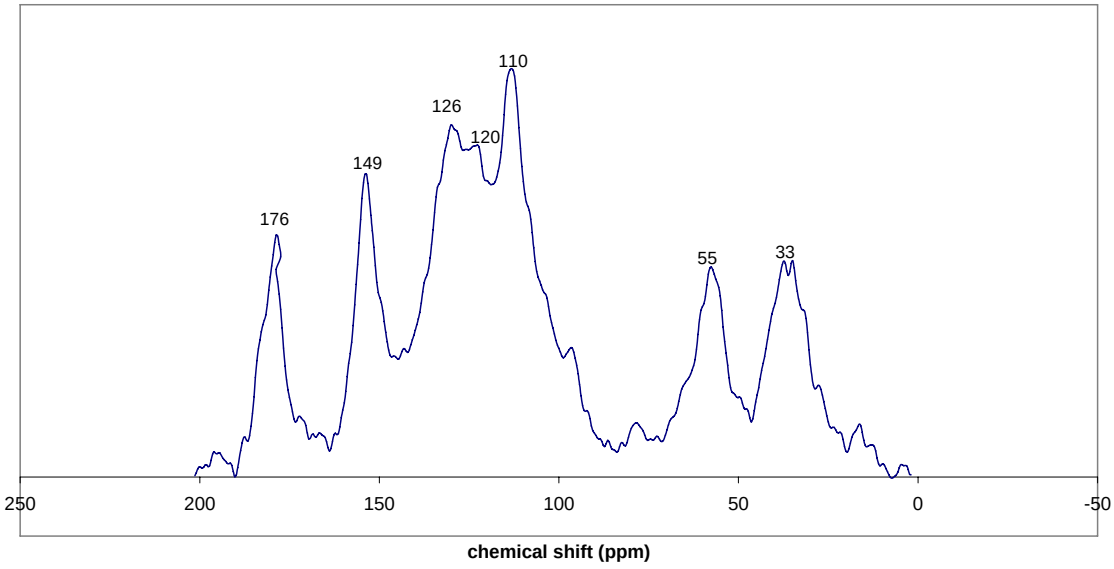

Figure 2.15. ^{13}C solid-state NMR spectrum of the electropolymerised melanin film (synthesised from 0.02 M l-dopa in borax buffer)

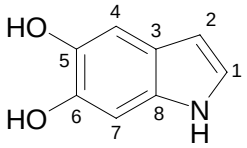

C1, C2, C8: 110-130
C3, C4, C7: 120-130
C5, C6: 140-155

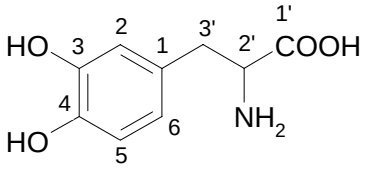

C1': 177 C1: 127
C2': 59 C2,C5,C6: 121-116
C3': 38 C3,C4 : 142-144

Figure 2.16. Literature chemical shift[162] of 5,6-dihydroxyindole (top) and dopa (bottom)

The NMR spectra also showed that there was dopa present in the polymer material, as indicated by the aliphatic carbons in dopa (peaks at 32 and 55 ppm). Our electrochemical analysis previously showed that there was only a small amount of dopa left in the solution, so the excess dopa found in the polymer was likely due to dopa molecules trapped within the polymer matrix. Since the polymer is highly hydrated when synthesised and vigorous washing was not possible, any dopa molecules trapped within the polymer would have been left behind within the polymer matrix despite the repeated washing. However at this point it was still unknown whether the dopa was chemically bound to the melanin.

2.4.2. Scanning Electron Microscopy

SEM analysis of electrochemically synthesised melanin showed that the polymer formed as a continuous film (See Figure 2.17), without the granules previously observed in natural melanin and chemically synthesised melanin[168, 173]. The cross section was smooth and uniform, with only some irregularities on the surface which seems to be due to the drying process.

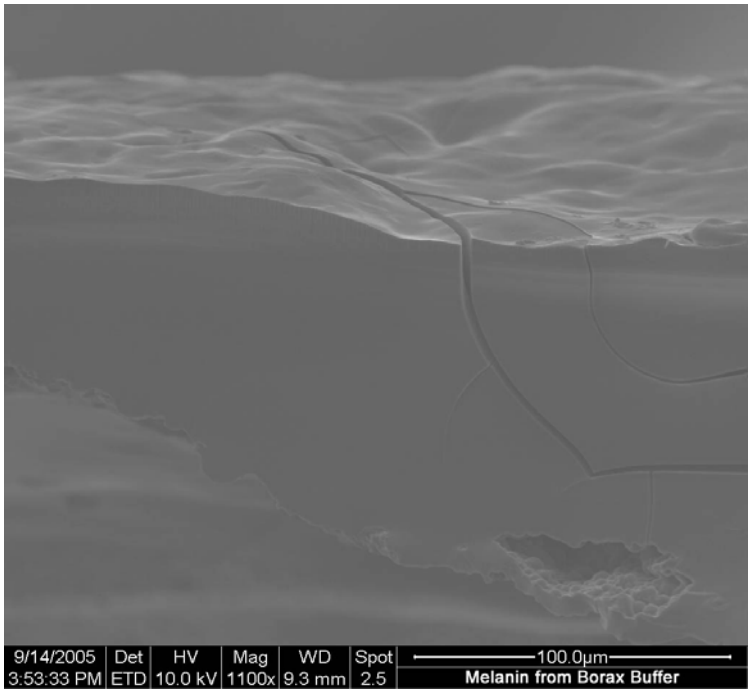

Figure 2.17. SEM images of the cross section of the melanin film synthesised from 30 mM l-dopa in borax buffer for 8 days

At higher magnification, some of the samples exhibited a grain structure similar to wood. In some cases it was also found that although the film appears smooth and continuous, an underlying structure can become apparent due to stress (See Figure 2.18).

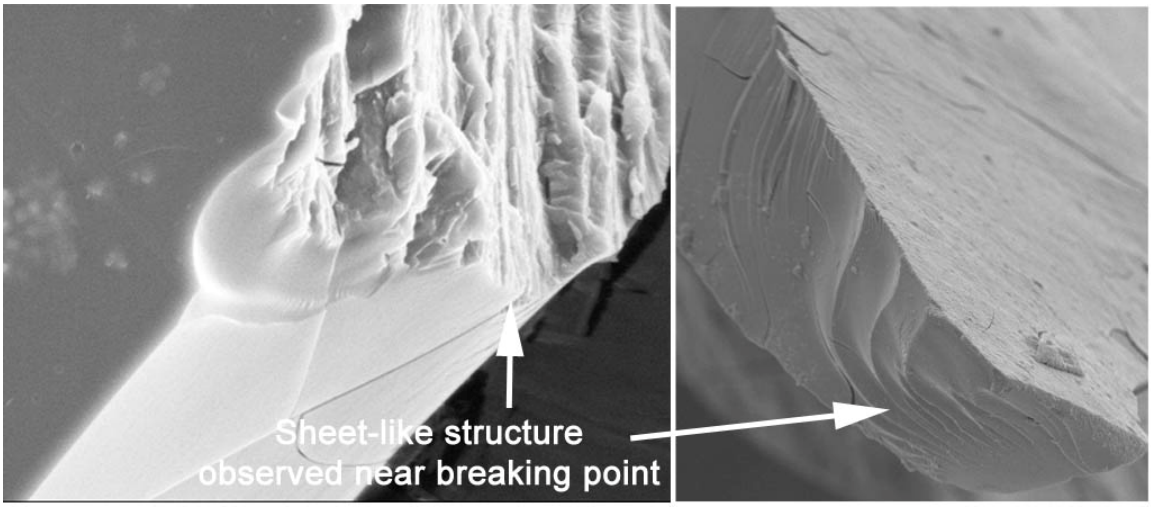

Figure 2.18. SEM images of melanin with an underlying structure apparent due to stress

At first, it was thought that this underlying layered structure may be due to a macrocylic sheet structure[27, 174-176] similar to what has been previously postulated by Zajac[103]. However, XRD analysis of the material showed a single broad peak indicating small domains of π-stacked planar moieties, the interposition of which makes the polymer essentially amorphous. Furthermore, the majority of the polymer would most likely be the randomly linked, conjugated structure of the Nicolaus[100] model (Section 1.2.3).

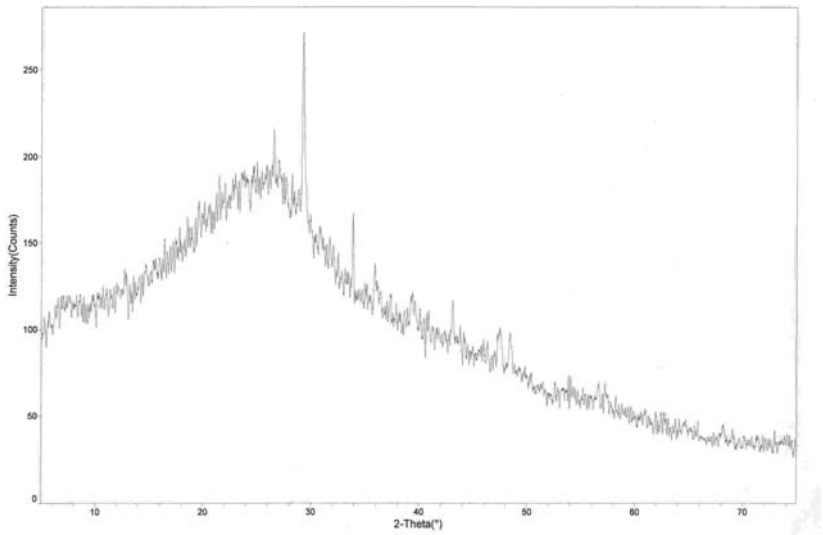

Figure 2.19. XRD spectra of melanin film electropolymerised from 0.02 M l-dopa in borax buffer at 0.5 mA/cm^2 for 8 days.

The layered structure observed was likely caused by film growth from the electrode surface where the reactive intermediates would be most abundant (See Figure 2.20). As a new sheet of polymer was formed, it grew parallel to the electrode surface, and more precursor molecules diffused through the newly formed sheet onto the electrode surface to be oxidised into a new polymer layer. This resulted in the polymer being formed as sheets, which upon drying collapsed together to form a continuous film, but reappeared upon stress.

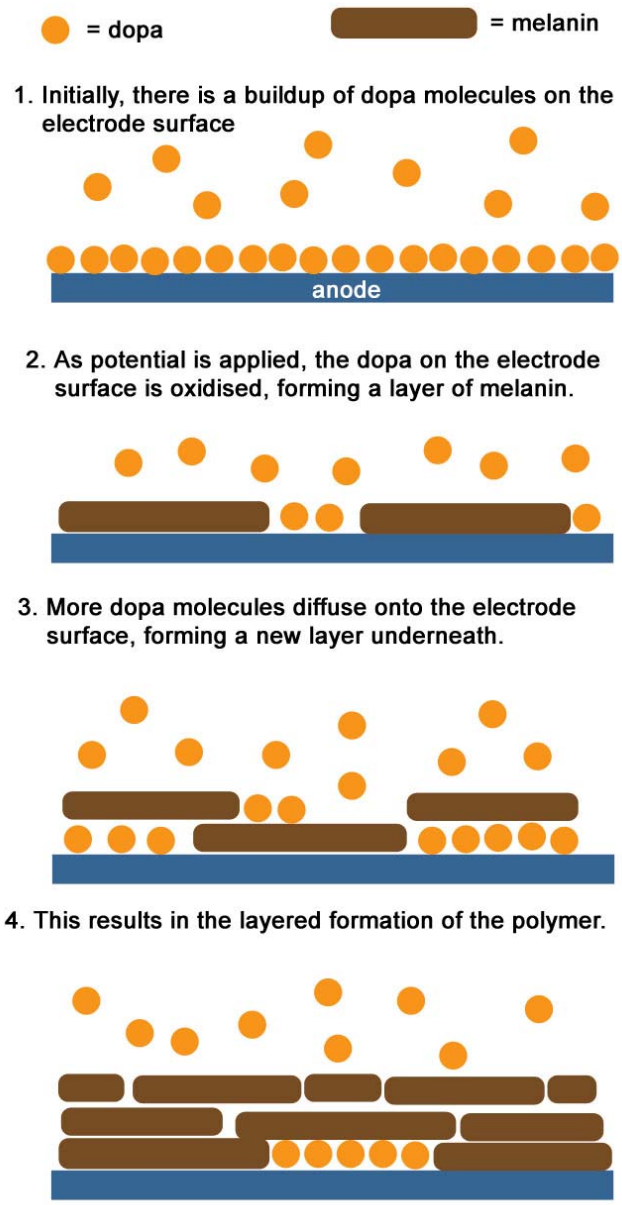

Figure 2.20. Layer formation during electropolymerisation of melanin at an electrode surface

2.4.3. Elemental Analysis

Elemental analysis of the electrochemically synthesised melanin (done by the University of Queensland Microanalytical Service - See Table 2.1) quite closely agrees to the literature value for *Sepia* melanin.

Element	Percentage	Literature Value[173] (*Sepia* melanin)	Expected Value (approx.)
C	47 %	43.3 %	65 %
H	4 %	3.3 %	3.4 %
N	7 %	7.2 %	9.5%

Table 2.1. Result of elemental analysis of electrochemically synthesised melanin compared to literature value of extracted *Sepia* (squid ink) melanin[173] and expected value based on a poly-DHI bonded at 2 positions.

The observed carbon and nitrogen content is lower than expected, and this has been previously noted in literature[173] and may be caused by tightly bound water or impurities such as starting material. Table 2.2. shows the results in terms of C/H and C/N ratio.

Element Ratio	Experimental Result	Literature Value (*Sepia* melanin)	Expected Value
C/N	8:1	8:1	8:1
C/H	1:1	1.2 : 1	2:1

Table 2.2. C/H and C/N ratio of the elemental analysis result observed in table 2:1

In the electrochemically synthesised melanin, the C/N ratio was 8:1 as expected of an indolic monomer unit, and supports our assumption that the polymer consists predominantly of DHI and not dopa or DHICA, both of which has a C/N ratio of 9:1. However, the C/H ratio was 1:1 which was higher than the expected value, and this may have been due to excess dopa which has more hydrogens than DHI. Another possible cause of the higher hydrogen content were non-indolic units that may be present, as melanin has been previously postulated to contain pyrrolic and aliphatic units[101].

This result was also consistent with our previous analysis in that it supports the structure proposed by Nicolaus[100] and Swan[101] of randomly linked DHI rather than the macrocylic stacked island model proposed by Zajac[103] (See figure 2.21).

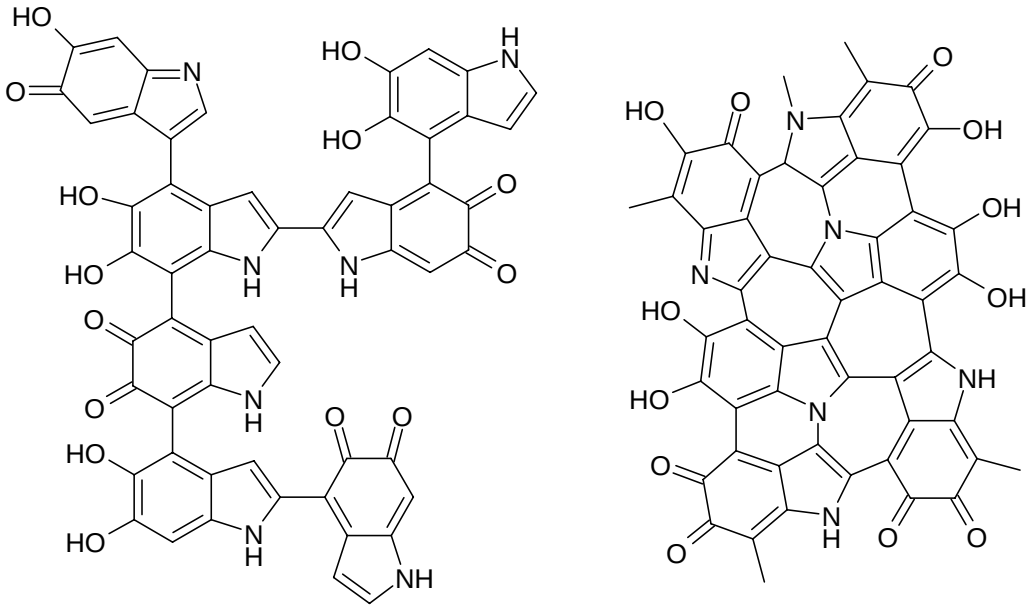

Figure 2.21. Possible structures of melanin and their expected elemental ratio; Left: Nicolaus structure; Right: Macrocyclic sheet.

2.4.4. X-Ray Photoelectron Spectroscopy

2.4.4.1. Comparison with dopa

Firstly, the N 1s XPS spectra of the electrochemically synthesised melanin showed a distinct difference from dopa (See Figure 2.22). The electrochemically synthesised melanin showed a binding energy shift of 3 eV compared to l-dopa. This was attributed to the self-protonation of the amine group in dopa (See Figure 2.23), which resulted in the observed shift corresponding to N^+ in the XPS spectra instead of a primary amine peak.

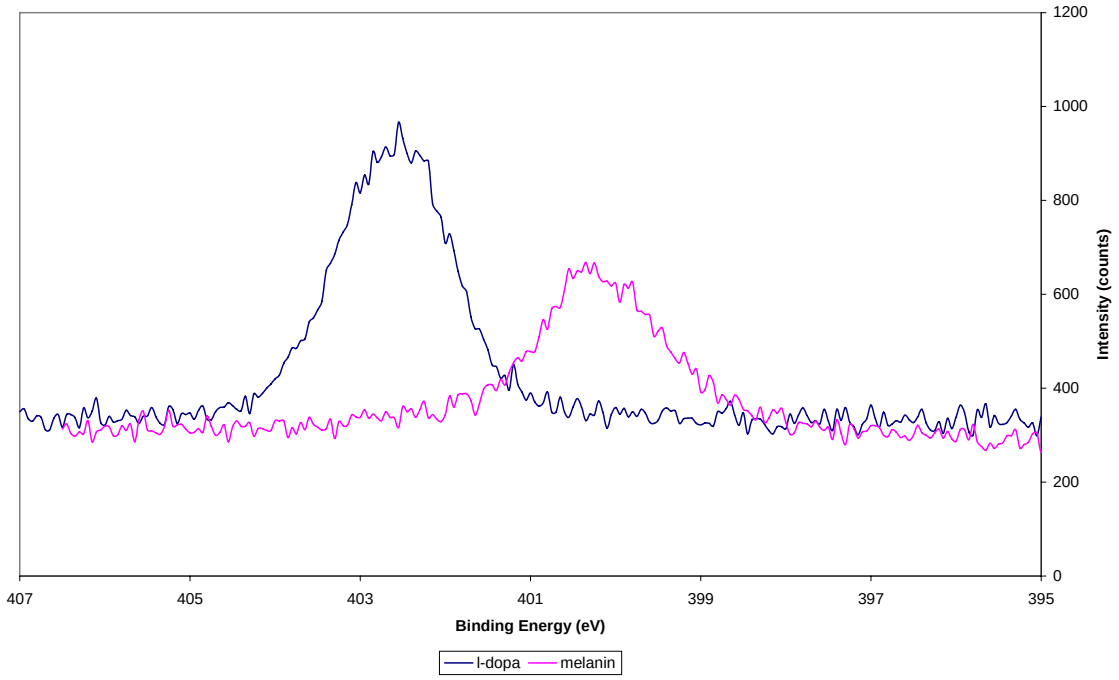

Figure 2.22. N 1s spectra of l-dopa and l-dopa melanin(electropolymerised from 30 mM l-dopa solution in borax buffer for 8 days at 0.5 mA/cm^2)

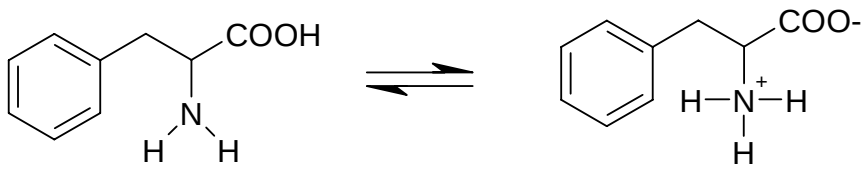

Figure 2.23. Acid-base tautomerisation of dopa

The N^+ species was not observed in melanin for several reasons: firstly, according to the Raper-Mason scheme, the carboxylic acid group had been lost in the oxidation process and hence no self-protonation can occur[97]. Secondly, in the case of DHICA, the nitrogen was bound within the aromatic ring and therefore could not readily donate its free electrons since they were required to maintain aromaticity.

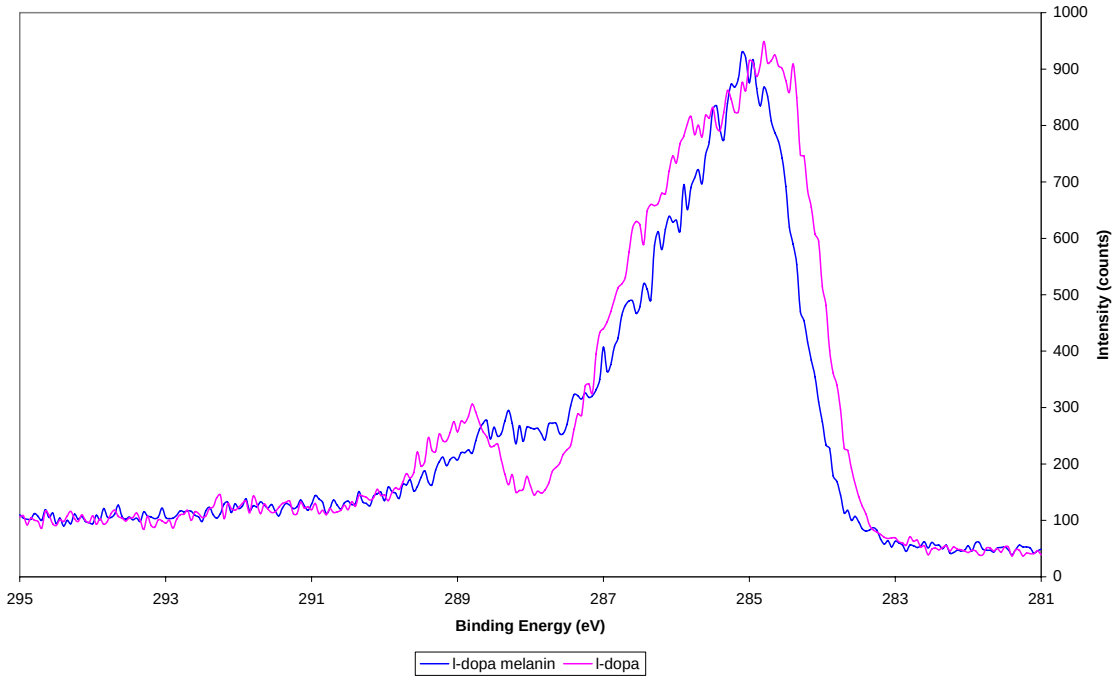

Figure 2.24. C 1s spectra of l-dopa and melanin samples electropolymerised from 30 mM of l-dopa or dl-dopa solution in borax buffer for 8 days at 0.5 mA/cm^2.

The comparison between electrochemically synthesised melanin and l-dopa (See Figure 2.24) showed the peaks in the melanin spectra having a less distinct shoulder to the main peak than the l-dopa spectrum. When peak-fitted, the l-dopa showed the expected 4 types of carbon (see Figure 2.25).

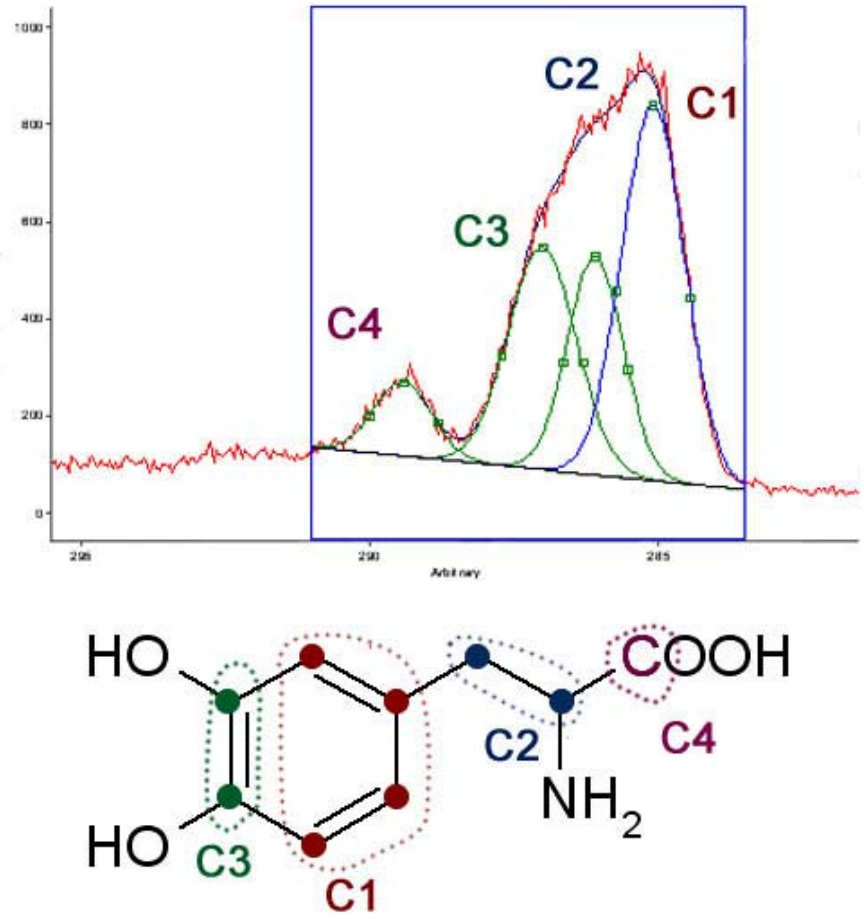

Figure 2.25. Peak fitting analysis of l-dopa C 1s XPS spectrum and their assignment

It must be noted, however, that due to the heterogeneity of melanin, quantitative peak fitting was not possible since we do not know the exact structure of the polymer. It has been previously published that melanin contains pyrrolic and unsaturated species in addition to the majority of indolic species[101], and other previous analysis indicates an excess of oxygen in the material[166] compared to theoretical expectations. Peak fitting can, however, provide indications as to the oxidation state and the overall composition of the material, and thus could not be ignored when looking at the XPS spectra.

Compared to l-dopa, peak fitting analysis of the C1s spectrum of melanin showed a shift in the binding energy as well as extra peaks required for a good fit. These extra peaks

could be attributed to leftover dopa, as their binding energy coincides with the carbonyl and carboxylic acid carbons (C3 and C4) of dopa (See figure 2.25).

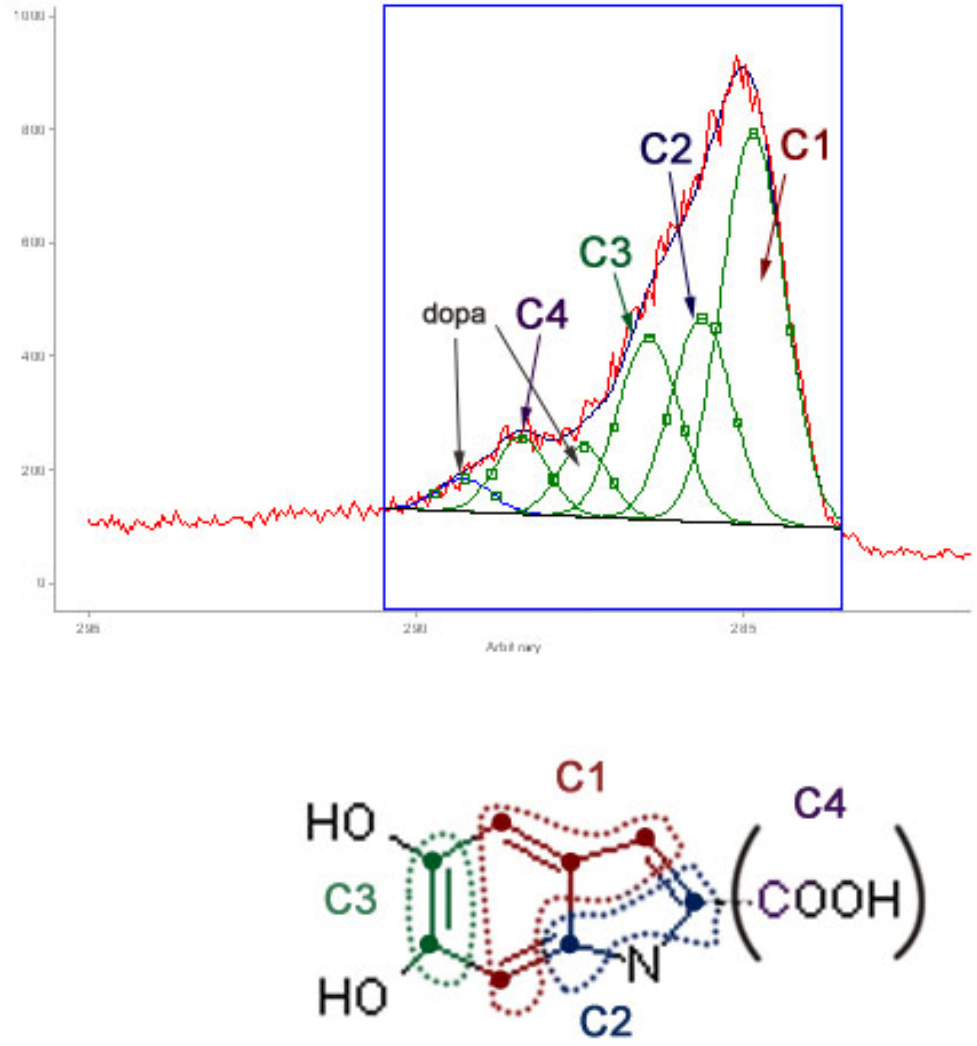

Figure 2.26. Peak fitting analysis of l-dopa melanin C 1s XPS spectrum

The peak fitting analysis for melanin (See Figure 2.26) showed that the peaks for the different carbons were now closer together, with a shift of 1 eV for the carbonyl carbons (C3) and the carboxylic acid carbon (C4). This was presumably due to greater aromaticity in the system, and again supports the previous hypothesis that melanin is made of indolic units, and is not merely poly(dopa).

Previously, in our NMR analysis, we observed the presence of carboxylic acid in the material, but since the analysis was qualitative we were unable to ascertain whether the carboxylic acid is due to presence of DHICA or dopa. The XPS confirmed that melanin contains some carboxylic acid functionality, but unlike the NMR the XPS analysis showed two types of carboxylic acid carbon, with a small peak where the dopa carboxylic acid was present and a larger peak at 288.4 eV was assigned to DHICA.

The difference between l-dopa and melanin was also reflected in the O1s spectra (See Figure 2.27). The O1s spectrum of l-dopa showed a greater tendency towards the higher binding energy compared to melanin (similar to what was observed in the C1s spectra), indicating a greater amount of single bonded oxygen.

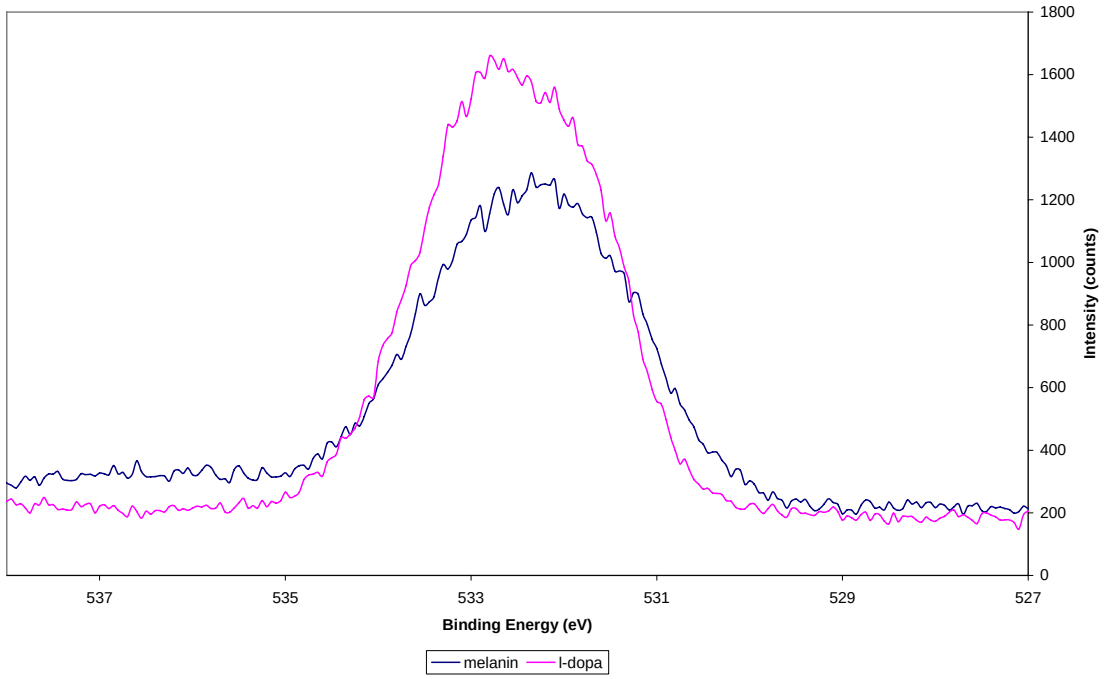

Figure 2.27. O1s spectra of l-dopa and melanin samples electropolymerised from 30 mM of l-dopa or dl-dopa solution in borax buffer for 8 days at 0.5 mA/cm^2.

The tendency towards lower binding energy in melanin indicates that there was a higher amount of double bonded oxygen in melanin compared to dopa. This was because in

dopa the predominant species was the single bonded oxygen of the hydroxyl groups, whereas melanin contained both hydroxyl and quinone forms of DHI.

Although the amount of quinone in melanin was likely to be pH dependant, one can expect a significantly higher amount of quinone in melanin than in dopa since the synthetic reaction was carried out at alkaline pH, and therefore a significant amount of the DHI unit would remain in quinone form.

2.4.4.2. Comparison with DAI melanin

DAI melanin can be described as a 'model' melanin polymer. Unlike the dopa melanin, DAI hydrolyses directly into DHI which then further oxidises into melanin, resulting in a poly-DHI melanin with no carboxylic acid or aliphatic content. In the case of dopa, due to the lengthy oxidation process, intermediates and products such as DHICA can be incorporated into the polymer, making it less homogenous. A small amount of chemically synthesised DAI melanin was obtained to study and compare to the electrochemically synthesised dopa melanin.

Initially, the DAI melanin spectrum seems to resemble that of dopa (See figure 2.28), with a greater proportion of carbon-oxygen bond and a large secondary peak at 289.5 eV which initially appeared to be due to carboxylic acid. There was also another peak at 293.2 eV, which was initially thought to be an impurity.

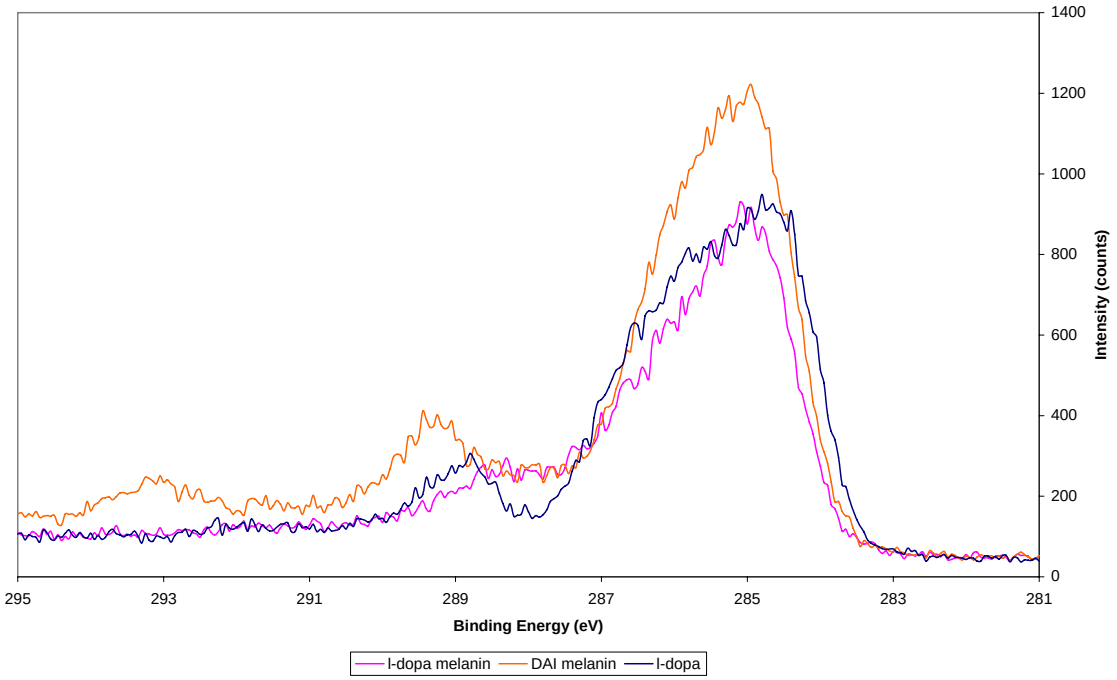

Figure 2.28. C 1s spectra of DAI, l-dopa, and dl-dopa melanin

The peak at 289.5 eV of the DAI spectra may appear to be due to carboxylic acid, but this was most likely a satellite peak since the material should not contain any carboxylic acid functionality. Furthermore, the second peak at 293.2 eV did not correspond to any of the other element present, and in an extended scan it appears that there was also a third peak at 295.8 eV. The extended C1s spectrum of DAI melanin (See Figure 2.29) showed that the satellite peaks are visible up to 292 eV.

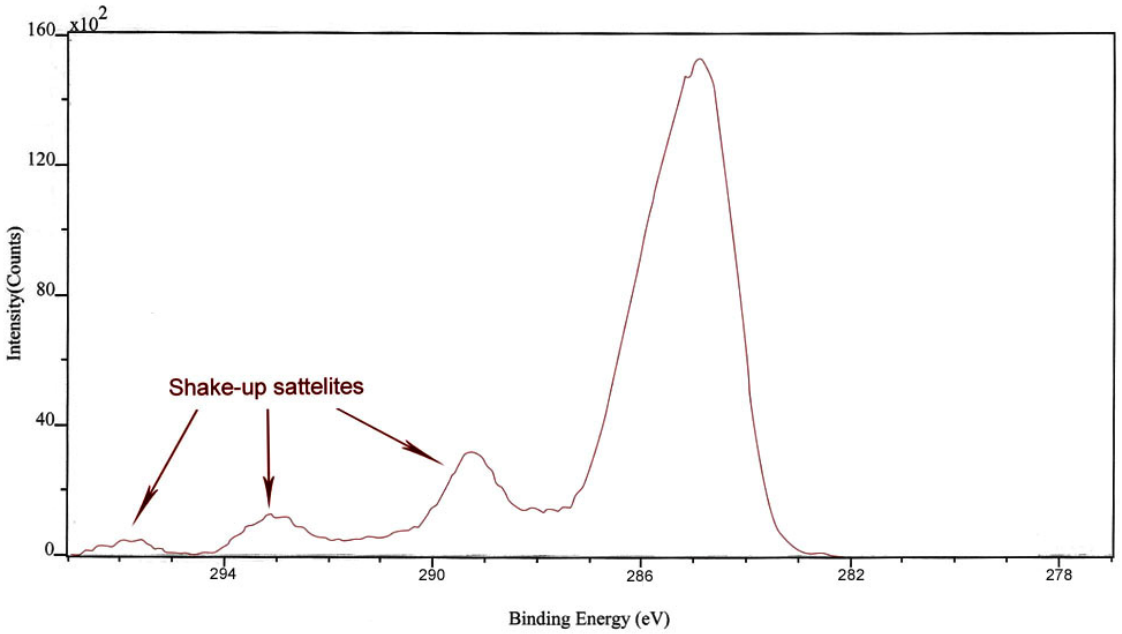

Figure 2.29. C1s spectra of DAI melanin showing the presence of shake-up satellite peaks. Spectrum taken as a survey scan with lower resolution than previous spectra.

The first satellite peak at 289 eV was not due to carboxylic acid functionalities because DAI melanin should contain only DHI units. The acetic acid produced from the hydrolysis of DAI would have been removed during extraction, and therefore should not be present in the material. Furthermore, the ultra high vacuum conditions used in XPS would have removed any acetic acid that was left in the material, so the extra peaks in the C 1s spectrum were likely shake up satellites rather than peaks due to a separate chemical species since the amount of carboxylic acid that may be present would be far too small to account for this peaks.

Shake-up satellites such as these are usually observed in aromatic polymers where π-stacking is possible due to planar moieties in the side or main chain such as graphite or polystyrene[177]. This indicates that the structure of DAI melanin may be that of the 'stacked island' model, with planar oligomers stacked together in a manner similar to graphite.

However, none of the dopa-melanin exhibited this behaviour, so it was likely that the polymerisation of DAI resulted in a more crystalline structure with better packing while dopa would polymerise into a more random conjugated units. However, since both the DAI and dopa-melanin were essentially amorphous, the structure of the polymer would not be a fully regular one such as graphite.

This observation, however, indicates that DAI melanin may share a structure similar to that of amorphous graphite where small clusters of stacked, graphitic domains are linked together by sp3 carbon. In the case of DAI melanin, it may be the case where small domains of the 'stacked island' model are linked by amorphous domains of the Nicolaus model. Since the dopa melanin did not show any shake up satellites, the predominant structure of dopa melanin is more likely that of the Nicolaus model with various randomly linked subunits.

Looking at the oxidation state of the material, the DAI melanin initially appeared to be at a lower oxidation state compared to the dopa melanin (See Figure 2.30). This was because in the O 1s spectra a shift in the DAI melanin towards the higher binding energy was observed, associated with single-bonded oxygen, while the dopa-melanin appeared as a more symmetrical, broad peak which indicated similar amounts of single and double-bonded oxygen.

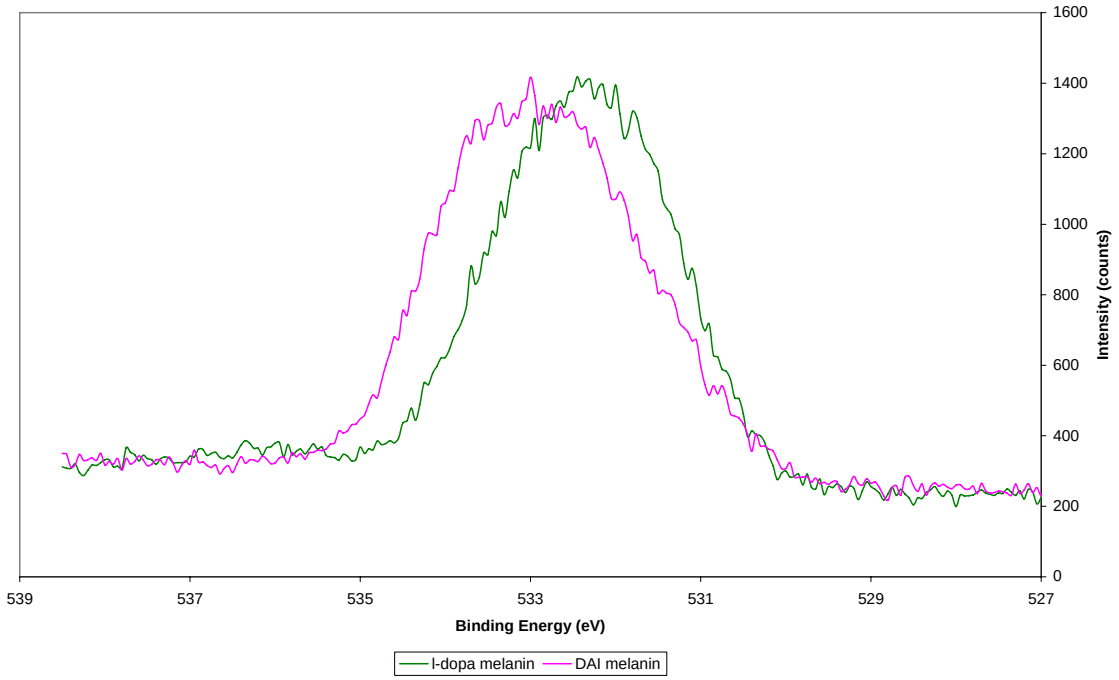

Figure 2.30. O1s spectra of l-dopa melanin (electropolymerised from 30 mM l-dopa solution in borax buffer for 8 days at 0.5 mA/cm^2) and DAI melanin

Initially, it may appear that the DAI melanin had a predominance of hydroquinone, and therefore was in a lower oxidation state than the dopa-melanin. However, the binding energy shift was greater than what can be accounted for by the hydroquinone alone. If DAI melanin were to consist primarily of hydroquinone then the peak would be a narrow one at around 533 eV similar to dopa, and not at a higher binding energy.

Therefore, it appears that evidence for the presence of quinone-imine in the DAI melanin had been found. In the N 1s spectra (See Figure 2.31), comparison between l-dopa melanin and DAI melanin showed that the DAI melanin contained another species of nitrogen at a lower binding energy which can be attributed to the quinone-imine. This presence of the quinone imine shows that the DAI melanin was more highly oxidised than dopa melanin, since the quinone imine would be a result of further oxidation of the quinone.

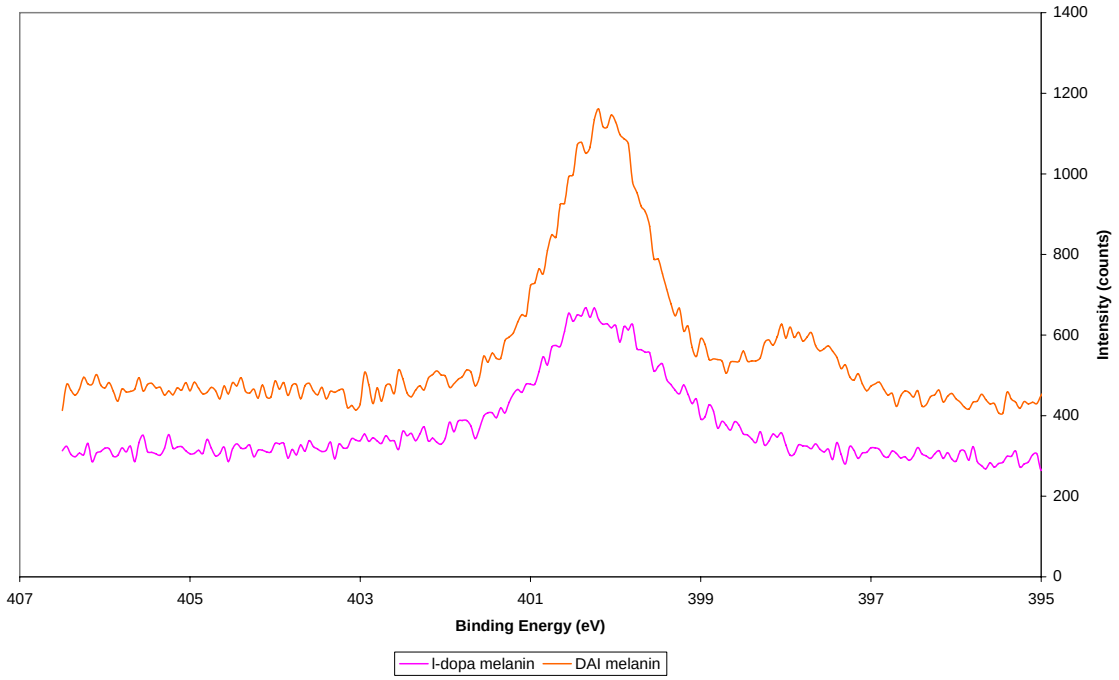

Figure 2.31. N 1s spectra of l-dopa melanin (electropolymerised from 30 mM l-dopa solution in borax buffer for 8 days at 0.5 mA/cm^2) and DAI melanin

The higher oxidation states observed may be due more to the fact that DAI was oxidised into melanin faster than dopa, so the chemically synthesised DAI melanin analysed may have been over oxidised during synthesis. This was because the DAI melanin has been synthesised using the same oxidant concentration and oxidation time as a conventional dopa-melanin, whereas in fact it would have required a lot less in order to polymerise. As a result, when the polymer was formed there would be a large excess of oxidant, and the polymer may have been further oxidised resulting in the large presence of quinone imines observed.

2.4.4.3. Effect of dopa chirality

In a past study the chirality of the dopa has been postulated to affect the adsorption and packing of dopa molecules onto the electrode surface. Chia et al[178] found that in an edge-to-edge orientation the packing density is significantly greater in l-dopa melanin than in dl-dopa melanin.

Due to this, it was first thought that the l-dopa may give polymer of higher oxidation state through more efficient packing which would provide the film with more exposure to the applied potential over the same time period. However, upon further investigation it appeared that the oxidation states of the polymer seemed to be dependant more on the preparation procedure rather than the precursor, and that any effect that the dopa chirality may have was insignificant as far as the bulk polymer was concerned.

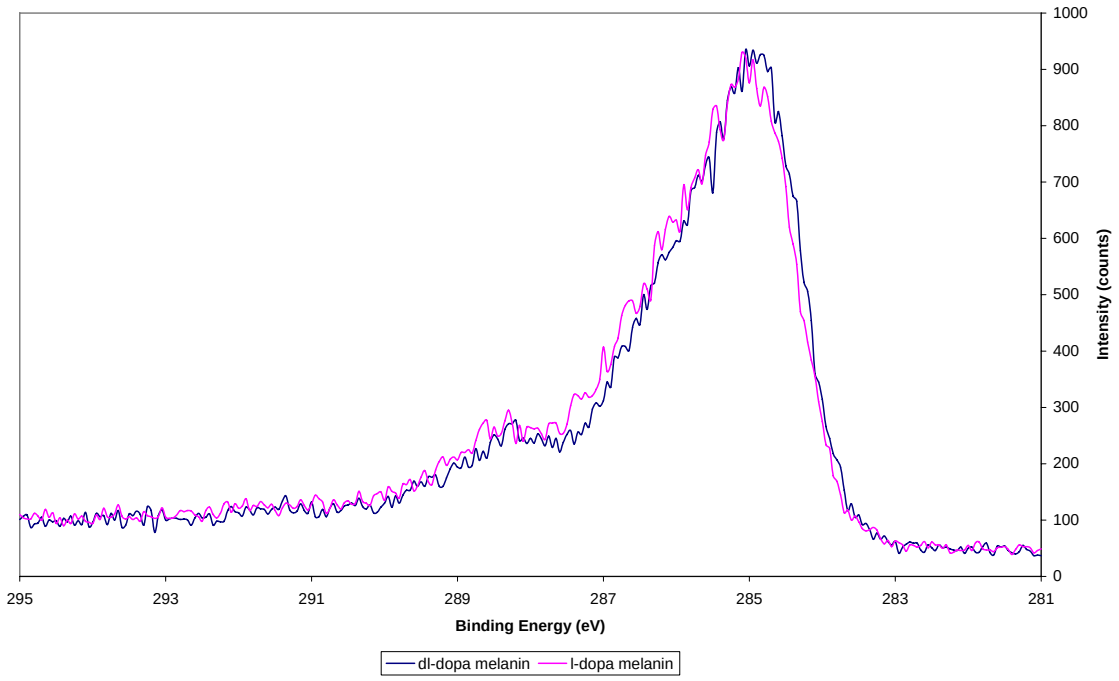

Figure 2.32. C1s spectra of melanin synthesised electrochemically from dl- and l-dopa. Sample synthesised from 30 mM dl/l-dopa in borax buffer at 0.5 mA/cm^2 for 8 days.

The C1s of two samples prepared in identical manner from dl- and l-dopa (See Figure 2.32) showed identical peaks, and the broad shoulder at 288.5 eV assigned to carboxylic acid groups were comparable in size indicating that the carboxylic acid content of the two samples were similar.

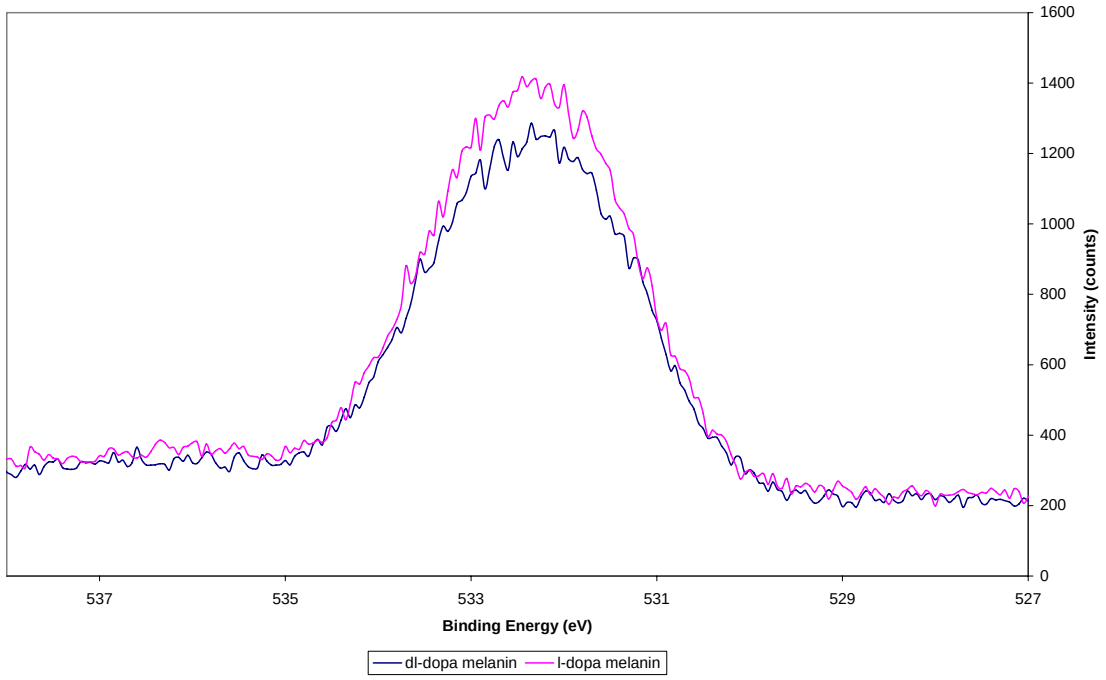

Figure 2.33. O 1s spectra of melanin synthesised electrochemically from dl- and l-dopa. Sample synthesised from 30 mM dl/l-dopa in borax buffer at 0.5 mA/cm^2 for 8 days.

The C1s spectra was supported by the O1s spectra (See Figure 2.33) which also showed little difference in the polymer made from l- and dl-dopa, both having similar peak width and distribution.

It was likely that any effect of the precursor's chirality would be very small, and since the melanin itself is not chiral the bulk property would be affected more by synthetic conditions than the chirality of the precursor. Furthermore, even if the chirality of dopa affects the packing of molecules on the electrode surface, this effect would be lost upon cyclisation of dopaquinone and therefore all the latter steps involving dopachrome and DHI would remain unaffected.

2.4.4.4. Elemental Analysis

In the fields of conducting polymer, one of the most important aspects in the design of the polymer is the counterion. Since XPS is able to analyse any element, it lends itself into studies of inorganic counterions, and indeed elemental analysis of the melanin

samples revealed some interesting clues with regards to the amount of counterions incorporated in the material.

In the electropolymerisation process the counterions incorporated is generally the supporting electrolyte used in solution. In the case of the borax buffer used, Sodium tetraborate hydrolyses in water to form sodium borate and boric acid, and hence the ions that could be incorporated into the polymer were borate (BO_3^-) and sodium (Na^+) ions. If the ions were present because of leftover solution trapped in the polymer, one can assume that they would be present in stochiometrically equal amount, while an excess of either would indicate the present of charges within the polymer.

Since the electropolymerisation was carried out at an alkaline pH, the hydroxyl groups on the hydroquinone is subject to deprotonation, and the resultant negative charge may be balanced by a sodium ion, and this could result in an excess of sodium in the material.

On the other hand, polyheterocycles such as polypyrrole are subject to p-doping, where oxidation creates positive charge along the polymer backbone, and we would expect to see an excess in the amount of borate ions present to balance the charge.

Sample	% Na	% B	Excess
A	3.7	3.9	0.2% B
B	3.9	4.3	0.4% B
C	4.2	4.6	0.4% B
D	0.7	0.7	n/a

Table 2.3. XPS elemental analysis of several melanin samples electrochemically synthesised from borax buffer. The samples were made from borax buffer by galvanostatic electropolymerisation at 0.5 mA from (A) 0.02 M l-dopa; (B) and (C) 0.03 M l-dopa; and (D) 0.03 M l-dopa with the sample vigorously washed after synthesised.

Based on our XPS analysis (See Table 2.3), the amounts of salt present were approximately 4 %, and in most cases were present in almost equal amount. This indicates that most of the sodium and borate ions present were merely trapped within the material. Sample B had been more vigorously washed compared to the other three samples, and this was reflected in the significantly lower amount of salt detected. Vigorous washing was generally not done since it damages the melanin film, however since the XPS was done with powdered sample there was no need to obtain an intact film.

In most cases there was a slight excess of boron compared to sodium. Sample D did not show any excess, however since XPS is much more sensitive to sodium than to boron the readings for sample B were not very precise. As for the other samples, the excess boron indicates that there were positive charges along the polymer backbone, and that melanin was indeed synthesised in its doped form.

The doping level observed was quite low, considering the doping levels in CPs such as polypyrrole commonly reaches 5-13%[9]. The low doping level may be a result of the self-doping in melanin. Other CPs such as polyaniline have been synthesised with an anionic side chain which enables it to act as its own counterion[179], and the hydroxyl groups in melanin may have acted in a similar fashion.

2.4.5. Mass Spectrometry

It is still debatable whether or not melanin is truly a polymer, or merely an aggregation of large oligomers. Certainly, the more recent studies on chemically synthesised melanin suggested that melanin has quite a low molecular weight, however there

Seraglia et al[180] and Serpentini et al[155] has analysed chemically synthesised melanin using Matrix-Assisted-Laser-Desorption-Ionisation Time-Of-Flight (MALDI-TOF) mass spectrometry, and their findings suggest that melanin is an aggregated clusters of large oligomers rather than a long continuous polymer chain. In Serpentini et al's study[155], the most abundant molecular weight was found around 2770 Da (which translates to approximately 20 monomer units).

In the study by Seraglia et al[180], they obtained better spectra by not using any matrix, but by solubilising the melanin in HCl directly on the stainless steel slides. With this method they were able to detect higher molecular weight species at 40000, 48000, and 78000 Da, but the most abundant were of 1700 and 2100 Da (approximately 12-15 monomer units). The abundance of low molecular weight species indicates that they were not merely fragment of the species at higher molecular weight,

In a follow-up study by Napolitano et al[167, 181] on DHI-melanin, it was found that melanin were made of predominantly low-molecular weight species of 500 to 1500 Da. Although they couldn't rule out the possibility that high molecular weight species simply remained undetected, this study further supports the theory that melanin does not consist of large molecular species, but rather a mixture of oligomeric species.

Unfortunately, we have been unable to obtain mass spectrometry results with electrochemically synthesised melanin. The main problem with the analysis comes from the intractability of the material, which remains mostly insoluble even in basic solvents. Although Seraglia claimed to have solubilised the melanin simply with HCl, we weren't able to do so with electrochemically synthesised melanin.

Although we do not possess hard data regarding the mass of our material, the indications were that the electrochemically synthesised melanin may have larger molecular weight than the chemically synthesised ones since it was less soluble. Horak[152] has performed SIMS analysis on electrochemically synthesised melanin, and found oligomeric units with molecular mass of less than 300. However, with techniques such as SIMS, as the material need not be in solution there is a danger of underestimating the molecular weight of the material as the heavier molecules may remain undetected, and in Horak's study the use of SIMS was to identify the molecular unit and not as a mean to identify molecular mass.

2.5. Conductivity Measurements

2.5.1. Effect of Water

Our previous study[171] estimated the conductivity of melanin at 1.4 x 10^{-6} S/cm under ambient conditions, however it has been noted in the literature that the conductivity of melanin is greatly affected by the relative humidity. McGuinness postulated that this was caused by the alteration to local dielectric constants, however the amount and linearity of the increase also suggests an ionic component to the conductivity. Since the conductivity of melanin under vacuum was very low, it is most likely that a higher amount of water in the material turns melanin into a gel electrolyte, with the conduction being due to the water rather than the melanin itself as a conducting polymer.

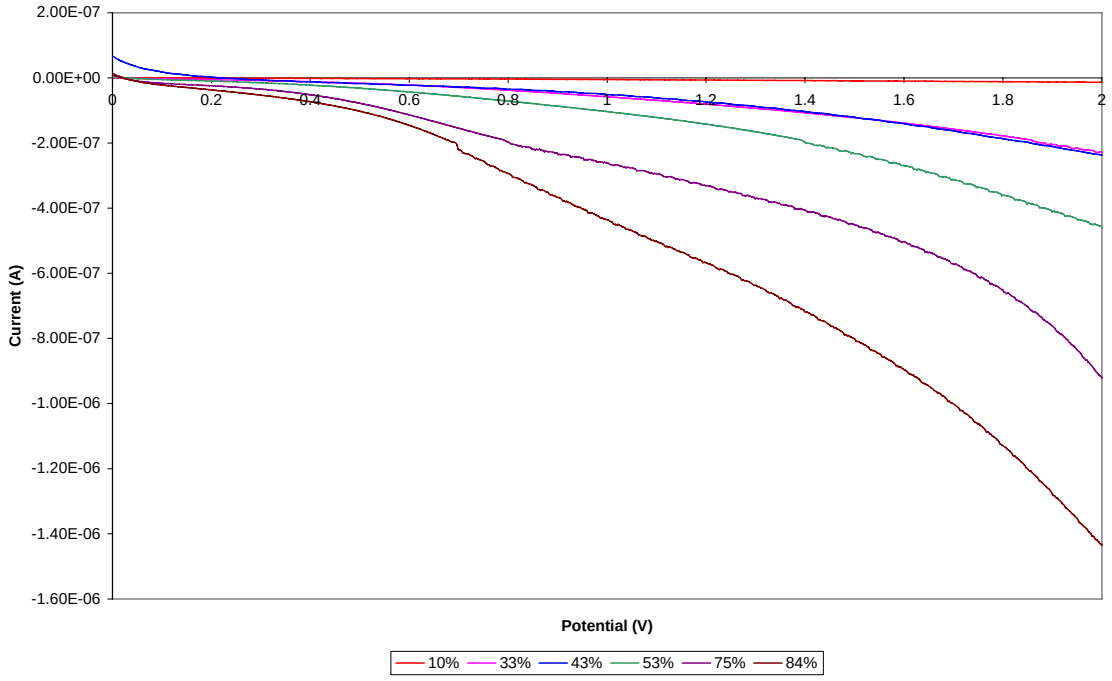

Figure 2.34. Effect of humidity on the IV curve of melanin synthesised in borax buffer

When the IV curve was performed at different humidity (See Figure 2.34), there was an increase in the slope of the line as the relative humidity increases. At high humidity there seems to be a steep downward slope after 1.6 V which may have been due to electrolysis of water.

As can be seen, the curve was not completely linear; however in all cases they are quite linear between 1-1.4 V. The conductivity value obtained by calculating the slope at this region was also close to values obtained by measuring the resistance with an ohmmeter. Thus it was decided that this region would be the most suitable for further measurements for the conductivity as a function of humidity (See Figure 2.35).

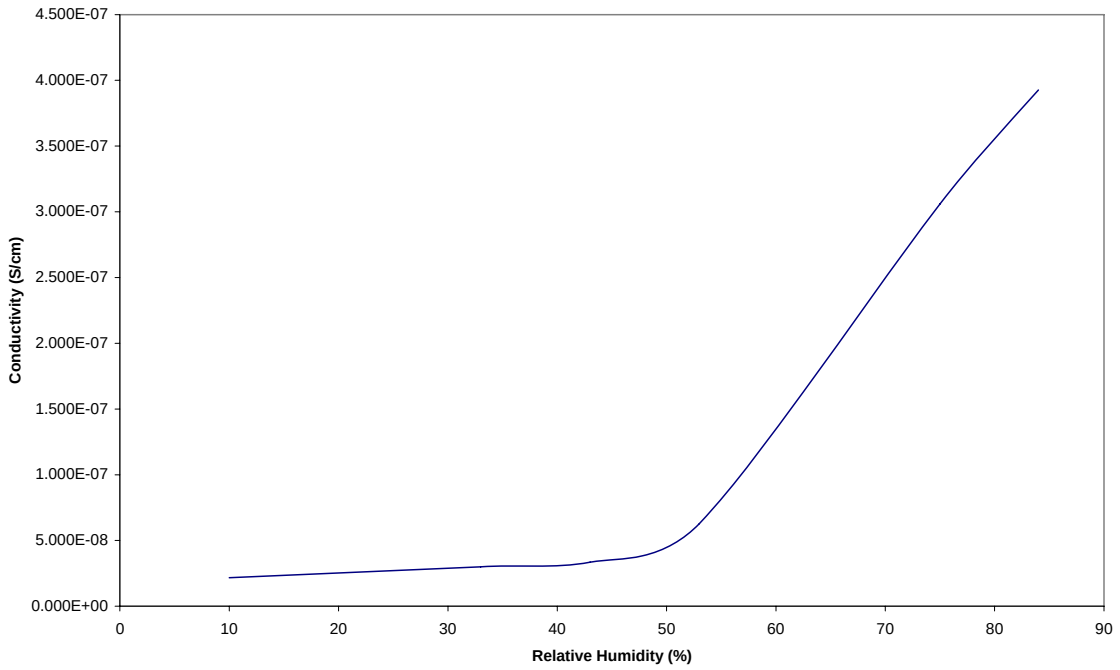

Figure 2.35. Conductivity of melanin as a function of Relative Humidity. Melanin synthesised by galvanostatic oxidation of 0.03 M l-dopa I borax buffer at 0.5 mA/cm^2 for 8 days.

The conductivity did not change significantly until 43% humidity, and increased linearly afterwards. This may be due to the presence of two types of water in the material as was previously postulated in the literature[134, 182, 183]. When dry, the material seems to have very little to no conductivity. The conductivity value increases as humidity increases with initial change corresponding to the tightly bound water in the melanin structure. This may have served to activate conduction in the material, and since the conductivity itself was due to tightly bound water it did not change significantly up to 43% humidity. Once the material is saturated (at 43% humidity) an ionic conductivity was imparted to the

material, which was directly proportional to the water content, hence the almost linear increase afterwards.

This observation was also supported by high-resolution TGA analysis (See Figure 2.36). The derivative of the mass loss vs temperature shows a non-gaussian peak above 100°C with a shoulder extending to 200° C compared to the expected single Gaussian peak at 100°C if there is only adsorbed water present.

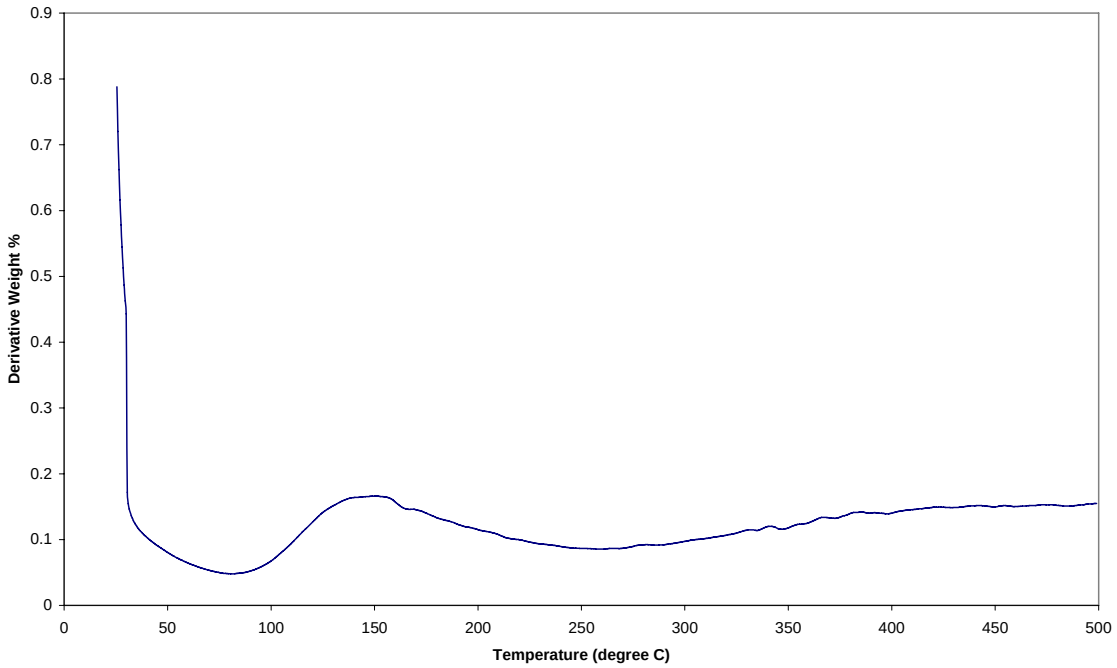

Figure 2.36. Derivative curve of the high resolution TGA of melanin synthesised by galvanostatic polymerisation of 0.03 M l-dopa at 0.5 mA/cm^2 for 8 days, sample mass 15 mg.

2.6. Summary

We have shown that melanin free-standing films can be synthesised from l-dopa by electrochemical means. The optimum method for the electrochemical synthesis was determined to be a galvanostatic method with a current density of 0.5 mA/cm^2 for 8 days with a precursor concentration of 20-30 mM. It was also found that melanin can only polymerise into free-standing films when ITO or FTO conducting glass was used as the

electrode, with the use of metallic electrodes resulting in the formation of a thin film which passivates the electrode.

The conductivity of the material was found to be highly dependent on hydration with a significant change in conductivity observed with changes in relative humidity, which is consistent with the literature.

Solid state NMR and XPS analysis confirmed that the polymer contains indolic moieties which showed that cyclisation had occurred. Comparison with DHI melanin and dopa showed that our material is made of a mixture of DHI and DHICA. Dopa was also evident in the material, but was thought to be trapped in the material and not chemically bonded to the polymer.

Elemental analysis by XPS indicates that dopant counterions were indeed incorporated in the material in small amounts, with the majority of salt present due to leftover solution. There was a slight excess of anions, indicating the presence of positive charges in the polymer. The doping level was low compared to conducting polymers such as polypyrrole or polythiophene, however the analysis may have been an underestimation of the doping level as it did not take into account the possibility of sodium ions being bonded to deprotonated hydroxyl groups or possible self doping in melanin.

Due to the lack of quantitative data, we were unable to determine the exact structure of the material. The main problem with structure determination in dopa-melanin is that the compound is very heterogeneous, with Swan[101] estimating that eumelanin consists of 65% indolic species, 10% indolinecarboxylic acid species, 15% pyrrolic species, and 10% uncyclised units.

The data supports the conclusion of Nicolaus[100] and Swan[101] in that electrochemically synthesised melanin was an amorphous solid made of predominantly indolic units linked together in a random manner. It was likely that macrocyclic sheet are also formed to some degree, although not quite in the ordered, crystalline fashion proposed by Zajac[103].

Chapter 3

Effect of Dopant and Additives

3.1. Introduction

3.1.1. Dopant Counterions in Melanin Synthesis

Dopant counterions are an important part of the electrochemical synthesis of conducting polymers, since the choice of dopants greatly affects the mechanical and electrical properties of the polymer. Initially most conducting polymers were doped with simple inorganic salts, such as iodide or chloride, however nowadays the most common dopants used in the synthesis of conducting polymers such as polypyrrole are organic dopants containing sulphonate group such as p-toluenesulphonate or dodecyl sulfate[9].

In the synthesis of melanin the use of buffer means that the dopant counterions are the inorganic buffer salts. Thus, the buffer used in the synthesis serves not only to maintain pH, but also to provide the dopant counterion. However, previous studies have generally used only borax (pH 9) or phosphate (pH 7), with most melanin synthesis done in caustic solution.

Furthermore, there has been no study in the use of organic dopants in melanin. Since the use of organic dopants in other heterocycles often results in materials with better conductivity, there was also the need to investigate the effect of these dopants on the electrochemically synthesised melanin.

Another possible dopant for use in melanin synthesis are metal ions, since it has been shown that metal ions such as Cu^{2+} or Zn^{2+} affects the oxidation of melanin[99, 119, 124, 184-186] and may affect the ratio of DHICA to DHI in the polymer.

In the study by Gidanian et al[99], they incorporated metal ions into electrochemically synthesised DHI melanin in order to study its effect. However, the main problem with the use of metal ions as dopant in synthesis is that these metal ions can form a complex with the dopa in solution and hinder the oxidation process.

3.1.2. The Use of Fillers

Fillers and additives are often used in polymer synthesis in order to improve the mechanical properties of the material. It has been demonstrated in literature that melanin can be incorporated into synthetic polymers, and previous works has been done with coupling melanin with Polyethylene Glycol (PEG) and Poly-2-Hydroxylethyl Methacrylate (HEMA).

Chirila et al[187] synthesised melanised poly(HEMA) hydrogels for use as materials for intraocular lenses. A main difference in this study compared to a lot of other studies is that they used epinephrine (adrenaline) as a starting material which resulted in a melanin polymer with a methyl group attached to the nitrogen. Ishii et al[188] studied the modification of natural pigments by conjugation with PEG. The PEG-melanin was found to have increased solubility in organic solutions, while still maintaining the desired photoprotective properties. In this study the synthesis was done chemically with activated PEG and natural melanin extracted from human hair.

3.2. Alternative Buffer Systems

As discussed in Section 2.3.4, the electropolymerisation proceeds most efficiently at higher pH. At neutral pH the dopa-dopaquinone equilibrium is reversible, while at pH of 9 and above, the equilibrium shifts towards dopaquinone since protonation of the quinone is suppressed. Although a borax buffer is used predominantly in this study it is possible that different buffers may have an effect on the synthesis.

The main criteria for the required buffer would be that it needs to be in the pH range of 9-10. At lower/neutral pH, the reaction becomes much less efficient due to the reversibility of the oxidation reaction, while at higher pH (11-12) most of the melanin formed remained soluble and hence film formation is hindered. Furthermore, autooxidation proceeds very rapidly in solution at high pH.

With that criteria, we tested 4 buffer systems that possess the required pH range. The buffers were:

- Sodium Tetraborate (Borax) (pH 9)
- Sodium Carbonate/Sodium Hydrogen Carbonate (pH 9-10)
- Ammonia/Ammonium Chloride (pH 10.5)
- Triethanolamine (pH 10)

3.2.1. Borax Buffer

The borax buffer was the buffer system used in our previous study, and it provides sufficiently alkaline pH for dopa oxidation without excessive autooxidation in solution. The CV (See Figure 3.1) of dopa oxidation in borax buffer shows a peak at 0.9 V vs Ag/AgCl, which was the only oxidation peak present in the first cycle. The intensity of this peak initially increases, but then decreases over subsequent cycles. This may be due to a build up of reagent initially, increasing the oxidation current, but as the melanin was formed on the electrode it presents a barrier to diffusion and hence the current decreases.

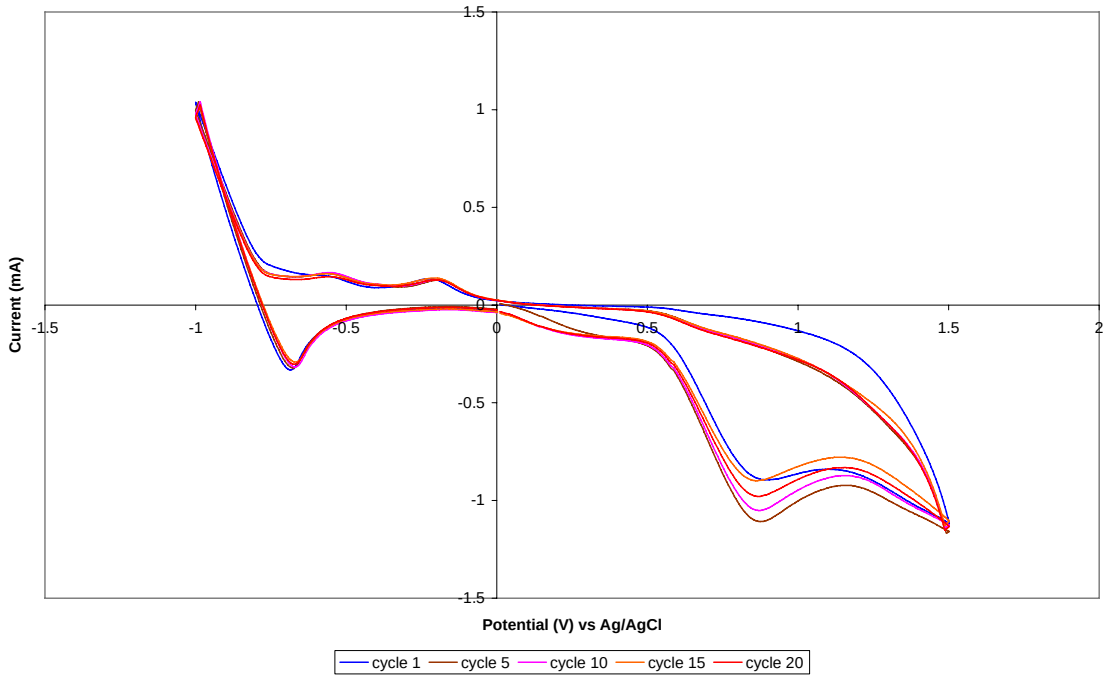

Figure 3.1. CV of 0.02 M l-dopa in borax buffer, scan rate 50 mV/s

In the subsequent cycle, a small peak appeared at 0.3 V vs Ag/AgCl which was attributed to dopachrome. In the first cycle this peak was not apparent as there was little dopachrome in solution, however in the subsequent cycles the peak increases until it reaches an equilibrium.

In the borax buffer, preoxidation of the dopa solution at higher current density with mechanical stirring improves film formation by increasing the initial concentration of dopachrome available for polymerisation, and therefore assisting in forming the initial melanin film (once mechanical stirring has been stopped) on the electrode. The preoxidation was visually monitored by the formation of a deep orange colour in the solution.

3.2.2. Carbonate Buffer

The carbonate buffer caused the solution darken significantly faster than with the borax buffer due to the slightly higher pH. It appears that in the carbonate buffer autooxidation of dopa occurs rapidly even without any applied potential. This means that unlike borax buffer, there was already a significant amount of dopachrome in the solution and therefore no preoxidation was required.

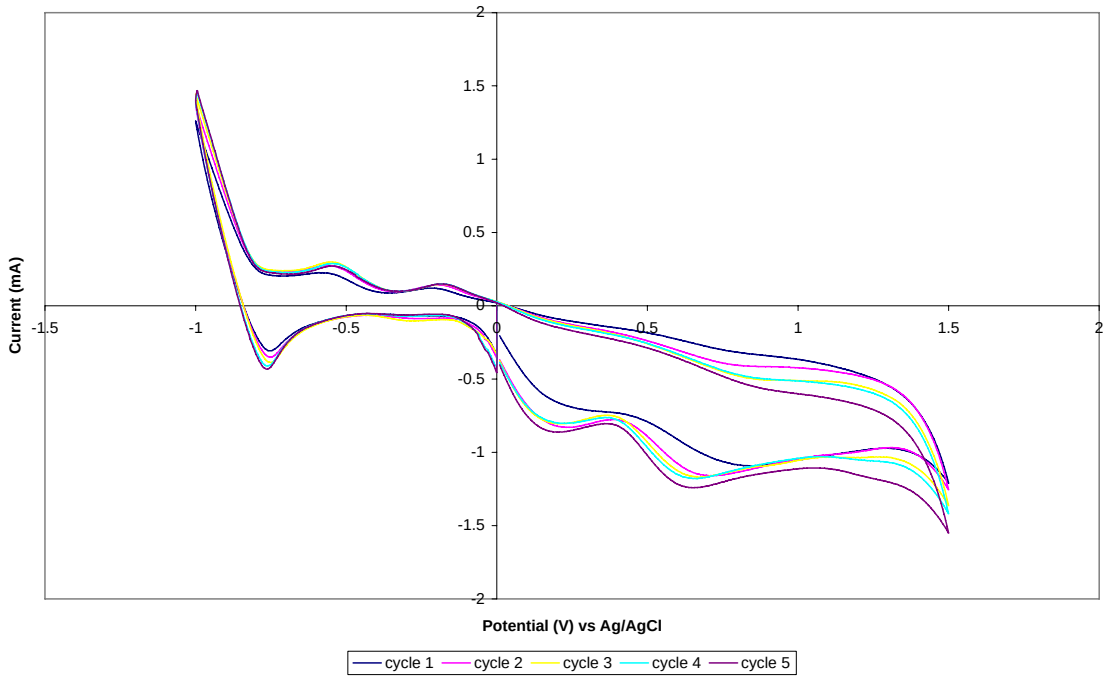

Figure 3.2. CV of 0.02M l-dopa in carbonate buffer (pH 10), scan rate 50 mV/s, solution degassed prior to analysis by bubbling nitrogen through the solution.

This was confirmed by CV (See Figure 3.2), where from the first cycle two oxidation peak in the CV at 0.2 and 0.7 V vs SCE could be observed corresponding to the oxidation of dopachrome and dopa respectively. The peak due to dopachrome was much more apparent compared to the CV of the solution in borax buffer since in this case the dopachrome was present in solution and not merely a product of the previous oxidation cycle. There was also two corresponding reduction peak present in all scans, in contrast to only one present when borax buffer was used. In the CV analysis the solution was degassed which slowed down initial dopachrome formation, however an orange colour still developed in the solution as the experiment were performed under normal conditions. This was reflected in the CV where the first cycle showed smaller peaks compared to the subsequent cycles.

3.2.3. Ammonia Buffer

When the ammonia buffer was used, rapid colouration of the solution was observed as soon as the dopa was added. This indicates that in the ammonia buffer the autooxidation

of dopa was proceeding at a faster rate than in the other buffer systems due to the more rapid colour evolution.

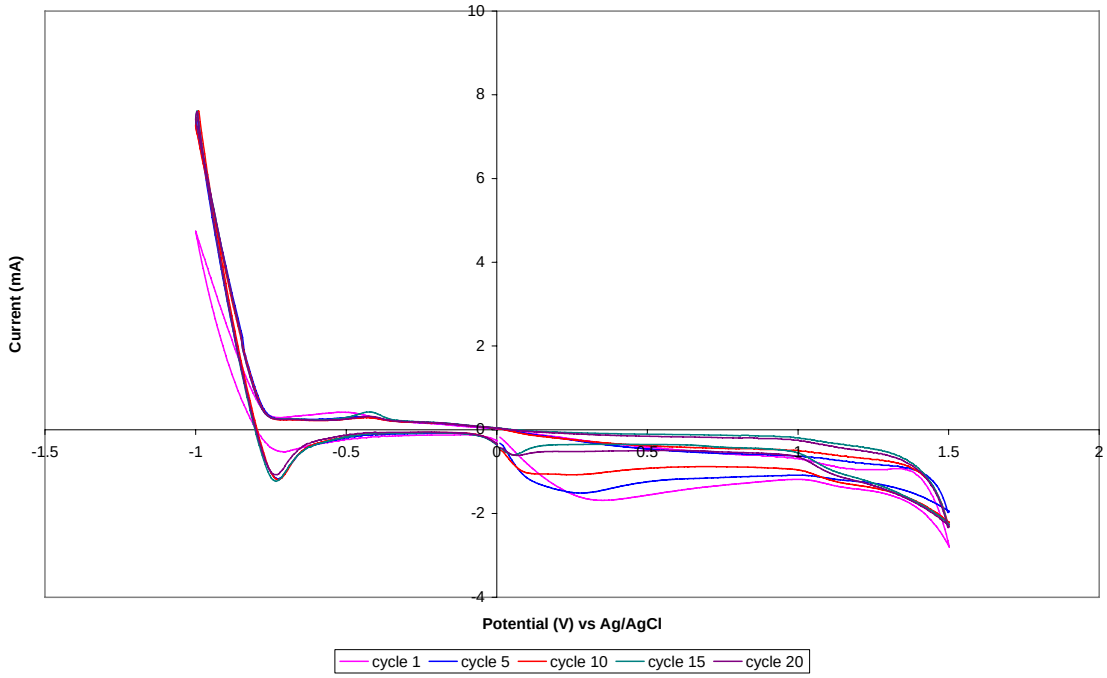

Figure 3.3. CV of 0.02M l-dopa in ammonia buffer (pH 10.5), scan rate 50 mV/s

The CV of l-dopa in ammonia buffer (see Figure 3.3) showed a lack of oxidation peaks. Unlike the CV of l-dopa in carbonate buffer (which shows both the dopa and dopachrome oxidation peak), the initial cycle shows a broad peak at 0.3 V, which weakens significantly upon further cycling, and eventually this peak also disappears, replaced by a very small oxidation peak around 0.07 V and a broad shoulder at 1.1 V. This indicates an oxidation of dopachrome during the initial cycles, and on repeated cycling the oxidation of dopa (peak at 1.1 V) can be observed.

This indicates that the autooxidation process in the ammonia buffer may be more dominant than the electrochemical oxidation. Thus the bulk of dopa in the immediate vicinity of the electrode was rapidly autooxidised into dopachrome, and hence the peak of dopachrome oxidation was greater than the peak due to dopa oxidation.

In the CV there was also a small peak at 0.07 V which could be due either to DHI or melanin. Since the peak was still present at lower scan rate (See Figure 3.4), it was most likely due to the melanin formed on the electrode surface rather than DHI. This was because at slower scan rate DHI would either oxidise into melanin during the forward scan or diffuse into solution, and its oxidation peak would not be observed in the subsequent scans. Furthermore, at the faster scan rate we also see a single, reversible reduction peak, which was similar to what has been observed previously in cases where melanin film has been formed.

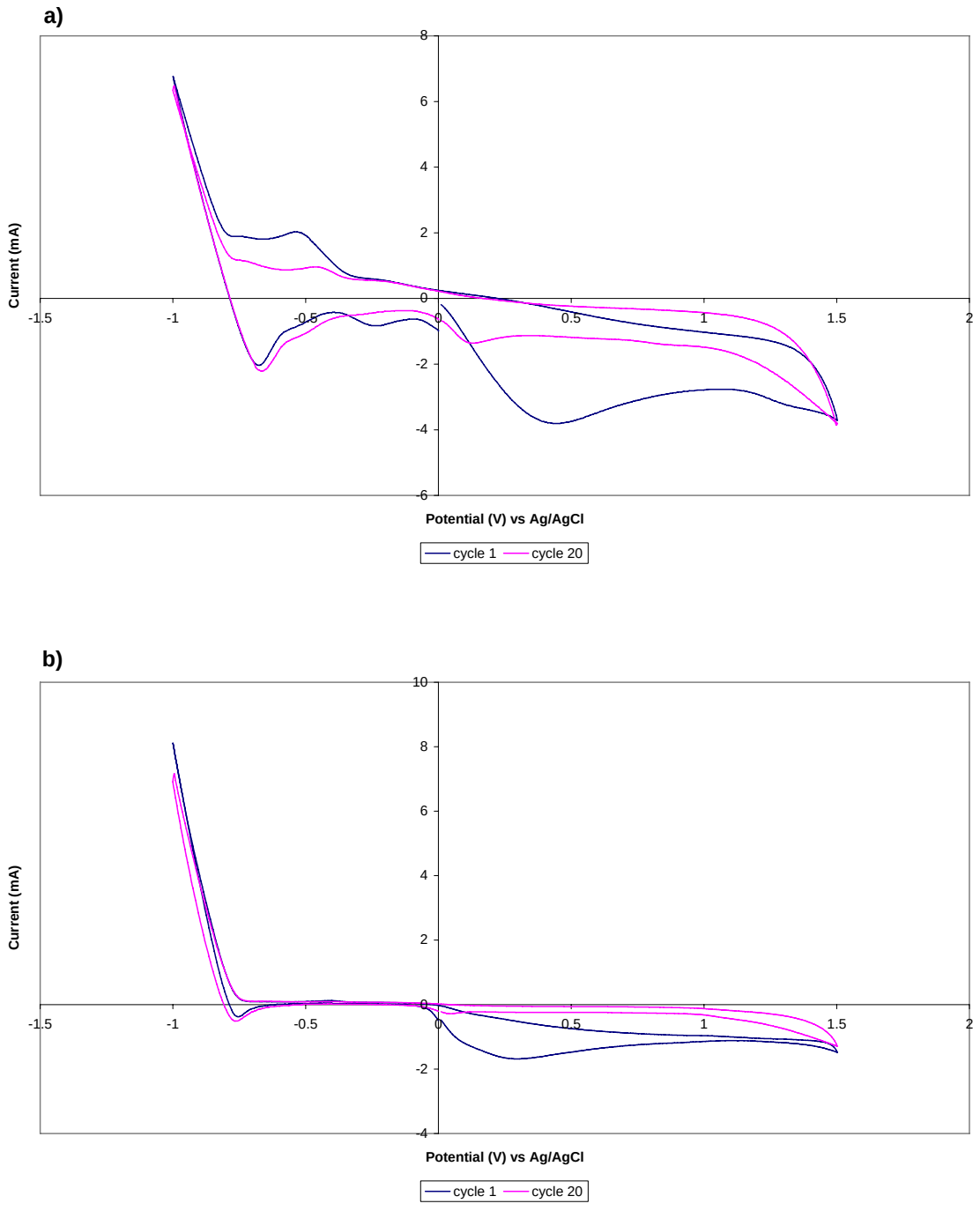

Figure 3.4. CV of 0.02M l-dopa in ammonia buffer (pH 10.5), scan rate of (a) 250 mV/s and (b) 10 mV/s

The lack of other peaks in the CV at latter cycles was due to the melanin film limiting diffusion of precursors onto the electrode surface. It appears that due to the higher pH film formation happens quite rapidly, in that sufficient amount of melanin has been deposited in 15 cycles (at a scan rate 50 mV/s) whereas with the borax and carbonate buffer at this stage the decay in peak current is still quite small. The polymer film would significantly lower the amount of dopa available for oxidation on the electrode surface, and hence the peak intensity decreases quite significantly. The peak at 0.07 V, however, being due to melanin, remains unaffected and hence was still present with the intensity practically unchanged after multiple cycles.

Despite the faster film formation, when ammonia buffer was used the film produced was notably thinner compared to the ones produced from borax and carbonate buffer, with less of the paste-like material on the side exposed to the solution. This indicates that the lower molecular weight species was still soluble in the ammonia buffer whereas they would have precipitated out in the borax buffer.

Since the autooxidation process proceeds quite rapidly in ammonias buffer there was also a significant amount of melanin being formed in solution. Degassing the solution did slow down the oxidation process, however since the intermediates have sufficiently long lifetime to diffuse away from the electrode melanin would still form in solution even when it was degassed.

When ammonia buffer was used, a thin film of melanin was also formed at the surface of the solution regardless of applied potential. This film has little to no mechanical integrity and will disintegrate upon physical contact and therefore could not be extracted. This surface layer formation was due to the slow but constant evaporation of ammonia from the solution, creating a region of lower pH on the surface of the solution. This causes the precipitation of melanin on the surface, forming the thin film observed.

Upon physical contact or stirring this surface layer redissolves into the bulk solution indicating that the melanin forming this layer consists mainly of low molecular weight

species since it was soluble in the polymerisation solution at which pH the film on the electrode was precipitated.

3.2.4. Triethanolamine Buffer

When triethanolamine buffer was used, film formation did not occur. The reason for this is still unclear, since there was visible colour evolution upon standing but the orange colour indicative of dopa autooxidation did not develop as rapidly as when the carbonate or ammonia buffer was used. This was also true when potential is applied, indicating that the oxidation of dopa is slower in the triethanolamine buffer system compared to other buffers.

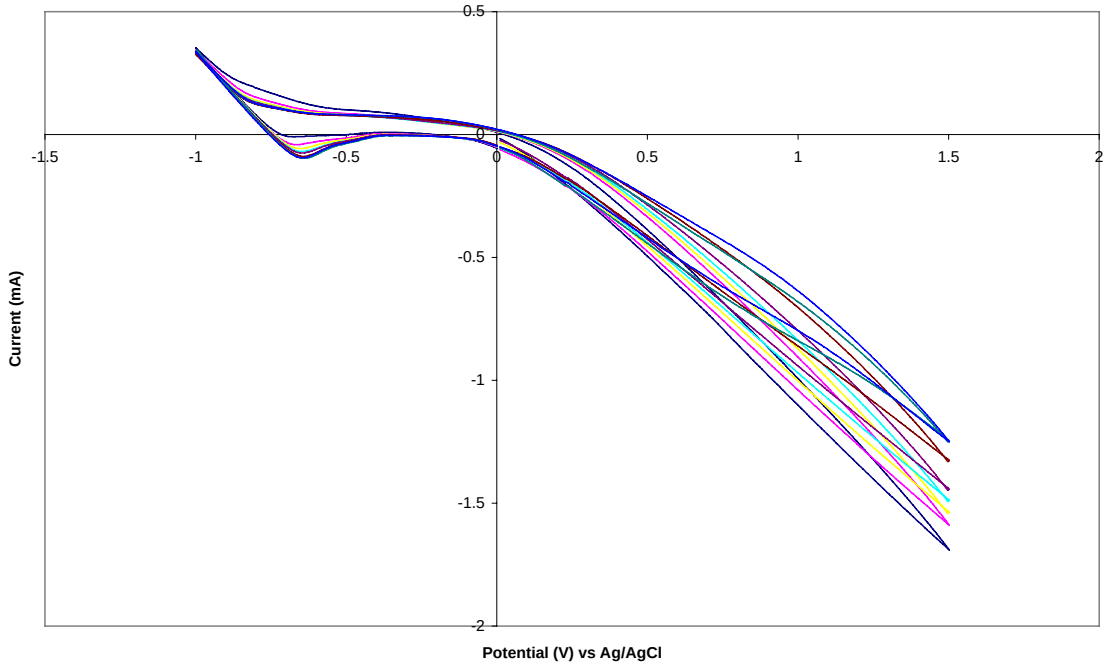

Figure 3.5. CV of 0.02M l-dopa in Triethanolamine buffer (pH 10), scan rate 50 mV/s

The CV of dopa in triethanolamine (See Figure 3.5) did not show any oxidation peak. There was some colouration observed near the electrode which meant that some of the dopa was oxidised into dopachrome, but this did not show as a peak in the CV. Analysis of a triethanolamine solution (without dopa) showed a very similar CV, therefore it appears that there was little dopa present on the electrode surface.

This may be due to triethanolamine being a strong complexing agent. The triethanolamine may have complexed the metallic electrode surface and form a layer that prevents diffusion of dopa or other melanin intermediates.

3.2.5. SEM Analysis

The use of different buffer system does have some effect on the morphology of the polymer film, but this was more likely due to the pH of the buffer rather than the difference in buffer salts incorporated as counterions, as the higher pH buffers produce rougher films.

At first it appears that both borax and carbonate buffer produces smooth, continuous melanin films, however, SEM investigation (See Figure 3.6) showed that the melanin synthesised from borax buffer has a smoother morphology compared to the one synthesised from carbonate buffer, resulting in lesser cracks and irregularities. This is attributed to the slightly higher pH of the carbonate buffer dissolving the lower molecular weight species of melanin whereas they would precipitate in the borax buffer.

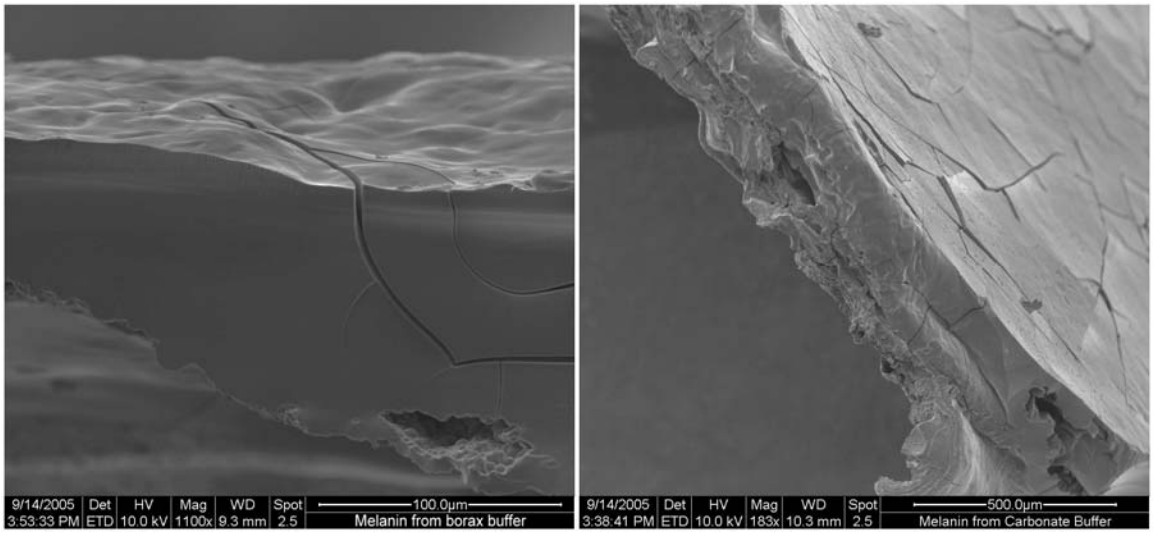

Figure 3.6. SEM images of the cross section of melanin film synthesised from borax (left) and carbonate buffer (right). Both films were synthesised from 30 mM l-dopa solution in their respective buffer at a current density of 0.5 mA/cm^2 for 8 days.

The melanin synthesised from the ammonia buffer showed the greatest difference, with a more porous, irregular structure (See Figure 3.7), and possessing poor mechanical properties, being brittle and crumbly. The SEM images showed large pores within an irregular, granular polymer structure, but without the underlying smaller spherical units found by Zeise et al[173] and Nosfinger et al[168].

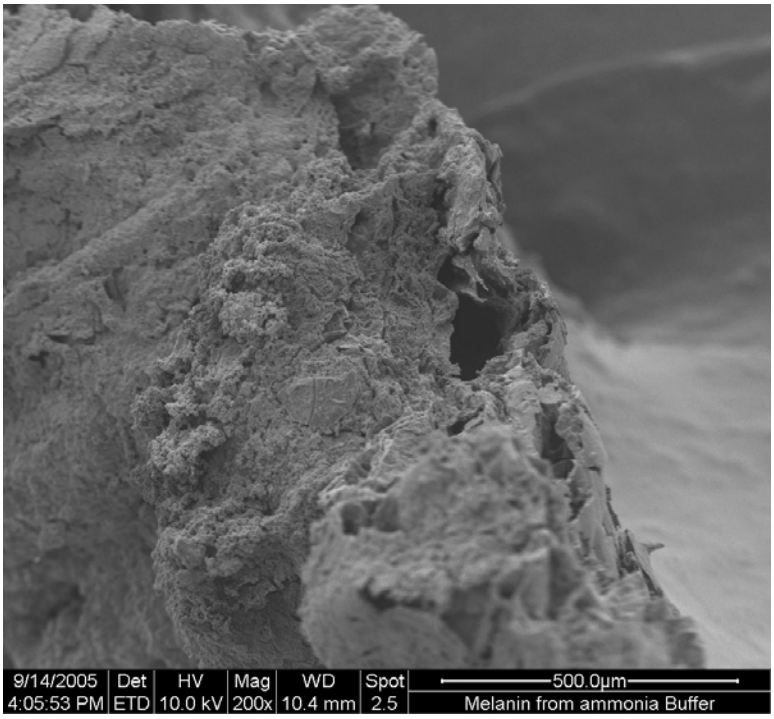

Figure 3.7. Melanin film synthesised from ammonia buffer. Film synthesised from 30 mM l-dopa solution at a current density of 0.5 mA/cm^2 for 8 days

Despite the porous, irregular structure, the lack of a granular microstructure indicates that although the bulk structure shows some dependence on pH, the underlying structure of all the electrochemically synthesised melanin was continuous and not granular as observed with natural and chemically synthesised melanin. This means that the granular microstructure of the natural melanin was likely due to the way it was synthesised within the melanosome and not a property of the polymer itself.

Looking at the morphology of these films, it appears that borax buffer was the best choice for electropolymerisation as it produces the smoothest film. It appears that by keeping the

pH slightly lower the polymer was better precipitated out of the solution and hence a smoother film was obtained.

Theoretically, at higher pH the electropolymerisation would proceed at a faster rate and therefore film formation would be more efficient. However, it appears the higher pH also causes the melanin to be more soluble, resulting in a more hydrated material and also more irregularities in the polymer film after drying.

3.2.6. XPS Analysis

In this work it was determined that the best buffer to use was the borax buffer and the carbonate buffer. Since they have a similar pH range, they yield similar materials. The carbonate buffer was thought to have facilitated autooxidation better due to the slightly higher pH than the borax buffer, and this may result in the carbonate buffer producing a more oxidised material with a greater amount of quinones (and perhaps some quinone-imines).

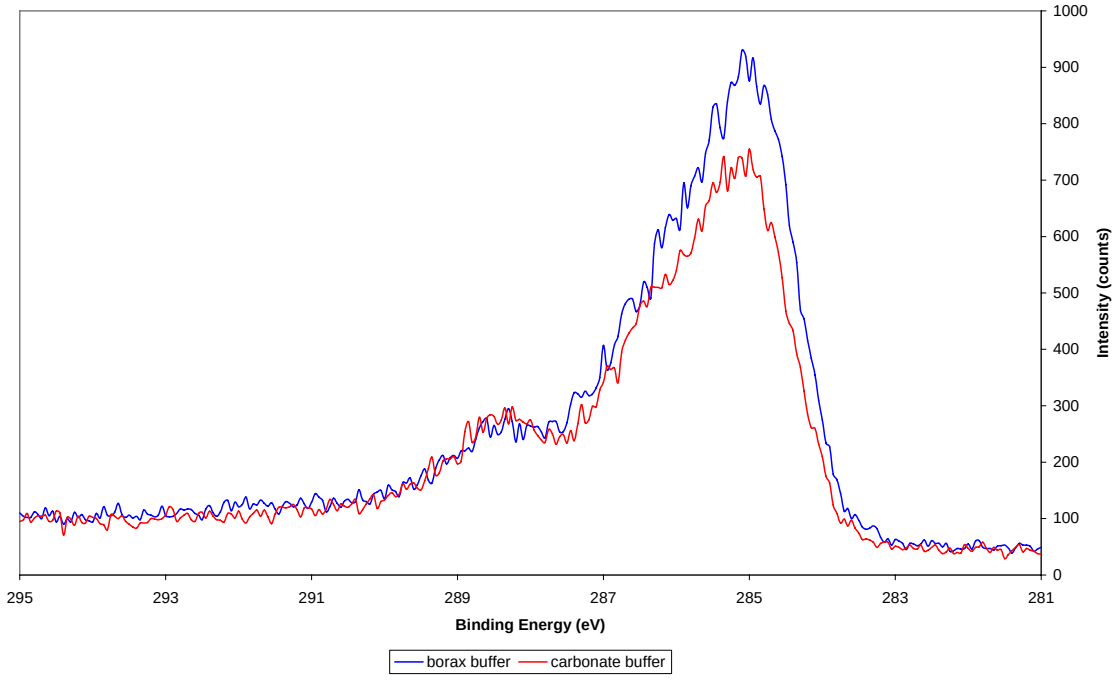

Figure 3.8. C 1s spectra of melanin samples (electrochemically synthesised from 30 mM l-dopa at 0.5 mA/cm^2 for 8 days) from borax and carbonate buffer.

The C1s spectra (See Figure 3.8) of melanin synthesised in borax and carbonate buffer did not show any significant differences. The difference in pH of the buffer would more likely affect the oxidation state of the material, however since the chemical shift for the C-O and C=O bond are very close together the effect on the C1s spectra would be minimal.

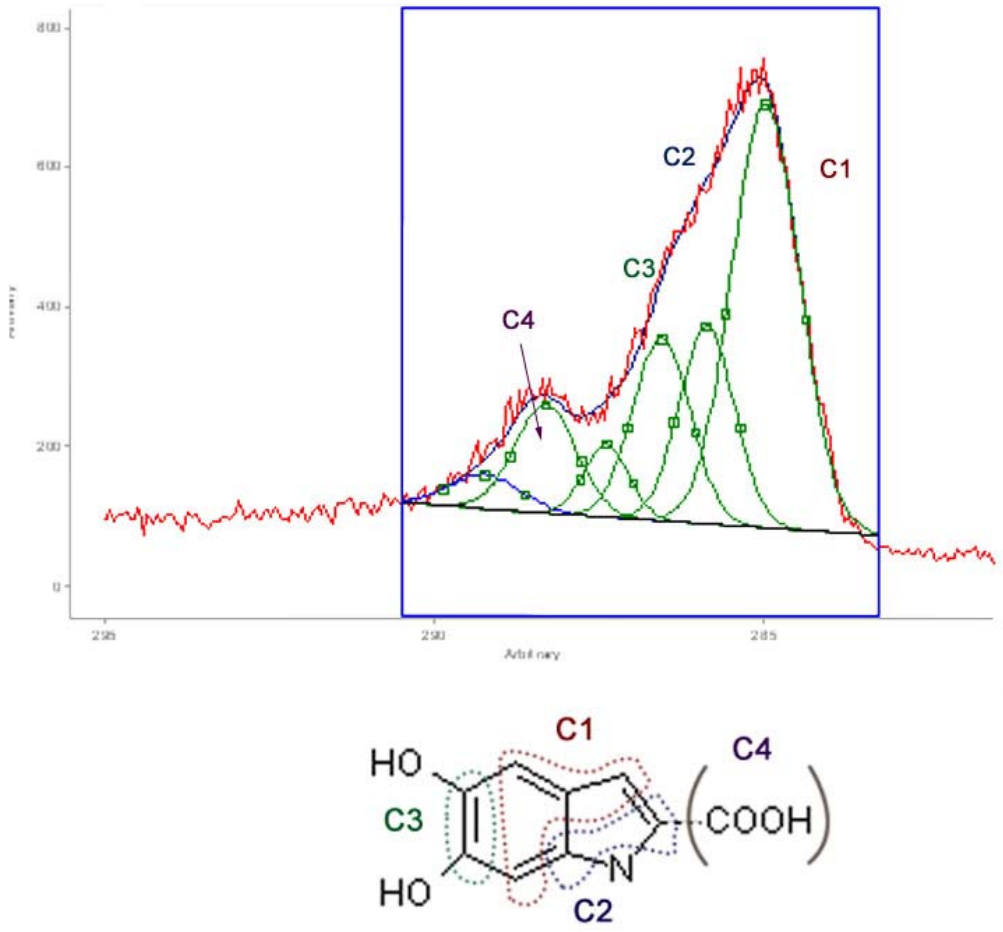

Figure 3.9. Peak fitting of the XPS C1s spectra for melanin synthesised from carbonate buffer

Peak fitting of the C1s spectra (See Figure 3.9) showed that the melanin synthesised from carbonate buffer was quite similar to the ones synthesised from borax buffer (Section 2.4.4). The amount of dopa present in the two samples was quite similar, since they

should be determined by the synthetic method rather than solution pH. The main difference in the two samples is that the amount of DHICA (indicated by C4) was larger in the sample synthesised from carbonate buffer, and therefore it appears that the faster oxidation in carbonate buffer led to a material with a higher DHICA content.

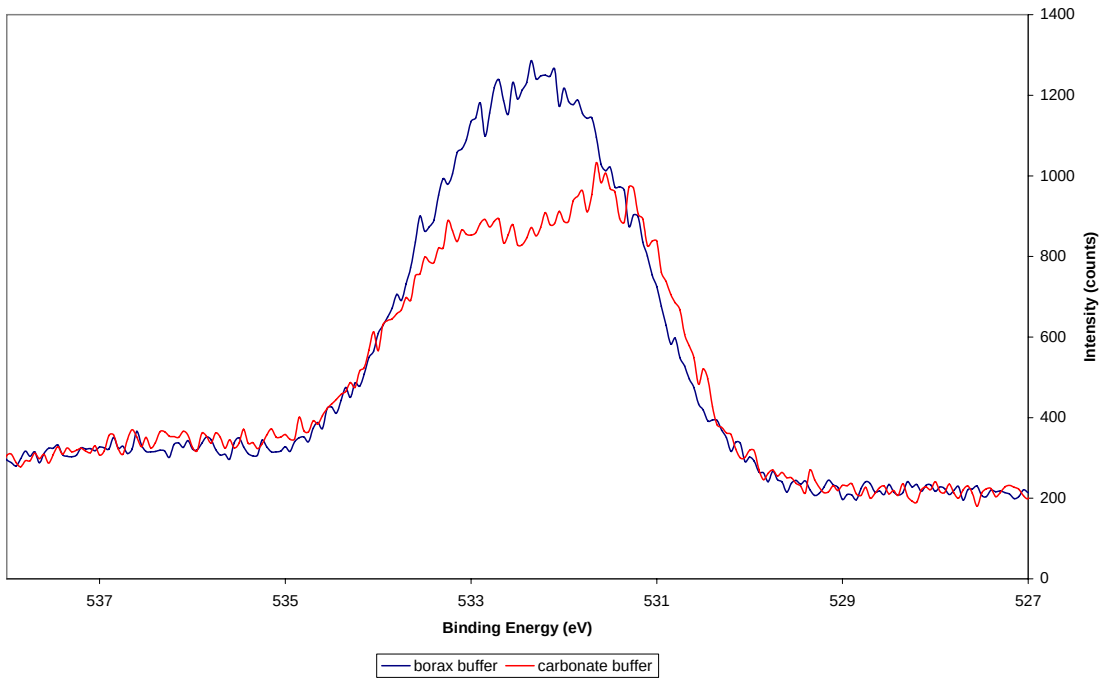

Figure 3.10. O 1s spectra of melanin samples (electrochemically synthesised from 30 mM l-dopa at 0.5 mA/cm^2 for 8 days) from borax and carbonate buffer

Unlike the C 1s spectra, The O 1s spectra (See Figure 3.10) showed distinct differences between the two samples, with the melanin from carbonate buffer producing a peak that appears split compared to the melanin from borax buffer. There was no shift in the actual peak position, as the chemical species remain the same. However, peak fitting of the two peaks (See Figure 3.11) showed that no significant differences in the oxidation state of the sample exist.

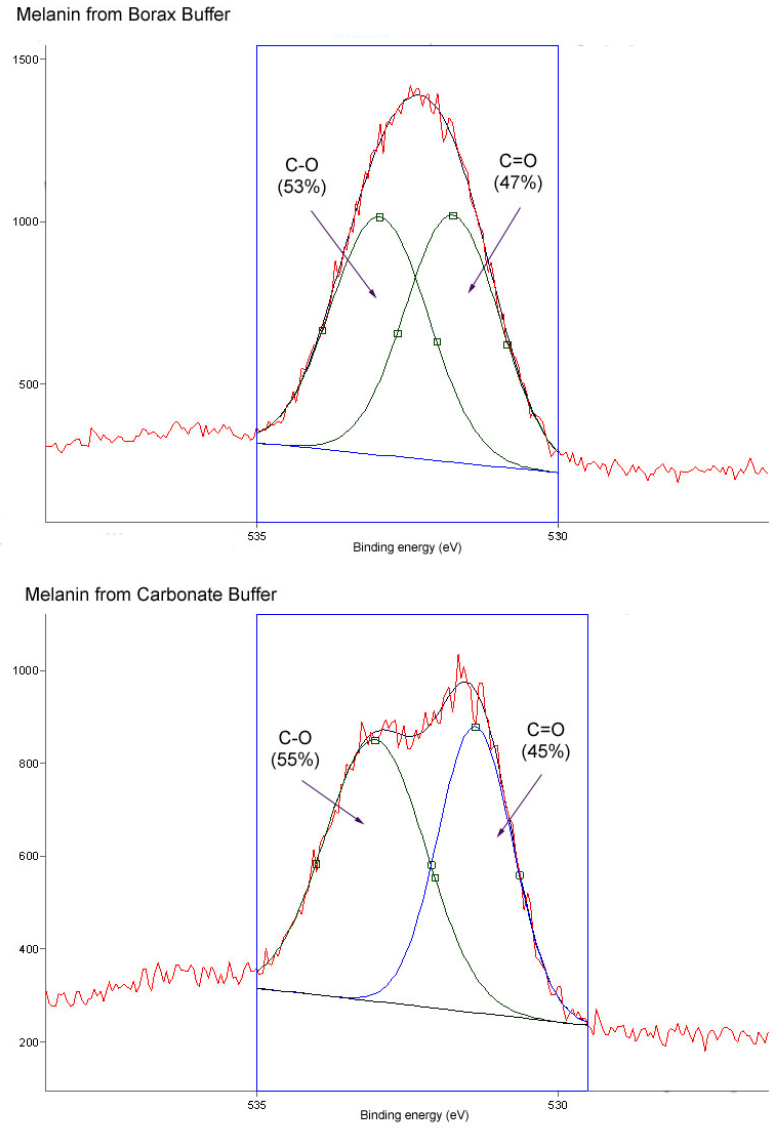

Figure 3.11. Peak fitting of the O 1s spectra of melanin electrochemically synthesised from borax and carbonate buffer.

As the peak fitting shows, despite the difference in the appearance of the peak the percentage of single to double bonded oxygen in the two samples were quite similar, with both exhibiting a slight excess of double bonded oxygen. The sample synthesised from borax buffer did show a slightly higher oxidation state (increased quinone content as indicated by the higher amount of double-bonded oxygen), however the difference between the two was only 2%. Swan[101] previously postulated that the ratio of quinone to dihydroxy units in melanin is roughly equal, and our result supports this theory.

Regarding the peak fitting, small differences may have resulted from other unaccounted factors such as the assumption that DHI is the sole monomer unit present and no contributions of leftover dopa or DHICA were considered. Some of the double-bonded oxygen would also be due to the buffer salts, however since the concentration of the buffer incorporated in the material are generally quite low (<2% based on elemental analysis) they are unlikely to have any significant impact on the XPS spectrum. Furthermore, since the two buffers were quite similar (BO_3^- and CO_3^{2-}) their effect would be quite similar in both samples.

3.2.7. Conductivity Measurements

The conductivity was measured by means of IV curves (See Figure 3.12), and the resultant value (See Table 3.1) was significantly lower than previous conductivity value measured under ambient conditions[171], being about 2 or 3 orders of magnitude less. This lowered value is expected, as previous measurements were done under ambient conditions, and it has been well documented that the conductivity of melanin is greatly affected by humidity.

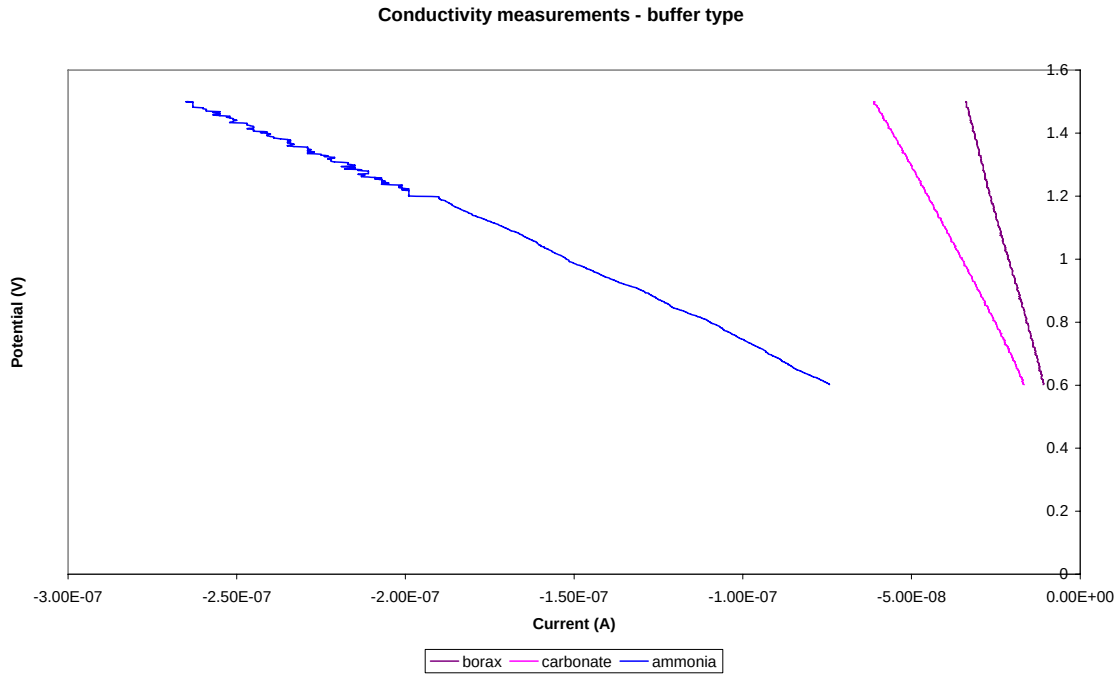

Figure 3.12. I-V measurements of melanin films made by electropolymerisation of 0.02M l-dopa in various buffer solutions. Measurements done over silica gel in a desiccator. The current notation in the graph was negative as it was an oxidative current, and for the purpose of conductivity measurement the absolute value of the slope was taken as the resistance.

Buffer (pH)	Conductivity (Scm^{-1})
Borax	$1 \pm 2 \times 10^{-8}$
Carbonate	$1 \pm 1 \times 10^{-7}$
Ammonia	$2 \pm 2 \times 10^{-7}$

Table 3.1. Conductivity value of melanin synthesised from different buffer solutions, measured in a dry atmosphere.

Unexpectedly, melanin synthesised from ammonia buffer showed the greatest conductivity value despite being the most morphologically irregular based on the SEM

analysis. Since the measurements were performed in a desiccator under a dry atmosphere, it shouldn't be affected by water content in the atmosphere. However, in this analysis the sample was measured by sandwiching the film in between two conducting glass plates, and thus it may not have taken into account the morphology of the film. The melanin synthesised from ammonia buffer (having the highest pH) would most likely have a higher average molecular weight compared to the ones synthesised from the other buffers since species that were insoluble in the borax and carbonate buffer would still be soluble in the ammonia buffer.

Another possibility is that although the experiment was done in a desiccator, it was not done under vacuum and thus some tightly bound water might have remained in the material. Thus, the samples may not have been sufficiently dried, and the more porous material synthesised from ammonia may have higher water content than the other samples.

Therefore, rather than measurement in dry (but not vacuum) condition, a better indication might be a measurement done in a constant humidity. This would also provide us with a higher value compared to the vacuum conductivity which can be more accurately measured within our instrumental limitations (as melanin has been shown to be an insulator under vacuum). As previous measurement showed that the conductivity remain relatively unchanged up to 43% humidity, it was decided to measure the conductivity at this humidity, and Table 3.2 below listed the results of conductivity measurements performed after the samples have been left overnight at 43% humidity.

Buffer	Conductivity
Borax	$(5 \pm 2) \times 10^{-7}$
Carbonate	$(8 \pm 3) \times 10^{-8}$
Ammonia	$(1 \pm 2) \times 10^{-7}$

Table 3.2. Conductivity (at 43% humidity) of melanin synthesised from different buffers.

At 43% humidity the melanin synthesised from borax buffer was the most conductive, and the other two samples showed little change inconductivity which indicates that they may have been more hydrated in the previous measurement. However, there was quite a large error in the values, and overall there was little difference in the conductivity between the three samples. The small differences were likely due to the morphology of the film, with the borax buffer being the most conductive as it provided the smoothest film, while the conductivity values obtained from the carbonate buffer and ammonia buffer were quite close to each other.

3.3. Addition of PEG

For our study, we chose to attempt to introduce PEG into the electrochemical synthesis mainly due to water solubility, availability, and the fact that a similar previous study has been done. The main difference would be that in the Ishii study[188], the melanin was incorporated into PEG chemically, while in our study we would attempt to incorporate PEG into melanin during the electrochemical synthesis.

3.3.1. Electrochemical Analysis

CV of dopa-PEG solution (See Figure 3.13) showed that the PEG itself was not involved in the oxidation process. There were no new peaks in the CV of dopa-PEG, indicating that the PEG did not undergo oxidation under the conditions used, and was therefore unlikely to form a chemical bond with the melanin. The dopa and the dopachrome oxidation were still visible, and there was no significant decay in peak current which meant that the rate of film formation was not affected.

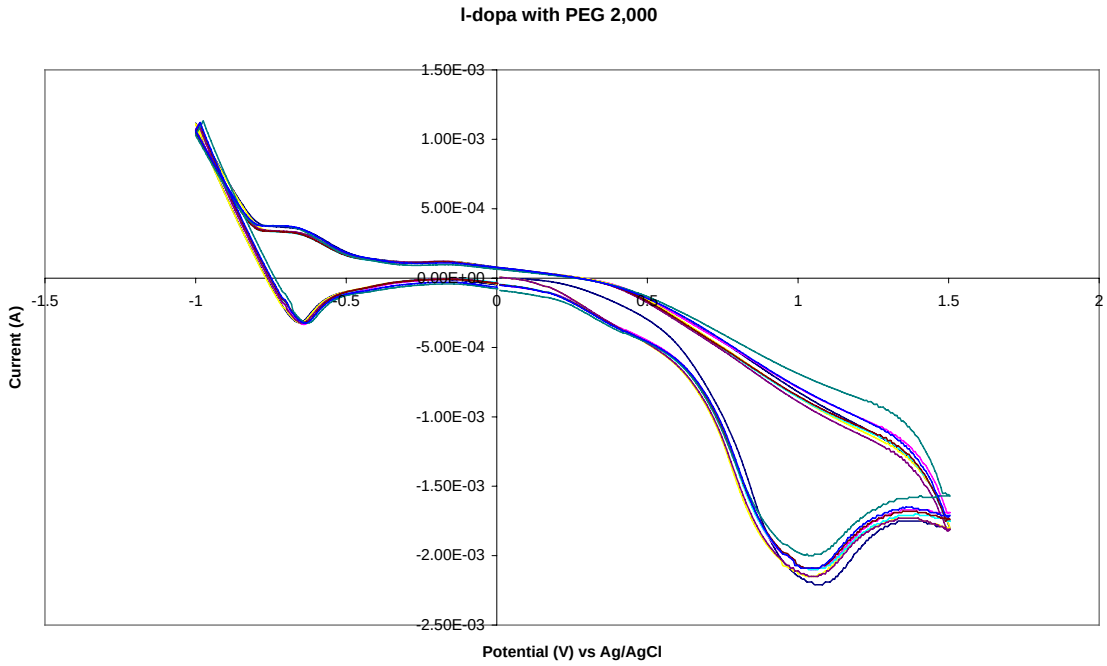

Figure 3.13. CV of 0.02M l-dopa in borax buffer with 0.1 mM of PEG (average m.w. 2,000) added. Scan rate 50 mV/s

Using PEG of a higher molecular weight did seem to alter the CV (see Figure 3.14) in that the slope of the oxidation peak was steeper with a slight shoulder at 0.7 V vs Ag/AgCl. The dopa oxidation peak seems to have shifted from 0.9 V to 1.1 V vs Ag/AgCl, and the shoulder on 0.7 V may have been due to the dopachrome peak experiencing a similar shift. The shift in peak potential may have been caused by the higher molecular weight PEG lowering the diffusion rate of molecules to and from the electrode surface.

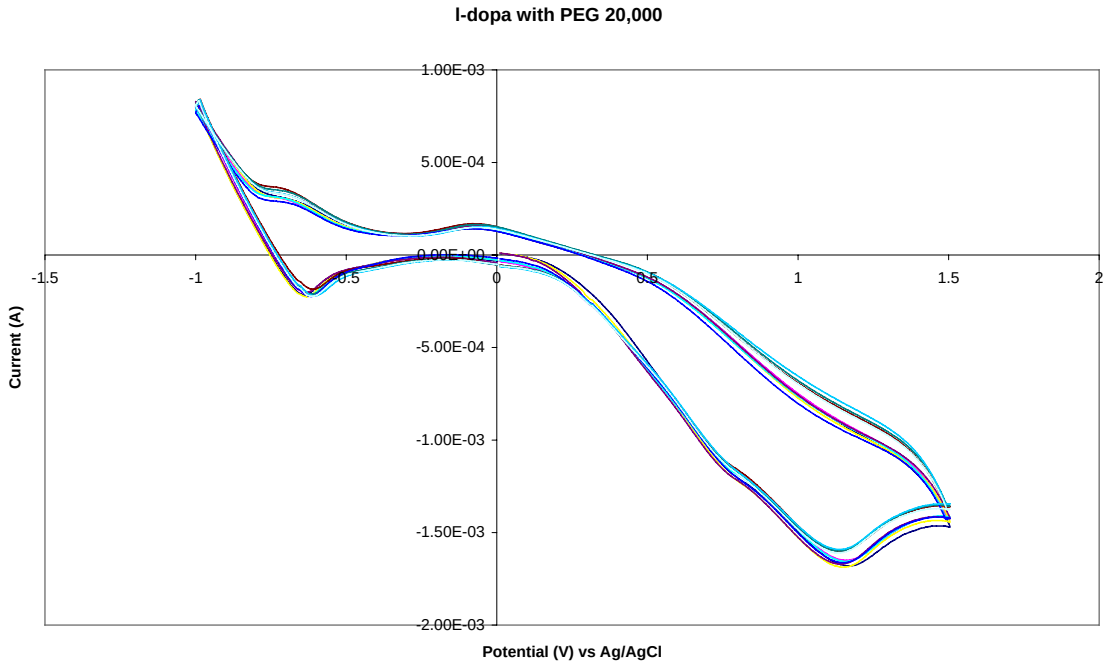

Figure 3.14. CV of 0.02M l-dopa in borax buffer with 0.1 mM of PEG (average m.w. 20,000) added. Scan rate 50 mV/s

Reducing the scan rate of the CV to facilitate film formation indicates that PEG has been incorporated into the material as observed with the significant decay in peak current. Increasing the concentration of PEG also led to a larger decay in peak current (see Figure 3.15).

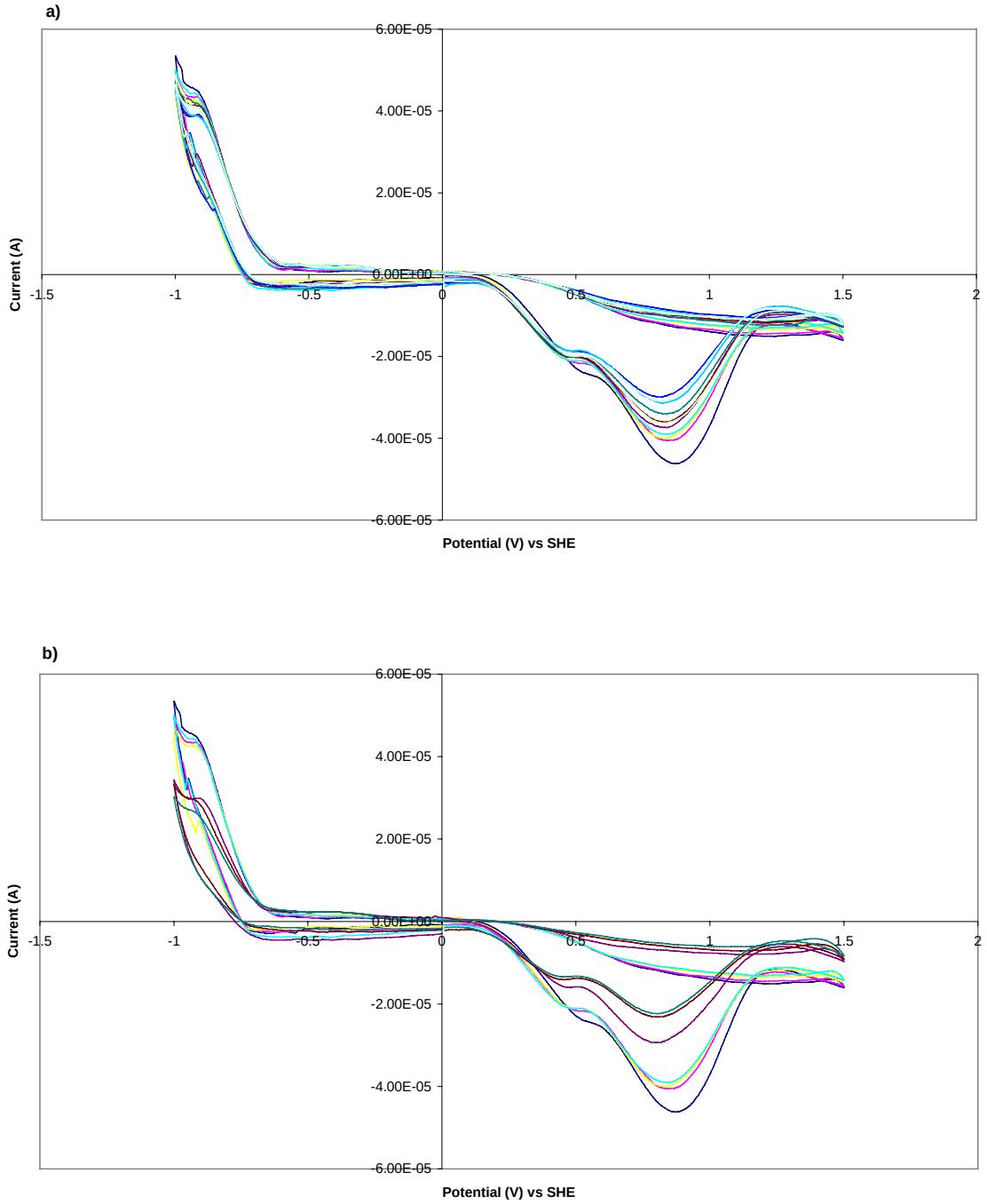

Figure 3.15. CV of 0.02M l-dopa in borax buffer with PEG (average m.w. 2,000) added with concentrations of a)0.1 mM b)1 mM ; scan rate 10 mV/s, experimental setup referenced to the counter electrode.

As can be seen from the CV, when a higher concentration of PEG was used the peak current drops more rapidly. This dependence of the peak current decay on the concentration of added PEG indicates that it was the diffusion process controlling the rate, therefore the amount of PEG that gets incorporated in the melanin film would be a function of the concentration of PEG in solution.

In the end, although our analysis showed the PEG was incorporated into the melanin films they did not exhibit significantly greater mechanical properties compared to the non PEG samples and the dried polymer was still very brittle. It appears that although a significant amount of PEG has been incorporated into the material, it was not sufficient to impart extra mechanical strength and malleability into the material.

3.3.2. SEM Analysis

Interestingly, unlike the addition of dopant counterions, the addition of PEG seems to have a more pronounced effect on the morphology of the film. The PEG-melanin composites showed a porous structure, not unlike the films synthesised from ammonia buffer (See figure 3.16). However, unlike the irregular bulk of the ammonia melanin, the melanin PEG-composite form as a distinct film and were not as irregular, with several sheets being observed in the cross section of the film.

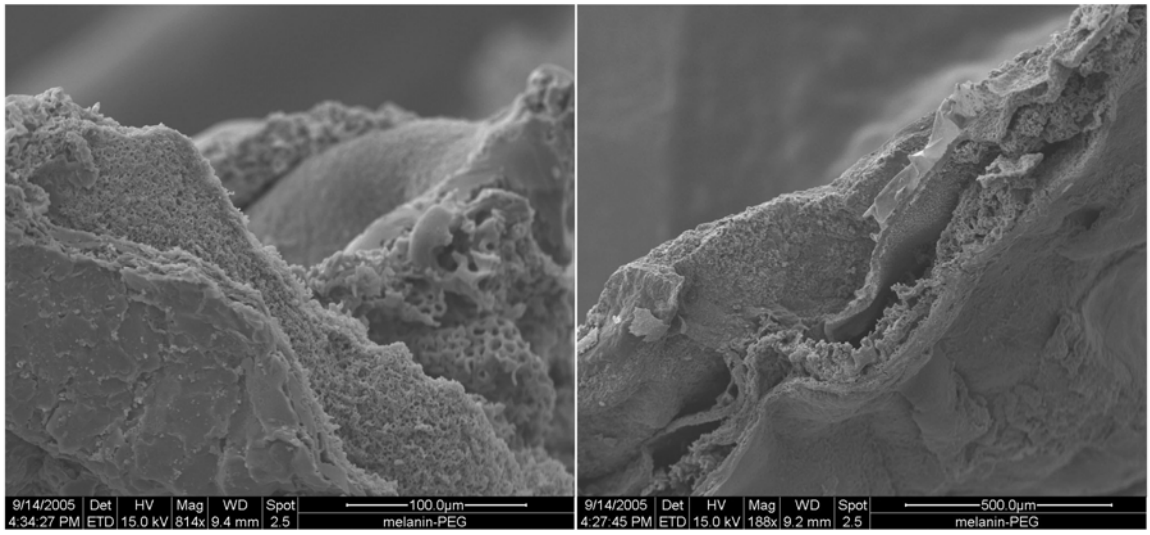

Figure 3.16. SEM image of melanin film electropolymerised from a 30 mM l-dopa solution containing 0.1 mM PEG (average m.w. 20,000)

This may be caused by a difference in solubility between the melanin and the PEG. Even if the PEG did not have a direct effect on the solubility of melanin it would have an effect on the drying process, as it may result in more water being adsorbed in the material.

3.3.3. XPS Analysis

XPS study of the PEG-melanin composite showed that PEG was incorporated into the material. This was evident from the C 1s spectra (See Figure 3.17), with a significant shift towards the C-O peak due to the presence of PEG. In the sample with PEG added, the major peak in the spectrum was now the one at 286.5 eV (indicative of carbon-oxygen bond), while in the control sample the main peak remained the one at 285 eV (indicative of carbon-carbon bond).

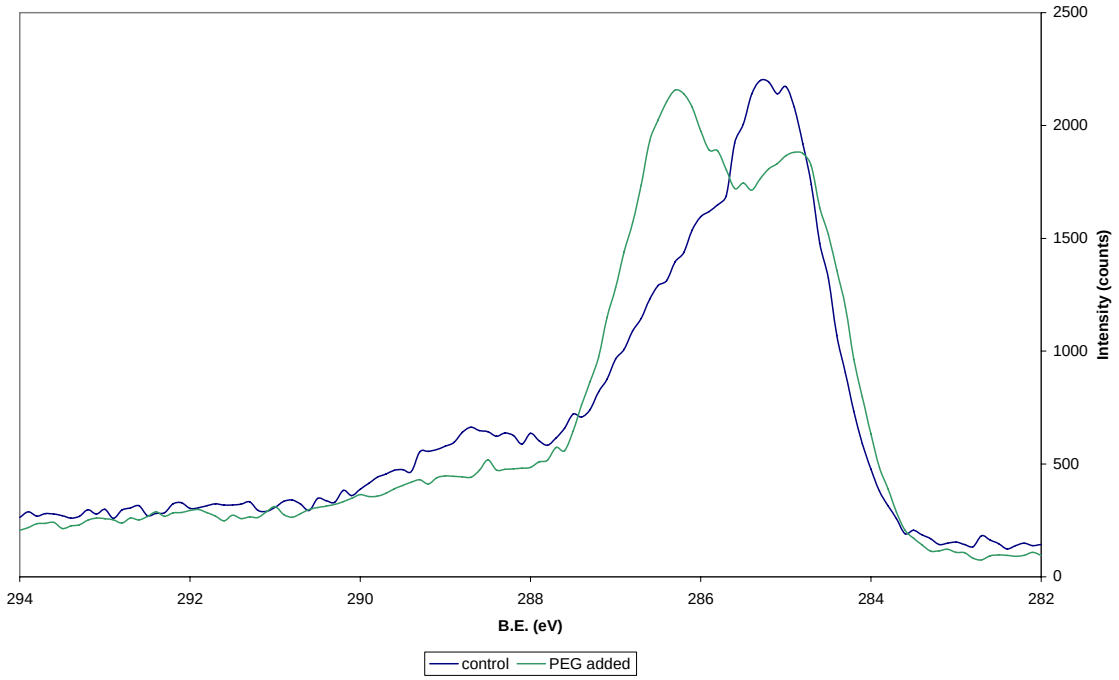

Figure 3.17. XPS C1s spectra of melanin-PEG composite made by electropolymerisation of a solution of 30 mM l-dopa and 0.1 mM PEG in borax buffer.

In the C 1s spectra the control sample also exhibited a broader "shoulder" on the higher binding energy side, which indicates a higher percentage of carboxylic acid in the material. This was because assuming the same percentage of DHI:DHICA and leftover dopa in both samples, the overall carboxylic acid ratio of the sample with PEG added would decrease since the PEG did not appear to react or become oxidised to affect the actual carboxylic acid content of the material.

Peak fitting of the C1s spectra (See Figure 3.18) confirmed the large increase of the C-O content of the material. The percentage of carbon-oxygen bond in the material has increased to 31% compared to the expected amount of 25 % in samples with no PEG content (assuming that the material contains only DHI monomer unit). This indicates that a significant amount of PEG has been incorporated in the material. However, as mentioned before, this figure was only an estimate, and not a quantitative analysis on the amount of PEG incorporated.

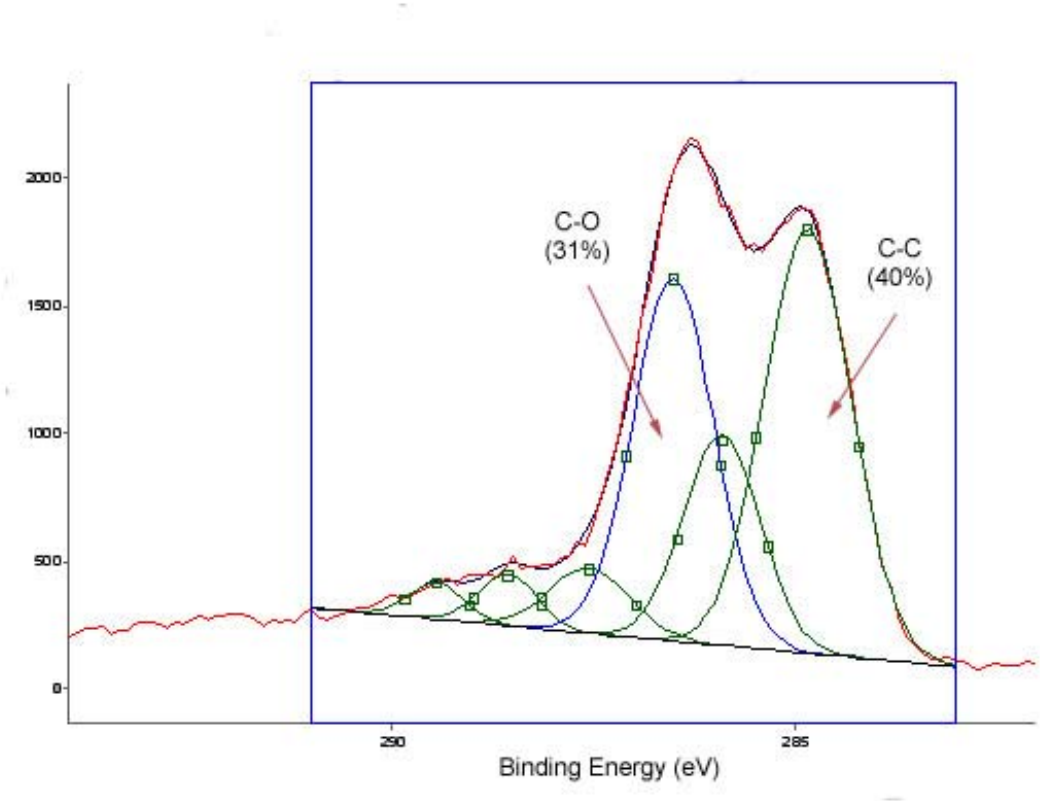

Figure 3.18. Peak fitting of the C1s spectra of the melanin-PEG composite.

The incorporation of PEG was also reflected in the O1s spectra (See Figure 3.19) where the melanin-PEG composite showed a tendency towards the higher binding energy indicative of an increased amount of single-bonded oxygen. Since the sample was prepared with the same electrochemical parameters as the control sample, the excess C-O would be due to PEG and not to a change in the oxidation state of the material.

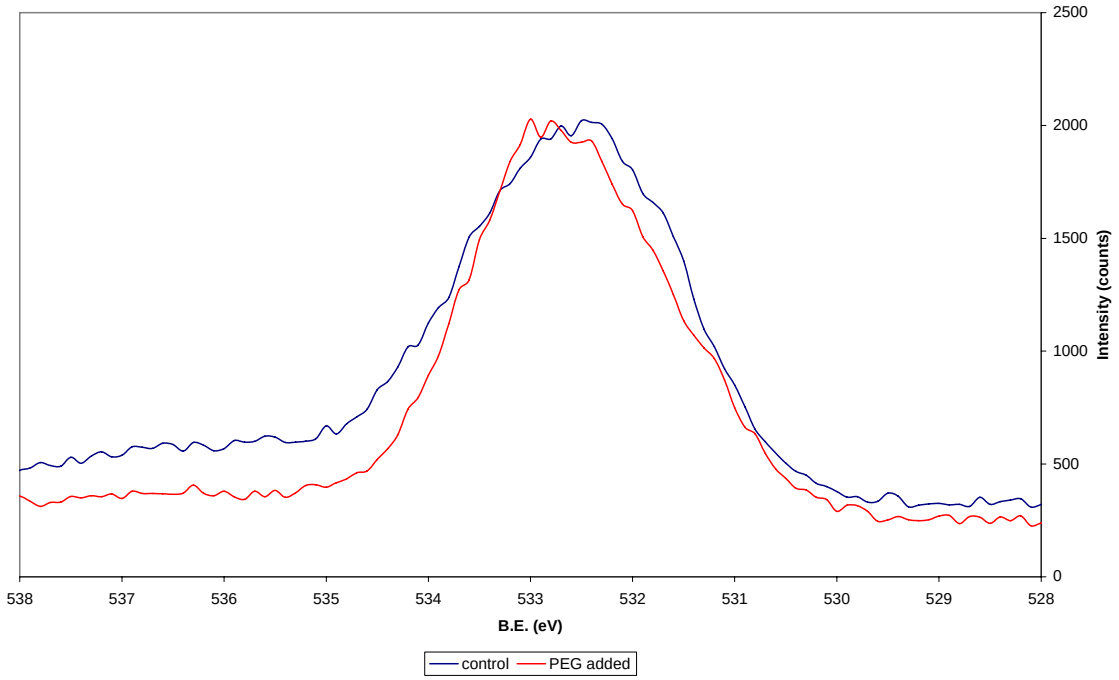

Figure 3.19. O1s spectra of melanin and melanin-PEG composite made by electropolymerisation of a solution of 30 mM l-dopa and 0.1 mM PEG in borax buffer.

Peak fitting of the O1s spectrum of the PEG-melanin (See Figure 3.20) confirmed that the melanin-PEG composite had a much higher percentage of single-bonded oxygen, which would be due to the presence of PEG. The electropolymerised melanin showed a 53:47 ratio of single to double bonded-oxygen while in the melanin-PEG composite this ratio had increased to 63:37 due to the ether linkages of the PEG.

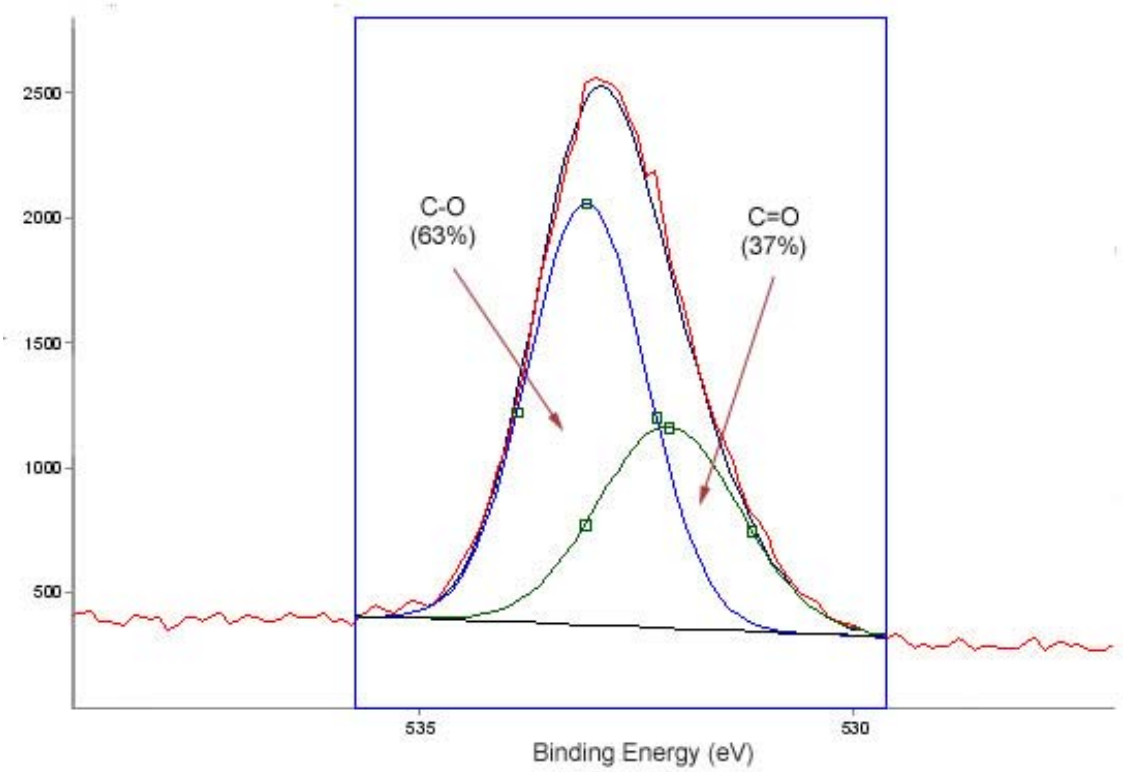

Figure 3.20. Peak fitting of the O1s spectrum of the melanin-PEG composite

Overall, it appears that PEG has been incorporated in the material, as there was a significant increase in the amount of C-O bonds in the material. However, based on our previous electrochemical investigation, it was most likely only incorporated as fillers and were not chemically bound to the melanin as it appears to be inert in the potential range where dopa oxidises.

3.4. Addition of Organic dopant

3.4.1. Electrochemical Analysis

The addition of the dopant itself did not have any effect on the dopa oxidation (See Figure 3.21). No change to the dopa oxidation peak when p-toluenesulfonate was present could be observed. This indicates that the dopant was merely present as an electrolyte, and did not have any effect on the electrochemical oxidation process.

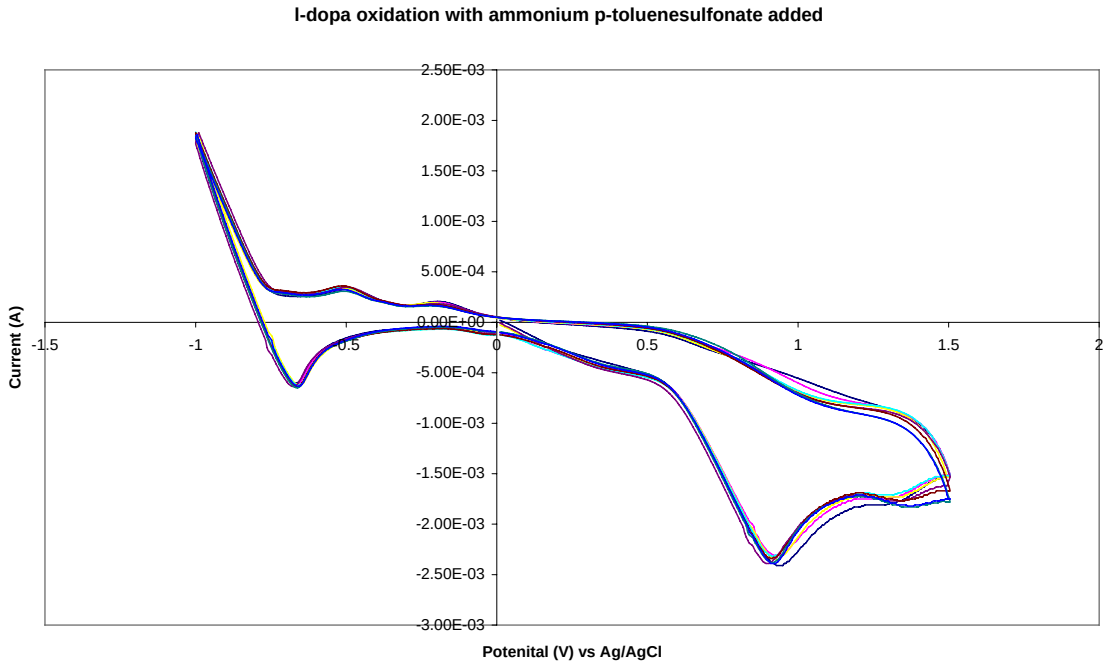

Figure 3.21. CV of 0.02M l-dopa in borax buffer with 0.005M ammonium p-toluenesulfonate added, scan rate of 50 mV/s.

When these organic dopants were used in the electrochemical synthesis, the resultant polymer seems to have poorer mechanical properties, and appeared to be formed of thin layers that flaked off quite easily (Section 3.4.2). This flaky layer was more apparent at higher dopant concentration of 10 mM or more, whereas films synthesised using dopant concentration of 5 mM or less showed reasonable mechanical integrity.

3.4.2. SEM Analysis

When p-toluenesulfonate was added into the dopa solution in borax buffer, the resultant melanin film was found to exhibit more sheet-like structure compared to those synthesised from borax buffer alone, with sheets visibly seen flaking off the film (see Figure 3.22). At first it was thought that the p-toluenesulphonate, being a small aromatic dopant would help facilitate layer formation by fitting in between the semi-planar melanin molecules.

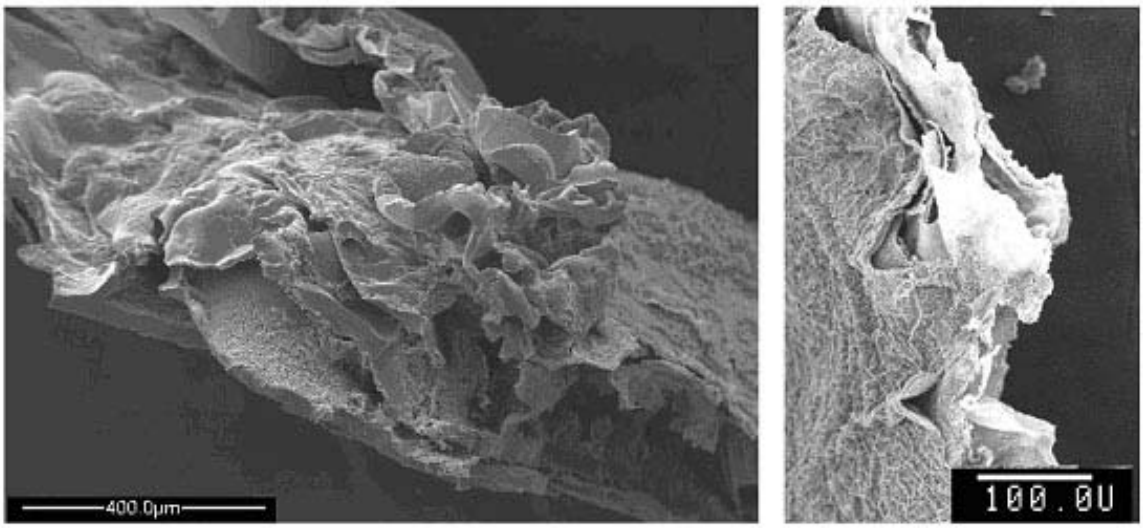

Figure 3.22. SEM image of melanin film electropolymerised from a 30 mM l-dopa solution containing 10 mM ammonium p-toluenesulphonate

In order to test this, it was thought that other small, aromatic molecules may have the same effect as toluenesulfonate, and we attempted to dope the polymer with phthalate. A phthalate ion with two carboxylic acid groups would be sterically smaller and more planar than the toluenesulfonate, presenting less disruption to the polymer structure. Furthermore, phtalate share a similar structure to the monomer unit DHI.

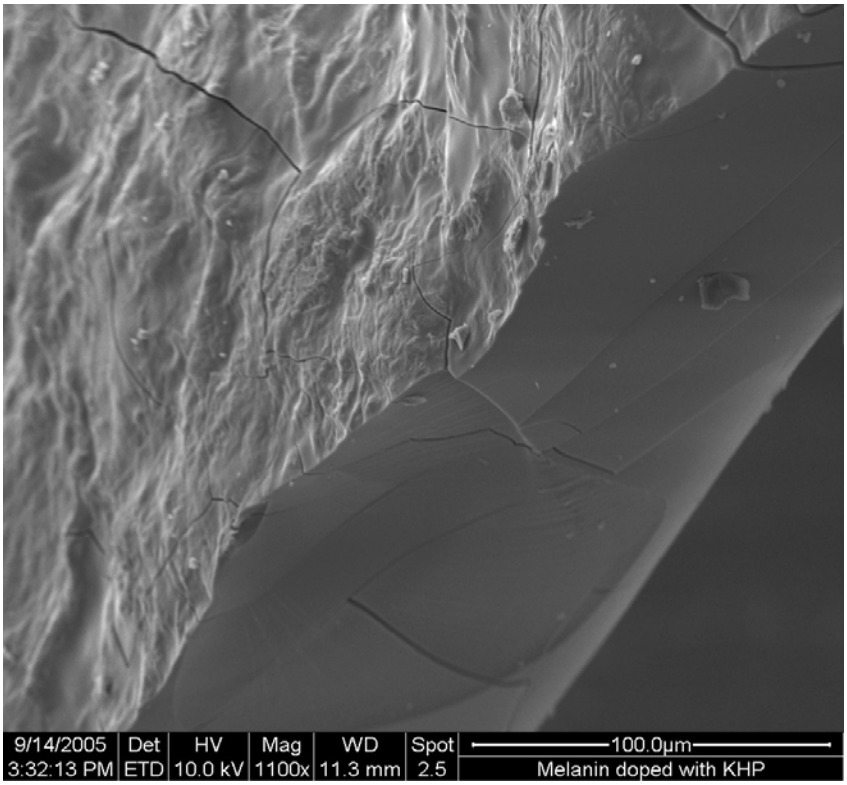

Figure 3.23. SEM image of melanin film electropolymerised from a 30 mM l-dopa solution containing 10 mM KHP

Looking at the SEM image of the cross section of the phthalate-melanin (See Figure 3.23), it showed a smooth continuous film similar to the film synthesised from borax buffer alone, without the layers that were present on the surface of the toluenesulfonate-melanin.

In this case, it is possible that the dopants may have been incorporated randomly in the space between the polymer molecules, and not regularly in between the planar sheets as previously thought. Furthermore, the underlying sheet structure was also present in the undoped sample (which would only contain borate counterions) which was essentially amorphous.

The more visible layered structure present in toluenesulfonate-doped polymer was probably due to the hydrophobic functionality of the dopant adding to the disorder in the material. In this case the toluenesulfonate may have acted as a surfactant, isolating the

newly formed polymer sheets and preventing them from forming a compact, continuous structure. Upon drying, the sheets that were formed during synthesis remained separated, resulting in the structure seen. This was supported by the fact that when lower concentrations of ammonium p-toluenesulfonate was used during synthesis, the melanin was formed as a continuous film without the flaky, layered sheets previously observed (See Figure 3.24).

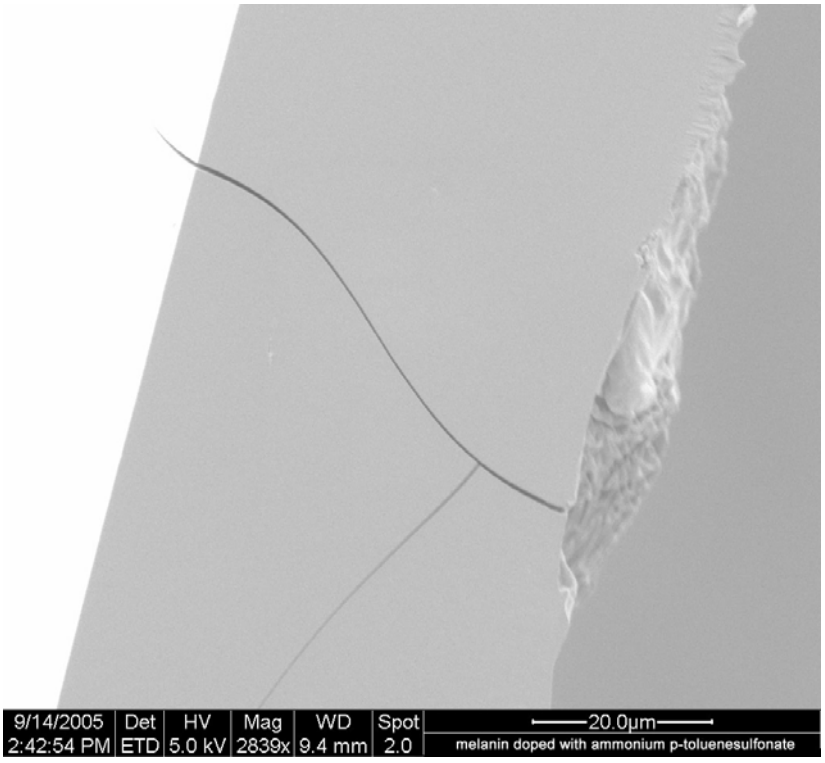

Figure 3.24. SEM image of melanin film electropolymerised from a 30 mM l-dopa solution containing 3 mM ammonium p-toluenesulphonate

3.4.3. Conductivity Measurements

In the electrochemical synthesis of conducting polymer, the polymer is synthesised in its doped form with the supporting electrolyte acting as the dopant counterion. In our synthesis, as the melanin was synthesised in a buffer solution, the buffer ions were incorporated into the material as the dopant counterion.

However, for conducting polymers such as polypyrrole it has been known that polymers doped with organic dopants containing sulphonate groups such as p-toluenesulfonate or dodecyl sulphate possesses better conductivity compared to polymers doped with inorganic salts. In the case of melanin, there has not been any literature with regards to the effect of organic dopant counterions to the electrical properties of the material, and thus there was a need to investigate whether or not organic dopants can improve the conductivity of the polymer. Table 3.3 shows the conductivity measured at 43% humidity of melanin doped with organic dopants:

Dopant	Conductivity
Control (borate)	$(5 \pm 1) \times 10^{-7}$
p-toluenesulfonate	$(6 \pm 3) \times 10^{-7}$
Dodecyl sulphate	$(4 \pm 2) \times 10^{-7}$
Phtalate	$(6 \pm 2) \times 10^{-7}$

Table 3.3. Conductivity of melanin synthesised from borax buffer and various organic dopants at dopant concentration of 0.003 M.

In all cases the conductivity values were quite low and were very close to each other, despite the fact that since they were electrochemically synthesised they would have been formed in their oxidised, doped form, with the dopant counterion being incorporated in the material.

Elemental analysis with XPS also failed to find any correlation between synthetic method and amount of dopant incorporated, with a very small amount (<1%) of organic dopant incorporated in most cases. Thus, the small differences in conductivity may be related more to the morphology of the film and not to the nature of the dopant ion. This may be caused by organic dopants being bulkier than the inorganic salts already present in the solution and therefore was less likely to be incorporated into the polymer.

3.5. Addition of Metal Ions

3.5. 1. Effect of Cu^{2+}

The addition of Cu initially resulted in precipitation of a greenish brown substance which was most likely a Cu-dopa complex, as the precipitate did not form when the metal ions was added to the buffer solution alone. The precipitate redissolves upon stirring, however when higher concentration of 10 mM of $CuSO_4$ or more (in 30 mM l-dopa) was added a slight cloudiness remained in solution. CV analysis on $CuSO_4$ alone (See Figure 3.25) showed only one reduction peak at -0.3 due to reduction of Cu^{2+}, with no oxidation peak observed.

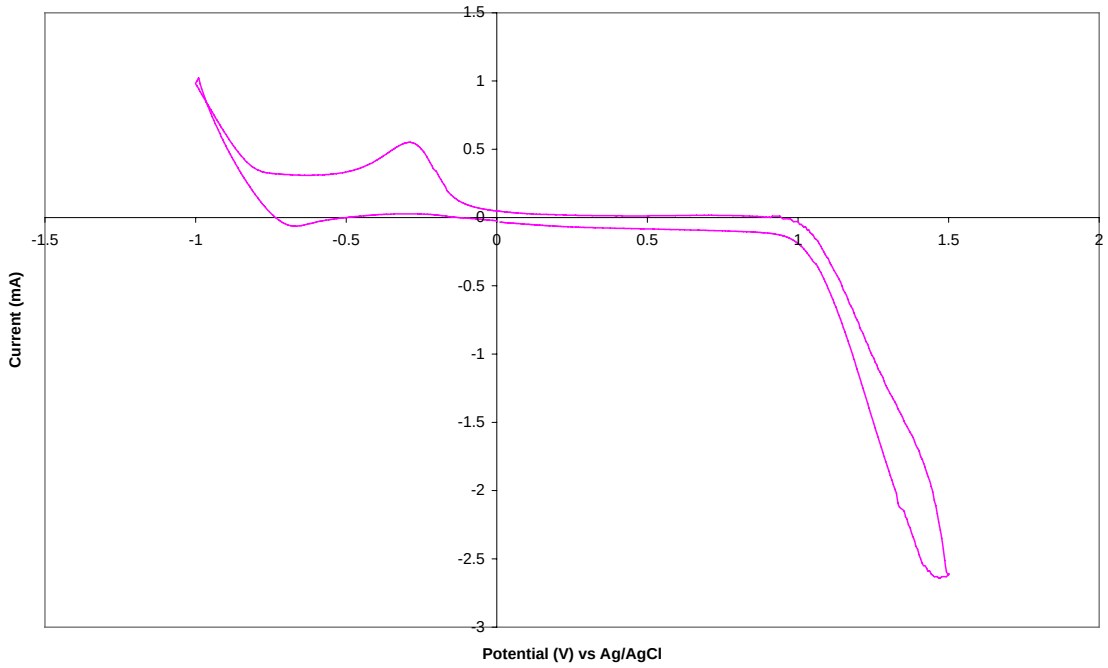

Figure 3.25. CV of 0.005 M $CuSO_4$ in borax buffer, scan rate 50 mV/s

When Cu was added to a solution of l-dopa (See Figure 3.26), it appears that the Cu ions formed a complex with the dopa and the reduction peak of Cu at -0.3 V was no longer observed.

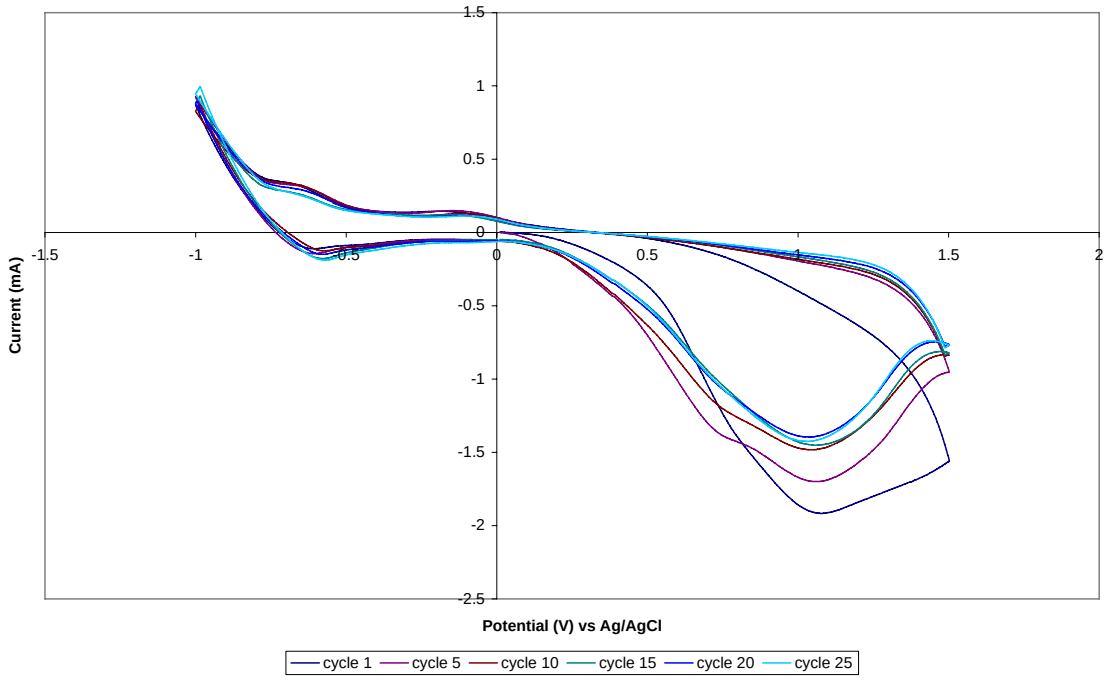

Figure 3.26. CV of 0.02M l-dopa in borax buffer with 0.001M $CuSO_4$ added, scan rate 50 mV/s

The dopa oxidation peak can be seen at 1 V, but in the subsequent scans the dopachrome oxidation peak at 0.3-0.5 V was not observed (there is only a slight increase in intensity over this potential range). Instead, there is a small peak at 0.7 V which decreases in intensity over subsequent scans. This peak may be due to a copper-dopaquinone complex as it was not observed in the first scan.

An increase in the concentration of Cu caused the CV to show a single peak at 0.8 V (See Figure 3.27) in the subsequent scan, with the dopa oxidation peak at 1 V only observed in the first scan. This means that in the subsequent scans the copper-dopaquinone complex has become the main peak due to the increased copper concentration, and it may have overlap the dopa oxidation peak resulting in the single peak observed. Also, as observed in the previous CV, the dopachrome peak was very weak and there was also no peak in the reduction cycle.

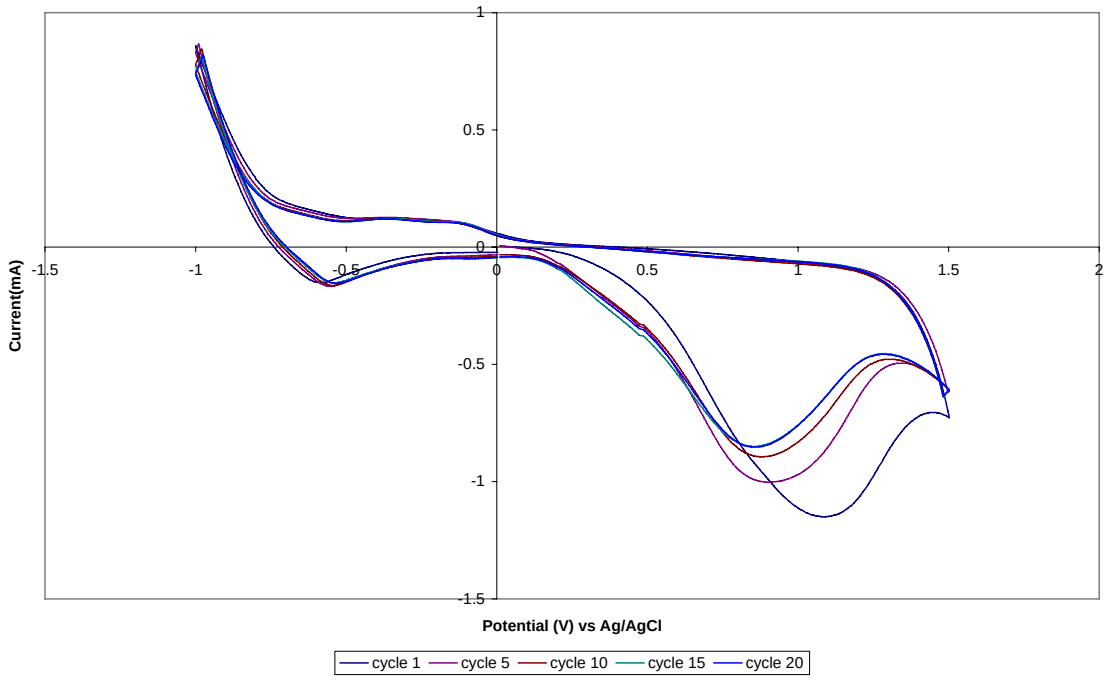

Figure 3.27. CV of 0.02M l-dopa in borax buffer with 0.005M $CuSO_4$ added, scan rate 50 mV/s

Although Cu forms a complex with dopaquinone, it seems to have little effect in the oxidation of dopachrome. This can be seen from the CV in carbonate buffer (See Figure 3.28), where there appears to be little change in the dopachrome oxidation peak with the addition of Cu. The dopachrome oxidation and reduction peaks were still present in all cycles, indicating that dopachrome was still able to oxidise in the presence of Cu.

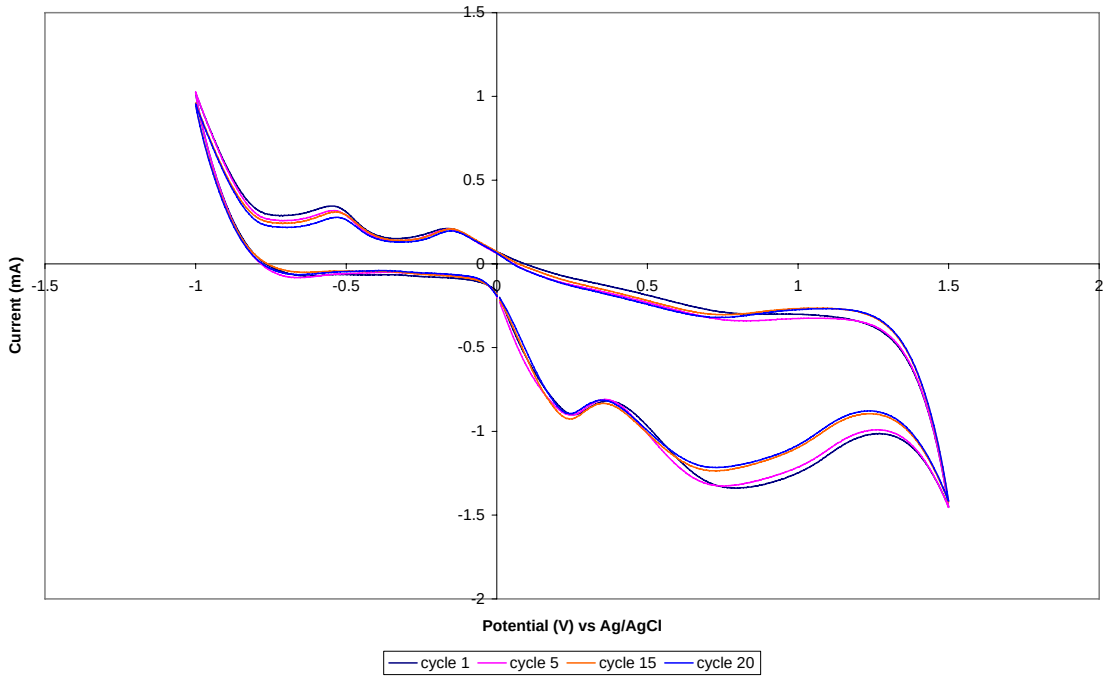

Figure 3.28. CV of 0.02M l-dopa in carbonate buffer with 0.005M $CuSO_4$ added, scan rate 50 mV/s

Compared to when no Cu is present, the oxidation peak decreases steadily with subsequent cycles. Since the dopachrome concentration should have increased as more dopachrome is produced by dopa oxidation, the dopachrome peak should have shown an increase in intensity as more dopa was oxidised, but the opposite trend was observed. This supports our previous observation in that copper hinders the formation of dopachrome, presumably by complexing the quinone, and hence little dopachrome is produced and the oxidation peak is due only to the dopachrome formed by autooxidation of dopa in solution and not from dopachrome produced on the electrode surface.

3.5.2. Effect of Zn^{2+}

The addition of Zn did not seem to have significant effect to the oxidation of dopa, in that the CV remained quite similar to the control (See Figure 3.29). There was a slight shift in the dopa oxidation peak, but unlike the addition of Cu there did not appear to be any new peaks in the scan.

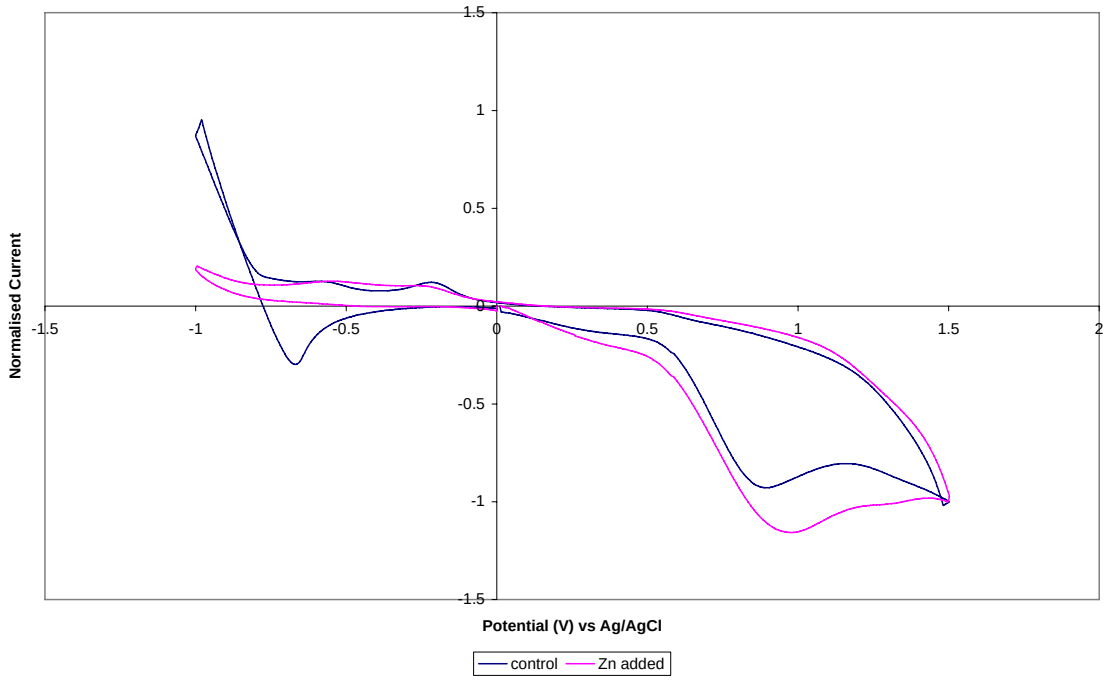

Figure 3.29. CV of 0.02M l-dopa in borax buffer with 0.001M $ZnSO_4$ added, scan rate 50 mV/s

Unlike what was observed with Cu, the most significant effect from the addition of Zn appears to be the significant reduction of the oxidation current upon repeated cycling. When Zn is present the oxidation current decreases quite rapidly upon repeated cycling, indicating formation of a passive film on the electrode surface.

The reason for this is unclear, however it has been previously postulated that the presence of Zn results in an increased amount of DHI compared to DHICA in the final polymer. This may have facilitated the formation of a dense film which hinders diffusion. In a previous study by Gidanian et al[99], when DHI is subjected to CV there is quite a significant peak current decay observed.

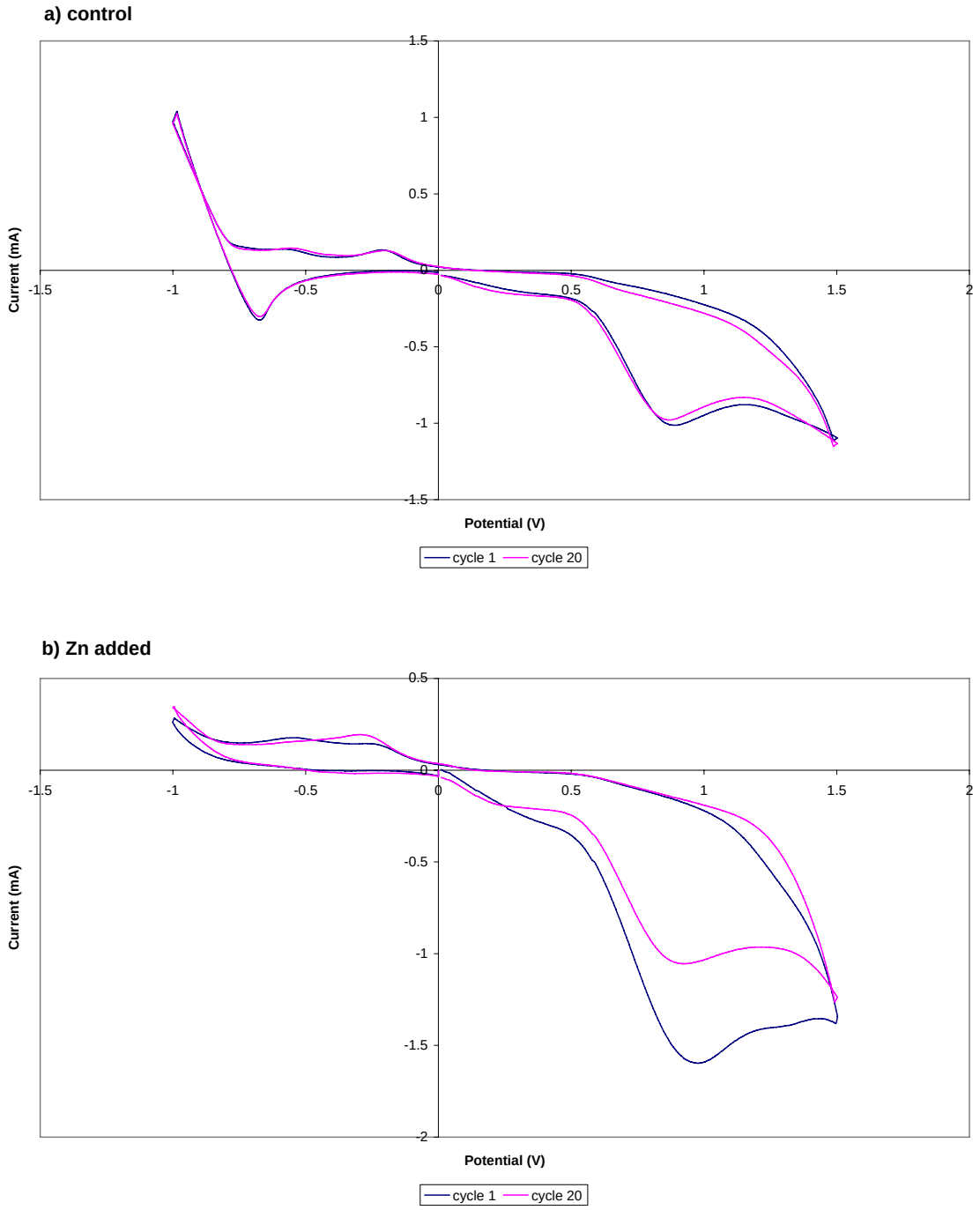

Figure 3.30. CV of l-dopa oxidation with a scan rate of 50 mV/s in (a) borax buffer only; (b) borax buffer and 1 mM $ZnSO_4$ added

CV analysis (See Figure 3.30) showed that when Zn was present the oxidation peak has significantly decreased after 20 cycles, compared to the control where the reduction in the

oxidation current was negligible. Furthermore, after 20 cycles there was only one reduction peak (corresponding to dopaquinone) with the dopachrome reduction peak at -0.5V disappearing. This effect was much more apparent when the concentration of Zn was increased to 5 mM, where upon repeated cycling there was a significant decrease in the dopa oxidation peak (See Figure 3.31). There was also a lack of dopachrome peaks, both in the oxidation and reduction cycle. In the control sample, the intensity of the dopachrome peak increases in subsequent scans, however when Zn was present this was not the case as there was a decrease in the dopachrome oxidation peak, and a lack of the dopachrome reduction peak altogether.

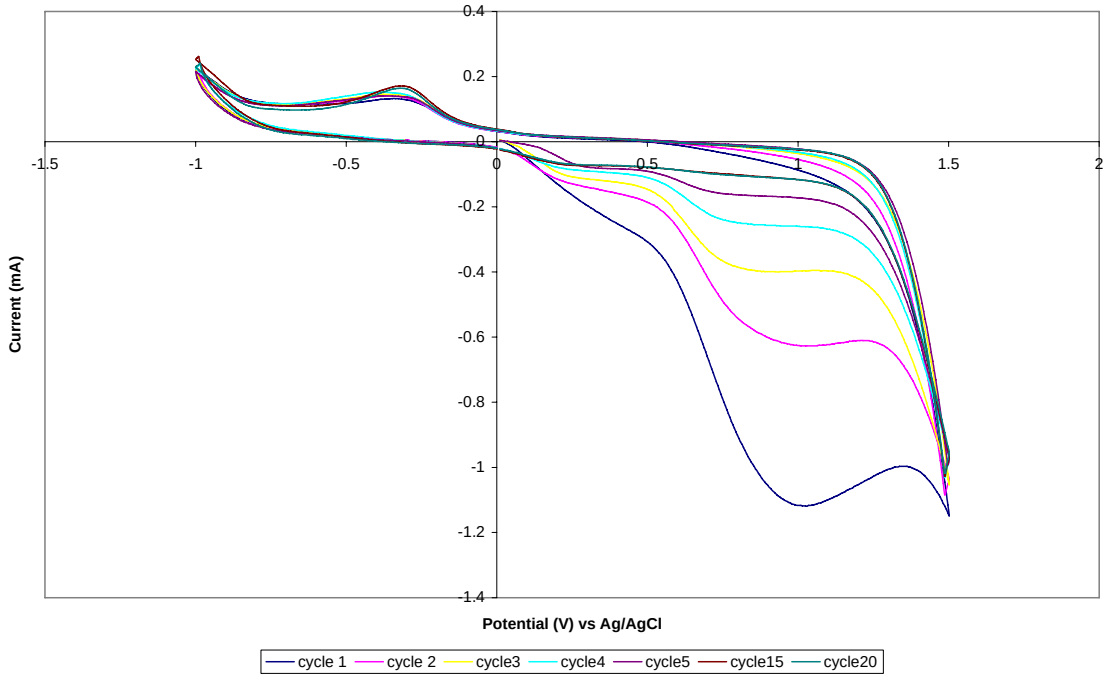

Figure 3.31. l-dopa oxidation on borax buffer with 0.005 M of $ZnSO_4$ added, scan rate of 50 mV/S

The passivation was not caused by deposition of metal ions as repeated oxidation-only cycles also bear the same result. Furthermore, should the metal ion itself be responsible for forming the passive film, there would have been another peak in the reduction cycle of the CV due to the reduction of the metal ions. It therefore appears that the addition of metal ions may have formed a dense film of melanin-Zn complex on the electrode surface.

3.5.3. Effect of Fe^{2+}

Fe has been postulated as one of the main influence on the role of melanin in biological systems[119, 125, 126, 189], and it appeared that Fe ions do complex dopa very strongly, in that a dark purple colour developed when Fe^{2+} was added to a solution of dopa in borax buffer. CV investigation (see Figure 3.32) showed that when Fe ions were present there did not appear to be any dopa oxidation.

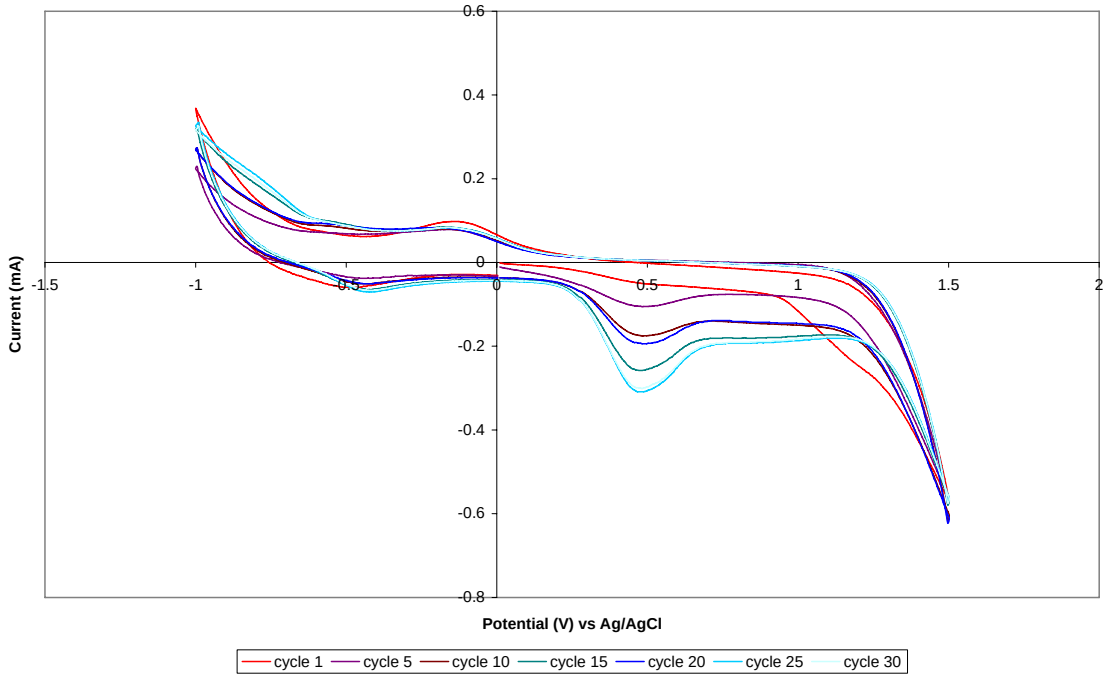

Figure 3.32. CV of 0.02M l-dopa in borax buffer with 0.005M $FeSO_4$ added, scan rate 50 mV/s

In the first cycle there was only a weak shoulder where the dopa oxidation peak should be, and in subsequent cycles the major peak at 0.5 V increases in intensity. This peak was not apparent on the CV of $FeSO_4$ alone which shows only one small oxidation peak at 1.1 V vs Ag/AgCl (see Figure 3.33), which indicates that the peak was due to an Fe-dopaquinone complex since the peak at 0.5 V was absent in the first cycle and increases in intensity with subsequent cycles.

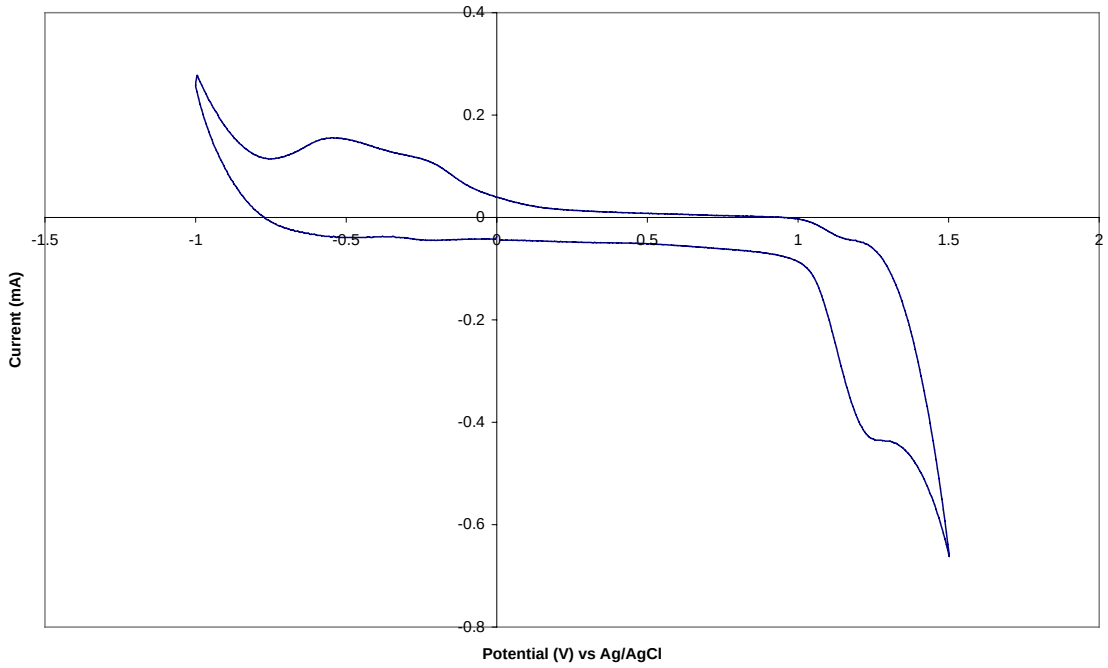

Figure 3.33. CV of 0.005M $FeSO_4$ in borax buffer, scan rate 50 mV/s

3.6. Summary

It was found that borax was the best aqueous buffer system for use in the electrochemical synthesis of melanin. Films produced from borax buffer were the smoothest and most uniform, with the ammonia buffer faring the worst, producing a more porous film. The film from borax buffer was also the most conductive when measured under 43% humidity.

XPS analysis supports previous observation by Swan that melanin contains approximately equal amounts of hydroxyl and quinone forms of DHI, and that the use of carbonate instead of borax buffer did not significantly affect this ratio.

Doping with organic dopants did not result in a more conductive material, with a negligible increase in conductivity compared to those synthesised from borax buffer only. Doping with metal ions was unsuccessful as metal ions interfere with the polymerisation

process. The addition of Cu^{2+} and Fe^{2+} interferes with the oxidation of dopaquinone, while the addition of Zn^{2+} causes passivation of the electrode.

The morphology of the film was affected by the pH and additives. Borax and carbonate buffer produces continuous film, whereas ammonia buffer produces a more granular film but without the ordered, spherical granules previously observed in natural melanin. The addition of small amounts of organic dopants did not affect the morphology, however the addition of PEG resulted in an irregular surface structure.

Chapter 4

Electrochemically Synthesised Melanin as a Light Harvester In Dye-Sensitised Solar Cells

4.1. Introduction

4.1.1. Solar Energy and Solar Cells

Due to the ever-increasing demand for energy and the finite resource of fossil fuels, there has been a great interest in the field of alternative energy. Amongst the various available energy sources, solar energy has received attention due to its potential as a clean, abundant source.

The field of solar energy conversion is equally rich and diverse, and there are many available materials for the conversion of solar radiation into electricity. The majority of these photovoltaic systems are based on the p-n junction of a semiconductor, and nowadays silicon solar cells are the mainstay of solar energy conversion. However, the performance of these silicon solar cells are greatly affected by their crystallinity, and thus incur a high cost due to the energy intensive manufacturing process associated with purifying and processing the material.

An alternative that has been developed in the last 15 years is the Dye-Sensitised Solar Cells (DSSC)[190], which utilised a metal oxide semiconductor coupled with a dye. These DSSCs have attracted considerable attention due to their lower cost, and excellent in service performance potential. Their efficiency has been shown to be lower than the crystalline silicon cell and the next generation of solid-state thin film technologies, but they still present commercially viable efficiencies[191]. Furthermore, DSSCs are still relatively new and thus are still far from their theoretical efficiencies, presenting a high potential for improvements.

4.1.2. The Dye-Sensitised Solar Cell (DSSC)

In a DSSC the dye which is the element responsible for light absorption is separated from charge-carrier transport, and therefore it is possible for DSSC to use low to medium purity semiconductor materials. This means that unlike silicon solar cells (which require highly pure, crystalline materials), DSSCs can be manufactured using cheap material and simple assembly techniques.

At the heart of the DSSC (See Figure 4.1) is a metal oxide semiconductor, commonly a mesoporous TiO_2 film which is placed in contact with a transparent Indium-Tin Oxide conducting glass electrode. Attached to the TiO_2 is a monolayer of a charge transfer dye (typically an organometallic complex) responsible for capturing solar radiation.

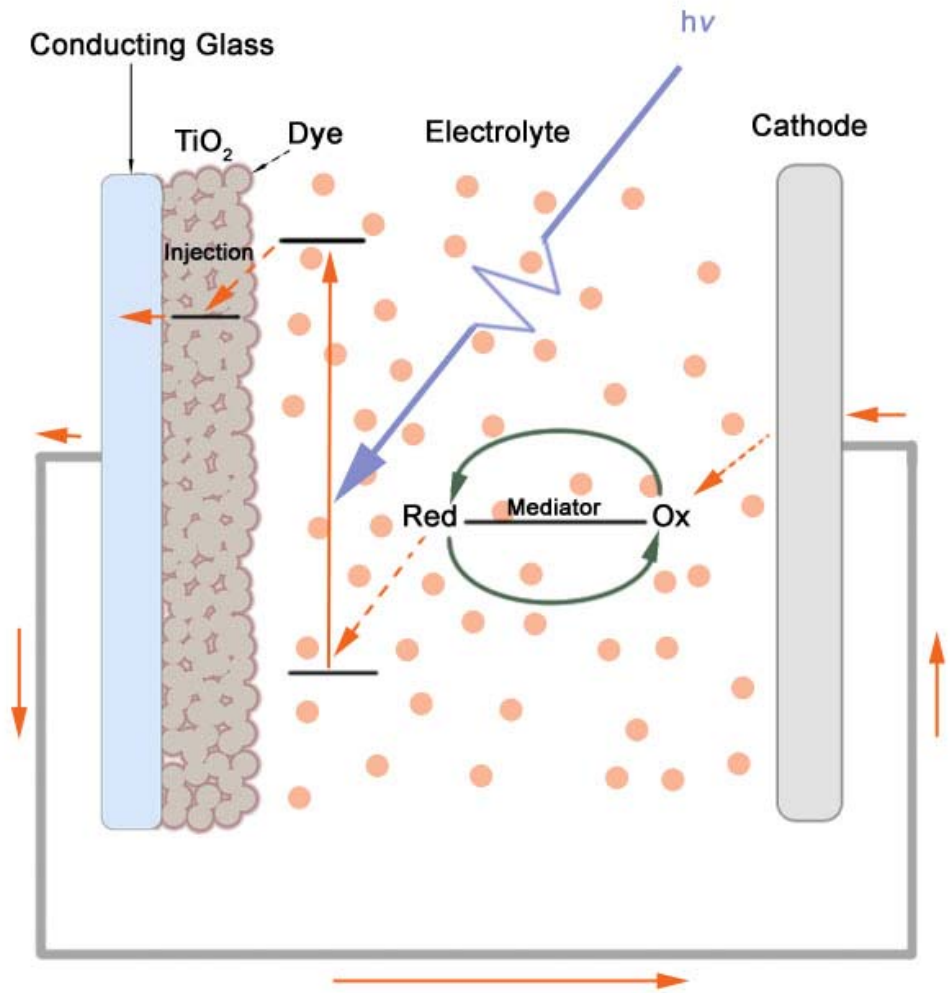

Figure 4.1. Schematic of a DSSC

Upon photoexcitation, the dye molecules inject electrons into the conduction band of the metal oxide semiconductor. The dye is subsequently regenerated by the redox electrolyte (typically an Iodide/Triiodide redox couple dissolved in an organic electrolyte), which in turn is regenerated at the counter electrode.

Since the dye is responsible for the actual light absorption of the system, it is important that the dye absorbs as much visible light as possible in order to maximise the efficiency of the cell. Most of the work in this area have been centered around organometallic dyes such as the N3 dye (Ru(4,4'dicarboxy-2,2'-bipyridine)$_2$*cis*(NCS)$_2$). These organometallic dyes give very good cell efficiency, however, the main drawback is that unlike the rest of the component of the DSSC, they are quite expensive and often require the use of toxic materials in their synthesis, and they only absorb certain portions of the electromagnetic spectrum.

4.1.3. Conducting polymer in DSSCs

Due to their good conductivity, the interests with regards to conducting polymers in the field of DSSCs has mainly centered around their use as solid electrolytes or electrode materials rather than dye sensitisers[30, 192]. However, it has been shown in the literature that conducting polymers can act as an electron donor when combined with a wide band gap semiconductor such as TiO_2. Conducting polymers possess a broad visible absorption due to the extensive electron delocalisation on the polymer backbone leading to efficient light harvesting properties.

Nogueira et al[193] have showed that it is possible using poly(*o*-methoxy aniline) doped with p-toluenesulphonic acid (PoAni-TSA) as a sensitiser in a quasi-solid state DSSC. In their experiment the PoAni-TSA was used as the dye sensitiser, with an ion conducting gel polymer based on poly(epichlorohydrin-co-ethylene oxide) filled with NaI/I_2 as the electrolyte. Their cell produced an open circuit potential and closed circuit current of 48 mV and 12.2 μA cm^{-2} under 120 mW cm^{-2} of AM (Air Mass) 1.5 illumination. This translates to an overall efficiency of around 1.6 x 10^{-4} %, significantly less than what can be obtained with organometallic dyes (>10%[190]), but it again showed that conducting polymer can indeed act as a sensitiser in a DSSC. The low efficiency may also due to the solid electrolyte, which has higher resistance and less charge transfer mobility compared to liquid electrolytes.

Savenjie et al[194] has reported energy conversion efficiency of 0.15% in their use of poly(2-methoxy-5(2`-ethyl-hexyloxy) para-phenylene vinylene (MEH-PPV) in a TiO_2 DSSC with a mercury drop counter electrode. They reported an open circuit potential and closed circuit current of 0.92 V and 0.32 mA cm^{-2} under AM 1.5 illumination. In their study the MEH-PPV acts as both the dye and the electrolyte, so it is possible that higher efficiency may have been achieved with a liquid electrolyte. They also studied the theoretical charge separation in a TiO_2/PPV system and found that the maximum theoretical efficiency of this system would be around 6 %.

A. van Hal et al[195] studied electron injection from poly(p-phenylenevinylene) (PPV) derivative on TiO_2, and confirmed photoinduced electron transfer and revealed the reversible formation of polymer cation radicals, supporting Savenjie et al's[194] experiment.

Yanagida et al[196] reported the use of a polythiophene as a sensitizer in DSSC, giving high photocurrents which increases in the presence of electron-donating ionic liquids. Their cells utilised poly(3-thiophene acetic acid) (P3TAA) and were able to achieve photocurrents of 9.75 mA cm^{-2} with an open circuit potential of 0.405 V and a total power conversion efficiency of 2.4 %. Lower efficiencies of 1.6% were obtained with poly(3-thiophene acetic acid)-poly(hexyl thiophene). They attributed this efficiency to the presence of carboxylic acid groups which provides a good electronic connection with the TiO_2.

In a similar manner, Moss et al[197] have reported the use of electropolymerised thin films of polypyridyl metal complexes. They found that the electropolymerised films have comparable performance to their conventionally dyed counterparts, but their main advantage was in their greatly increased stability against dye desorption.

It has been well documented that melanin exhibits photoelectric responses. In the study by Rosei et al[132], melanin was described as nanometer-sized conjugated clusters, where photogenerated electron-hole pairs undergo either germinate recombination or dissociation depending on the photon energy. Similarly, the photoconductivity of melanin

has been studied by Jartzebska et al[131] who studied the photoconductivity of melanin as a function of wavelength and temperature. Furthermore, it has been recently published that natural dyes extracted from various sources can act as a photosensitizer in DSSC[198]. Despite all this, no study has been published so far regarding the use of melanin in DSSC.

Since melanin is a natural photoprotective agent, it possesses a broadband absorbance in the UV and visible region of solar radiation. It also possesses COOH and OH groups which would be free to bind to the surface. Also, melanin can be synthesised using simple electrochemical means from aqueous solutions, and may therefore be an attractive alternative to traditional organometallic dyes.

4.2. Experimental

N3 dye (Ru(4,4'dicarboxy-2,2'-bipyridine)$_2$*cis*(NCS)$_2$) was purchased from Solaronix and l-dopa was purchased from Sigma Aldrich and used as received.

Titania paste (Degussa P25) was made according to the method by Ito et al[199]. Titania powder was refluxed in dilute nitric acid at 80°C for 8 hours, and the solvent was subsequently removed to yield $TiO_2NO_3^-$ powder. P25 TiO_2 contains 70% wt anatase and 30% wt rutile, with a primary particle diameter of 21 nm. Titania paste was made by adding Polyethylene Glycol (M.W. 20,000) and water until the solution reaches the consistency of a thick paste. P25 TiO_2 contains 70% wt anatase and 30% wt rutile, with a primary particle diameter of 21 nm.

Hydrothermally treated TiO_2 was made following the method of Wilson et al[200]. 20 cm^3 of isopropanol and 125 cm^3 of titanium isopropoxide was mixed in a dropping funnel, and the solution was added dropwise into 750 cm^3 of ultrapure deionised water (conductivity of 10^{-8} S) over 20 minutes with vigorous stirring. After all the titanium isopropoxide was added, 5.3 cm^3 of 70% HNO_3 was added as the peptizing agent and the solution was stirred at 80° C for a further 8 hours.

The resultant titania colloid was then put into a stainless steel autoclave Parr bomb and hydrothermally treated in a convection oven at 200° C for 15 hours. The resultant solution was cooled to room temperature and dried in a rotary evaporator until it became a thick paste, upon which Polyethylene Glycol (m.w. 20,000) was added to the titania paste with vigorous stirring.

The titania paste was then applied to the Fluorine doped-Tin Oxide conducting Glass (FTO) by the doctor blade method. The glass was first bound at three sides using a clear plastic tape, and the titania paste was placed onto the plastic tape opposite the uncovered side. A glass rod was then used to spread the paste by sliding it over the glass in a smooth linear motion. The resultant film was then put in a furnace and calcined at 450°C for 10 hours, with the furnace heating rate set at 120°C/hour.

The electrochemical polymerization of melanin onto titania film was done in a three electrode setup using a PAR 273A Potentiostat/Galvanostat controlled through a computer using the virtual potentiostat function in the PAR PowerSuite software package (See Figure 4.2). The titania film was used as the working electrode, with stainless steel counter electrode and calomel reference electrode. The electropolymerisation solution was 5 mM l-dopa in borax buffer unless otherwise stated. The solution was made by dissolving the required amount of l-dopa in a minimum amount of 1M borax stock solution and then diluting it to the required volume. The area of the counter electrode used was always larger than the area of the titania film to ensure that the current density was dependent on the working electrode.

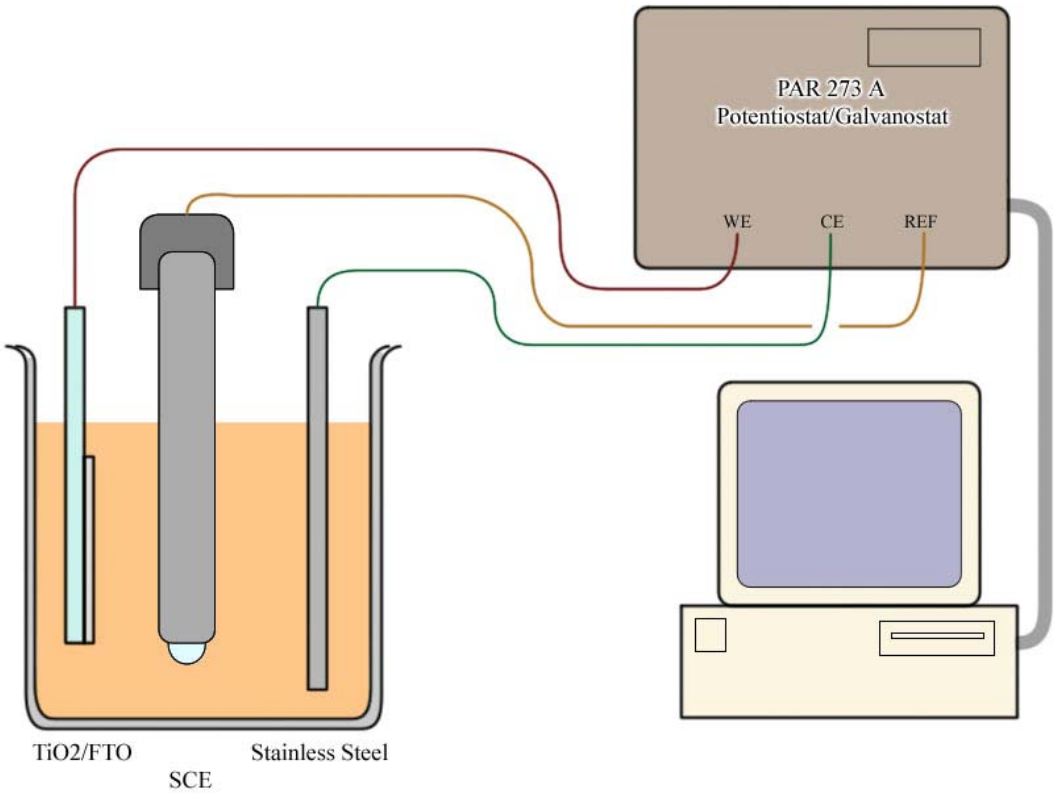

Figure 4.2. Experimental setup for the electropolymerisation of melanin onto TiO_2 film

The counter electrode used for the DSSC was platinised FTO conducting glass, which was made by potentiostatic cathodic deposition of platinum from a solution of H_2PtCl_6. The cathodic deposition current was maintained as to provide a suitably uniform deposition of platinum onto the conducting glass, with a current density of approximately 1 mA/cm^2.

The electrolyte used in all measurements was 0.05 M I_2 / 0.5 M LiI in Propylene Carbonate unless otherwise stated. Due to the hygroscopic nature of propylene carbonate, the electrolyte was kept in a sealed container with molecular sieves added in order to minimize water absorption from the atmosphere.

The dye sensitized solar cell was made by combining the two electrodes with the electrolyte in between. Stretched laboratory film was used as a spacer to prevent shorting

between the two electrodes and confine the cell to the desired cell area (See Figure 4.3). Copper sheets were used as contacts.

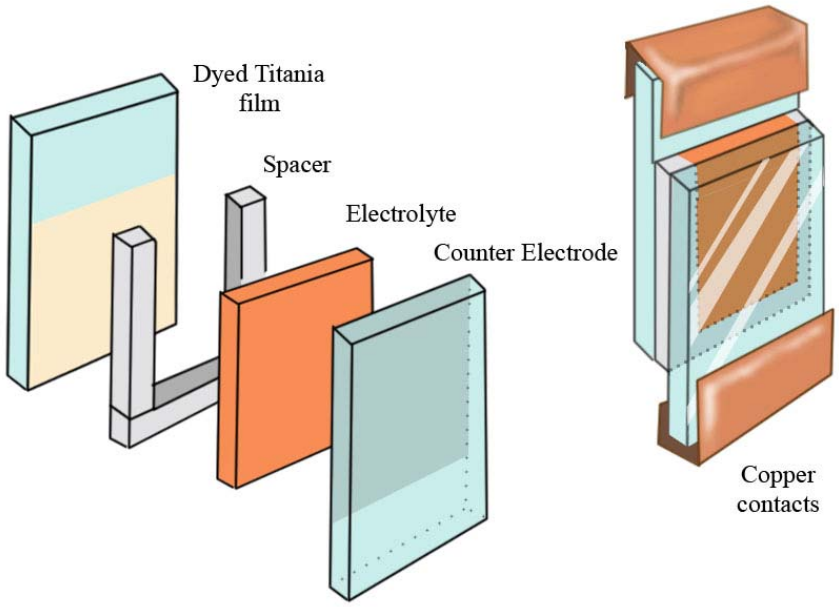

Figure 4.3. Schematic of the melanin DSSC

The light source used was a 150 W Ozone-free Xenon lamp integrated as part of Oriel 96000 Solar Simulator (See Figure 4.4). An Air Mass or/and a 420 nm cutoff optical filters were used as specified, and a dichroic filter was used to remove infrared radiation. The maximum output of the solar simulator was 162 mW/cm^2.

Initial photocurrent and IV measurements were performed using a Keithley 236 Source Measure Unit coupled to a Fluke 8050A digital multimeter with the solar simulator in a linear configuration with an appropriate filter (See Figure 4.4). The Keithley was used in linear stair mode between -1 to +1 V with a step size of 50 mV every 5 seconds. The use of 5 second delays between each potential step was due to limitations in the data recording.

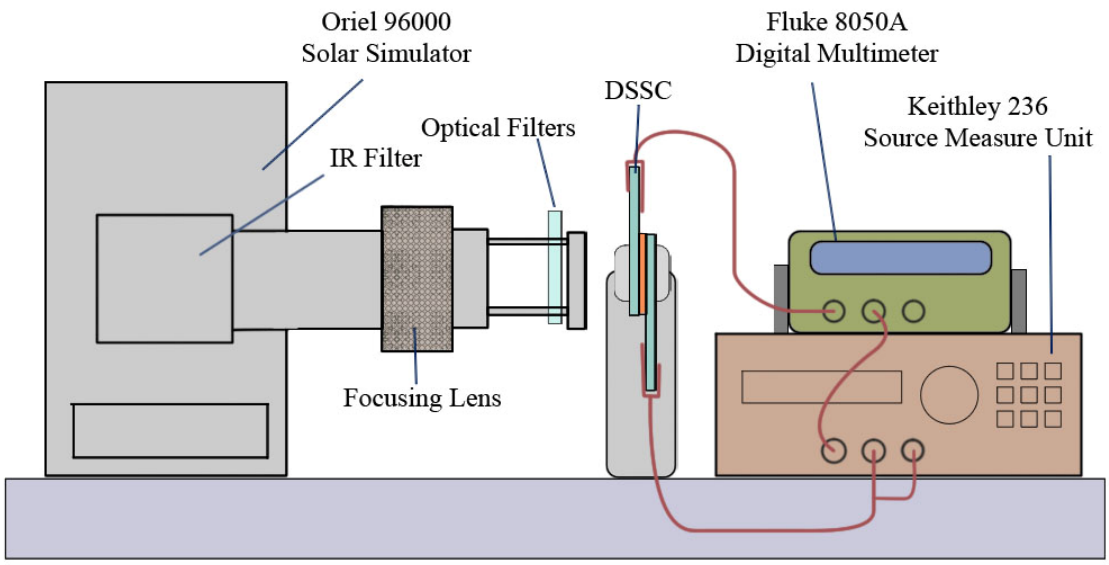

Figure 4.4. Experimental setup for IV curve measurement

More accurate IV measurements and measurements at different light intensity were done using an EDAQ ECorder 401 coupled to a PC with the EDAQ Echem 401 software. For these measurements a dichroic filter was used to remove IR radiation, in conjunction with the Air Mass and cutoff filters. The EDAQ potentiostat was used in linear staircase voltammetry mode with a potential range of -1 to +1 Volts with a scan rate of 50 mV/s and a step size of 1 mV. The DSSCs were tested with the counter electrode set as the reference. In the case of melanin DSSCs due to the need for UV activation (which will be discussed later in Section 4.3.6. p 163) the cell was first exposed to a light power of 140 mW/cm^2 (with A.M.1.5 filter) until the observed photocurrent did not show any further changes upon repeated IV measurements.

Measurements at a varied light intensity was used by placing a series of Air Mass filter (Schott KG1 to KG5) in front of the sample, with the light power measured before the reading was taken. For very small light intensity (below 30 mW/cm^2) the light source was set on a broad focus (to ensure the absence of hotspots of stronger light density), then the sample was placed on a rail and the distance between the sample and the light source was varied, with the light power first measured at the intended sample position on the rail before every measurement (See Figure 4.5).

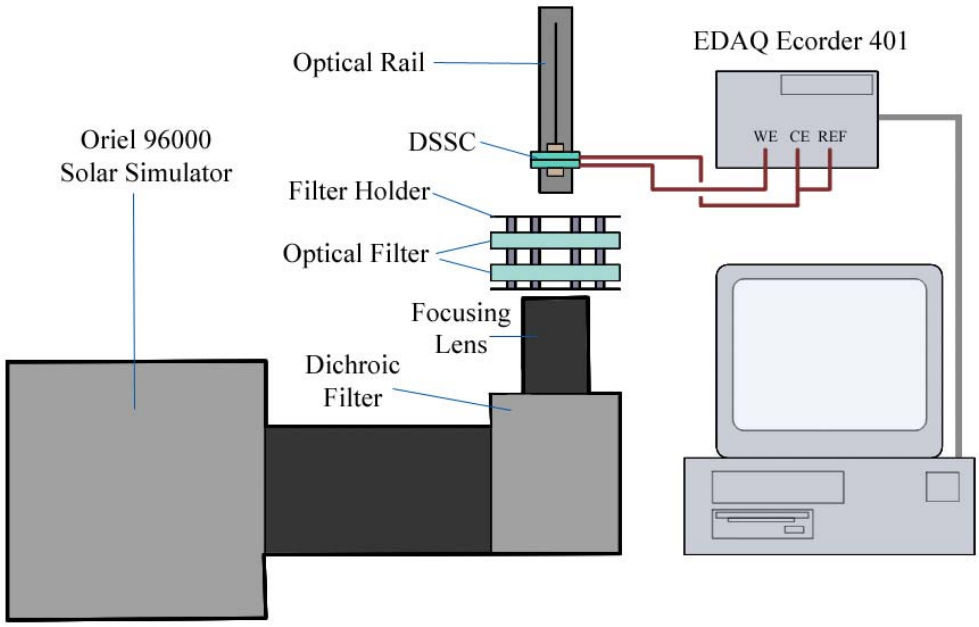

Figure 4.5. Experimental setup for IV curve measurement at varying light intensity.

Photodynamic spectra was taken by coupling the solar simulator to an Oriel Cornerstone 130 monochromator and a multimeter, with both the entry and exit slits of the monochromator set at the maximum of 10 x 3.9 mm in order to gain maximum power output (See Figure 4.6). The absence of a focusing lens on the exit slit ensure that the light output was uniform for the slit area, and power measurements for the monochromator output was taken with a calibrated power meter. For measurements above 600 nm a 420 nm cutoff filter was used in order to filter out the half-wavelength output. Below 600 nm a filter was not deemed necessary due to the lack of monochromator output below 300 nm. The photovoltaic response was read as photocurrent rather than photovoltage in order to avoid capacitance effects, however, in cases where potential was measured, the scan rate was significantly slowed down in order to ensure equilibrium potential was achieved before the data was sampled. For the photocurrent measurements the step size for the scan was set at 10 nm at 5 s intervals.

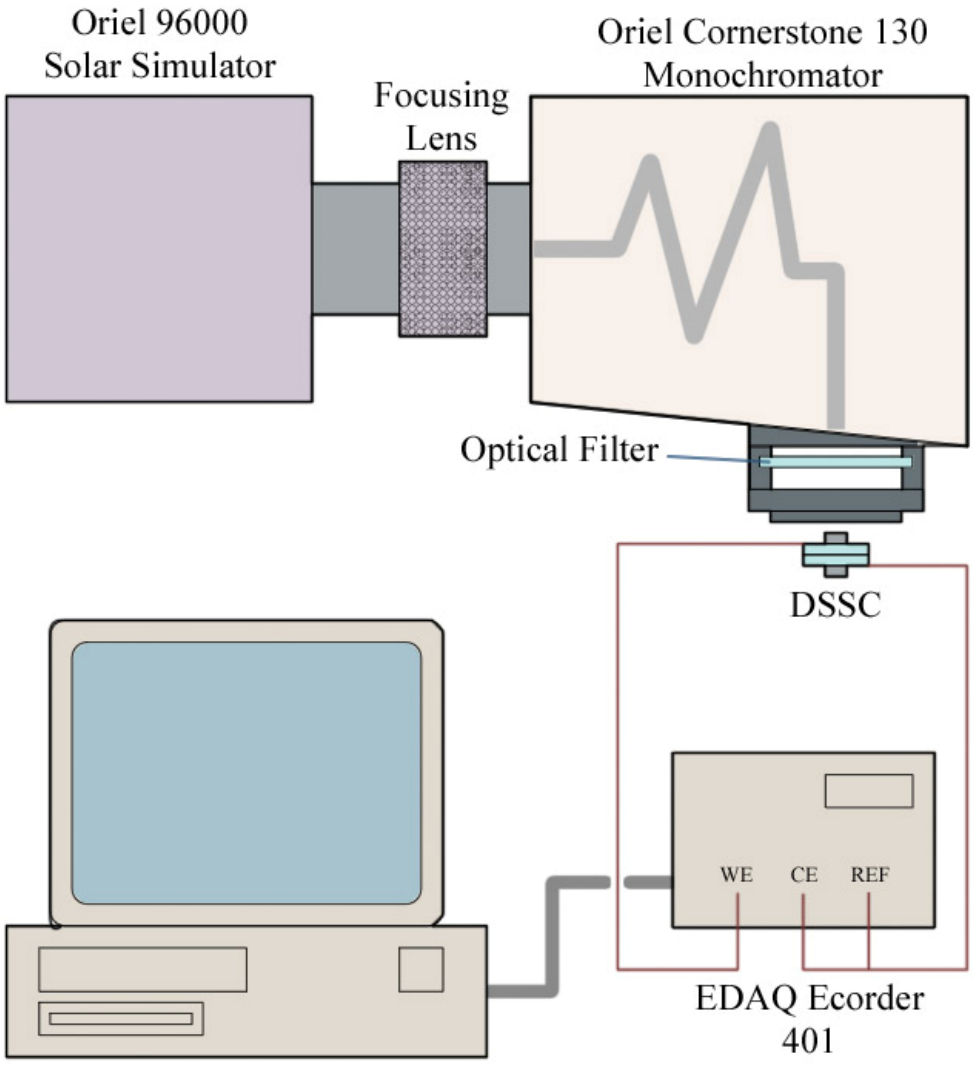

Figure 4.6. Experimental setup for photodynamic action spectra measurement.

All measurements were done by illumination through the conducting glass on the titania side of the cell to minimize light scattering and absorption by the platinised FTO counter electrode and the electrolyte.

4.3. Results and Discussion

4.3.1. Initial Cell Preparation

Traditionally, DSSCs are dyed by immersing the titania film in a dye solution, and therefore initial experiments were to dye the titania film using a solution of chemically synthesised melanin. The melanin was synthesised by bubbling air to a solution of l-dopa accompanied with mechanical stirring, and after several days a melanin solution is obtained. The titania film was then immersed in this solution overnight, and then made into a DSSC and tested for photocurrents.

Despite several attempts, the photocurrent produced was very small, and in some cases the photocurrent under A.M 1.5 condition was found to be less than that of a blank TiO_2 DSSC. This was rather unexpected, since there was visible colouration on the titania itself, and therefore at first it appeared that the titania has been successfully dyed with melanin.

Since the colouration indicates that melanin has been absorbed onto the titania surface, the lack of observed photocurrent may be due to the interface between melanin and the titania. Since the melanin appears to act as a filter, it shows that there is insufficient interaction between the titania and the melanin, and the melanin simply absorbs light and dissipates the energy through some other means rather than injecting electrons into the titania.

The chemically synthesised melanin may have formed as granules or aggregates which would not have a good contact area with the titania. Furthermore, the size of the melanin granules may make it harder for the melanin to fully diffuse through the pores of the titania, and the bulk of it would be deposited on the outermost surface, acting as an optical filter rather than a dye-sensitizer.

This result shows that chemical synthesis was inefficient in the synthesis of melanin DSSC due to the lack of interaction between the titania and the melanin. Since electrochemical synthesis deposits melanin film directly on the electrode surface, it was thought that it may be able to overcome this problem and produce a functioning melanin DSSC.

4.3.2. Electrochemical Deposition of Melanin

By using similar conditions as to that were used in the electrochemical synthesis, we successfully synthesised melanin as a thin film on the titania. The resultant film had a dark brown colour which depends upon the thickness of the titania film and oxidation time.

However, this melanin DDSC only produces a small photocurrent when tested, despite the strong colouration. Again, the melanin seemed to act as a filter, in that it suppresses the photocurrent of titania in the UV region. Upon further investigation, it was found that the melanin DSSC would only give a photocurrent when it is only lightly dyed with melanin, while films saturated with melanin gave less photocurrent than a blank TiO_2 cell (See Figure 4.7). The melanin DSSC also requires irradiation with UV light in order to reach its maximum efficiency, and this will be discussed later in Section 4.3.6.

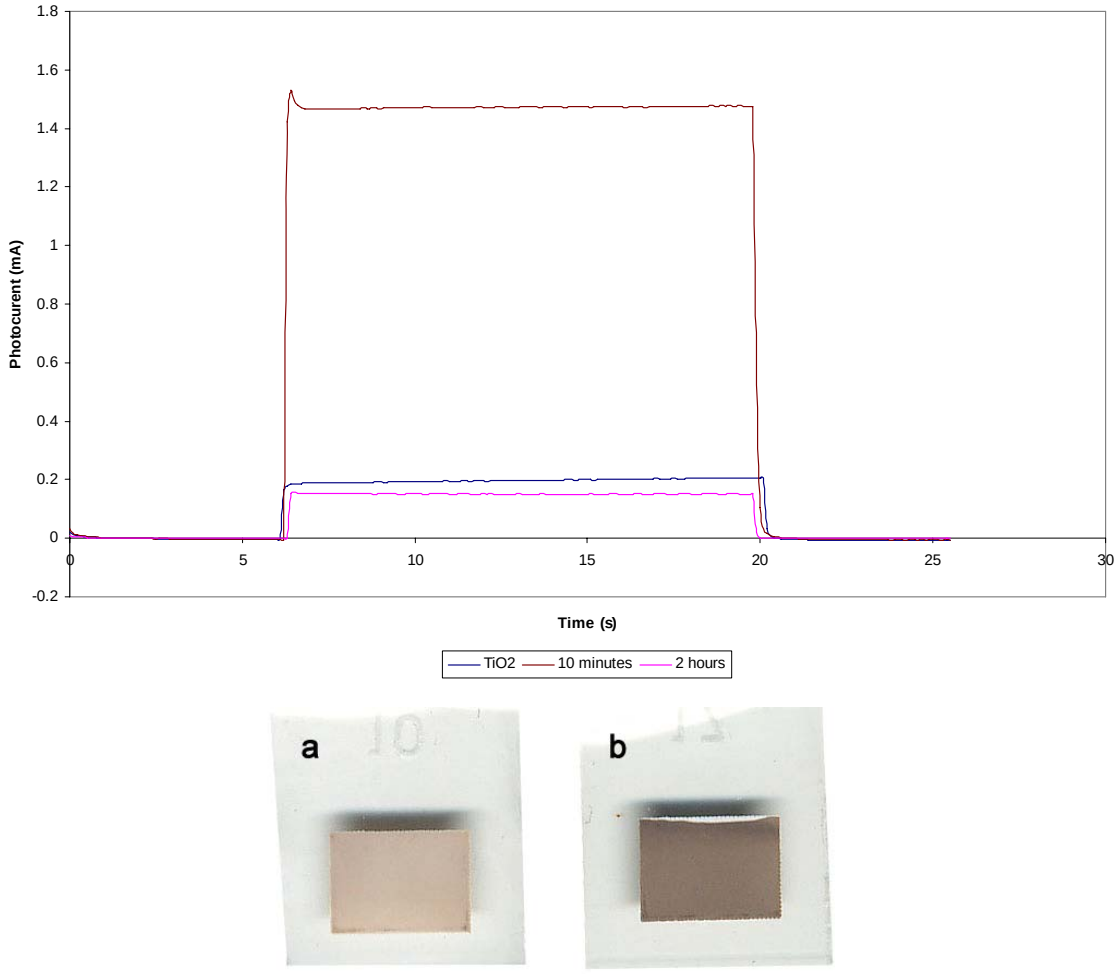

Figure 4.7. Comparison of dyeing level of melanin DSSC synthesised by potentiostatic oxidation of 0.005 M l-dopa at 1.5 V for: (a) 10 minutes and (b) 2 hours. DSSC illuminated with 95 mW/cm^2 AM 1.5 illumination after irradiation with UV light for 1 hour

Since melanin have a much lower conductivity than titania, if the melanin layer is too thick it would act as a resistor and the charges created by incident radiation on the polymer surface may not reach the interface between the polymer and the titania, preventing electron injection and therefore reducing the efficiency of the cell. Likewise, the charge separated at the melanin-titania interface would have to travel to the melanin-electrolyte interface to be regenerated, and this would be more difficult in a thick film.

Furthermore, previous studies[131, 132] have shown that melanin have a high concentration of traps and recombination centres. This would pose a barrier to charge transfer between the melanin and the titania, and thus as the film thickness increases, charge recombination may become the dominant process, effectively turning the melanin film into a filter.

In addition, it is likely that if the melanin film is grown to sufficient thickness it may also block the pores of the titania film, therefore preventing diffusion of electrolytes into the pores of the titania film, reducing the effective surface area of the DSSC.

Despite similar colouration, DSSC dyed using chemically synthesised melanin produces much smaller photocurrents (See Figure 4.8). This indicates that electrochemical synthesis results in a better interaction between the melanin and the titania as postulated, and previous lack of result with chemically synthesised melanin was not due to film thickness.

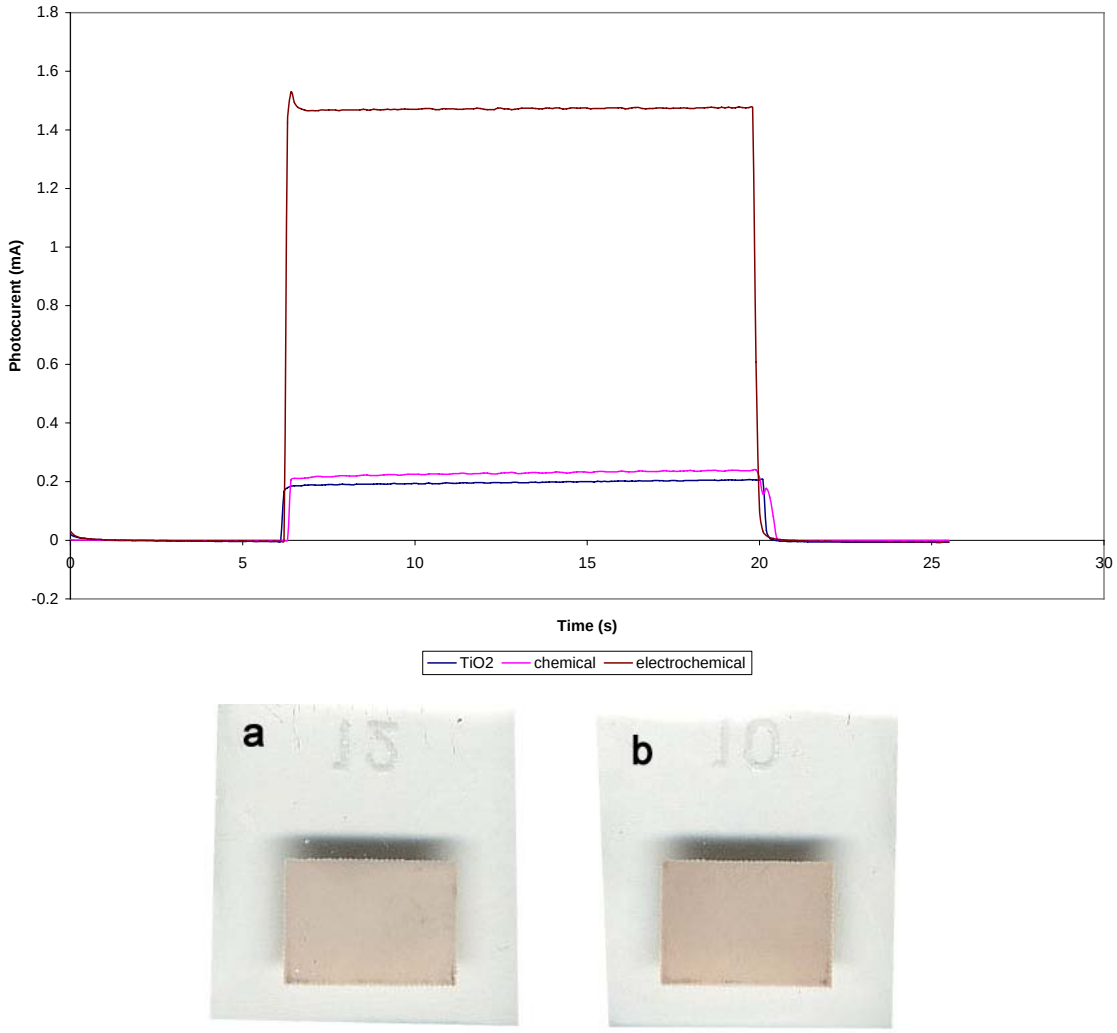

Figure 4.8. Comparison of melanin DSC dyed with: (a) chemically synthesised melanin (overnight immersion of TiO_2 film in an autooxidised solution of melanin from 0.015 M l-dopa in borax buffer) and (b) electrochemical method (potentiostatic oxidation of 0.005 M l-dopa in borax buffer at 1.5 V for 10 minutes). DSSC illuminated with 95 mW/cm^2 AM 1.5 illumination after irradiation with UV light for 1 hour.

Although this does present a drawback in that it places a limit on how much light it can absorb, this also shows that melanin can act as a reasonably efficient light harvester even when it is only present in small quantities. This would open up the possibilities of its use in semi-transparent solar cells, where the melanin may act as both a dye sensitizer and a UV filter while still letting sufficient visible light through the glass.

4.3.3. Optimisation of Synthetic Method

The polymerisation potential required depends partially on the surface area of the electrode, but it was found that an oxidation potential of 1 to 1.5 Volts on a cell area of 4-6 cm^2 gave a sufficient rate of oxidation without overoxidising the titania. Similarly, the optimum polymerisation time was determined to be between 10-20 minutes oxidation in 5 mM l-dopa solution. Under these conditions melanin was deposited as a light yellowish brown film on the titania.

This observation was also supported by Yanagida et al[196] who claimed that the efficiency of their polythiophene-sensitised DSSC showed a decrease in quantum efficiency with increasing film thickness. Since the photocurrent is produced mainly at the junction between the semiconductor and the polymer, increasing film thickness would decrease electron collection and increase electron recombination, contributing to the lower efficiencies observed.

Horak and Weeks[152] claimed that redox cycling seems to result in mechanically stronger, more adherent melanin film, which was the desired properties of melanin used in DSSC. In the synthesis of free standing films, redox cycling was avoided since the resultant film passivates the electrode. However in the DSSC only a very thin film is required and hence it was thought that redox cycling can be used to improve the adherence of the melanin film and increase the cell efficiency. Initially this appears to be the case, with the best performing film being the one subjected to short potentiostatic redox cycles. However, when tested under more intense light source, it appears that the performance of the DSC seems dependent only on the oxidation cycle, with the film subjected to redox cycles producing less photocurrent than the film that was subjected to oxidation only (See Figure 4.9).

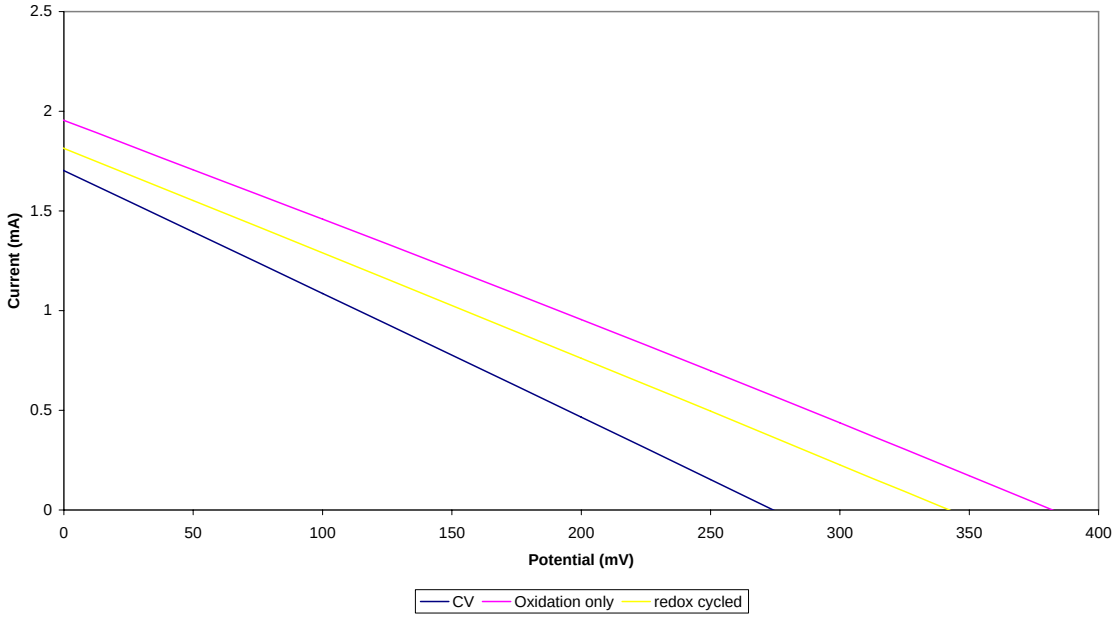

Figure 4.9. IV curve of melanin DSSC with opaque P25 under 110 mW/cm^2 AM 1.5 illumination. Melanin synthesised by: CV scan between 1.5 to -1 V at 50 mV/s for 30 minutes ; Potentiostatic oxidation at 1.5 V for 15 minutes followed by reduction at -1 V for 5 minutes; A series of 2 minute potentiostatic oxidation/reduction at +1.5 and -1 V for 30 minutes.

The difference was more significant when the 420 nm cutoff filter was used, indicating that the melanin subjected to potentiostatic oxidation was more highly oxidised and therefore was able to absorb more visible light (See Figure 4.10).

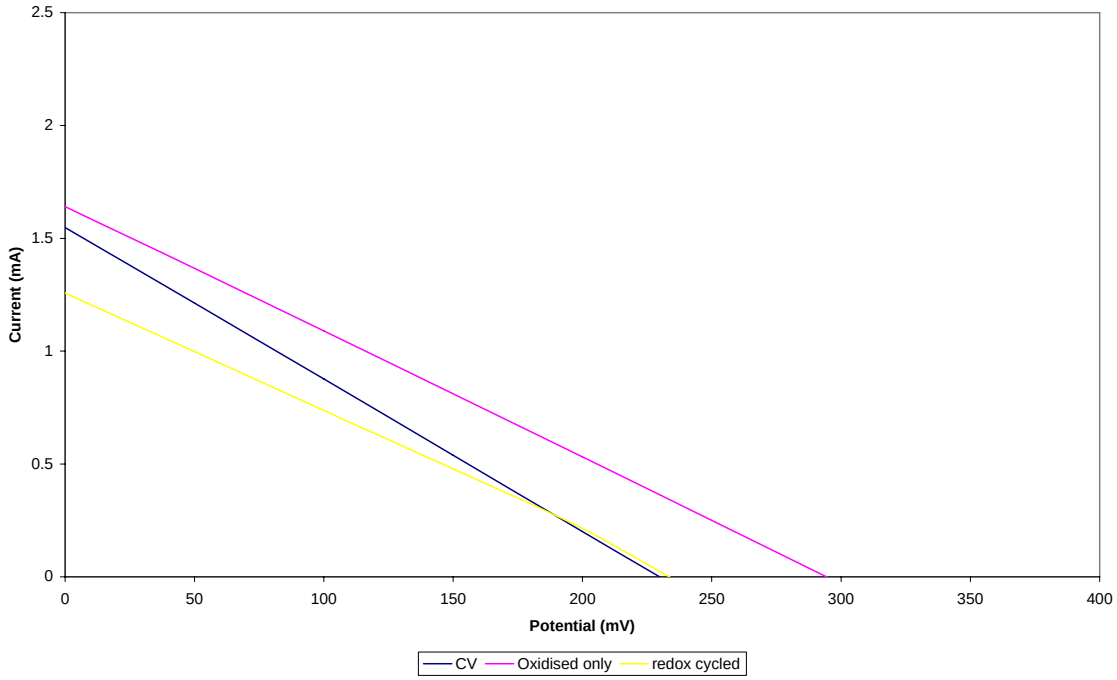

Figure 4.10. IV curves of the melanin DSSC tested under 420 nm cutoff filter. Cells were made as per Figure 4.7.

Amongst the oxidation methods tested, it appears that potentiostatic methods gave the best result. When CV was used, the DSSCs gave lower photocurrent and this was attributed to the idle time during a CV where the potential was below that of the oxidation potential of the melanin intermediates. In potentiostatic polymerization these idle times were eliminated, providing a more efficient polymerisation. It must be noted that the IV curves was linear due to a capacitance effect, which will be discussed later in this chapter.

It does appear, however, that the redox cycles increases the mechanical integrity of the melanin film, since films produced by cyclic methods showed less decay over time when subjected to a light source with high infrared radiation content. However, under normal conditions there were no difference in stability observed between the films that were cycled and ones subjected to oxidation only, and therefore it was concluded that the single-step oxidation process would be the most efficient and effective way to produce melanin DSSC.

In the electrochemical synthesis of free standing films galvanostatic method was preferred, however in the synthesis of melanin DSSC potentiostatic method gave better results. This is because in galvanostatic method the resistance increases as the melanin film builds up on the TiO_2 and an increasingly large potential was required to maintain the current. Although galvanostatic method would give a more stable rate of polymerisation, the higher potential seems to have a negative effect on the titania film as it seems to oxidize the titania and reduce its mechanical integrity. Furthermore, due to the low concentration of dopa used, the electropolymerisation was diffusion controlled, and increasing the current does not increase the rate of polymerisation. Instead, it may result in oxygen formation which was detrimental to the formation of melanin since the newly formed bubbles would push the intermediates away from the titania surface.

The optimum concentration of dopa was found to be 5 mM, which provided sufficient melanin formation within a short period of time. When very low concentrations of below 1mM were used, the reaction proceeds slowly and significantly more time was needed to deposit an equivalent amount of melanin onto the titania film. Higher concentration of l-dopa did not result in any significant improvement to the DSSC, and thus would only result in higher amount of wasted starting material.

The optimum pH was found to be pH 8-9, which was slightly lower than the pH used in our electrochemical synthesis. This was because unlike the electrochemical synthesis which was aimed at free standing films, our DSSC required thin, adherent films and when the oxidation was done at pH 10 and above the rate became too great and the process became more difficult to control, resulting in highly dyed films which performed poorly as a DSSC. Furthermore, the concentration of l-dopa required was significantly lower than those used in the electrochemical synthesis, and hence a lower pH was sufficient to dissolve the dopa completely. Similarly to the electrochemical synthesis, best result was obtained when the concentration of the borate buffer was minimised by dissolving the dopa in minimum amount of the borax stock solution before diluting to volume.

Mechanical stirring was also not used for a similar reason in that it reduced the amount of reactive intermediates available for polymerisation and the resultant film would be too thin even after extended oxidation period (See Figure 4.11). The polymers that were formed within the pores of the titania should be relatively unaffected by stirring, however, due to the several steps required for melanin formation, the intermediates exist for a significant amount of time and mechanical stirring would strip these intermediates away from the titania film before they have a chance to oxidise further into melanin.

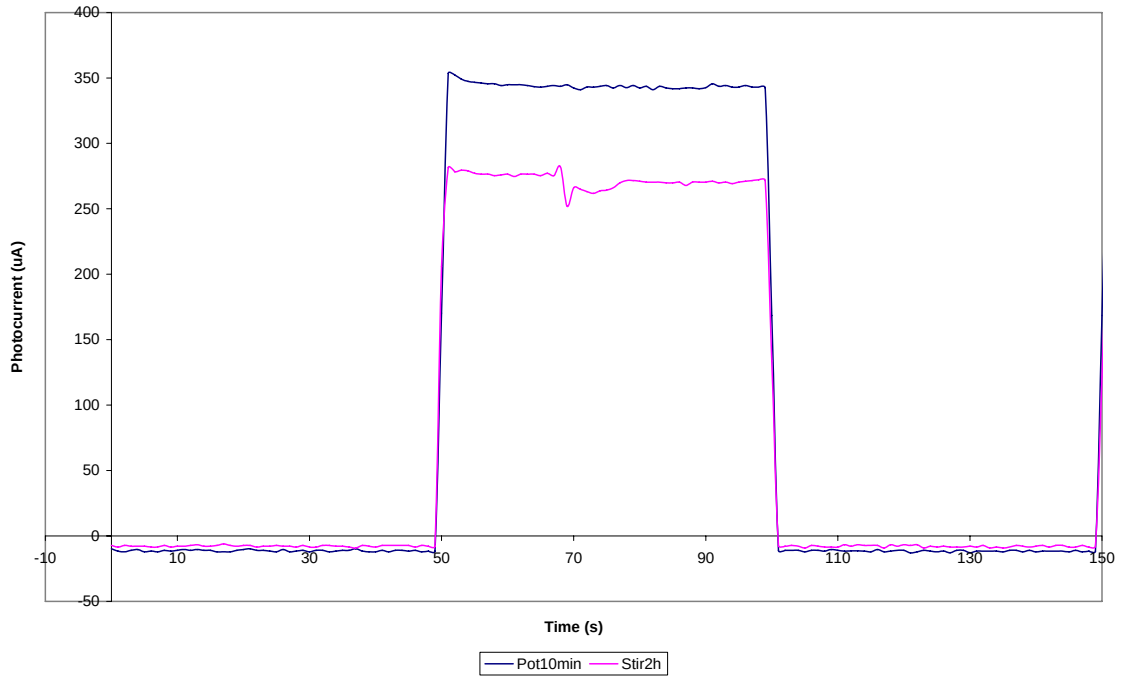

Figure 4.11. Photocurrent under 38 mW/cm^2 AM 1.5 illumination of melanin DSSC made by: Potentiostatic oxidation at 1.5 V for 10 minute; Potentiostatic oxidation at 1.5 V for 2 hours with mechanical stirring.

The melanin film seems to perform best when it is synthesised from a dopa solution rather than a preoxidised melanin solution. Unlike the electrochemical synthesis, preoxidation of the solution at higher potential resulted in a cell with less photocurrent (See Figure 4.12). Our attempt to coat the titania by dipping it into a more concentrated preoxidised solution and oxidising it an a separate salt solution was also unsuccessful in that very little melanin was actually deposited. This was attributed to the fact that the monomer and intermediates would be better able to penetrate into the titania pores

compared to melanin granules present in a preoxidised melanin solution. This observation agrees with our previous result regarding film thickness, in that thicker film would act as a filter rather than a sensitizer.

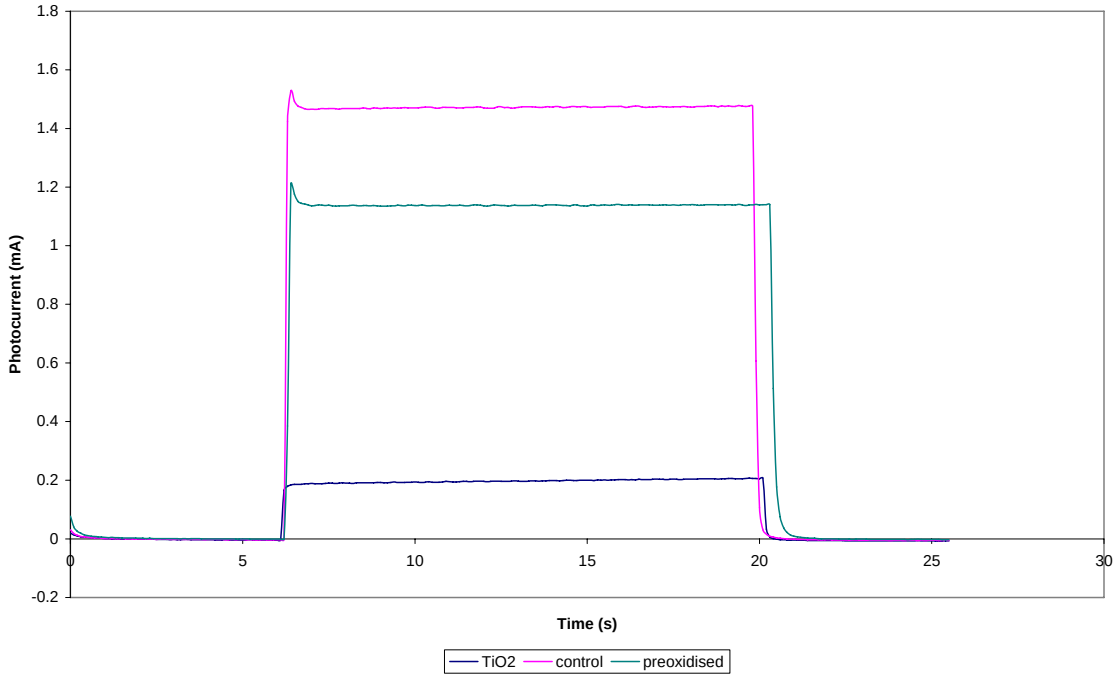

Figure 4.12. Photocurrent of melanin DSSC made by potentiostatic oxidation at 1.5 V for 10 minutes with and without preoxidation of the solution. DSSCs tested under 95 mW/cm^2 of AM 1.5 illumination

4.3.4. Choice of Titania

The choice of titania affects the cell quite significantly. Best results were obtained using Degussa P25, and when hydrothermally treated titania were used very little to no photocurrent was observed. Since the two films were of similar thicknesses, this was most likely due to the pore size of the titania, since the hydrothermally treated titania has a smaller particle size arranged in a more compact structure. SEM investigation showed that the P25 film was rougher and more porous than the hydrothermally treated one (See Figure 4.13). The smaller pore size would mean that it was more difficult for the melanin oligomers to diffuse through and polymerise inside the titania, so most of the polymer would simply coat the outer surface of the titania film. This resulted in a much smaller

effective area of the cell since only the outermost layer would be able to harvest visible light.

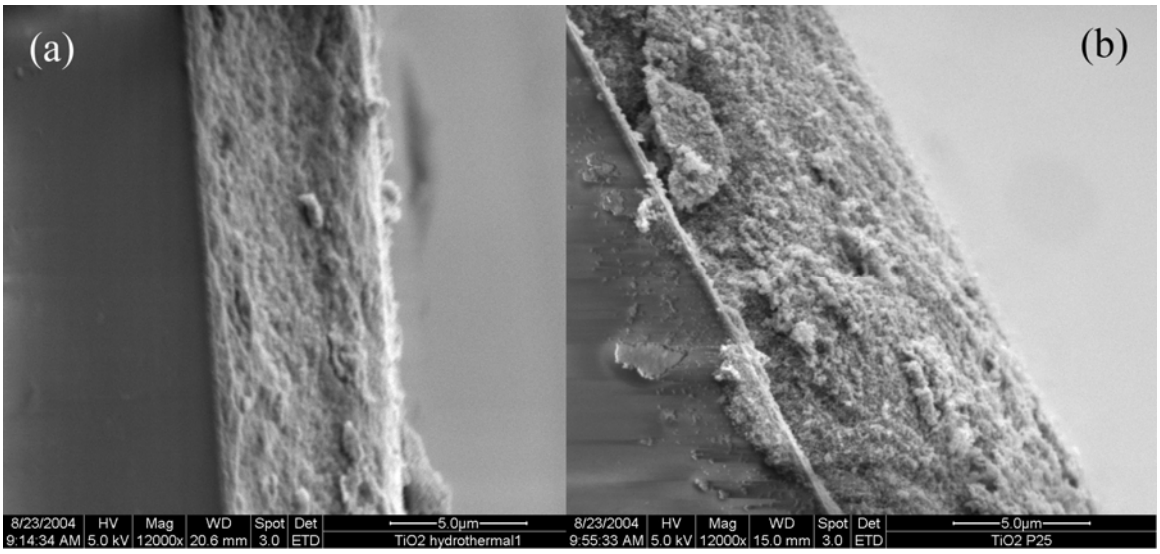

Figure 4.13. Cross section of the titania films (a) hydrothermally treated (b) P25

4.3.5. Incident Photon conversion Efficiency (IPCE)

Being a natural photoprotective agent, melanin exhibit a very high absorbance in the UV region, and this absorbance tails off into the visible region as far as 600 nm (See Figure 4.14) The shape of the absorption spectra does not show any significant peak, and this may be due to the various possible oxidation states and different molecular weight species absorbing at slightly different wavelength, producing an almost smooth featureless profile.

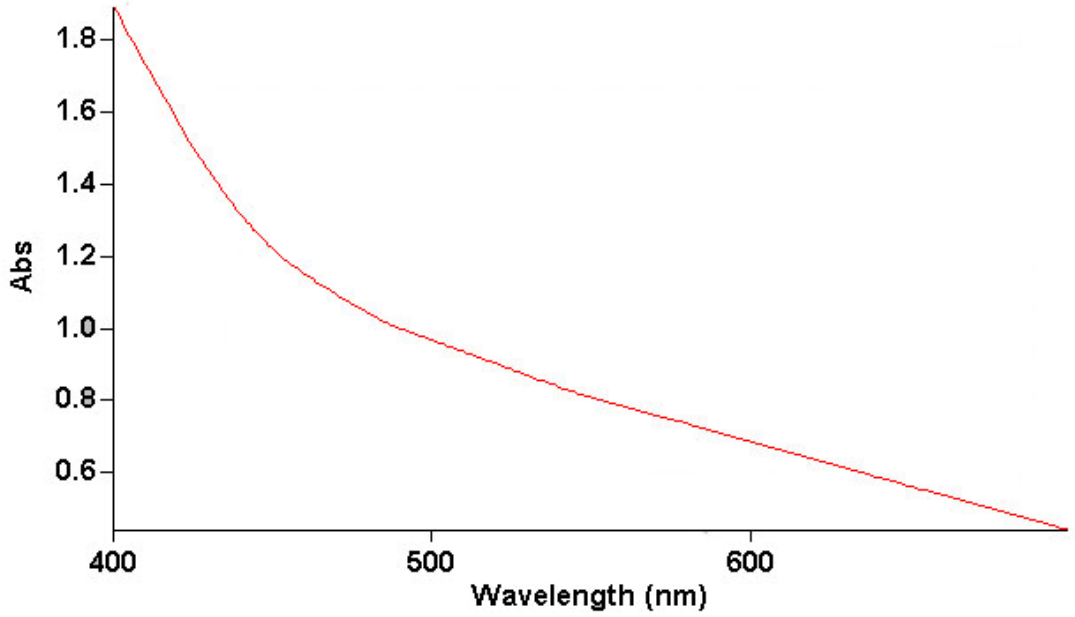

Figure 4.14. UV-Visible absorbance of melanin dissolved in caustic solution

The photodynamic response of the melanin DSSC showed a peak at around 470 nm and tails off towards the NIR region, with the peak at 350 nm being attributed to TiO_2 rather than the dye. The melanin DSSC displays its greatest photocurrent in the 400-470 nm region and the photocurrent steadily decreases after that with very little photocurrent observed past 600 nm. The photocurrent profile was very reproducible in that cells dyed with varying amount of melanin shows the same photodynamic spectrum (See Figure 4.15).

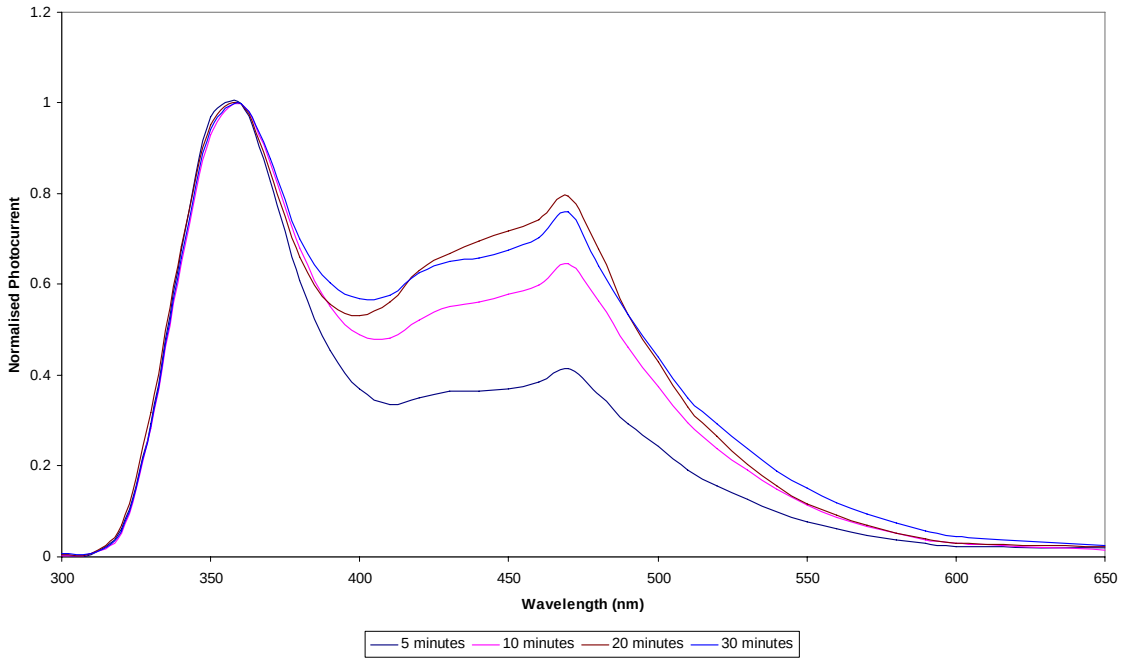

Figure 4.15. Photodynamic spectrum of melanin DSSCs dyed by potentiostatic oxidation at 1.5 V of 0.003 M l-dopa in borax buffer on opaque P25 TiO_2 films with varying amount of time

Due to instrumental restraints, we were unable to determine the response under 300 nm, however this was deemed to be insignificant since most of the photovoltaic response below 400 nm would be due to the TiO_2 and not the melanin, and therefore would not be a true reflection of the efficiency of the dye itself.

Comparison with the N3 dye (See Figure 4.16) shows that melanin is not quite as efficient in harvesting visible light, since the melanin response tails off where the N3 is still absorbing strongly towards the NIR. Furthermore, the N3 dye shows its greatest absorbance in the visible region, while the melanin absorbs more strongly in the UV.

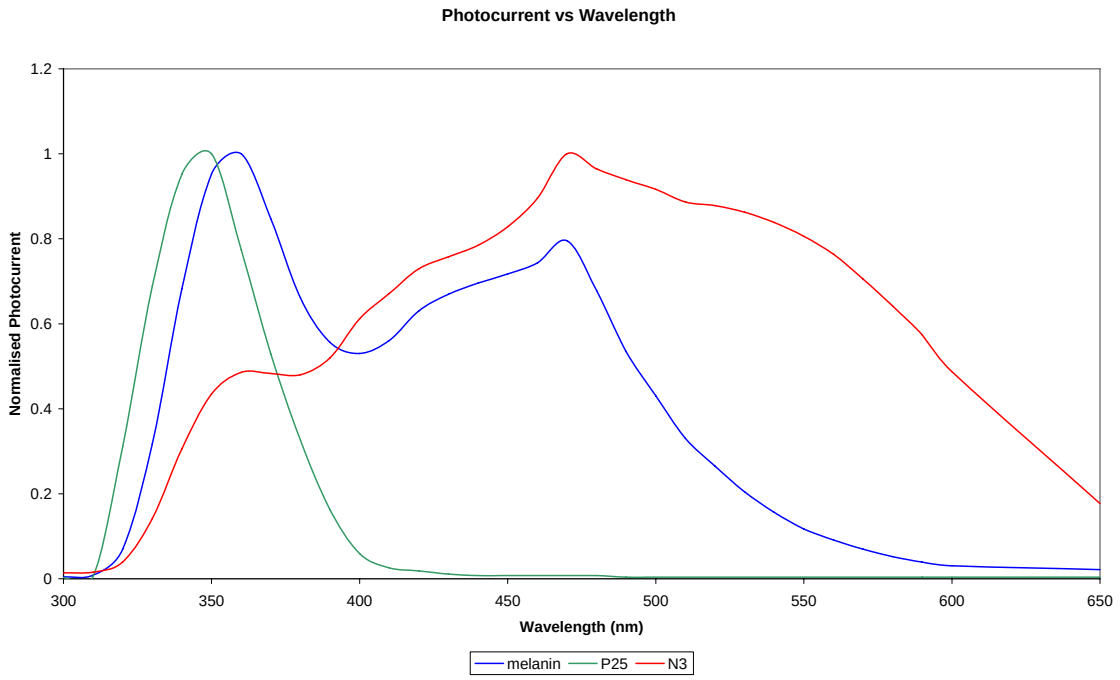

Figure 4.16. Photodynamic action spectra of melanin DSSC, N3 DSSC, and a blank TiO_2 cell as control.

Theoretically, further oxidation of melanin would lead to more absorbance in the visible since a higher molecular weight would result in more conjugation and hence absorbance at higher wavelengths. This was not the case because when further oxidation was done in the electropolymerisation process, we encounter the problem of having an overly thick film where light filtering occurs due to the low conductivity of the material.

Furthermore, CV of a melanin film (see Figure 4.17) showed that after a thin film of melanin is formed, a single oxidation cycle was sufficient to fully oxidise the polymer. There was a significant shift in the reduction peak at -0.5 V between cycle 1 and 2, which may be due to the oxidation of the oligomers and lower molecular weight species still present in the first scan into the species detected in subsequent scans. In the subsequent cycle there was no further shift which indicates that there is no further change to the oxidation potential of the polymer, indicating that the polymer have reached a maximum conjugation length.

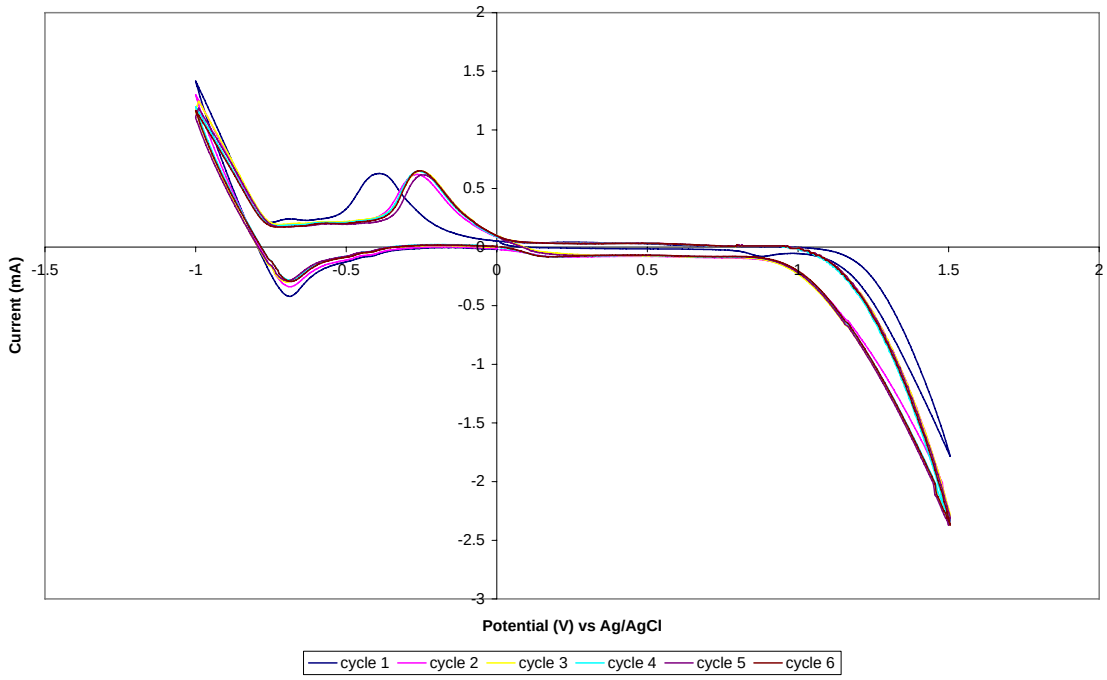

Figure 4.17. CV of a thin film of melanin on platinum electrode synthesised from 0.02M l-dopa in borax buffer by potentiostatic electropolymerisation for 12 hours at 1.5 V. CV taken in a 0.05 M borax solution with a scan rate of 50 mV/s.

As a measure of efficiency as a function of wavelength, the Incident Photon Conversion Efficiency (IPCE) was calculated by comparing the power output of the cell at a particular wavelength to power of absorbed light at that wavelength:

$$IPCE_{\lambda} = (P_{incident} - P_{transmitted}) / P_{out}$$

In order to obtain the IPCE, the power output of the monochromator was first measured as a function of wavelength, and it was found that the monochromator output peaks at around 450 nm, with a significant decrease afterwards. Between 400-600 nm, this output is quite similar to the photocurrent action spectra of the cell, with a peak at around 480 nm and a steadily decreasing response afterwards. We were unable to accurately measure the light power below 400 nm due to instrumental limitations, however, looking at the photocurrent profile it is likely that the response below 400 nm would be mostly due to the titania and not the melanin itself.

The IPCE (See Figure 4.18) differs from the photodynamic spectrum, with the melanin cell showing a broad peak efficiency between 400-450 nm. Compared to the photocurrent action spectra, the IPCE had a peak of 13% between 420 -450 nm, with a sharp decrease after 480 nm. The maximum IPCE was around 13.3 % at 430 nm, which was quite low compared to the IPCE of the N3 dye which had a peak IPCE of 55 % at 510 nm.

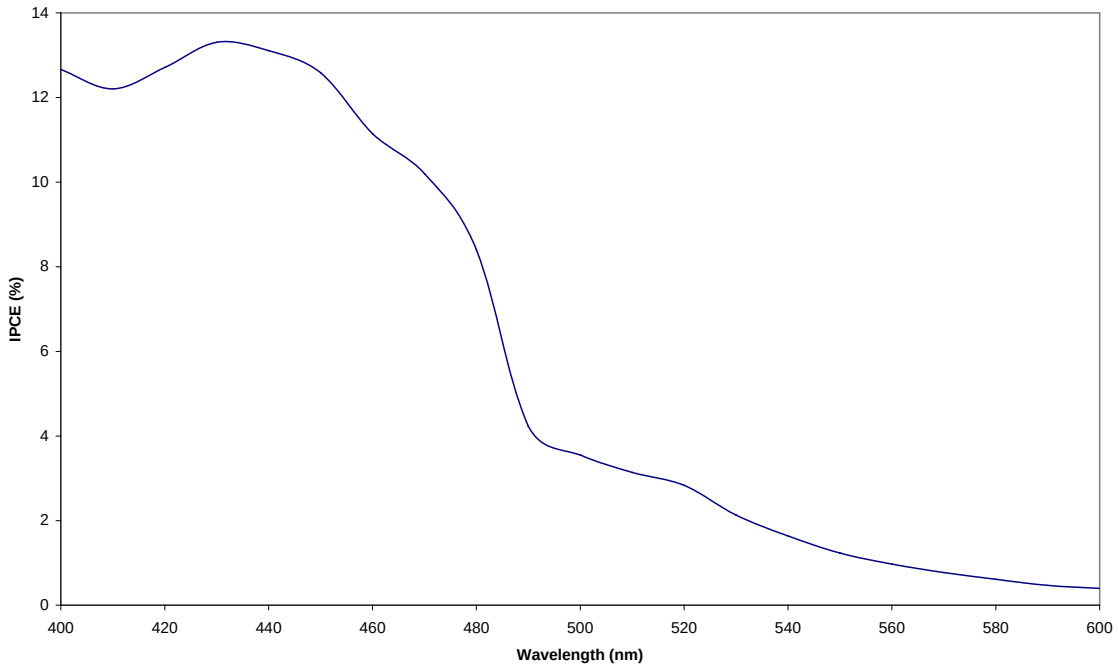

Figure 4.18. IPCE of the melanin DSSC

Like the photodynamic action spectrum, the IPCE showed a departure from the absorption spectra of melanin, since in the IPCE there was a shoulder in the 400-480 nm range whereas the absorption spectra was practically featureless at that particular wavelength region (see Figure 4.19).

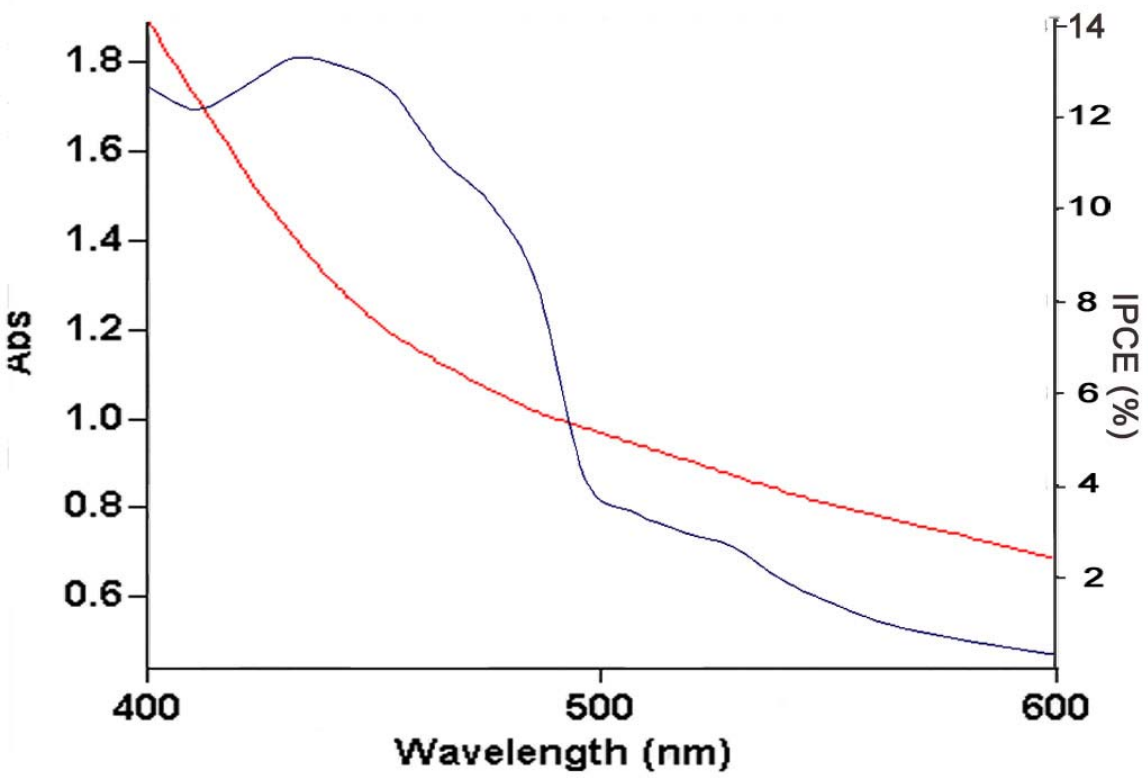

Figure 4.19. Comparison between the absorption spectra and the IPCE of melanin

This deviation has been observed by Jartzebska et al[131] who found a minimum in photocurrent at 600-700 nm and they postulated that the mechanism of trap emptying determines the spectral range of the photoconductivity in melanin. Carriers captured by traps can be released by the radiation of the UV-VIS and IR range, resulting in the appearance of photocurrents which depends on the concentration and the degree of filling of the traps. The IPCE profile obtained for melanin was also similar to the one obtained by Yanagida et al[196] for their polythiophene-sensitised DSSCs, but so far there has not been any in-depth study regarding this effect and it was beyond the scope of this research project.

4.3.6. UV Post Treatment

Interestingly, in order for the melanin DSSC to reach their maximum output they needed to be 'activated' by irradiation with UV light. Initially the output of the melanin cell was

very poor, however, the photocurrent of the cell increased almost linearly with UV irradiation up to a point where it stabilizes (See Figure 4.20). After this activation process the cell performed at that level even when the UV light is removed. The cell returned to its previous efficiency after being stored for 24 hours in the dark, but could be reactivated by the same method.

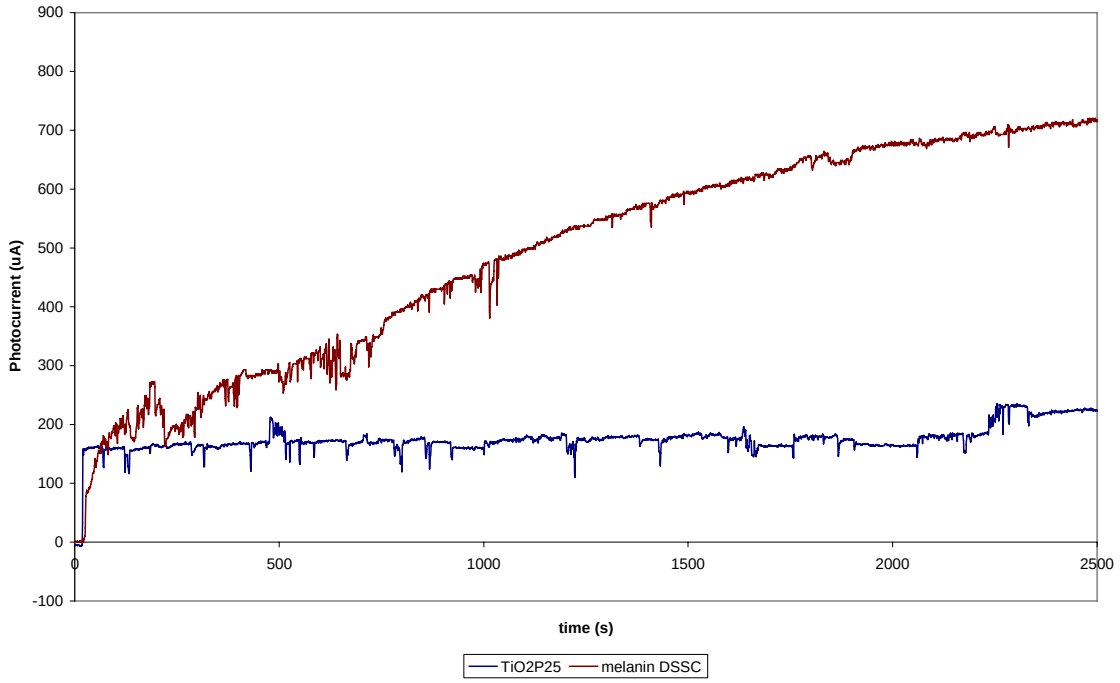

Figure 4.20. The increase in photocurrent of the melanin DSSC upon irradiation with 38 mW/cm^2 of light from a Xe lamp with an IR filter only. The blue line is of a blank TiO_2 cell and indicates the contribution of TiO_2 to the photocurrent.

This was attributed to photodoping, where the UV irradiation increased the number of charge carriers in the polymer, thus making the polymer a more efficient conductor and increases its efficiency. This also increased the delocalisation of electrons in the polymer and shifted its absorbance towards the visible light region of the spectrum (See Figure 4.21) hence increasing the amount of light it absorbs and the resulting photocurrent.

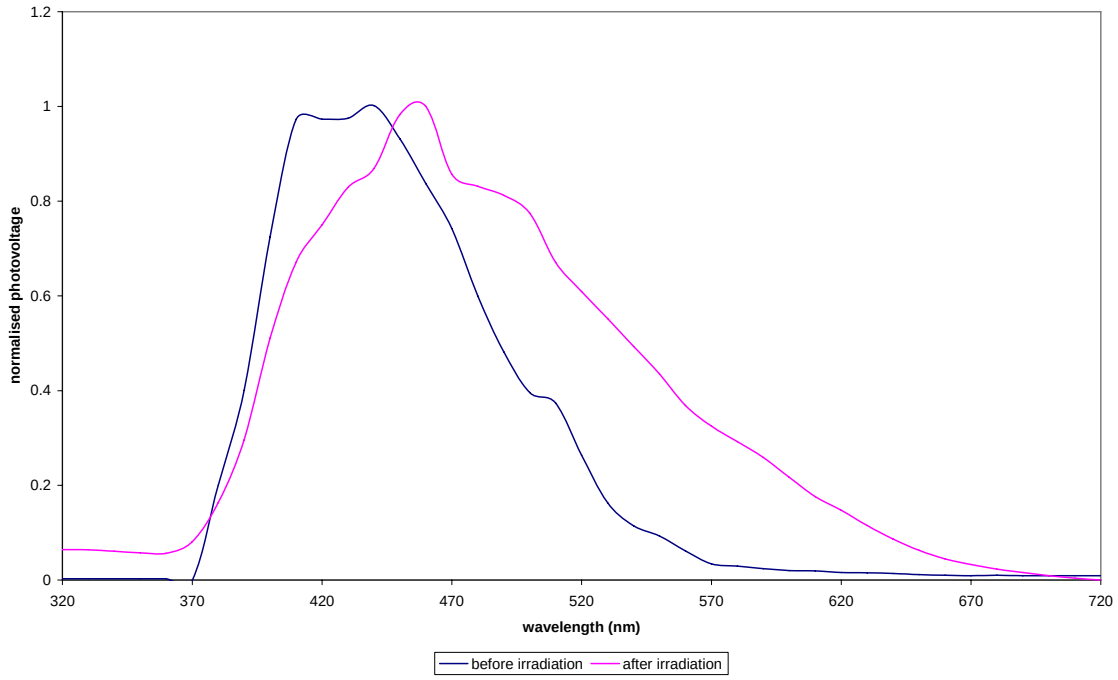

Figure 4.21. Photodynamic action spectra of the melanin DSSC before and after irradiation with 38 mW/cm^2 illumination from a Xe lamp with an IR filter only.

Despite the need for UV activation, the reproducibility of the cell activation process was quite good and the activation process had been repeated up to five times with a 38 mW/cm^2 light source without significant loss in photocurrent. There has not been longer testing with the activation cycles due to problem with loss of electrolyte in the cell, however, an activated cell showed a stable photocurrent of around 220-240 μA under fluorescent light for 4 days, with a loss of photocurrent afterwards due to loss of electrolyte.

Furthermore, this activation effect was also more observable with lower light energy, since when a lamp of higher power density (upwards of 100 mW/cm^2) was used, the activation period was shortened significantly (See Figure 4.22). At light density of higher than 150 mW cm^{-2} the activation period was shortened to a matter of minutes.

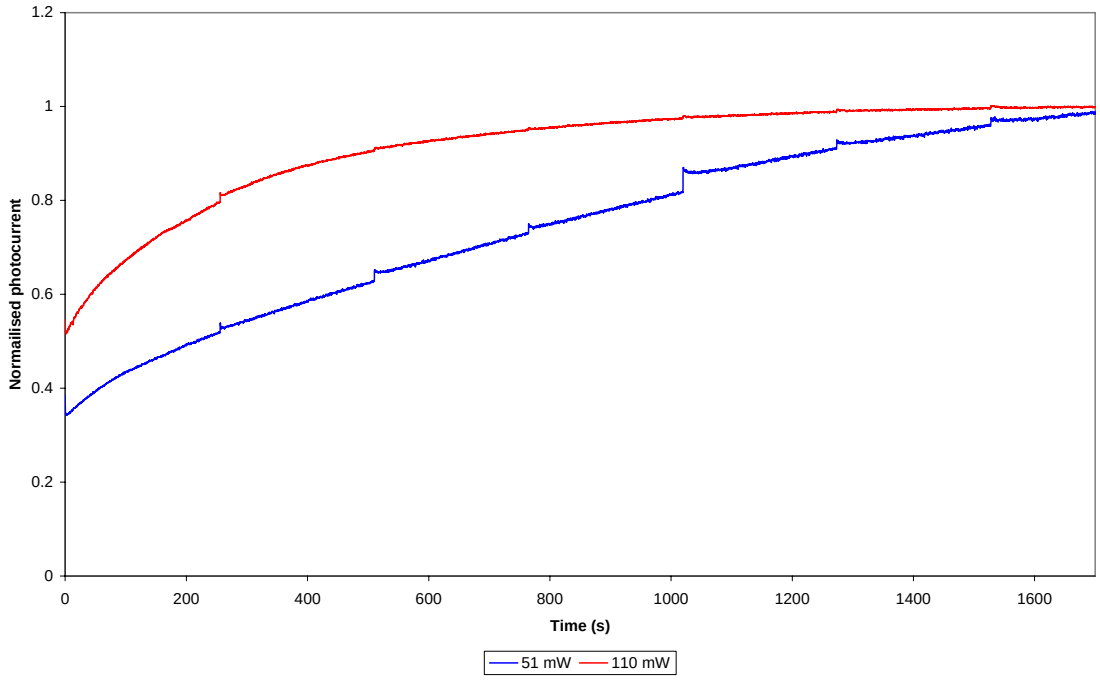

Figure 4.22. Increase in photocurrent upon irradiation with differing light intensity from a Xe lamp with IR filter only.

4.3.7. Electrochemical Post Treatment

Since it appears that the efficiency of the melanin DSSC depended on the oxidation state of the polymer, several post treatments were considered to see if the cell could be made more efficient or be 'activated' through electrochemical means rather than by UV radiation.

However, it seemed that post-synthesis oxidation did not have any effect on the performance of DSSC. Although it was thought that by oxidising the melanin further we can increase the amount of quinone in the polymer and therefore increase the efficiency of the cell, it is very likely that since the initial concentration of dopa in the solution was quite small some of the potential supplied would be used to oxidise the melanin already formed on the titania rather than to oxidise new precursor molecules from the solution, resulting in a highly oxidised polymer film. Even though the film was subjected to electrochemical reduction afterwards, the reduction would affect mainly the interface

between the melanin and the titania and not the bulk of the melanin itself since the high pH used would suppress reprotonation/reduction of the quinone.

The application of potential across the cell to activate the melanin by oxidation was also unsuccessful. When a small potential was applied, there was no effect on the cell, and when the potential was increased it seemed that hydrogen/oxygen production occurs and this was detrimental to the DSSC. It appears that the potential required to activate the cell is higher than that for hydrogen/oxygen formation, and therefore the titania and the melanin film would be damaged by gas formation before it could be activated electrochemically.

Since the efficiency of the cell depends quite significantly on the conductivity of the melanin film, it was thought that by doping the film we can not only improve its conductivity but may also alter its oxidation state to make it perform better in a DSSC. However, attempts at doping the polymer with common organic dopants such as p-toluenesulfonate and dodecyl sulphate were unsuccessful, with the doped melanin film showing no significant improvement over the undoped film. This is attributed to the low conductivity gain of the melanin polymer upon doping, since the conductivity of the melanin seems to be more dependant upon hydration rather than dopant (Section 3.4.4), with the conductivity gain of the melanin upon hydration greatly exceeds that by doping.

Since organic dopants did not seem to have any significant effect, another possibility was the use of metal ions as dopants. Post synthesis doping was required since if the metal ions are present during synthesis they would interfere with the oxidation process by forming a complex with dopa, preventing it from further oxidation and hence little or no melanin formation was observed. It was thought that these metal ions may help influence the oxidation state of the polymer in a similar way that UV radiation does, increasing the amount of quinone and hence making it a more efficient light harvester.

Metal ions have also been postulated to affect the DHI:DHICA ratio in the polymer. Since the amount of DHICA (and hence the carboxylic acid groups that could bind to the

titania) in the final polymer would influence the electronic connection between the polymer and the titania, it is possible that the cell efficiency would increase if we were able to synthesise melanin in the presence of metal ion catalyst such as zinc which has been postulated to increase the DHICA:DHI ratio in the final polymer.

However, doping with metal ions was unsuccessful, with cells dyed electrochemically with melanin and subjected to post-synthesis doping with metal ions giving less photocurrent over the control sample. It appeared that post synthesis doping with metal ions did not improve the electronic properties of the melanin, while the extended oxidation time was actually detrimental to the melanin DSSC and therefore the photocurrent was significantly reduced.

This indicates that metal ions have their greatest effect on the oxidation process of melanin rather on the melanin itself. Metal ions that form square planar complexes are known to influence the oxidative pathway of dopa and affect the ratio of DHI to DHICA in the final polymer, but it appears that these metal ions have little effect on the melanin itself once it is formed. It is possible that when they are introduced after synthesis, these metal ions would simply form a complex with available hydroxyl and quinone groups in the monomer unit without affecting the overall structure or oxidation state of the polymer itself.

And unfortunately, our attempts so far at introducing metal ions during synthesis have been unsuccessful. This same problem was encountered in the synthesis of free-standing films in that the metal ions would form a complex with the precursor (l-dopa) and prevent its oxidation into melanin, and as a result the oxidation process became highly inefficient and filming was hindered.

When metal ions were introduced during synthesis, melanin films were only formed when the metal ions were present in a very low or trace concentration, but this did not seem to have any effect on the performance of the DSSC. It was possible that the metal ions that are present are simply complexed by dopa and were not present in sufficient

concentration on the electrode surface in order to affect the oxidation reaction, therefore having little effect on the properties of the material.

4.3.8. Effect of electrolyte pH

Since the oxidation state of melanin depends on the pH, it is likely that altering the pH of the electrolyte will also affect the efficiency of the melanin DSSC by altering its oxidation state. From our previous observation with UV irradiation, it would appear that the higher oxidation state of the melanin was responsible for the absorption in the visible region, and thus it was thought that by increasing the pH we may be able to achieve the same effect or shift the equilibrium further to enable greater visible light absorption.

However, addition of alkaline salts into the electrolyte solution did not improve the photocurrent of the cell, in fact the alkaline pH seems to have the opposite effect in that the photocurrent was lowered. It appears that the use of alkaline pH may have been detrimental to the titania, in that the cell seemed less stable when alkaline pH was used.

4.3.9. Cell Efficiency

IV measurements were performed in order to test the efficiency of the solar cells. The efficiency is given by

$$\eta = \text{Fill Factor} \times I_{sc} \times V_{oc} / P_{in}$$

where η = efficiency

FF = Fill Factor, defined by $FF = (I_{max} \times V_{max}) / (I_{sc} \times V_{oc})$

I_{sc} = Short circuit current

V_{oc} = Open circuit potential

The maximum power region is determined from the IV curve in the area between zero potential (closed circuit current) and open circuit potential. The maximum I and V are taken from the point of infliction in the curve (see Figure 4.23)

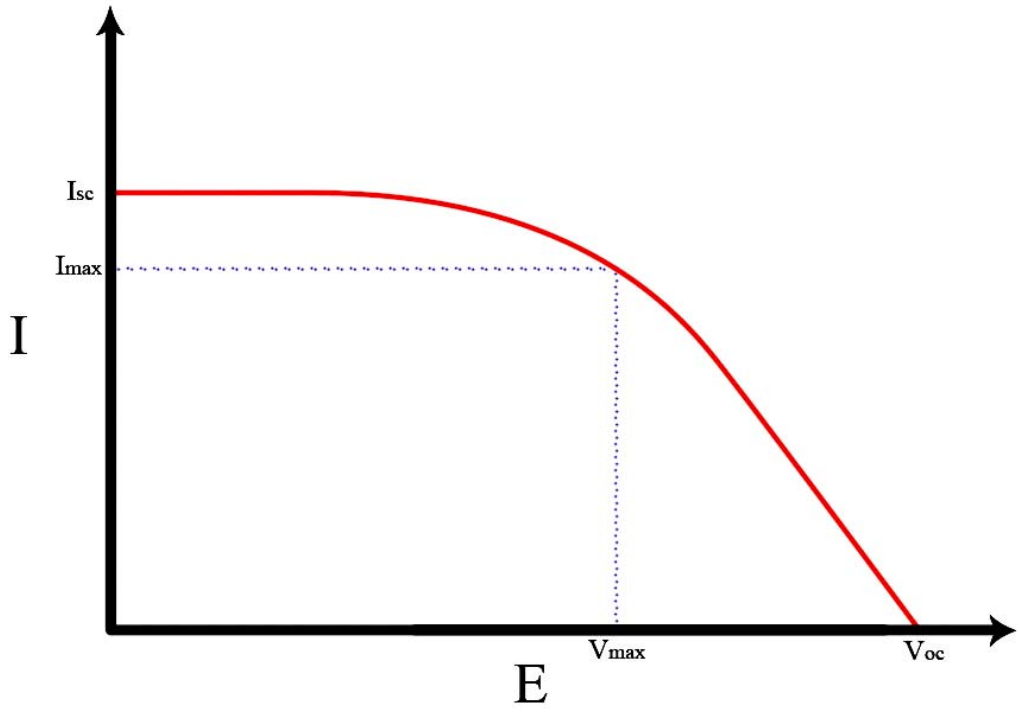

Figure 4.23. the IV curve and the maximum power region

When tested, however, our cells seemed to produce a more linear response compared to the standard diode response expected. The cause for this is still unknown, but it was not due to short circuit within the cell since the dark current of the cells gave a typical diode response with the flat region in the middle, both before and after being irradiated (See Figure 4.24).

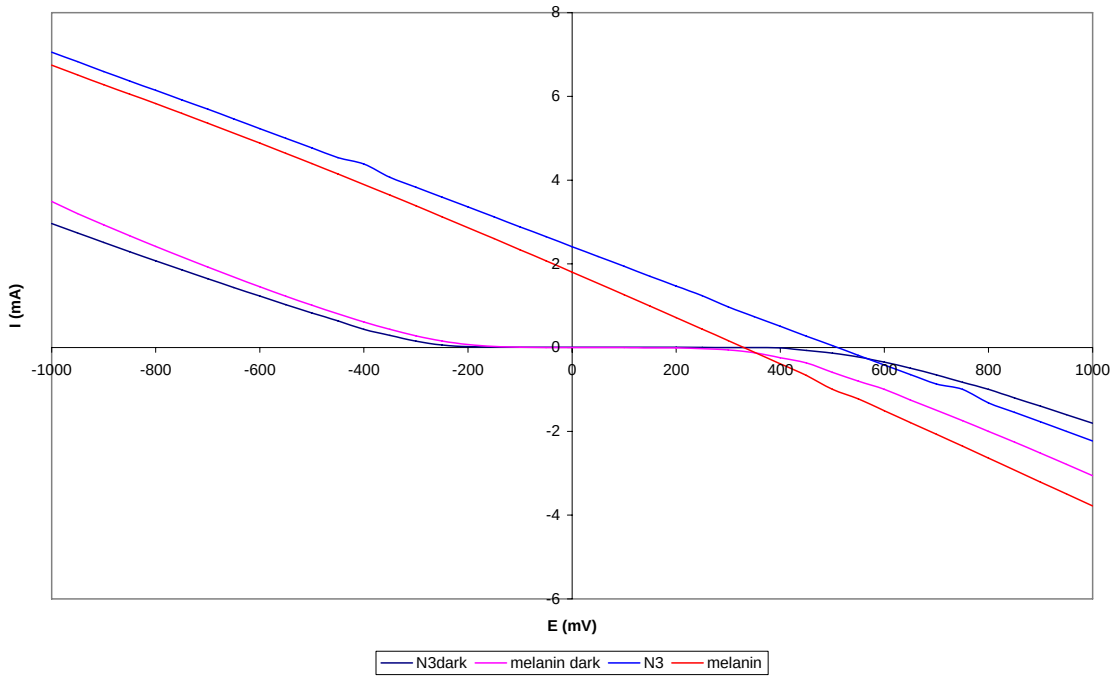

Figure 4.24. IV curves of light and dark currents of melanin and N3 DSSC. Cells irradiated with Xe lamp with AM 1.5 and 420 nm cuttoff filter used to remove UV radiation.

As can be seen the dark current followed a typical pattern for a diode, indicating that the cell was functioning normally. Furthermore, a short circuit current and open circuit potential was still observed, whereas a short circuit in the cell would result in the IV curve passing through zero.

This linearity seems to have resulted from capacitance effect which causes a shift in the curve, resulting in the linear tail end of the actual curve being observed in the region of interest around 0-600 mV. This effect was found to be dependent on the light intensity (and hence cell output) (See Figure 4.25).

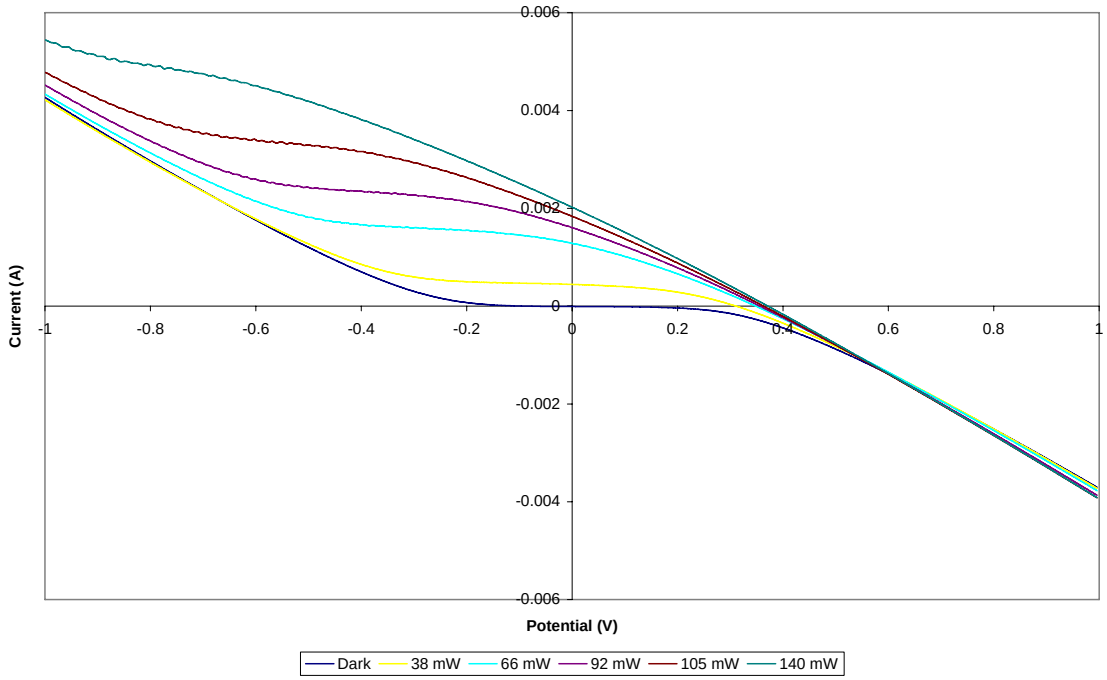

Figure 4.25. The capacitance effect in a melanin DSSC irradiated with light at different intensity. Cell dyed by potentiostatic oxidation at +1.5 V for 20 minutes followed by reduction at -1 V for 5 minutes.

The increasing light intensity caused the flat region of the curve to be shifted upwards, resulting in a linear response in the region of interest between 0-500 mV where the maximum power region was calculated. This was not limited to our melanin DSSC, with the same trend observed when N3 dye was used (See Figure 4.26), indicating that this capacitance effect was inherent to the DSSC and was not an effect of the sensitizer used.

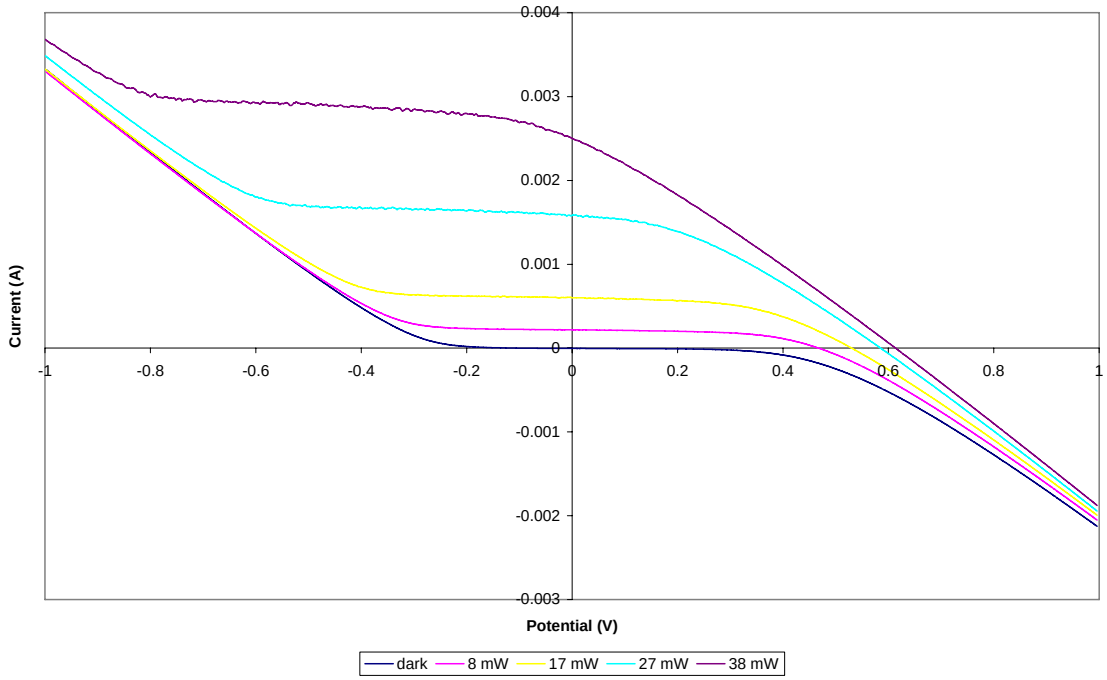

Figure 4.26. The capacitance effect in an N3 DSSC

Since the ohmic region seems to be unchanged, this effect may be due to charge build up in the cell, causing a potential shift. Initially we thought that by increasing the electrolyte concentration (and hence its conductivity), we may be able to reduce the charge buildup that occurs. However, it appears that doubling the electrolyte concentration did not eliminate this effect, with the capacitance effect still clearly visible, and the same type of shift being observed as the current increases (see Figure 4.27).

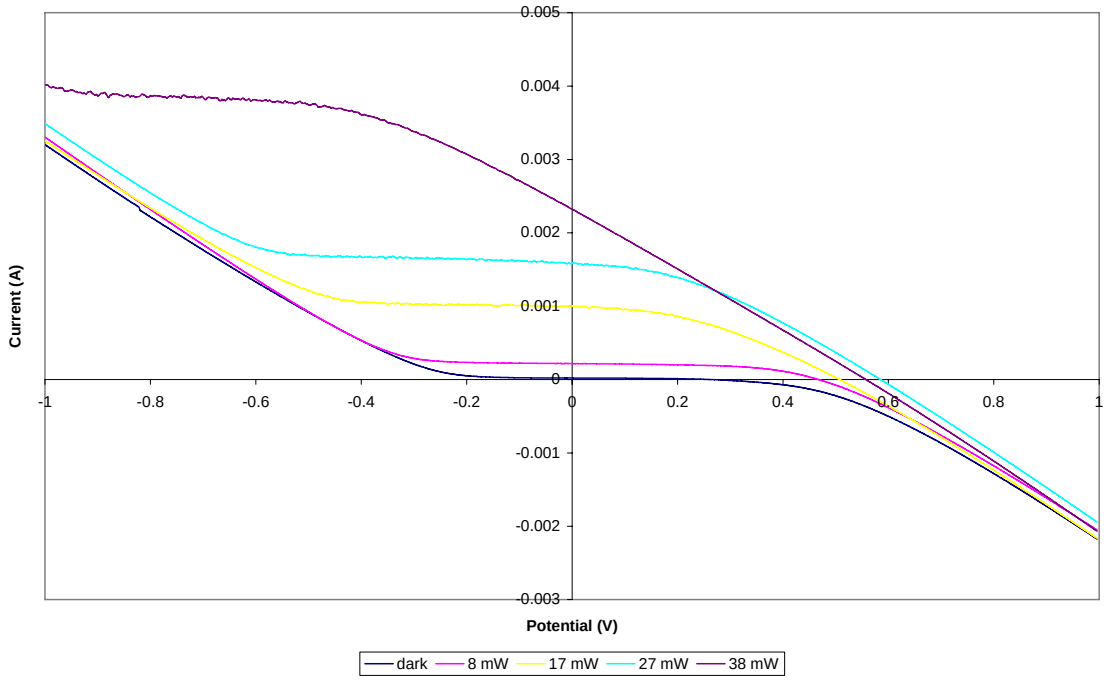

Figure 4.27. IV curve showing the capacitance effect in an N3 DSSC at higher electrolyte concentration.

There was, however, a slight increase in the photocurrent intensity which we believe is due to increased efficiency of the cell, and despite the presence of the capacitance effect, its magnitude seems to have been lessened. At 0.5 M electrolyte concentration, the flat region of the curve at a light intensity of 38 mW flattens at 3.8 mA and -390 mV, while in the cell with higher electrolyte concentration the curve at 27 mW, which flattens at around 3.4 mA, reached that point at around -20 mV.

This result showed that the higher electrolyte concentration helps reduce this capacitance effect, but the electrolyte itself did not seem to be the source of the problem. It was most likely that the higher electrolyte concentration simply helps to dissipate the charge build-up, thereby we see a lessening in the rate of the shift, but the magnitude of the shift in the IV curve still seems to follow a linear relationship. If the electrolyte was the main factor in that the capacitance was due to charge buildup in the dye-electrolyte interface, then we should observe no shift in the lower current intensities when the electrolyte concentration was increased.

Since the P25 TiO_2 used is a mixture of anatase and rutile, another possibility was that the charge was building up on the titania on the interface between the two phases. If this was the case, then when the thickness of the titania film is reduced the charge can be better dissipated and the capacitance effect should be reduced. The main problem with this method was that for thinner films, the photocurrent response was also significantly reduced (See Figure 4.28). With the thinner film the short circuit current at the maximum light density was only around 1 mA for the N3 dye, and at this current region the DSSC still showed normal diode behaviour. However, comparing the thin film to the thick film it would appear that the capacitance effect was slightly more pronounced in the thin TiO_2 film compared to the thicker film.

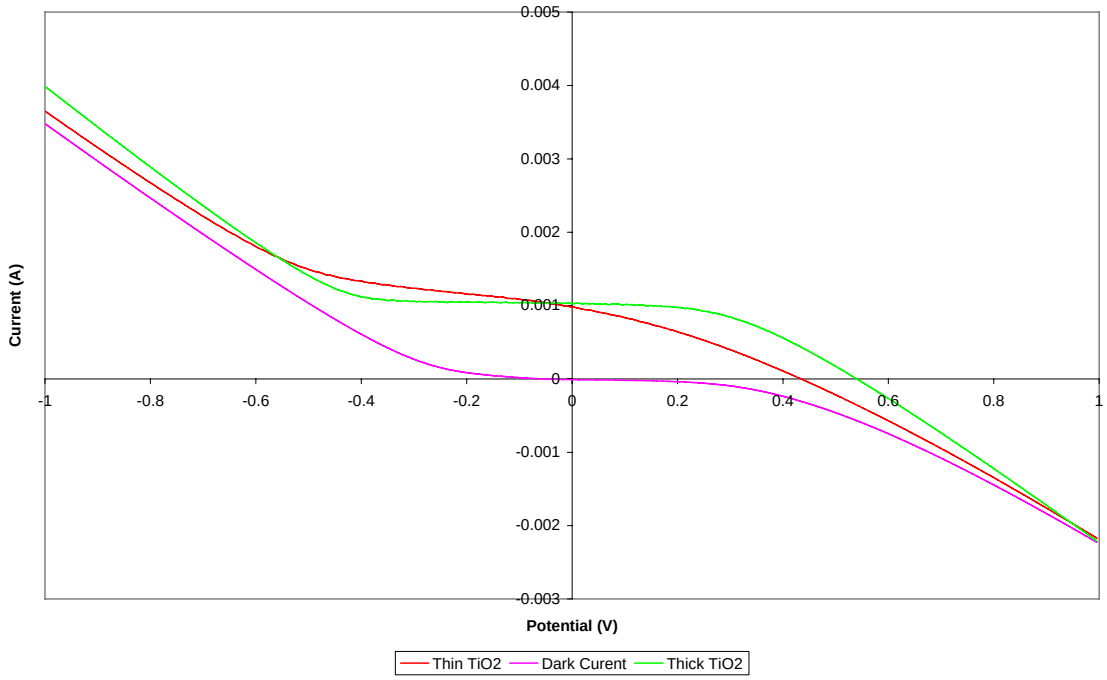

Figure 4.28. IV measurements of N3 DSSC made with differing TiO_2 film thickness. The thick film was made by the doctor blade method, while the thinner film was made by dip-coating (10 coats). Electrolyte used was 0.5 M LiI/0.05 M I_2 in Propylene Carbonate, with a cell area of 1 cm^2

This result was quite unexpected, since it was believed that by using a thinner TiO_2 film the resistance due to the titania would be smaller, and charge build up can be minimised. This observation indicates that the capacitance was not due to the thickness of the titania, but more likely due to the recombination of electrons that occurs in the interface between the titania/dye and the electrolyte. Since capacitance at the interface is dependent solely on surface area, it was possible that the thinner film actually provided relatively larger dye coverage whereas the thick film may not be entirely penetrated with the dye.

It was possible that the use of a more conductive titania such as the hydrothermally treated variety would help minimise this effect, but our melanin DSSC did not seem to function with the hydrothermally treated titania for reasons mentioned earlier, and hence it was decided that that particular experiment would be beyond the scope of this project.

Furthermore, the use of titania films purchased from Dyesol also resulted in the same capacitance effect when used in a DSSC with an N3 dye (see Figure 4.29). As can be seen the DSSC still exhibited a large shift with the flat region barely observable when illuminated despite the fact that the dark current shows that the cell was behaving as a diode and there was no short circuit within the cell. This shows that this effectwas not due to our preparation method with the titania, as it seems to be present regardless of the titania film used.

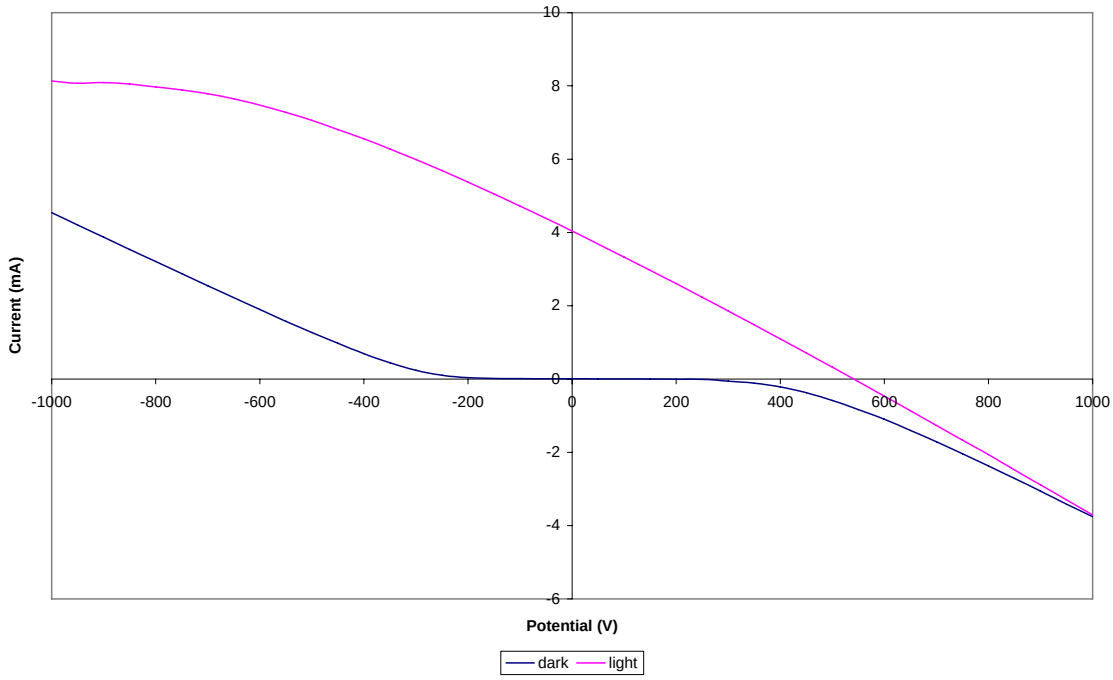

Figure 4.29. IV curve of an N3 DSSC made using TiO_2 film purchased from Dyesol

The problem with this observed linearity is that when the curve was shifted, not only would it result in a lowering of the short circuit current, but also a lowering of the fill factor which was calculated from the maximum power region due to the fact that the maximum potential and current were not extended as far as they should (See Figure 4.30). This results in a lower reading for the I_{max} and V_{max} which results in a lower fill factor.

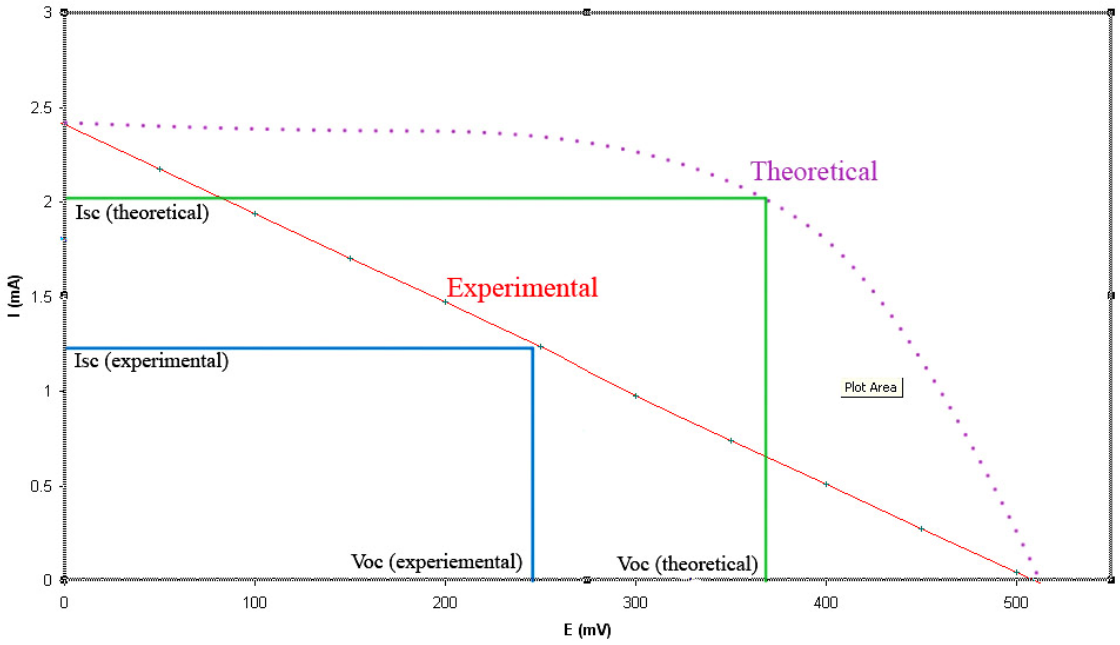

Figure 4.30. The influence of the capacitance effect on the maximum power region of an IV curve

Although there has been no specific literature investigation into this capacitance effect, this phenomenon has also been observed in the literature when less conductive polymer electrolytes was used instead of the traditional liquid electrolyte. Nogueira et al[193] reported that their DSSC utilising N3 dye and a poly(ethylene oxide-co-epichlorohydrin) copolymer electrolyte containing I_2/NaI electrolyte exhibit their greatest efficiency of 2.6% at 10 mW cm^{-2}, while at higher light intensity of 100 mW cm^{-2} the efficiency decreases quite significantly to 1.6%. Their IV curve shows an indication of a similar effect, with the curve at higher energy 'straightening out' towards linearity, albeit to a much lesser degree than what we observed.

They attribute this observation to a slower kinetic of electron transfer between the dye/TiO_2 and the electrolyte due to the higher series resistance (R_s) of the system. In their experiments their DSSC showed a series resistance (R_s) of 60 Ω with the glass electrode-polymer electrolyte system and 400 Ω when a polymer electrode is used, compared to 30 Ω for the usual system. This higher R_s creates a high capacitance at the electrolyte/dye-titania interface which was strongly dependent on light intensity.

In our case, by examining the linear region of the IV curve profile the series resistance was determined to be around ~180-190 Ω for both the melanin and N3 DSSC (See Figure 4.31). This value was obtained by plotting the linear region of the dark current and reversing the X and Y axis (with the potential on the y axis and current on the x-axis) in order to satisfy the ohm's law of V = IR, with the resistance of the cell being the gradient. It should be noted that the gradient in this case is negative in value due to the way the IV curves are measured with the current flow in the cell being the reverse of the current flow in the circuit, and anodic current being designated as having negative value.

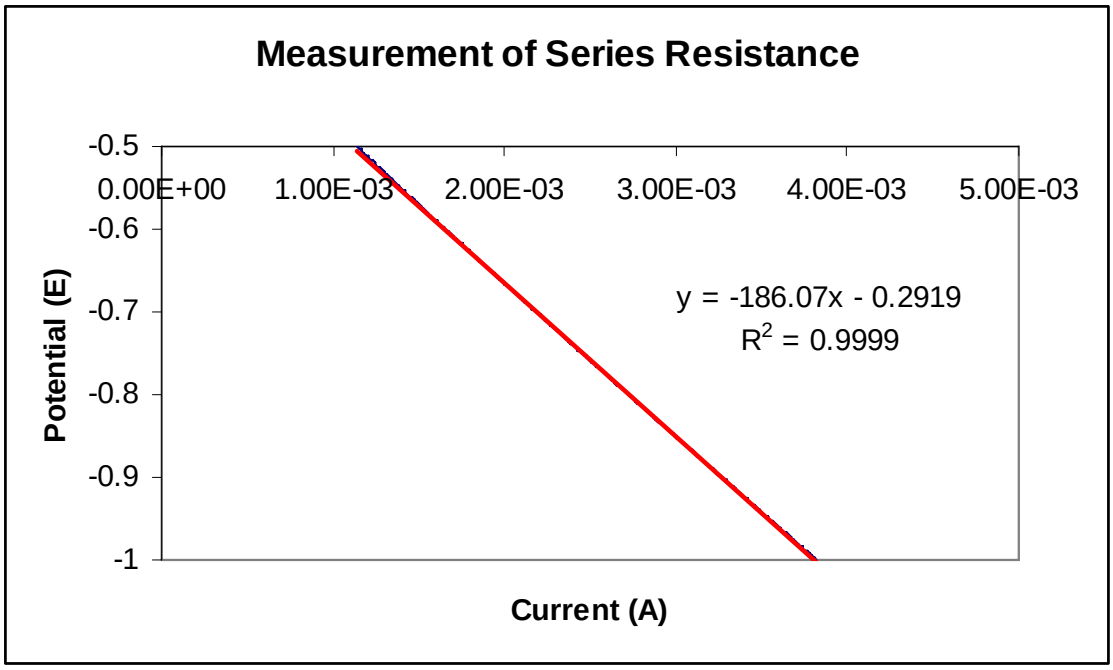

Figure 4.31. IV curve measurement of the series resistance of a melanin DSSC. The electrolyte used was 0.5 M LiI/0.05 M I_2 in Propylene Carbonate, with a cell area of 1 cm^2

Based on resistance alone, the value of 180-190 Ω, was much lower than the 400 Ω in the cell by Nogueira et al[193], but the shift in the IV curve we observe is much greater. A second conductivity measurement using electrochemical impedance method (see Figure

4.32) estimates the resistance of our DSSC at around 11000 Ω, and thus it would appear that our previous IV measurement may not have been fully accurate in that we may have induced conductivity in the titania, and the value for the resistance that we obtained may have been an underestimation of the actual resistance of the system.

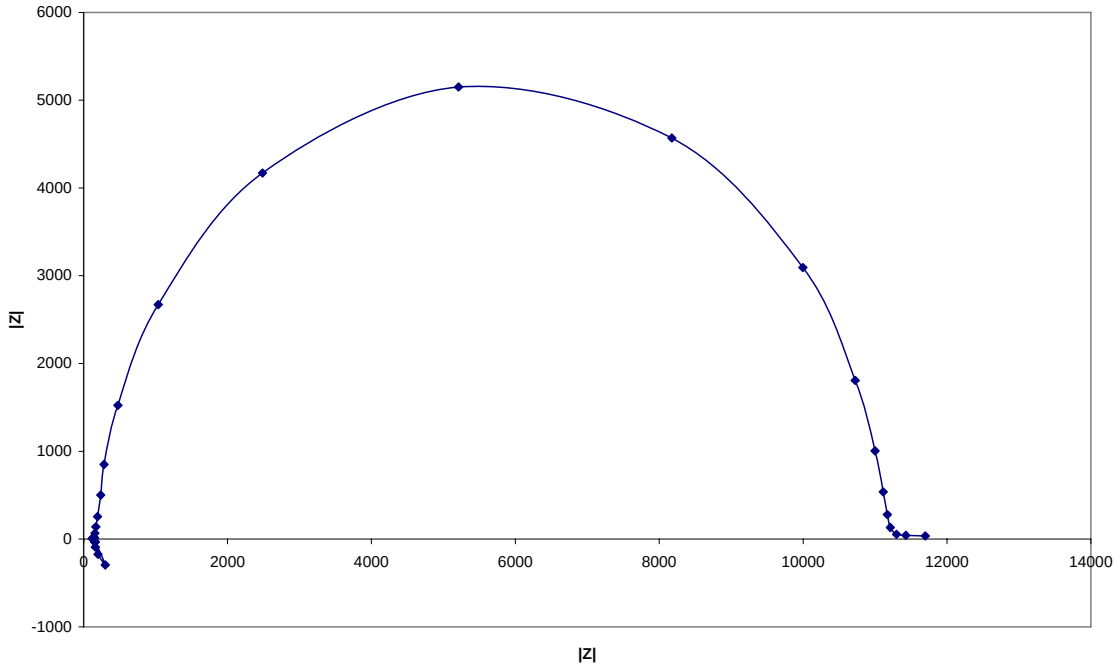

Figure 4.32.Nynquist plot obtained from electrochemical impedance measurement of our DSSC

Since the film thickness and electrolyte concentration did not seem to cause the observed shift in the IV curve, it was possible that this observed shift was due to the interface between the titania-dye and electrolyte. A full investigation into this effect was not possible due to time constraints, but this observed shift may be due to charge build-up and recombination at the titania-dye interface.

Since we were unable to overcome this capacitance effect, the efficiency of the cell was calculated at varying light intensity, with the IV curve taken and calculations performed at different light intensity. The IV curve of the melanin and N3 DSSC at various light intensity can be seen in Figure 4.33 and 4.34, with the data tabulated in Table 4.1 and 4.2.

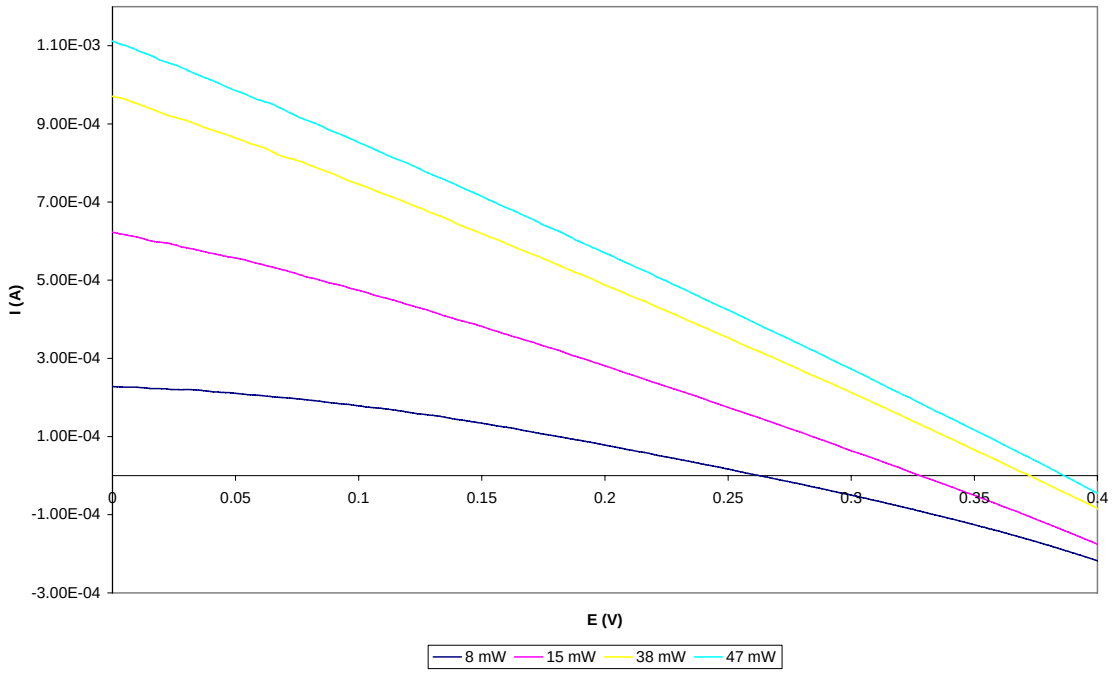

Figure 4.33. IV curve of the melanin DSSC at varying light intensity. Electrolyte used was 0.5 M LiI/0.05 M I_2 in Propylene Carbonate, with a cell area of 1 cm^2

Light Power (mW)	V_{oc} (V)	I_{sc} (A)	V_{max} (V)	I_{max} (A)	Fill Factor	Efficiency (%)
8	0.264	0.000227	0.203	0.0000746	0.25	0.19%
15	0.33	0.000621	0.225	0.000228	0.25	0.34%
38	0.374	0.000969	0.222	0.000429	0.26	0.25%
47	0.388	0.00111	0.213	0.000532	0.26	0.24%

Table 4.1. The efficiency of the melanin DSSC calculated at varying light intensity

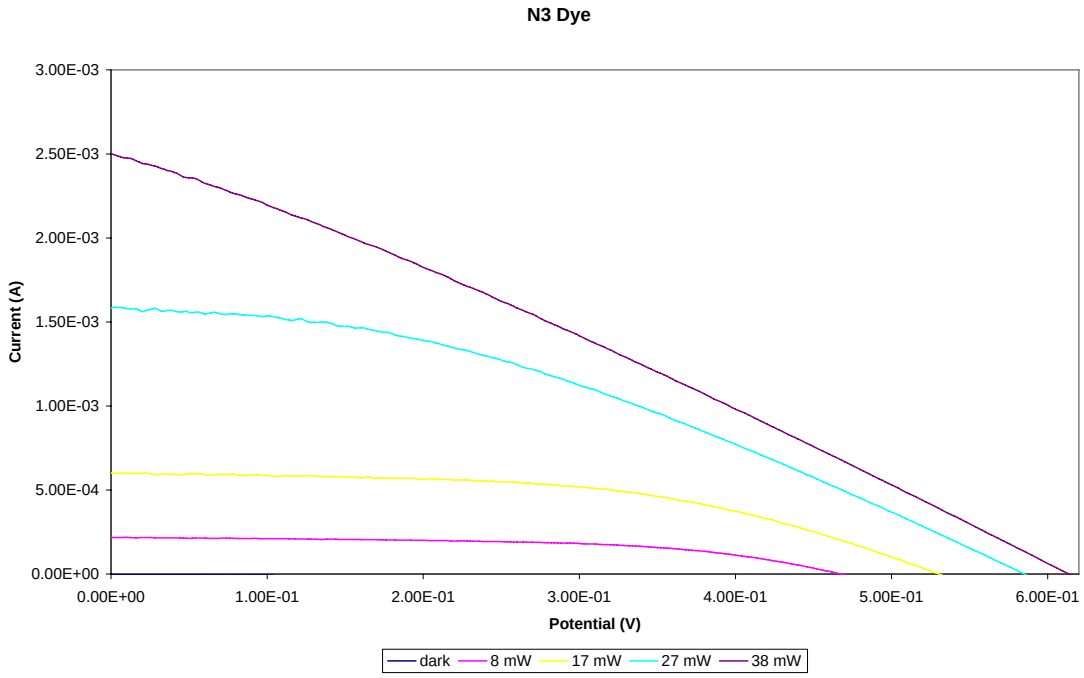

Figure 4.34. IV curve of the N3 DSSC at varying light intensity. Electrolyte used was 0.5 M LiI/0.05 M I_2 in Propylene Carbonate, with a cell area of 1 cm^2

Light Power (mW)	V_{oc} (V)	I_{sc} (A)	V_{max} (V)	I_{max} (A)	Fill Factor	Efficiency (%)
8	0.476	0.000218	0.408	0.000102	0.40	0.52%
17	0.534	0.000602	0.402	0.000371	0.46	0.88%
27	0.59	0.00159	0.332	0.00102	0.36	1.25%
38	0.62	0.00248	0.322	0.00132	0.28	1.12%

Table 4.2. The efficiency of the N3 DSSC calculated at varying light intensity

The data on Table 4.1 signifies that although the IV curve at 38 mW has the greatest fill factor, it appears that the closed circuit current was a lot lower than the profile at 66 mW, resulting in a lower overall efficiency. The N3 cell also showed a similar trend, with the

profile at 17 mW showing the greatest fill factor, but the best efficiency was found at the slightly higher light intensity of 27 mW.

From the data above, the melanin cell showed a peak efficiency of 0.34 %, while the N3 has a maximum efficiency of 1.25%. This efficiency was significantly less than the reported literature value for N3 dye, and this was most likely due to the experimental setup in that it is likely that our cell has a higher resistance and therefore lower efficiency compared to the literature.

The efficiency of the melanin DSSC was also quite low because of the fact that despite showing good photocurrents, the open circuit potential of the melanin DSSC was quite low, with the typical value of around 360 mV. This is quite similar to the values of around 400 mV in the literature for polythiophene-sensitised DSSC[196]. They believed that one of the reasons for this low V_{oc} is the shift of the conduction band edge of the inorganic semiconductor due to the protonation of the surface by the polymer[196].

4.3.10. Melanin as a gel electrolyte

As mentioned before, there has been significant interest in the use of solid or gel electrolytes in DSSC[190] due to the limitations of traditional liquid electrolytes. With solid electrolytes, the problem of sealing (and therefore leakage), and loss of electrolyte through evaporation would be removed, making the cell more suitable for various commercial applications.

Like the MEH-PPV sensitised DSSC[194] where the polymer acts as both the dye and the electrolyte, it was thought that melanin could act as both the dye and the electrolyte, but in order to achieve this melanin would require sufficiently high conductivity and a sufficient contact area with the titania, since that would determine the efficiency of the cell. Judging from the conductivity measurements done in previous chapter, the conductivity of the melanin itself may not be sufficient, but due to its hygroscopic nature it may be able to act as a gel electrolyte rather than a solid one.

However, our attempt at using the melanin as both the dye and the electrolyte was unsuccessful, with the resultant DSSC giving very little or no photocurrent. This was attributed to the low conductivity of the polymer, which even in its hydrated state still did not provide sufficient charge mobility for efficient charge transfer. Based on our previous measurement of melanin conductivity as a function of humidity, even in a hydrated state the conductivity of the melanin was only around 10^{-7} S/cm, which was still a few orders of magnitude lower than liquid electrolytes.

Despite the redox properties of melanin, due to the low conductivity of the material it was unlikely that the photogenerated charges would be able to move at a sufficient rate in the electrolyte, and thus the electrolyte would be unable to act as an efficient redox couple to regenerate the anode.

4.4. Summary

In conclusion, the traditional organometallic dyes such as the N3 dye were undoubtedly more efficient, with an efficiency of around 1.25% than the 0.34% of the melanin cell. This was mainly due to the fact that the open circuit potential of the melanin cell was a lot lower than the N3 dye even though the photocurrent produced was quite reasonable, resulting an a smaller overall efficiency.

It was shown that electrochemical oxidation can be used to synthesise melanin films for use in a DSSC, with the best method being a potentiostatic oxidation method. The optimum precursor concentration was found to be 5 mM of l-dopa in a borax buffer solution, which provided the most controlled oxidation which was important since film thickness was an important factor.

This low concentration required (compared to the synthesis of free-standing films) is advantageous from a production point of view since it would minimise the cost associated with the process. It was also found that the resultant DSSC needed to be irradiated with UV light in order to perform as its maximum efficiency, and this was attributed to photodoping of the melanin.

Despite the smaller efficiency, the melanin DSSC has the advantage over the N3 dye in cost efficiency and simplicity of synthesis. Unlike N3 dye, melanin can be synthesised at a fraction of the cost using a one step electrochemical synthesis from aqueous solutions. This would lend itself well for scale-up and use in industrial processes. The synthesis and dyeing process are also done in the same step, thus reducing the time required to manufacture the DSSC. The lower cost and ease of synthesis of melanin DSSC also opens the possibility of single-use applications where only a small amount of power is required.

Chapter 5

Conclusion
and
Future Works

5.1. Conclusion

Melanin free-standing films was synthesised from l-dopa by electrochemical means. The optimum method was the galvanostatic oxidation process was determined to be a current density of 0.5 mA/cm^2 for 8 days with a precursor concentration of 20-30 mM, with the most suitable buffer found to be the borax buffer. It was also found that melanin can only polymerise into free-standing films when ITO or FTO conducting glass was used as the electrode, with the use of metallic electrodes resulting in the formation of a thin film which passivates the electrode.

Solid state NMR and XPS analysis confirmed that the polymer contains indolic moieties which showed that cyclisation had occurred. The polymer is made of a mixture of DHI and DHICA, with an approximately 50:50 ratio of dihydroxyl to quinone species. The exact structure of the polymer remains unclear, but is most likely an amorphous solid made of predominantly indolic units linked together in a random manner as proposed by Nicolaus[100] and Swan[101], with possible small regions of the stacked macrocylic sheets structure proposed by Zajac[103]. Dopa was also evident in the material, but was thought to be trapped in the material and not chemically bonded to the polymer.

The conductivity of the material was found to be highly dependent on hydration, with a significant change in conductivity observed with changes in relative humidity, which is consistent with the literature. The conductivity and TGA result also indicated that there are two types of water within the material.

Attempts at doping the polymer was unsuccessful, with organic dopants having little to no effect on its conductivity. The use of metal ions was also unsuccessful as they interfere with the oxidation process.

PEG has been successfully incorporated into the electrochemically synthesised film. The PEG was not chemically bound to the melanin, but incorporated by mechanical entanglement. The addition PEG did not result in improved mechanical properties, but resulted in a more granular material.

We have also shown that melanin can be used as a sensitizer in DSSC. The optimum synthetic parameters have been determined, and it was also found that the cell required irradiation with UV light in order to reach its maximum efficiency. The melanin DSSC showed a power conversion efficiency of 0.34% compared to 1.25% of the N3 dye used in the same setup.

5.2. Future Works

For melanin to be of use as a polymer material, the mechanical properties of the polymer need to be further improved. In our study we have tried incorporating PEG into the material, and found that the PEG was only incorporated by mechanical entanglement. A possible extension to this study would be to use polymers with side chains that are able to bind to the 5,6-Dihydroxyindole (DHI) monomer, and thus may provide a better incorporation in the material.

Another option would be to polymerise the melanin onto a supporting structure. Due to time constraints we have not fully investigated this possibility, however it has been shown in the past that the use of inert scaffolds can improve the mechanical properties of conducting polymers[201, 202].

In this study, we have been unsuccessful in replicating the synthesis of 5,6-Diacetoxyindole (DAI)[170, 203-209], a direct precursor to DHI. It is likely that the use of DAI would provide a more homogenous material, and as such in the future successful synthesis of significant quantity of DAI may enable us to electrochemically synthesise melanin films with better mechanical properties. Functionalisation of the DAI monomer could also lead to novel structures.

The successful synthesis of DAI would also be of interest in melanin DSSC. The performance of DSSC dyed with DHI melanin which has no carboxylic acid functionality would help us to understand the nature of the bond between the TiO_2 and the melanin. This should be supported by the synthesis of 5,6-Diacetoxyindole-2-carboxylic acid

(DAICA), which would yield a polymer made entirely of 5,6-Dihydroxyindole-2-carboxylic acid (DHICA).

We also have not investigated other possible applications of this material. Since the conductivity of melanin is highly dependent on humidity, melanin can be used as a humidity sensor. In order to do this, firstly we would need to synthesise a more mechanically stable melanin film in order for electrical contacts to be successfully attached to the material. A more in depth study on the effect of humidity would also be required, and a possibility would be to use IR spectroscopy and chemometrics[210] to quantify the hydroxyl and quinone groups present in the material.

It has been shown in the literature that melanin shows selectivity towards certain ions[156], however we have not investigated the use of melanin as an electrode modifier. The electrochemical synthesis is a suitable way to deposit melanin onto an electrode surface, and this may lead to applications in electrochemical sensors.

Despite the low intrinsic conductivity, melanin may have good proton conductivity due to its hydrated nature, and as such may find use as proton-conducting polymer electrolytes. Polyheterocycles such as Poly(benzimidazole) are good proton conductors[211-213], and melanin with its abundance of hydroxyl and quinone groups may be able to function in a similar way.

References

(1) MacDiarmid, A. G. *Synthetic Metals* **1997**, *84*, 27-34.
(2) MacDiarmid, A. G. *Angew. Chem. Int. Ed.* **2001**, *40*, 2581-2590.
(3) Shirakawa, H. *Synthetic Metals* **2002**, *125*, 3-10.
(4) Naarman, H. *Science and applications on conducting polymers*; Adam Hilger Publ.: Bristol, 1991.
(5) Aldissi, M. *Critical reviews in surface chemistry* **1993**, *3*, 13-28.
(6) Chilton, J. A.; Goosey, M. T., Eds. *Special polymers for electronics and optoelectronics*; Chapman & Hall: London, 1995.
(7) Aldissi, M. *Inherently Conducting polymers*; Noyes Data Corporation: New Jersey, 1989.
(8) Ashwell, G. J., Ed. *Molecular Electronics*; Research Studies Press: Somerset, 1992.
(9) Chandrasekhar, P. *Conducting polymers, fundamentals and applications: a practical approach*; Kluwer academic publisher group: Dordrecht, 1999.
(10) Elsenbaumer, R. L.; Jen, K. Y.; Oboodi, R. *Synthetic Metals* **1986**, *15*, 169-174.
(11) Dufour, B.; Rannou, P.; Djurado, D.; Zagorska, M.; Kulszewicz-Bajer, I.; Pron, A. *Synthetic Metals* **2003**, *135-136*, 63-68.
(12) Heeger, A. J. *Synthetic Metals* **2002**, *125*, 23-42.
(13) Pron, A.; Rannou, P. *Progress in Polymer Science* **2002**, *27*, 135-190.
(14) Waltman, R.; Diaz, A.; Bargon, J. *J. Phys. Chem.* **1984**, 4343-4346.
(15) Salaneck, W. R.; Lundstrom, I.; Ranby, B., Eds. *Conjugated polymers and related materials: the interconnection of chemical and electronic structure*; Oxford University Press: New York, 1993.
(16) Patil, A. O. *Synthetic Metals* **1989**, *28*, 495-500.
(17) Zotti, G. In *Conductive Polymers: Synthesis and Electrical Properties*; Nalwa, H. S., Ed.; John wiley & Sons: West Sussex, 1997; Vol. 2, pp 137-170.
(18) Yoshino, K.; Morita, S.; Uchida, M.; Muro, K.; Kawai, T.; Ohmori, Y. *Synthetic Metals* **1993**, *55*, 28-35.
(19) Matsuda, H.; Shimada, S.; Takeda, H.; Masaki, A.; Keuren, E. V.; Yamada, S.; Hayamizu, K.; Nakanishi, F.; Okada, S.; Nakanishi, H. *Synthetic Metals* **1997**, *84*, 909-910.
(20) Ikkala, O. T.; Laakso, J.; Väkiparta, K.; Virtanen, E.; Ruohonen, H.; Järvinen, H.; Taka, T.; Passiniemi, P.; Österholm, J.-E.; Cao, Y.; al., A. A. e. *Synthetic Metals* **1995**, *69*, 97-100.
(21) Heeger, A. J. *Synthetic Metals* **1993**, *57*, 3471-3482.
(22) Angelopoulos, M.; Shaw, J.; Lecorre, M.; Tissier, M. *Microelectronic Engineering* **1991**, *13*, 515-518.
(23) Angelopoulos, M.; Patel, N.; Shaw, J.; Labianca, N.; Rishton, S. *Journal of Vacuum Science & Technology, B: Microelectronics and Nanometer Structures* **1993**, *11*, 2794-2797.
(24) Angelopoulos, M.; Shaw, J.; Kaplan, R.; Perreault, S. *Journal of Vacuum Science & Technology, B: Microelectronics and Nanometer Structures* **1989**, *7*, 1519-1523.

(25) Baughman, R. H. In *Science and Applications of Conducting Polymer*; Salaneck, R., Ed.; IOP Publishers, 1991, pp 47.
(26) Wosnitza, J. *Current Opinion in Solid State and Materials Science* **2001**, *5*, 131-141.
(27) Aldissi, M., Ed. *Intrinsically conducting polymer: an emerging technology*; Kluwer academic publisher: Dordrecht, 1993.
(28) Gurunathan, K.; Murugan, A. V.; Marimuthu, R.; Mulik, U. P.; Amalnekar, D. P. *Materials Chemistry and Physics* **1999**, *61*, 173-191.
(29) Arbizzani, C.; Mastragostino, M.; Scrosati, B. In *Handbook of Organic Conductive Molecules and Polymer*; Nalwa, H. S., Ed.; John Wiley & Sons: West Sussex, 1997; Vol. 4, pp 595-620.
(30) Nogueira, A. F.; Longo, C.; De Paoli, M.-A. *Coordination Chemistry Reviews* **2004**, *248*, 1455-1468.
(31) Gebeyechu, D.; Brabec, C. J.; Sacrifitci, N. S.; Vageneugden, D.; Kiebooms, R.; Vanderzande, D.; Kienberger, F.; Schindler, H. *Synthetic Metals* **2002**, *125*, 279-287.
(32) Arango, A. C.; Carter, S. A.; Brock, P. J. *Applied Physics Letters* **1999**, *74*, 1698-1700.
(33) Inzelt, G.; Pineri, M.; Schultze, J. W.; Vorotyntsev, M. A. *Electrochimica Acta* **2000**, *45*, 2403-2421.
(34) Ozaki, M.; Peebles, D. L.; Weinberger, B. R.; Chiang, C. K.; Gau, S. C.; Heeger, A. J.; MacDiarmid, A. G. *Applied Physics Letters* **1979**, *35*, 83-85.
(35) Smestad, G.; Spiekermann, S.; Kowalik, J.; Grant, C. D.; Schwartzberg, A. M.; Zhang, J.; Tolbert, L. M.; Moons, E. *Solar Energy Materials & Solar Cells* **2003**, *76*, 85-105.
(36) Luzzati, S.; Basso, M.; Catellani, M.; Brabec, C. J.; Gebeyechu, D.; Sacrifitci, N. S. *Thin Solid films* **2002**, *403-404*, 52-56.
(37) Spiekermann, S.; Smestad, G.; Kowalik, J.; Tolbert, L. M.; Gratzel, M. *Synthetic Metals* **2001**, *121*, 1603-1604.
(38) Bongini, A.; Barbarella, G.; Sotgiu, G.; Zambianchi, M.; Mastragostino, M.; Arbizzani, C.; Soavi, F. *Synthetic Metals* **1999**, *101*, 13-14.
(39) Arbizzani, C.; Mastragostino, M.; Soavi, F. *Electrochimica Acta* **2000**, *45*, 2273-2278.
(40) Chirvase, D.; Chiguvare, Z.; Knipper, M.; Parisi, J.; Dyakonov, V.; Hummelen, J. C. *Synthetic Metals* **2003**, *138*, 299-304.
(41) Umeda, T.; Hashimoto, Y.; Mizukami, H.; Shirakawa, T.; Fujii, A.; Yoshino, K. *Synthetic Metals* **2005**, *152*, 93-96.
(42) Armstrong, N. R.; Carter, C.; Donley, C.; Simmonds, A.; Lee, P.; Brumbach, M.; Kippelen, B.; Domercq, B.; Yoo, S. *Thin Solid films* **2003**, *445*, 345-352.
(43) Savenjie, T. J.; Vermeulen, M. J.; de Haas, M. P.; Warman, J. M. *Solar Energy Materials & Solar Cells* **2000**, *61*, 9-18.
(44) Yoshino, K.; Tada, K.; Fujii, A.; Conwell, E.; Zakhidov, A. *IEEE Transactions on Electron Devices* **1997**, *44*, 1315-1324.
(45) Lee, S. B.; Katayama, T.; Kajii, H.; Araki, H.; Yoshino, K. *Synthetic Metals* **2001**, *121*, 1591-1592.

(46) Kroon, J. M.; Wienk, M. M.; Verhees, W. J. H.; Hummelen, J. C. *Thin Solid films* **1999**, *101*, 223-228.
(47) Sonmez, G. *Chemical Communications* **2005**, *42*, 5251-5259.
(48) Zhang, F.; Inganaes, O. *Optical Science and Engineering* **2005**, *99*, 479-494.
(49) Chandrasekhar, P.; Zay, B. J.; McQueeney, T.; Birur, G. C.; Sitaram, V.; Menon, R.; Coviello, M.; Elsenbaumer, R. L. *Synthetic Metals* **2005**, *155*, 623-627.
(50) Nicho, M. E.; Hu, H.; López-Mata, C.; Escalante, J. *Solar Energy Materials & Solar Cells* **2004**, *82*, 105-118.
(51) Pagès, H.; Topart, P.; Lemordant, D. *Electrochimica Acta* **2001**, *46*, 2137-2143.
(52) Mortimer, R.; Dyer, A.; Reynolds, J. *Displays* **2006**, *27*, 2-18.
(53) Somani, R.; Radakrishnan, S. *Materials Chemistry and Physics* **2002**, *9299*, 1-17.
(54) Seo, S.; Kim, J.; Park, J.; Lee, H. *Applied Physics Letters* **2005**, *87*, 183503/183501-183503/183503.
(55) Tengstedt, C.; Crispin, A.; Hsu, C.-H.; Zhang, C.; Parker, I. D.; Salaneck, W. R.; Fahlman, M. *Organic Electronics* **2005**, *6*, 21-33.
(56) Shaukat, S. F.; Farooq, R.; Dong, Y. *Journal of Natural Sciences and Mathematics* **2003**, *43*, 133-139.
(57) Ampuero, S.; Bosset, J. O. *Sensors and Actuators B:Chemical* **2003**, *94*, 1-12.
(58) Farace, G.; Lillie, G.; Hianik, T.; Payne, P.; Vadgama, P. *Bioelectrochemistry* **2002**, *55*, 1-3.
(59) Bidan G, B. M., Livache T *Synthetic metals* **1999**, *102*, 1363-1365.
(60) Riul, A.; Malmegrim, R.; Fonseca, F.; Mattoso, L. *Biosensors and Bioelectronics* **2003**, *18*, 1365-1369.
(61) Mark, H.; Atta, N.; Ma, Y.; Petticrew, K.; Zimmer, H.; Shi, Y.; Lunsford, S.; Rubinson, J.; Galal, A. *Bioelectrochemistry and Bioenergetics* **1995**, *38*, 229-245.
(62) Joo, J.; Lee, J. K.; Baeck, J. S.; Kim, K. H.; Oh, E. J.; Epstein, J. *Synthetic Metals* **2001**, *117*, 45-51.
(63) Gardner, J.; Bartlett, P. *Sensora and Actuators A* **1995**, *51*, 57-66.
(64) Wallace, G.; Smyth, M.; Zhao, H. *TrAC Trends in Analytical Chemistry* **1999**, *18*, 245-251.
(65) Gerard, M.; Chaubey, A.; Malhotra, B. D. *Biosensors and Bioelectronics* **2002**, *17*, 345-359.
(66) Kotwal, A.; Schmidt, C. *Biomaterials* **2001**, *22*, 1055-1064.
(67) Seal, B.; Otero, T.; Panitch, A. *Materials Science and Engineering* **2001**, *R 34*, 147-230.
(68) Khan, G.; Wernet, W. *Thin Solid films* **1997**, *300*, 265-271.
(69) Campbell, T. E.; Hodgson, A. J.; Wallace, G. G. *Electroanalysis* **1999**, *11*, 215-222.
(70) Kane-Maguire, L.; Wallace, G. *Synthetic Metals* **2001**, *119*, 39-42.
(71) Gandhi, M. R.; Murray, P.; Spinks, G. M.; Wallace, G. *Synthetic Metals* **1995**, *73*, 247-256.
(72) Careem, M. A.; Velmurugu, Y.; Skaarup, S.; West, K. *Journal of Power Sources* **2006**, *In Press, Corrected Proof,*.
(73) Metz, P.; Alici, G.; Spinks, G. M. *Sensors and Actuators A* **2006**, *130-131*, 1-11.
(74) Baughman, R. H. *Synthetic Metals* **1996**, *78*, 339-353.

(75) Jager, E. W.; Smela, E.; Inganas, O.; Lundstrom, I. *Synthetic Metals* **1999**, *102*, 1309-1310.
(76) Hutchison, A. S.; Lewis, T. W.; Moulton, S. E.; Spinks, G. M.; Wallace, G. *Synthetic metals* **2000**, *113*, 121-127.
(77) Kilmartin, P. A.; Li, K. C.; Bowmaker, G. A.; Vigar, N. A.; Cooney, R. P.; Travas-Sejdic, J. *Current Applied Physics* **2006**, *6*, 567-570.
(78) Otero, T.; Sansena, J. *Bioelectrochemistry and Bioenergetics* **1995**, *38*, 411-414.
(79) Rossi, D. D.; Santa, A. D.; Mazzoldi, A. *Synthetic Metals* **1997**, *90*, 93-100.
(80) Radhakrishnan, S.; Kar, S. B. *Sensors and Actuators B:* **2006**, *In Press, Corrected Proof*.
(81) Nakano, T.; Takeoka, Y.; Rikukawa, M.; Sanui, K. *Synthetic Metals* **2005**, *153*, 121-124.
(82) Han, G.; Shi, G. *Journal of Electroanalytical Chemistry* **2004**, *569*, 169-174.
(83) Ding, J.; Spinks, G. M.; Zhou, D.; Wallace, G.; Gillespie, J. *Synthetic Metals* **2003**, *138*, 391-398.
(84) Hara, S.; Zama, T.; Takashima, W.; Kaneto, K. *Synthetic Metals* **2005**, *149*, 199-201.
(85) Madden, J. D.; D.Rinderknecht; Anquetil, P. A.; Hunter, I. W. *Sensors and Actuators A* **2006**, *In Press, Corrected Proof*.
(86) Reece, D. A.; Ralph, S. F.; Wallace, G. G. *Journal of Membrane Science* **2005**, *249*, 9-20.
(87) Price, W. E.; Too, C. O.; Wallace, G. G.; Zhou, D. *Synthetic Metals* **1999**, *102*, 1338-1341.
(88) Partridge, A. C.; Milestone, C.; Too, C. O.; Wallace, G. G. *Journal of Membrane Science* **1997**, *132*, 245-253.
(89) Partridge, A. C.; Milestone, C. B.; Too, C. O.; Wallace, G. G. *Journal of Membrane Science* **1999**, *152*, 61-70.
(90) Pile, D.; Hillier, A. *Journal of Membrane Science* **2002**, *208*, 119-131.
(91) Selampinar, F.; Akbulut, U.; Ozden, M.; Toppare, L. *Biomaterials* **1997**, *18*, 1163-1168.
(92) Bidan, G.; Lopez, C.; Mendes-Viegas, F.; Vielil, E.; Gadelle, A. *Biosensors and Bioelectronics* **1994**, *9*, 219-229.
(93) Wadhwa, R.; Lagenaur, C. F.; Cui, X. T. *Journal of Controlled Release* **2006**, *110*, 531-541.
(94) Lira, L. M.; de Toressi, S. C. *Electrochemistry Communications* **2005**, *7*, 717-723.
(95) Saxena, V.; Malhotra, B. D. *Current Applied Physics* **2003**, *3*, 293-305.
(96) Zinger, B.; Miller, L. *Journal of the American Chemical Society* **1984**, *106*, 6861-6863.
(97) Mason, H. S. *Advances in Biology of Skin* **1967**, *8*, 293-312.
(98) Pezzella, A.; Napolitano, A.; d`Ischia, M.; Prota, G. *Tetrahedron* **1996**, *52*, 7913-7910.
(99) Gidanian, S.; Farmer, P. *Journal of Inorganic Biochemistry* **2001**, *89*, 54-60.
(100) Nicolaus, R. A. *Melanins*; Hermann: Paris, 1968.
(101) Swan, G. A. *Fortschritte der Chemie Organischer Naturstoffe* **1974**, *31*, 521-582.
(102) Stark, K. B.; Gallas, J. M.; G.W., Z.; Golab, J. T.; Gidanian, S.; McIntire, T.; Farmer, P. *J. Phys. Chem. B* **2005**, *109*, 1970-1977.

(103) Zajac, G. W. *Biochimica et Biophysica Acta* **1994**, *1199*, 271.
(104) Haywood, R.; Lee, M.; Linge, C. *Journal of Photochemistry and Photobiology B* **2006**, *82*, 224-235.
(105) Nicolaus, B. J. R. *Medical Hypotheses* **2005**, *65*, 791-796.
(106) Riley, P. A. *International Journal of Biochemistry and Cell Biology* **1997**, *29*, 1235-1239.
(107) Cesarini, J. P. *Advance Space Research* **1996**, *18*, 1235-1240.
(108) Sone, M.; Takahashi, K.; Murakami, O.; Totsune, K.; Arihara, Z.; Sartoh, F.; Sasano, J.; Ito, H.; Mouri, T. *Peptides* **2000**, *21*, 245-249.
(109) Sionkowska, A. *Journal of Photochemistry and Photobiology A* **1999**, *124*, 91-94.
(110) Nikiforos, K.; M., R.; Zeise, S.; Chedekel, R. M. *Journal of Photochemistry and Photobiology B: Biology* **1991**, *9*, 135-160.
(111) Giacomoni, P. U. *Journal of Photochemistry and Photobiology B* **1995**, *29*, 87-89.
(112) Prota, G. *European Journal of Cancer* **1994**, *30*, 553-554.
(113) Sarna, T.; Pilas, B.; Land, E.; Truscott, G. *Biochimica et Biophysica Acta* **1986**, *883*, 162-167.
(114) Sarna, T.; Hyde, J.; Swartz, H. *Science* **1976**, *192*, 1132-1134.
(115) Prota, G. *Pigment Cell Research* **2000**, *13*, 283-293.
(116) Hung, Y.; Sava, V.; Yu. Makan, S.; J, C.; Hong, M.; Huang, G. *Food Chemistry* **2002**, *78*, 233-240.
(117) Sava, V. M.; Hung, Y. C.; Golkin, B. N.; Hong, M.-Y.; Huang, G. S. *Food Research International* **2002**, *35*, 619-626.
(118) Zbitniewski, Z.; Kanclerz, A.; Drewa, G. *Pol. Przeglad Zoologiczny* **1977**, *21*, 116-126.
(119) Hegedus, Z. L. *Toxicology* **2000**, *145*, 85-101.
(120) Rozanowska, M.; Sarna, T.; E, L.; Truscott, G. *Free Radical Biology and Medicine* **1998**, *26*, 518-525.
(121) Sarna, T.; Sealy, R. *Archives of Biochemistry and Biophysics* **1984**, *232*, 574-578.
(122) Geremia, E.; Corsaro, C.; Bonomo, R.; Giardinelli, R.; Papalardo, P.; Vanella, A.; Sichel, G. *Comp, Biochem. Physiol* **1984**, *79B*, 67-69.
(123) Zareba, M.; Bober, A.; Korytowski, W.; Zecca, L.; Sarna, T. *Biochimica et Biophysica Acta* **1995**, *1271*, 343-348.
(124) Bridelli, M. G.; Tampellini, D.; Zecca, L. *FEBS Letters* **1999**, *457*, 18-22.
(125) Zecca, L.; Shima, T.; Stroppolo, A.; Goj, C.; Battson, A.; Gerbasi, R.; Sarna, T.; Swartz, M. *Neuroscience* **1996**, *73*, 407-415.
(126) Thong, P.; Watt, F.; Ponraj, D.; Leong, S.; He, Y.; Lee, T. *Nuclear Instruments and Methods in Physics Research B* **1999**, *158*, 349-355.
(127) McGinness, J.; Corry, P.; Proctor, P. *Science* **1974**, *183*, 853-855.
(128) Strzelecka, T. *Physiological Chemistry and Physics* **1982**, *14*, 223-231.
(129) Strzelecka, T. *Physiological Chemistry and Physics* **1982**, *14*, 219-222.
(130) Osak, W.; Tkacz, K.; Czternastek, H.; Slawinski, J. *Biopolymers* **1989**, *28*, 1885-1890.
(131) Jartzebska, M.; Kocot, A.; Tajber, L. *Journal of Photochemistry and Photobiology B* **2002**, *66*, 201-206.
(132) Rosei, M.; Mosca, L.; Galuzzi, F. *Synthetic Metals* **1996**, *76*, 331-335.
(133) Lundstrom, I.; Svensson, S. *Current Applied Physics* **2002**, *2*, 17-21.

(134) Jartzebska, M.; Isotalo, H.; Paloheimo, J.; Stubb, H. *Journal of Biomaterials Science. Polymer Edition* **1995**, *7*, 577-586.
(135) Meredith, P.: International Patent Application, 2002.
(136) Subianto, S. Honours, Queensland University of Technology, Brisbane, 2002.
(137) Jerome, C.; Jerome, R. *Angew Chem Int Ed Eng* **1998**, *37*, 2488-2490.
(138) Kupila, E.; Kankare, J. *Synthetic Metals* **1995**, *74*, 241-249.
(139) Nalwa, H. S., Ed. *Conductive polymers: synthesis and electrical properties*; John wiley & sons: Chicester, 1997.
(140) Penner, R. M.; Martin, C. R. *Journal of the Electrochemical Society* **1986**, *133*, 2206-2207.
(141) Sadki, S.; Schottland, P.; Brodie, N.; Saboraud, G. *Chemistry Society Reviews* **2000**, *29*, 283-293.
(142) Wood, G. I., J *Journal of Applied Polymer Science* **1996**, *61*, 519-528.
(143) Wood, G. I., J *European polymer Journal* **1997**, *33*, 107-114.
(144) Zhou, M.; Heinze, J. *Journal of Physical Chemistry B* **1999**, *103*, 8451.
(145) Zhou, M.; Heinze, J. *The Journal of Physical Chemistry B* **1999**, *103*, 8443.
(146) Otero, T. F.; Santamaria, C.; Bunting, R. K. *Journal of Electroanalytical chemistry* **1995**, *380*, 291-294.
(147) Kupila, E. K., J *Synthetic Metals* **1996**, *82*, 89-95.
(148) Drekylev, P.; Granstrom, M.; Inganas, O.; Guaratne, L.; Senadeera, G.; Skaarup, S.; West, K. *Polymer* **1996**, *37*, 2609-2613.
(149) Choi, K. M.; Kim, C. Y.; Kim, K. H. *J. Phys. Chem.* **1992**, *96*, 3782-3788.
(150) Brun, A.; Rosset, R. *Electroanalytical Chemistry and Interfacial Electrochemistry* **1974**, *49*, 287-300.
(151) Zielinski, C.; Pande, M. *Synthetic Metals* **1990**, *37*, 350-351.
(152) Horak, V.; Weeks, G. *Bioorganic Chemistry* **1993**, *21*, 24-33.
(153) Deziderio, S. N.; Brunello, C. A.; da Silva, M. N.; Cotta, M. A.; Graeff, C. F. O. *Journal of Non-Crystalline Solids* **2004**, *338-340*, 634-638.
(154) Robinson, G. M.; Iwuoha, E. I.; Smyth, M. R. *Electrochimica Acta* **1998**, *43*, 3489-3496.
(155) Serpentini, C.; Gauchet, C.; de Montauzon, D.; Comtat, M.; Ginestar, J.; Paillous, N. *Electrochimica Acta* **2000**, *45*, 1663-1668.
(156) Rubianes, M. D.; Rivas, G. A. *Analytica Chimica Acta* **2001**, 99-108.
(157) Bard, A. J. *Electrochemical methods: fundamentals and applications*, 2 ed.; John Wiley: New York, 2001.
(158) Li, J.; Christensen, B. M. *Journal of Electroanalytical chemistry* **1994**, *375*, 219-231.
(159) Wang, J. *Analytical electrochemistry*, 2 ed.; Wiley-VCH: New York, 2000.
(160) Scholz, F. *Electroanalytical Methods*; Springer-Verlag: Berlin, 2002.
(161) Young, T. E.; Babbitt, B. W. *J. Org. chem* **1983**, *48*, 562-566.
(162) Duff, G.; Roberts, J.; Foster, N. *Biochemistry* **1988**, *27*, 7112-7116.
(163) Reinheimer, P.; Hirschinger, J.; Granger, P.; Breton, P.; Lagrange, A.; Gilard, P.; Lebefve, M.; Goetz, N. *Biochimica et Biophysica Acta* **1999**, *1472*, 240-249.
(164) Katritzky, A. R.; Akhmedov, N.G; Denisenko, S. N.; Denisko, O. V. *Pigment Cell Research* **2002**, *15*, 93-97.

(165) Williams-Smith, D.; Dunne, J.; Evans, S.; Pritchard, R.; Evans, E. *FEBS Letters* **1976**, *69*, 291-294.
(166) Clark, M.; Gardella, J.; Schultz, T.; Patil, D.; Salvati, L. *Analytical Chemistry* **1990**, *62*, 949-956.
(167) Napolitano, A.; Pezzella, A.; Prota, G.; Seraglia, R.; Traldi, P. *Rapid communications in Mass Spectrometry* **1996**, *10*, 468-472.
(168) Nofsfinger, J.; Forest, S.; Eibest, L.; Gold, K.; Simon, J. *Pigment Cell Research* **2000**, *13*, 179-184.
(169) Liu, Y.; Simon, J. *Pigment Cell Research* **2003**, *16*, 72-80.
(170) Atkinson, S.; Meredith, P. *Synlett* **2003**, *12*, 1853-1855.
(171) Subianto, S.; Will, G.; Meredith, P. *Polymer* **2005**, *46*, 11505-11509.
(172) Subianto, S.; Will, G.; Kokot, S. *Journal of Polymer Science, Part A: Polymer Chemistry* **2003**, *41*, 1867-1869.
(173) Zeise, L.; Addison, R.; Chedekel, M. *Pigment Cell Research Supplement* **1992**, *2*, 48-53.
(174) Schmeiber, D.; Bartl, A.; Dunsch, L.; Naarman, H.; Gopel, W. *Synthetic Metals* **1998**, *93*, 43-58.
(175) Chen, S. A.; Chen, S. H. *Journal of Polymer Science: Part C: Polymer Letters* **1989**, *27*, 93-101.
(176) Yin, W. L., H, Gan, L *Journal of Applied Polymer Science* **1999**, *72*, 95-101.
(177) Kang, E. T.; Neoh, K. G.; Tan, K. L. In *Advances in Polymer Science*; Springer-Verlag: Berlin, 1993; Vol. 106, pp 135-189.
(178) Chia, V.; Soriaga, M.; Hubbard, A.; Anderson, S. *J. Phys. Chem.* **1983**, *87*.
(179) Malinauskas, A. *Journal of Power Sources* **2004**, *126*, 214-220.
(180) Seraglia, R.; Traldi, P.; Elli, G.; Bertazzo, A.; Costa, C.; Allegri, G. *Biological Mass Spectrometry* **1993**, *22*, 687-697.
(181) Napolitano, A.; Cresceni, O.; Prota, G. *Tetrahedron Letters* **1993**, *34*, 885-888.
(182) Bridelli, M.; Capelletti, R.; Crippa, P. R. *Journal of Electroanalytical Chemistry* **1981**, *128*, 555-567.
(183) Bridelli, M.; Capelletti, R.; Crippa, P. R. *Bioelectrochemistry and Bioenergetics* **1981**, *8*, 555-567.
(184) Stainsack, J.; Mangrich, A.; Maia, C.; Machado, V.; dos Santos, J.; Nakagaki, S. *Inorganica Chimica Acta* **2003**, *356*, 243-248.
(185) Szpoganicz, B.; Gidanian, S.; Kong, P.; Farmer, P. *Journal of Inorganic Biochemistry* **2001**, *89*, 45-53.
(186) Palumbo, A.; dÍschia, M.; Misuraca, G.; Prota, G. *Biochimica et Biophysica Acta* **1987**, *925*, 203-209.
(187) Chirila, T. *journal of Biomaterials Applications* **1993**, *8*, 106-145.
(188) Ishii, A.; Furukawa, M.; Matsushima, A.; Kodera, Y.; Yamada, A.; Kanai, H.; Inada, Y. *Dyes and Pigments* **1995**, *27*, 211-217.
(189) Sotomatsu, A.; Tanaka, M.; Hirai, S. *FEBS Letters* **1994**, *342*, 105-108.
(190) McConnell, R. D. *Renewable and Sustainable Energy Reviews* **2002**, *6*, 273-295.
(191) Gratzel, M. *Nature* **2001**, *414*, 338-344.
(192) Li, B.; Wang, L.; Kang, B.; Wang, P.; Qiu, Y. *Solar Energy Materials & Solar Cells* **2006**, *90*, 549-573.

(193) Nogueira, A. F.; Alonso-Vante, N.; De Paoli, M.-A. *Synthetic Metals* **1999**, *105*, 23-27.
(194) Savenjie, T. J.; Warman, J. M.; Goossens, A. *Chemical Physics Letters* **1998**, *287*, 148-153.
(195) A. van Hal, P.; Christiaans, P. T.; Wienk, M. J.; Kroon, J. M.; Janssen, R. A. J. *Journal of Physical Chemistry B* **1999**, *103*, 4352-4359.
(196) Yanagida, S.; Senadeera, G.; Nakamura, K.; Kitamura, T.; Wada, Y. *Journal of Photochemistry and Photobiology A* **2004**, *166*, 75-80.
(197) Moss, J.; Stipkala, J.; Yang, J.; Bignozzi, C.; Meyer, G.; Meyer, T.; Wen, X.; Linton, R. *Chemistry of Materials* **1998**, *10*, 1748-1750.
(198) Hao, S.; Wu, J.; Huang, Y.; Lin, J. *Solar Energy* **2006**, *80*, 209-214.
(199) Ito, S.; Kitamura, T.; Wada, Y.; Yanagida, S. *Solar Energy Materials & Solar Cells* **2003**, *76*, 3-13.
(200) Wilson, G.; Will, G.; Frost, R.; Montgomery, S. *Journal of Materials Chemistry* **2002**, *12*, 1787-1791.
(201) Wang, J.; Chen, J.; Wang, C. Y.; Zhou, D.; Too, O.; Wallace, G. *Synthetic Metals* **2005**, *153*, 117-120.
(202) Subianto, S.; Queensland University of Technology: Brisbane, 2001.
(203) Benigni, J. D.; Minnis, R. L. *Journal of Heterocyclic Chemistry* **1965**, *2*, 387-392.
(204) Murphy, B.; Schultz, T. *Journal of Organic Chemistry* **1985**, *50*, 2790-2791.
(205) Novellino, L.; d`Ischia, M.; Prota, G. *Synthesis* **1999**, *5*, 793-796.
(206) Wakamatsu, K.; Ito, S. *Analytical Biochemistry* **1987**, *170*, 335-340.
(207) Beer, R.; Clarke, K.; Khorana, H.; Robertson, A. *Nature* **1948**, *161*, 525.
(208) Beer, R.; Clarke, K.; Khorana, H.; Robertson, A. *Journal of the Chemical Society* **1948**, 2223-2226.
(209) Bu`lock, J. D.; Harley-mason, J. *Journal of the Chemical Society* **1951**, 2240-2252.
(210) Watanabe, A.; Morita, S.; Kokot, S.; Matsubara, M.; Fukai, K.; Ozaki, Y. *Journal of Molecular Structure* **2006**, *In Press, Corrected Proof*.
(211) Itoh, T.; Hamaguchi, Y.; Uno, T.; M.Kubo; Aihara, Y.; Sonai, A. *Solid State Ionics* **2006**, *177*, 185-189.
(212) Jannasch, P. *Current Opinion in Colloid & Interface Science* **2003**, *8*, 96-102.
(213) Kreuer, K. D. *Journal of Membrane Science* **2001**, *185*, 29-39.